



A University of Sussex PhD thesis

Available online via Sussex Research Online:

<http://sro.sussex.ac.uk/>

This thesis is protected by copyright which belongs to the author.

This thesis cannot be reproduced or quoted extensively from without first obtaining permission in writing from the Author

The content must not be changed in any way or sold commercially in any format or medium without the formal permission of the Author

When referring to this work, full bibliographic details including the author, title, awarding institution and date of the thesis must be given

Please visit Sussex Research Online for more information and further details



PSEUDO-GOLDSTONE BOSONS
IN EARLY UNIVERSE PHYSICS

Author:

Djuna Lize Croon

Submitted for the degree of Doctor of Philosophy

University of Sussex

May 2017

DECLARATION

I hereby declare that this thesis has not been and will not be submitted in whole or in part to another University for the award of any other degree.

The work in this thesis has been completed in collaboration with Veronica Sanz, Jack Setford, Ewan Tarrant, Barry Dillon, Stephan Huber, and is comprised of the following papers:

- Djuna Croon, and Veronica Sanz, 'Saving Natural Inflation', published in JCAP 1502 (2015) no.02, p. 008. arXiv: 1411.7809 [hep-ph].
- Djuna Croon, Veronica Sanz, and Jack Setford, 'Goldstone Inflation', published in JHEP 1510 (2015) no.20. arXiv:1503.08097 [hep-ph].
- Djuna Croon, Veronica Sanz, Ewan R. M. Tarrant, 'Reheating with a Composite Higgs', published in Physical Review D94 (2016) no.4, p. 045010. arXiv:1507.04653 [hep-ph]. The reheating calculation in this paper was performed by Ewan Tarrant, and the exclusion limits in figure 7 are the work of Veronica Sanz.
- Djuna Croon, Barry M. Dillon, Stephan J. Huber, Veronica Sanz, 'Exploring holographic Composite Higgs models', published in JHEP 1607 (2016) no.72, arXiv:1510.08482 [hep-ph]. The scans for the figures 1-12 in this paper were done in collaboration with Barry Dillon.
- Djuna Croon, 'Model Building with Non-Compact Cosets', Physics Letters B762 (2016) p. 543-548. arXiv:1605.06772 [hep-ph].

I have led or corroborated all the original research presented in this thesis.

Signature:

Djuna Lize Croon

‘The pleasure lies not in discovering truth, but in searching for it.’

Leo Tolstoy, Anna Karenina

‘The Universe is too big to care about something so small.’

Rick and Morty

UNIVERSITY OF SUSSEX

DJUNA LIZE CROON, DOCTOR OF PHILOSOPHY

PSEUDO-GOLDSTONE BOSONS IN EARLY UNIVERSE PHYSICS

ABSTRACT

This thesis aims to give an approach to dealing with Hierarchy problems in theoretical physics, plaguing theories that span a wide range of energy scales. At present, any theory that is formulated to connect observations of the Early Universe to results in present day particle physics, exhibits the necessity of (at least one) *unnaturally* fine-tuned parameter. This has encouraged the sectioning of many separate, highly specialized fields - each dealing with *Effective Field Theories* (EFTs) valid at a limited range of energy scales only. Here I describe an effort to connect different energy scales while dynamically accounting for hierarchies.

This thesis discusses the appeal of pseudo-Goldstone bosons (pGBs) for the generation of scales in Early Universe cosmology. In particular, I will show how models with pGBs address the radiative instability of mass scales in quantum mechanical theories.

I will start with an introduction to the two hierarchy problems that will be the primary focus of the thesis: the electroweak hierarchy problem, or the puzzle of the lightness of the Higgs mass; and the inflationary hierarchy problem, or the flatness of the inflaton potential demanded by the nearly scale invariant spectrum of the Cosmic Microwave Background. I will briefly introduce how pGBs arise, and can be described, using an example of a compact Special Orthogonal group $SO(n)$ breaking to its largest coset $SO(n-1)$.

I will then explore various models that address the electroweak and the inflationary hierarchy problem, using appropriate EFT tools such as the Callan-Coleman-Wess-Zumino mechanism and 5D approaches. I will discuss the relative strength of these models compared to existing models in the literature.

After this discussion I will show that it is possible to address both hierarchy problems in a unified model, in which an inflaton decays into the Higgs field after inflation, in a process called reheating. This section will include a detailed derivation of the model, and will explore the regions of parameter space that lead to inflation, reheating, and electroweak symmetry breaking compatible with the relevant experimental data.

This is followed by an excursion in which I will discuss non-compact models, based on $SO(n,1)/SO(n)$ cosets. I will show how such setups can also give rise to inflation compatible with the current data, and discuss different scenarios for reheating.

I will finish with an epilogue of the prospects of (holographic) Composite Higgs models - in which the Higgs is a pGB of the breaking of a strong compact symmetry - at particle colliders.

ACKNOWLEDGEMENTS

In the four years of this doctoral course, I have had a humbling amount of help and friendship from some great people.

My supervisor, role model, and friend, Veronica Sanz.

My PhD peers, in particular Chris Harman, Tugba Buyukbese, Heather McAslan, and Jack Setford, for sharing this experience, but also a moral framework and a lot of fun.

My amazing friends, the Independent Woemans: Marianna, Alexandra, Mariska, Steven, and Jesse, for celebrating life and sharing ups and downs; Alejandra, for always being a phone call away; Lisa, for your inspiring drive, and for travels and adventures; ABC: Astrid, Brita, and Cecilie, for an unbreakable international bond; Floortje and Lottie, for your reliable and longterm friendship; Samar, for political and intercultural contemplations; Paco, for cultural explorations and inspiration.

My family, for enthusiasm, confidence, literature, and music.

My love, Luke, for endless patience and support. I am a much stronger scientist and a much happier person with you in my life.

CONTENTS

List of Figures	xi
1 Introduction	1
1.1 Prelude	1
1.2 Hierarchy problems	3
1.2.1 A paradigm	3
1.2.2 Dynamical solutions to hierarchy problems	6
1.3 Theoretical input for Model Building	10
1.3.1 Internal consistency	10
1.3.2 Fine-tuning	12
1.3.3 Reproducing the Standard Model	12
1.4 Experimental Constraints	13
1.4.1 Collider bounds	13
1.4.2 CMB data	15
1.5 Outline of this thesis	19
2 Saving Natural Inflation	22
2.1 Introduction	23
2.2 The general set-up of Natural Inflation	25
2.3 Vanilla Natural Inflation: Instanton-like potential	27
2.3.1 The problem with vanilla natural inflation	28
2.4 Extra-natural inflation: a 5D model and its duals	30
2.4.1 The issue with the original Extra-natural inflation model, and how to solve it	33
2.5 Realistic 4D Inflation: Coleman-Weinberg Inflation	35
2.5.1 Fermionic contributions	36
2.5.2 Inflationary models inspired on the Higgs as a pseudo-Goldstone boson .	37
2.5.3 Inflating with a Higgslike PNGB	38
2.6 The effect of UV completions: Higher-Dimensional Terms	40

2.6.1	Adding Higher-Dimensional Operators to Vanilla Natural Inflation	41
2.7	Conclusions	43
3	Goldstone Inflation	45
3.1	Introduction	46
3.2	A successful Coleman-Weinberg potential	48
3.3	Constraints from Inflation	55
3.3.1	Fine-tuning	58
3.3.2	Non-Gaussianity and its relation to Goldstone scattering	59
3.4	Link to UV models	62
3.5	Light resonance connection	63
3.6	Discussion and Conclusions	66
4	Reheating with a Composite Higgs	72
4.1	Introduction	73
4.2	The Lagrangian of the Higgs and the Inflaton	75
4.2.1	Inflaton–Higgs couplings for perturbative reheating	75
4.2.2	Symmetry breaking: the minimal coset	76
4.2.3	Composite Higgs limit: CP assignment in the fermion sector	79
4.2.4	Spontaneously broken CP by the inflaton ($\alpha \neq 0$)	80
4.3	Inflation	81
4.3.1	Tuning	83
4.4	Reheating	85
4.4.1	Equations of Motion	85
4.4.2	Bogoliubov Calculation	90
4.4.3	Boltzmann Equations	92
4.4.4	Parameter Constraints from Reheating	95
4.5	TeV Inflaton and its consequences	96
4.6	Conclusions	98
5	Model Building with Non-Compact Cosets	104
5.1	Introduction	105
5.2	Models of hyperbolic space	106
5.3	Compact potentials from non-compact cosets	108
5.4	Inflation along the compact direction	111
5.5	Conclusions	114

6	Exploring Holographic Composite Higgs Models	116
6.1	Introduction	117
6.2	Overview of the MCHM ₅	120
6.3	A holographic model	121
6.3.1	The 5D gauge sector	122
6.3.2	The 5D quark sector	124
6.3.3	The effective action	124
6.4	Higgs potential and EWSB	126
6.4.1	Yukawa couplings in the holographic MCHM ₅	127
6.5	Top partners in holographic MCHM ₅	127
6.6	Higgs couplings to the top sector	133
6.6.1	Higgs differential distributions as a test of compositeness	135
6.7	Conclusions	136
7	Conclusion	139
7.1	Summary of the thesis	139
7.2	Directions for further study	140
7.2.1	A full classification of pGB potentials for inflation	140
7.2.2	A conclusive analysis of spectator fields during inflation	140
7.2.3	Tachyonic reheating after Goldstone Inflation	141
7.2.4	Electroweak Baryogenesis after Goldstone Inflation	141

LIST OF FIGURES

1.1	An illustration of the inflationary hierarchy problem	5
2.1	Predictions of Natural Inflation	29
2.2	Shape of the Extra-natural inflationary potential for different particle content . . .	33
2.3	Predictions of Extra-natural Inflation for different choices of particle content . . .	34
2.4	n_s - r plot for Composite Higgs-like Inflation	38
2.7	f - n_s plot for Composite Higgs-like Inflation	39
2.5	Form of the potential for Composite Higgs-like Inflation	39
2.6	n_s - r plot for Composite Higgs-like Inflation	39
2.8	Predictions of vanilla Natural Inflation with non-renormalizable corrections . . .	42
2.9	Maximal tensor to scalar ratio in vanilla Natural Inflation with non-renormalizable corrections	43
3.1	Subgroups of a global $SO(N)$ symmetry	50
3.2	Shape of the inflaton potential (3.34)	57
3.3	Inflationary predictions of the model (3.34)	58
3.4	Fine-tuning of the parameters in (3.34)	59
3.5	Sound speed predictions of (3.34)	61
3.6	Goldstone quartic interactions in (3.93)	70
4.1	Mass hierarchy in Goldstone Inflation	74
4.2	Form of the inflationary potential in the $SO(6)/SO(5)$ coset	82
4.3	Predictions of the model in the n_s - r plane	84
4.4	Fine-tuning of the $SO(6)/SO(5)$ potential	84
4.5	Matching of the reheating parameters to an exact numerical expansion	88
4.6	Inflaton-Higgs couplings in $SO(6)/SO(5)$	90
4.7	Schematic illustration of Higgs-inflaton interactions	95
4.8	Present and future 95% C.L. exclusion limits in the (m_η, c_3) plane	98

5.1	Models of the $SO(n, 1)/SO(n)$ coset	108
5.2	Mapping of transformations between models of $SO(n, 1)/SO(n)$, in two dimensions	109
5.3	In red: inflationary predictions of a model based on $SO(n, 1)/SO(n)$ in the $n_s - r$ plane	113
6.1	Correlation between c_u and $\ln(\Omega)$ when $ m_u < 1.4$	129
6.2	Correlation between c_u and $\ln(\Omega)$ when $ m_u > 1.4$	129
6.3	Correlation between c_u and the top partner masses when $ m_u < 1.4$	129
6.4	Correlation between c_u and the top partner masses when $ m_u > 1.4$	129
6.5	Correlation between s_h and the top partner masses when $ m_u < 1.4$	130
6.6	Correlation between s_h and the top partner masses when $ m_u > 1.4$	130
6.7	Dependence of the value of s_h on fermion masses	131
6.8	Mass scan of top partner for $c_q = 0.4$	131
6.9	Mass scan of top partner for $c_q = 0.2$	131
6.10	Scan of the relation (6.25) for $c_q = 0.4$	132
6.11	Scan of the relation (6.25) for $c_q = 0.2$	132
6.12	Scan of Δ_{BG} from (6.26) plotted against c_u and $\ln \Omega$	133
6.13	Profile contributions to the Yukawa coupling	134
6.14	Profile contributions to the Yukawa coupling plotted against ATLAS data	135
6.15	Momentum dependence of the form factor for the $Ht_L t_R$ coupling	136

INTRODUCTION

1.1 PRELUDE

The measurements of temperature fluctuations in the Cosmic Microwave Background (CMB) by COBE, WMAP, and Planck [1]–[3] have marked the advent of precision cosmology: physicists proposing models for the Early Universe now have experimental data to test their predictions. The energy scale associated with the CMB (the surface at which photons last scattered) is model dependent, but typically lies around $10^{14} - 10^{15}$ GeV for successful models (with the highest Bayesian likelihood [4]). Experimental access to a very different spectrum of energy scales comes from particle colliders, with the discovery of the Higgs boson [5], [6] at 125.09 ± 0.24 GeV [7] thus far its latest triumph.

Perhaps the biggest challenge in modern particle physics is to bridge the large energetic gap between these different data sets. Certainly, this gap can be utilized to separate the fields of particle physics and cosmology, by integrating out the heavy degrees of freedom associated with the Early Universe, characterizing the success of Effective Field Theories (EFTs) as accurate descriptions of the Late Universe and collider physics. Such EFTs only require knowledge of the low energy field content, and parametrize the (undetermined) UV theory in terms of an operator expansion in inverse powers of the scale at which the UV processes occur. But although EFTs have shown to be very successful descriptions within their restricted domains of validity, there remain theoretical problems with large gaps between energy scales. This is because unless protected by a symmetry, mass hierarchies between coupled physical theories tend to be flattened out by higher order quantum effects. Such effects give rise to associated *hierarchy problems* [8], [9], most familiarly occurring for ElectroWeak Symmetry Breaking (EWSB) and the Higgs boson mass, but also for inflation in the Early Universe (characterized by the Lyth bound and the η problem) [10], the Cosmological Constant [11], and the flavour sector of the Standard Model (SM) [12].

An approach to solving hierarchy problems is defined by the distinction of *technical natural-*

*ness*¹ as first defined by 't Hooft [13]. A model is deemed technically natural if its free parameters are insensitive to its quantum mechanical evolution over the full range of known energetic scales. The difficulty in finding solutions to hierarchy problems is exemplified by the fact that very few particle physics models capture both the Early Universe and physics at collider scales.

A further motivation for linking cosmological events comes from experimental verification. Although the data from the CMB can be seen as the most important boundary condition for Early Universe model building, the experimental information it offers is limited. The existing abundance of models of the Early Universe, and the lacking prospect of discriminating between them, have lessened the appetite for further contenders. An enhanced exposure to data would therefore be a desirable asset for a new class of models.

The efforts in this thesis are directed towards capturing different scales in unified models of particle physics. Linking cosmological events on a fundamental level is a theoretical challenge, which exposes the model builder to different experimental datasets. Hierarchies of scales can be generated dynamically, determined by the evolution of the symmetries of the interactions of fundamental particles. The lightness of Goldstone Bosons (GBs), degrees of freedom associated with the spontaneous breakdown of a symmetry upon evolving to a lower scale, as compared to the symmetry breaking scale, results in a gap of scales in the theory. Concurrently, the GB is insensitive to quantum corrections from above the scale of its emergence; and the resulting hierarchy is technically natural and radiatively stable.

It is evident that fine-tuning considerations constitute major challenges to such encompassing particle physics models. Boldly, however, I would argue that the precise numerical assessment and elimination of models based on fine-tuning is of limited meaning, when the EFTs do not address open UV problems. If the overarching goal of theoretical physics is to describe the complete cosmological evolution of the Universe, EFTs at different scales will eventually have to be coupled, and thus the associated hierarchy problems addressed. Advocating a focus on EFTs with limited energetic range (to keep numerical fine-tuning small) only promotes a stay of execution.

For example, in a future, complete theory (of everything), the physics of inflation (or alternative scenarios such as ekpyrosis) will inevitably have to be coupled to the particles of the SM. Thus a consideration of fine-tuning in models Beyond the SM (BSM) is necessarily incomplete without the inclusion of a source of fine-tuning from the microphysics in the Early Universe. Fine-tuning arguments organized around a single cosmological event may indeed be used as guiding principles, but cannot set the standard for the fine-tuning that arises in more encompassing models.

¹With the exception of the flavour hierarchies; which are technically stable (quantum corrections to the masses of flavour eigenstates do not have cut-off dependence).

1.2 HIERARCHY PROBLEMS

1.2.1 A PARADIGM

The radiative instability of fundamental scalars has plagued the theoretical physics community for almost four decades: the original realization that fundamental scalars are always accompanied by quadratic mass divergences has been attributed to Kenneth Wilson in 1978 [9]. Besides aesthetic considerations, the search for "naturalness" stipulates one (naively uncontroversial) requirement for theories of new physics. Qualitatively,

The experimental predictions of a theory should be stable when its (dimensionless) input parameters are varied by a small amount.²

With few other theoretical guiding principles in the ambitious quest of discovering how nature works at unobserved energies, reasoning along these lines has developed itself into the most important corner-stone for model building.

The hierarchies that will be discussed in this thesis are *technically unnatural*. This means that they can be formulated in terms of a small parameter in the classical theory, such as a ratio of energy scales, which is no longer expected to be small when quantum corrections are taken into account. Thus the experimental confirmation of the smallness of this parameter (and equivalently the hierarchy of scales), while unproblematic classically, points to an issue with the full quantum theory.

An insightful way to see if a theory is *technically natural*, as identified by 't Hooft [13], is by identifying whether setting the small parameter to zero enlarges its symmetry content. If that is the case the parameter has arisen from the scale of the symmetry breaking, and the theory has a limited range of validity; in particular, it will be insensitive to effects from higher scales. If that is not the case, it is impossible to satisfy the naturalness criterium as defined above. Notable examples of such hierarchy problems in theoretical physics include:³

- *The Cosmological Constant problem*: the measured accelerated expansion of the Universe [14] suggests a small cosmological constant, of order 10^{-47} GeV^4 (or 3×10^{-122} in reduced Planck units). However, a (quantum-mechanical) computation of the zero-point energies of the known components of the Universe points to a large cosmological constant, at least of the order M_p^4 . The discrepancy of order $O(120)$ between the theoretical and experimental

²"Stable" here means "not subject to large variation".

³This is not meant to be an exhaustive list.

findings arguably constitutes the most prominent theoretical question today. It is a thorn in the eyes of the community, ever since it came into existence as Einstein's "blunder", and has appropriately been described "the worst theoretical prediction in the history of physics" in a textbook [15].

- *The strong CP problem*: the QCD θ -parameter is experimentally found to be very small, $\theta < 10^{-104}$. Unless forbidden by a currently unknown symmetry, such a small value is unnatural. Since CP is broken maximally by the weak interaction, it is surprising that it may be conserved by the strong interaction. In particular, the breaking of chiral symmetry and instanton effects both contribute to a non-zero θ .
- *The Electroweak Hierarchy Problem* (or simply: "the hierarchy problem" in the literature): the lightness of the Higgs boson, as confirmed by experiments, is in tension with theoretical predictions of radiative corrections to its mass from loops of Standard Model particles. Such corrections, in particular from the Standard Model top-quark, will be of order of the cut-off scale of the theory, which in the absence of new physics is given by the Planck scale. The discrepancy between the Higgs boson mass and the Planck mass has provided a popular challenge for model building, possibly fuelled by the prospect of access to detailed experimental tests in the near future.

In this thesis, I will also discuss what can be called the *hierarchy problem of inflation*: the flatness of the inflationary potential against radiative corrections. For an effectively single field model, this can be illustrated by the tension between the Lyth bound [16],

$$\Delta\phi \sim \left(\frac{r}{0.002}\right)^{1/2} \left(\frac{N}{60}\right) M_P \quad (1.1)$$

and the measurements of the CMB anisotropies [14],

$$\Lambda_{inf}^4 = \left(2.2 \times 10^{16} \text{ GeV}\right)^4 \left(\frac{r}{0.2}\right) \quad (1.2)$$

The Lyth bound is a measure of the field excursion necessary to solve the problems inflation was invented to solve, given in terms of the number of e-foldings N . When one plots the scalar potential of the inflaton, the Lyth bound and the scale Λ_{inf} constitute the vertical and the horizontal axes respectively (Fig.1.1). For good measure, one may appreciate that the axes are of the same order only for very small tensor-to-scalar ratio $r < 10^{-13}$, pointing to a very flat potential. While such a stretched inflationary model can be a feature of a theory, the challenge of the inflationary hierarchy problem is to ensure that this flatness is stable against radiative corrections.

⁴From measurements of the electric dipole moments of hadrons and nuclei.

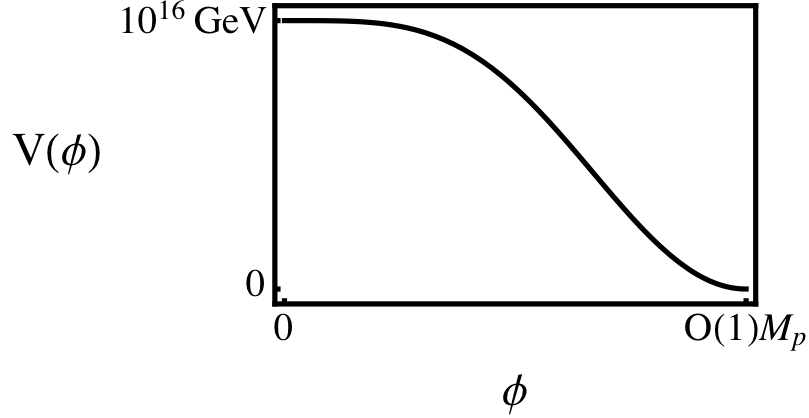


Figure 1.1: Illustration of the hierarchy problem of inflation.

The hierarchy problem of inflation can be described in the more familiar form of an unstable mass hierarchy: the well known η -problem, where η is the second slow-roll parameter,

$$\eta = M_p^2 \frac{V''(\phi)}{V(\phi)} \sim \frac{m_\phi^2}{H^2} \ll 1. \quad (1.3)$$

The inflationary predictions of the slow-roll paradigm crucially depend on the smallness of η (and the other the slow-roll parameters), and therefore on the relative lightness of the inflaton. The problem is that one generically expects higher dimensional corrections to the inflation potential, induced either by the inflaton's self couplings or couplings to new physics. They can be cast in the form

$$\frac{c_n}{M_p^{n-4}} \phi^n = c_n \left(\frac{\phi^{n-2}}{M_p^{n-4}} \right) \phi^2, \quad (1.4)$$

and as one typically expects that

$$\phi \sim \Delta\phi \sim M_p \quad (1.5)$$

in generic inflation models, it is clear that these contributions are unsuppressed, and will ruin the lightness of the inflaton and the inflationary predictions. Therefore any plausible inflation model must address the η -problem in some way.

Solving hierarchy problems, particularly the Electroweak hierarchy problem and the cosmological constant problem, has been the object of the creativity and intellect of a generation of physicists. Proposed solutions may roughly be divided into two main groups:⁵ solutions that propose a new symmetry, which stabilizes the hierarchy between energy scales, and those that propose that hierarchies are dynamically generated. In this thesis we will undemocratically focus on the latter category.

⁵Of course, different authors have proposed solutions that fall in between, or completely out of these categories. Among these are recent proposal such as relaxions [17], and the Higgsplasion [18].

1.2.2 DYNAMICAL SOLUTIONS TO HIERARCHY PROBLEMS

The key notion of a class of solutions to hierarchy problems is that large hierarchies between scales may be stable against radiative corrections, if they were generated dynamically. The basic ingredient of such a dynamical generation of scales is the existence of a *approximate* global symmetry, broken spontaneously at some energy scale. Hence, by Noether's and Goldstone's theorem, one expects a new scalar degree of freedom below that scale. But because the global symmetry was not exact, the scalar generated is a pseudo-Goldstone boson (pGB).

A pGB, as opposed to an exact Goldstone boson, may acquire a potential at the loop level. However, the parameters in a pGB potential are protected from large corrections, as they are insensitive to virtual effects above the cutoff scale of the effective theory - the scale at which the approximate global symmetry spontaneously broke. In the low energy theory, the Goldstone boson has a shift symmetry, that is, the Lagrangian is invariant under

$$\Phi \rightarrow \Phi + C \quad (1.6)$$

where C is a constant. For exact Goldstone bosons C is a continuous parameter; for pseudo-Goldstone bosons it can take on discrete values. While the shift symmetry does not necessarily imply that the scalar potential is bounded in energy, it forbids the existence of effective operators proportional to powers of the field.

Let us now consider the effective field theory (EFT) of the pGB, originated by the breaking of a global symmetry \mathcal{G} to a subgroup \mathcal{H} at the scale f . An EFT is characterized by the field content and symmetries of the low energy theory - the SM - and captures the effect of the UV theory in an operator expansion in powers of the energy scale at which processes of interest occur. These will be suppressed by a cut-off scale, at which one expects new physics to appear: in this case, the symmetry breaking scale f . The EFT Lagrangian for pGBs can be derived most easily using a 'trick': one first assumes that the full global symmetry \mathcal{G} is gauged, such that all physical fields fall into complete representations of the group. The Goldstone bosons will couple non-linearly to such representations, as we will see below. Upon writing down all structures that are invariant under \mathcal{G} , one can switch off the unphysical fields to find the low energy EFT Lagrangian.

We will denote the generators of \mathcal{G} as $T^a \in H$ and $T^{\hat{a}}$, where $T^{\hat{a}}$ are the broken generators. The resulting pGBs are associated with these broken generators, and we will assume in this thesis that the inflaton field and Higgs field are linear combinations of them. The mass and couplings of the pGBs depend on the explicit breaking of the global symmetry. The Goldstone bosons couple non-linearly, as part of the Σ field,

$$\Sigma(x) = \Sigma_0 e^{i\Pi(x)/f} \text{ where } \Pi = T^{\hat{a}} \Phi^{\hat{a}} \quad (1.7)$$

where $\Sigma_0 = \langle \Sigma \rangle$ contains the symmetry breaking vacuum expectation value, and $T^{\hat{a}}$ are the broken generators of the global symmetry \mathcal{G} . The exponential form in which $\Phi^{\hat{a}}$ appears exemplifies that its potential will be forbidden by the shift symmetry, Eq. 1.6: here, discrete shifts of $2\pi f$ leave the Lagrangian invariant.

One can proceed to write down the terms that are invariant under the global symmetry. For gauge fields, these are given by,

$$\mathcal{L}_{gauge} = \frac{1}{2} P^{\mu\nu} \left(\Pi_0(p) \text{Tr}(A_\mu A_\nu) + \Pi_1(p) \Sigma A_\mu A_\nu \Sigma^T \right) \quad (1.8)$$

where $P^{\mu\nu} = (\eta^{\mu\nu} - q^\mu q^\nu / q^2)$ projects out the transverse gauge fields.

The form factors Π_i parameterize our ignorance about the strongly coupled UV-theory. In analogy with QCD and technicolour, they can be seen to be proportional to towers of meson exchange.⁶ The Π_0 are related to the currents of the unbroken group (such that one may redefine $\Pi_0 = \Pi_a$)

$$(P_T)^{\mu\nu} \Pi_a(q^2) = \langle T \{ J_a^\mu(q) J_a^\nu(-q) \} \rangle = (q^2 \eta^{\mu\nu} - q^\mu q^\nu) \sum_n \frac{f_{\rho_n}^2}{q^2 - m_{\rho_n}^2} \quad (1.9)$$

where J_a^μ are the currents of the unbroken group, and m_{ρ_n} the mass of the n^{th} meson. The constant $f_{\rho_n} = \langle 0 | J | n \rangle$ gives the amplitude for creating the n^{th} meson from the vacuum. It is related to the spectral density (or density of states) of the theory and is also referred to as the decay constant. A linear combination of Π_0 and Π_1 will be related to the currents of the broken part of the gauge group (such that one may redefine $\Pi_{\hat{a}} = \Pi_0 + \frac{\Pi_1}{2}$),

$$(P_T)^{\mu\nu} \Pi_{\hat{a}}(q^2) = \langle T \{ J_{\hat{a}}^\mu(q) J_{\hat{a}}^\nu(-q) \} \rangle = (q^2 \eta^{\mu\nu} - q^\mu q^\nu) \sum_n \left(\frac{f_{a_n}^2}{q^2 - m_{a_n}^2} + \frac{f^2}{2q^2} \right) \quad (1.10)$$

The Goldstone bosons are excited by $\Pi_{\hat{a}}$, and the fact that this expression does not vanish at $q = 0$ ensures the mass for the vector bosons.

Now one can obtain an effective Lagrangian by expanding the form factors for low momenta (compared to the resonance masses), keeping only the physical fields. From the effective Lagrangian one can read of the gauge boson masses, as well as the scalar-gauge couplings.

Partial compositeness

As long as the global symmetry \mathcal{G} is not explicitly broken (as well as spontaneously), the goldstone bosons will not have a potential at any order in perturbation theory. An explicit breaking can be

⁶The pGBs in QCD are pions; in the chiral limit, pions are exact Goldstone bosons, and the charged pions get a radiative potential from loops of photons. Experimentally, this radiatively generated mass of the charged pions is consistent with the measurement of the difference $m_\pm^2 - m_0^2$.

induced by interactions between external fields and the states of the strong sector. In Composite Higgs models, this is achieved through the mechanism of partial compositeness, in which gauge fields and fermions mix with the composite states of the strong sector, analogously to photon- ρ mixing in QCD. By integrating out the dynamics of the strong sector it is possible to find the effective Lagrangian for the external fields.

As is intuitive, the contribution from $SU(2)_L \times U(1)$ gauge bosons to the potential will not break electroweak symmetry, as it will align in an $SU(2)_L \times U(1)$ preserving manner.⁷ The misaligned contribution can however come from fermion loops, most importantly the top quark, as it is heaviest (and thus has the strongest coupling to the Higgs). In partial compositeness fermions couple linearly to the strong sector: $\mathcal{L} \ni \lambda \psi O$ where ψ is an SM fermion field and O an operator of the strong sector with the right quantum numbers.

Similar to the previous sector, one can employ a "trick" to derive the effective potential: to uplift the fermion states to fill complete representations of the global gauge group \mathcal{G} , such that the Lagrangian can be written in a \mathcal{G} invariant way. Besides the SM fields, the representations are filled with non-dynamical (auxiliary) spurion fields. For instance for the Minimal Composite Higgs Model (MCHM) $\mathcal{G} = SO(5)$, which has a spinorial representation $4 = (2, 1) + (1, 2)$ (a Dirac spinor in 5D is composed of two Weyl spinors in 4D⁸) [19], one can write

$$\Psi_q = \begin{bmatrix} q_L \\ \cdot \end{bmatrix} \quad \Psi_u = \begin{bmatrix} \cdot \\ u_R \\ \cdot \end{bmatrix} \quad \Psi_d = \begin{bmatrix} \cdot \\ \cdot \\ d_R \end{bmatrix} \quad (1.11)$$

where the dots should be filled by spurion singlets and doublets. The incompleteness of these representations signifies the explicit breaking of the global $SO(5)$, and (as is seen below) contributes to the a scalar potential via fermion loops.

Now one can write down the part of the Lagrangian that contains the interactions between fermions and Goldstone bosons. The form of this Lagrangian will depend on the choice of fermion representation; here I will give the two simplest examples, the fundamental and the spinorial representation of \mathcal{G} . It is usually sufficient to consider only the contributions of the fermion generation that couples most strongly to the scalar sector, as it will give the dominant contribution to the potential, but the generalization is straightforward. The spinorial representation (such as the MCHM multiplets above), at the quadratic order in the fermion fields and treating Σ as a constant

⁷The reader is referred to [19],[20] or [21] for an explicit computation.

⁸Technically this is a statement about the Lorentz group $SO(4, 1)$ and $SO(3, 1)$, but it is true for $SO(5)$ and $SO(4)$ in much the same way.

background, gives

$$\mathcal{L}_{quarks} = \sum_{r=L,R} \bar{\Psi}_r \not{p} \left(\Pi_0^r(p) + \Pi_1^r(p) \Gamma^i \Sigma_i \right) \Psi_r + \bar{\Psi}_L \left(M_0(p) + M_1(p) \Gamma^j \Sigma_j \right) \Psi_R \quad (1.12)$$

Here $i = 1, 2, \dots, d$ is the \mathcal{G} index (remember that Σ transforms as a vector under \mathcal{G} , $d = \dim \mathcal{G}$) and Γ^i are higher dimensional gamma matrices. Contrarily, fermions in the fundamental representation couple as

$$\mathcal{L}_{quarks} = \sum_{r=L,R} \bar{\Psi}_r^i \not{p} \left[\Pi_0^r(p) \delta_{ij} + \Pi_1^r(p) \Sigma_i \Sigma_j \right] \Psi_r^j + M(p) \bar{\Psi}_L^i \Sigma_i \Sigma_j \Psi_R^j + h.c. , \quad (1.13)$$

As above, the form factors Π_i encode the strong dynamics, and cannot be determined perturbatively. However, there are clues: their momentum scaling can be determined, and their poles give the spectrum of the fermions of the strong sector, as above for gauge fields.

From \mathcal{L}_{quarks} one can find the scalar potential using the 1-loop Coleman Weinberg mechanism [22]. The (1-loop) Coleman Weinberg mechanism resums the series of 1-loop diagrams with an arbitrary number of external scalar legs, with zero external momentum:

$$V(h) = - \sum_{n=0}^{\infty} \frac{1}{n!} \Gamma(0, \dots, 0) h^n$$

where $\Gamma(\Phi_c)$ is the Legendre transform of the generating functional $W(J)$ of the connected diagrams ($Z[J] = e^{iW(J)/\hbar}$) and Φ_c is the 1PI generating functional. For the MCHM Lagrangian, the Coleman Weinberg potential from loops of top quarks is given by [19],

$$V(h) = -2N_c \int \frac{d^4 p}{(2\pi)^4} \left(2 \log \left(1 + \frac{\Pi_1^{tL}}{\Pi_0^{tL}} \cos \frac{h}{f} \right) + \log \left(1 - \frac{\Pi_1^{tR}}{\Pi_0^{tR}} \cos \frac{h}{f} \right) \right. \\ \left. \log \left(1 - \frac{(M_1 \sin(h/f))^2}{p^2 (\Pi_0^{tL} + \Pi_1^{tL} \cos(h/f)) (\Pi_0^{tR} + \Pi_1^{tR} \cos(h/f))} \right) \right) \quad (1.14)$$

$$\approx \alpha \cos \frac{h}{f} - \beta \sin^2 \frac{h}{f} \quad (1.15)$$

where the last equality stems from expanding the logarithms to first order. This is a good approximation in the assumption that the (ratios of) form factors decrease fast enough at high momentum.

In models with both the quartic coupling and the mass generated at the same order (as above) one requires an amount of tuning between the parameters to match the measured Higgs mass.⁹ To obtain a fully natural Higgs potential, one may think of inducing a tree-level quartic coupling, while only inducing a loop-level mass term. Models in which this is realized are called "Little Higgs" models [24]–[32]. Generically this tree-level term arises from mixing with an elementary scalar ϕ , which (unlike the Higgs boson) is not protected by symmetry. It therefore has a mass of

⁹Models with this tuning were classified as "Holographic" in [23]. Holographic Composite Higgs models are the subject of chapter 6 of this thesis.

order of the cutoff scale and is integrated out in the effective theory. If this elementary scalar had a bilinear coupling to the composite Higgs, $O_\phi O_\Sigma^2$ (where O_X creates X), an effective tree-level quartic coupling for the Higgs can arise. By choosing the quantum numbers of ϕ carefully, one can avoid a tree level mass term for h . Unfortunately, in fully natural Little Higgs models the Higgs mass generically too high: $m_h = 2v\sqrt{\lambda} \sim 2vg_{SM} \sim 500$ GeV, such that one cannot avoid some tuning at a later stage. Although heavily constrained, in some region of the parameter space Little Higgs models are still compatible with the Higgs mass and electroweak precision data [33].

1.3 THEORETICAL INPUT FOR MODEL BUILDING

There is no recipe to construct a model that addresses a hierarchy problem. That is lucky, because theoretical physicists tend to hate recipes; it is why many skipped as many undergraduate lab courses as they could.¹⁰ Nevertheless, there is a theoretical toolkit to be aware of; and a generic range of minimal conditions to fulfil. This section will survey some of these (often unspoken) theoretical rules that underly the models in this thesis.

1.3.1 INTERNAL CONSISTENCY

A self-consistent quantum field theory satisfies a host of theoretical constraints. Of particular interest in the current thesis¹¹ are the non-existence of negative energy (ghost) states, the conservation of (perturbative) unitarity, and the Weak Energy Condition (WEC).

Unless called upon as a theoretical device (such as in the case of "good" Faddeev-Popov ghosts), theories should not contain ghost fields. Usually, this is a statement of the signature of the metric tensor: for example, for a scalar field ϕ , the kinetic term $\dot{\phi}^2$ should have a positive definite coefficient. It also places a degeneracy condition on higher derivative field theories; the equations of motion need to be (equivalent to) first order [34], otherwise an instability characterized by an Ostrogradsky ghosts occurs [35].

For the model building in this thesis, the no-ghost condition warrants special consideration of theories with a negatively curved internal space. In such models the presence or absence of ghosts is more obvious in some coordinates than in others. In particular, field spaces based on

¹⁰The author pleads guilty.

¹¹Without claiming that this is an exhaustive list of theoretical input even for the present works.

non-compact internal symmetries may appear to have ghost terms for scalar fields, such as

$$\mathcal{L} \ni (\partial_\mu \phi_0)^2 - (\partial_\mu \phi_i)^2 \quad (1.16)$$

but such terms will be eliminated when the non-compact symmetry is broken to its maximal compact subgroup, a fact that has long been used by the supergravity community [36]. We will see examples of this in the chapters below.

Perturbative unitarity is a well defined concept for model building. It is expressed in terms of the scattering S-matrix, which gives the evolution of states from $t = -\infty$ to $t = +\infty$, decomposed as

$$S = 1 + iT \quad (1.17)$$

Unitarity then prescribes $S^\dagger S = 1$, which leads to the optical theorem for the partial wave components T_{ii} ;

$$(\text{Re}T_{ii})^2 + \left(\text{Im}T_{ii} - \frac{1}{2}\right)^2 = \frac{1}{2}. \quad (1.18)$$

This can be interpreted geometrically in that the eigenvalues of the scattering matrix are constrained to lie on the Argand circle (for elastic scattering) or inside it (for inelastic scattering).

The optical theorem holds for exact matrix elements and not order-by-order in perturbation theory. In particular, it is noted that the amplitude of tree level processes necessarily is real, and therefore violates the optical theorem. To avoid having to calculate the the contributions of all orders in perturbation theory, one can rely on the weaker statement: a theory is likely to have issues with perturbative unitarity if the real and imaginary parts of the partial wave amplitudes are of the same order. This may give an upper bound to the range of validity of the EFT.

The Higgs particle provides a minimal solution to the violation of perturbative unitarity by longitudinally polarized modes of the W and Z gauge bosons. Without the Higgs mechanism, the four point function of these vector bosons is expected to grow quadratically with energy. Any model that aims to replace the Higgs particle of the SM, should address the question of perturbative unitarity in vector boson scattering. In Composite Higgs models, the pGB Higgs unitarizes scattering amplitudes partially, that is, up to the scale

$$\Lambda \approx \frac{4\pi f}{\sqrt{\xi}} \quad (1.19)$$

Above that scale, strong resonances are expected to come in.

The WEC implies that the energy in the inflaton field, and in particular the scalar potential, should be positive definite. In some popular models of inflation, such as the vanilla Natural Inflation [37], this observation forces the authors to add a phenomenological constant to the potential. Of course, since such a constant serves as a vacuum energy and is therefore formally part of the

Cosmological Constant problem, an explanation for its necessity is often taken to be outside of the scope of the analysis. Notwithstanding, it will be seen that this thesis contains models that do not require the addition of a constant.

1.3.2 FINE-TUNING

While different ways of quantifying the naturalness of a model have been adopted, the most widely adopted criterium was defined by Barbieri and Giudice [38], and reads

$$\text{Fine-tuning} = \left| \frac{\Delta y/y}{\Delta x/x_0} \right| = \left| \frac{\partial \ln y}{\partial \ln x} \right| \quad (1.20)$$

where x_0 is an input parameter of the Lagrangian evaluated at an appropriate scale¹², and where y is the model's prediction, for instance a coupling or a mass. While the usefulness of this parameter, and in particular the value of a meaningful upper bound for the naturalness criterium, can be debated, the definition above is used most widely across the literature and thus lends itself best to model comparison for the purposes of this thesis.

1.3.3 REPRODUCING THE STANDARD MODEL

As the Standard Model is in excellent agreement with collider and low energy data, it can be interpreted as the low energy effective theory of any model for the Early Universe. It may seem very obvious that candidate theories should produce (conceivably only) the Standard Model particle content and couplings at low energy, but it is an important boundary condition which has the power to rule out potential models¹³. For example, it is generically difficult in supersymmetric models to find the measured Higgs mass without light stops and gluinos.

Any complete UV theory should therefore at least contain the Standard Model group structure and quantum numbers. For composite models involving the Higgs boson, this means that the global symmetry should at least contain $SU(2)_L \times U(1)$; or more preferably, the custodial $SU(2)_L \times SU(2)_R$ which protects the electroweak parameters as we will discuss below.

¹²For models with Goldstone bosons this will be given by the compositeness scale f .

¹³Any extra light particles are necessarily very weakly coupled to the SM, and should evade cosmological bounds as well. For example, extra light particles may impact on inflation [39], give rise to spectral distortions [40], Dark Matter direct detection [41], galaxy rotation curves [42], or are constraint by BBN [43]

1.4 EXPERIMENTAL CONSTRAINTS

A good particle physics model is in a constant conversation with experimental data. While the chronicles describe an era in which science worked through a linear sequence (model \rightarrow hypothesis \rightarrow test), the modern particle physicist is motivated by, aware of, and adaptive to new experimental results. Experiments have changed, too, and are not designed to test a single prediction, but test many different theories at once.

This section will give an overview - again, far from exhaustive, but relevant to the present effort - of experimental data to test theoretical models against. This section is subdivided into two parts: the data acquired by collider experiments and the cosmological data from the Cosmic Microwave Background.

1.4.1 COLLIDER BOUNDS

Electroweak precision tests

Electroweak Precision tests (EWPT) are powerful tests to distinguish electroweak BSM models from the Standard Model, and have led to the demise of (vanilla) Technicolor [44]. Deviations from the Standard Model are effectively captured by the Peskin-Takeuchi S and T parameters [45],¹⁴

The S parameter gives the difference between the number of left- and- right handed fermions charged under weak isospin,

$$\alpha S = 4s_w^2 c_w^2 \frac{\partial}{\partial q^2} \left(\Pi_{ZZ}(0) - \Pi_{\gamma\gamma}(0) - \frac{c_w^2 - s_w^2}{s_w c_w} \Pi_{Z\gamma}(0) \right) \quad (1.21)$$

where α is the fine structure constant. Theories that add extra (chiral) fermion doublets are strongly constrained by the upper bounds on S . The T parameter is a measure of isospin violation in the weak gauge bosons,

$$\alpha T = \Delta\rho = \frac{\Pi_{WW}(0)}{M_W^2} - \frac{\Pi_{ZZ}(0)}{M_Z^2} \quad (1.22)$$

where $\rho \equiv \frac{m_W^2}{m_Z^2 \cos^2 \theta_W}$ (θ_W is the Weinberg angle).¹⁵ Equivalently, one can define the experimental parameters ϵ_i , linear combinations and shifts of the Peskin-Takeuchi parameters [46].

¹⁴The U parameter is subdominant, as the first operator to contribute to it is at least dimension-8. It is therefore not usually applied to constrain BSM models.

¹⁵In the SM, $\rho = 1$.

As mentioned above, a straightforward way to protect the T-parameter in BSM models is to postulate the UV theory to be (approximately) invariant under $SU(2)_L \times SU(2)_R$ under which the Higgs field transforms as a bidoublet [47].

Top partner searches

In Composite Higgs models with partial compositeness, the SM quarks couple linearly to the strong sector, through

$$\mathcal{L} \ni \lambda \bar{Q}_L O + \text{h.c.} \quad (1.23)$$

where O is an operator of the UV strong sector. This opens up the opportunity to produce top partners directly at colliders.

There are several ways in which top partners can be produced in collider experiments. Because they necessarily carry QCD charge, as can be seen from the mixing (1.23), they can be pair produced in QCD interactions. The cross sections of such interactions are functions of the top partner mass and known parameters [48]. They can also be produced in association with a SM top or bottom quark, via an interaction with a (SM) vector boson.

Top partners can decay to a top quark (or a lighter top partner) and a SM vector boson. This gives a particularly clean signal for the lightest top partner decay, with an associated top quark from either the single or the double production channel.

It might be that new states are too heavy to be directly produced. In that case, their effects might be detected from the deviations from the SM predictions for the top-quark couplings to other SM particles.

Higgs couplings

In Composite Higgs models, it is useful to expand around the Higgs vacuum expectation value v . This allows for a comparison between models using the parameters a , b , and c in the following expansion

$$\begin{aligned} \mathcal{L}_{\text{eff}} = & \frac{1}{2}(\partial_\mu h)^2 + \frac{v^2}{4} \text{Tr} \left[(D_\mu \Sigma)^\dagger (D_\mu \Sigma) \right] \left(1 + 2a \frac{h}{v} + b \frac{h^2}{v^2} + \dots \right) \\ & - \frac{v}{\sqrt{2}} \sum_{i,j} \left(\bar{u}_L^{(i)} d_L^{(i)} \right) \Sigma \left(1 + c \frac{h}{v} + \dots \right) \left(\lambda_{ij}^u u_R^{(j)}, \lambda_{ij}^d d_R^{(j)} \right)^T + V(h) \end{aligned} \quad (1.24)$$

where for the SM $a = b = c = 1$.

Experimentally, the deviations of the Higgs couplings from the standard model are expressed in terms of κ -factors,

$$\kappa_i^2 = \frac{\sigma_i}{\sigma_{SM}} \quad (1.25)$$

where σ_i is the cross section for a particular process in the BSM model, and σ_{SM} the corresponding cross section in the Standard Model. For example, the Higgs decaying to vector bosons is captured by κ_V^2 , which for generic composite models is given by [49]

$$\kappa_V = a = \sqrt{1 - \chi} \quad (1.26)$$

where $\chi = v^2/f^2$.

The deviation from the SM value of the Yukawa coupling of the top quark is described by the parameter κ_t . The measurement of the $t\bar{t}H$ coupling is an experimental priority and is expected to be constrained to $O(10\%)$ with the Large Hadron Collider High-Luminosity Upgrade data [50]. Because the largest contribution to the Electroweak hierarchy problem comes from this coupling, this measurement can be seen as its most important probe. In this thesis, prospects for holographic Composite Higgs models are discussed in section 6.6.

If the Higgs couples to an extended scalar sector, an array of further constraints applies [51]. For the purposes of this thesis, we will consider the inflaton to be an $SU(2)$ scalar. The most important constraint in this case comes from mass mixing in the scalar sector after electroweak symmetry breaking, in the presence of the trilinear coupling $c_3\phi h^2$, where ϕ is the inflaton and h is the Higgs. Collider constraints from this effect are discussed in section 4.5.

1.4.2 CMB DATA

The discovery of the cosmic microwave background (CMB) by Penzias and Wilson in 1965 [52] is often cited as the birth of modern cosmology. The promise of such a powerful probe of the early universe makes models falsifiable and cosmology a physical science. Alas, careful excavation has shown that the CMB is more featureless than we hoped and more perfect than we dreamed. The philosophical arguments¹⁶ for homogeneity and isotropy have been confirmed to an exceptional degree.

The cosmic microwave background consists of photons from the last scattering surface, at the time of recombination of the light elements, and as such is the earliest directly observable probe of our cosmic history. The spectrum of the CMB is consistent with a black body at a temperature of 2.725 K [53], and is almost uniform in every direction, with small anisotropies varying with the size of the patch one considers. These small temperature fluctuations encode a wealth of information about our universe.

The primary anisotropy is given by the two point temperature correlation function, or equivalently the angular temperature distribution of the CMB, which probes the geometry and the

¹⁶Simplicity, and the belief that the Earth does not occupy a "special" position.

dynamics of the (Early) Universe. The late time anisotropy, given by spectral distortions and frequency perturbations, probes the thermal history. In this thesis we will mainly be concerned with the primary anisotropy as encapsulated in the CMB power spectrum, but we recognize that a complete theory should address reheating, baryogenesis, and the electroweak phase transition as well and as such be consistent with the late time anisotropy.

The CMB power spectrum

The scalar power spectrum (expanded on super-Hubble scales) reads,

$$\mathcal{P}_R(k) = \frac{k^3}{2\pi^2} |\mathcal{R}_k|^2 \quad (1.27)$$

$$= A_s \left(\frac{k}{k_*} \right)^{(n_s-1) + \frac{1}{2} dn_s / d \ln k \ln(k/k_*) + \frac{1}{6} d^2 n_s / d \ln k^2 (\ln(k/k_*))^2 + \dots} \quad (1.28)$$

It encodes the two-point function of CMB scalar modes, in Fourier space. Similarly, the tensor power spectrum is given by

$$\mathcal{P}_t(k) = A_t \left(\frac{k}{k_*} \right)^{n_t + \frac{1}{2} dn_t / d \ln k \ln(k/k_*) + \frac{1}{6} d^2 n_t / d \ln k^2 (\ln(k/k_*))^2 + \dots} \quad (1.29)$$

where the difference in normalization between n_s and n_t is by convention.

To great disappointment of the community, the primordial information extracted from the CMB today can be summarized in three independent primordial numbers (and a multitude of constraints consistent with zero) [54]:

- The amplitude of the CMB power spectrum

$$\ln(10^{10} A_s) = 3.089 \pm 0.036 \quad (1.30)$$

which can be related to the scale of cosmic inflation, as in (1.2).

- The deviation from scale invariance, as expressed in the tilt of the power spectrum,

$$n_s = 0.9655 \pm 0.0062 \quad (1.31)$$

which is a statement of the shape of the inflaton potential and has ruled out some proposals (such as a class of models based on string moduli fields), but is consistent with a multitude.

- The amount of inflation, captured by the number of e-foldings before the end of inflation, at which the pivot scale k_* exits the Hubble horizon,

$$N = \int_{t_i}^{t_e} H(t) dt \quad (1.32)$$

of which no precise measurement exists, but which sits roughly between 50 and 60.

All quoted measurements are at the pivot scale by $k_* = a_* H_* = 0.05 \text{ Mpc}^{-1}$ (for TT modes) by the Planck collaboration [14], with error bars at at 68 % (or 1σ) confidence level.

Many other important parameters have been constraint with upper and lower bounds, but are still consistent with zero. Important examples include,

- The amount of primordial gravitational waves, as measured by the polarization of the CMB, and frequently normalized to the scalar power spectrum as expressed with the tensor-to-scalar ratio,

$$r = \frac{\mathcal{P}_t(k_*)}{\mathcal{P}_R(k_*)} < 0.11 \quad (1.33)$$

where the upper bound depends on polarization mask and prior choices.

- The non-Gaussianity of the spectrum, as expressed using the parameters f_{NL} and g_{NL} ¹⁷,

$$f_{NL}^{local} = 2.5 \pm 5.7 \quad (1.34)$$

$$g_{NL}^{local} = (-0.9 \pm 7.7) \times 10^4, \quad (1.35)$$

which measure the higher-order correlation functions (the bi- and- trispectrum respectively). These null results imply that the consistency with the concordance Λ CDM model is overwhelming, and that the seeds of structure formation were adiabatic and Gaussian. The results favour single field inflation models over multi-field models.

- The number of (extra) effective neutrinos species,

$$N_f = 3.15 \pm 0.23 \quad (1.36)$$

(compared to the SM value $N_f \approx 3.046$) points to a standard big bang nucleosynthesis (BBN) scenario with no extra light species.

- The running of the spectral tilt,

$$\frac{dn_s}{d \ln k} = -0.0084 \pm 0.0082 \quad (1.37)$$

favours simple slow roll models of inflation with a hierarchy of slow roll parameters.

- The fraction of primordial isocurvature modes,

$$\beta_{iso} = \frac{\mathcal{P}_S}{\mathcal{P}_R + \mathcal{P}_S} \leq O(10^{-3} - 10^{-1}) \quad (1.38)$$

¹⁷For a full definition the reader is referred to [55].

which measures the relative importance of fluctuations normal to the inflationary trajectory.¹⁸ Isocurvature modes can be correlated with adiabatic perturbations, and source non-gaussianity as measured by the parameters f_{NL} and g_{NL} above. As these fluctuations are only present for models in which other fields fluctuate, this measurement also favours the single field cases.

Again all quoted data from the pivot scale by $k_* = a_* H_* = 0.05 \text{ Mpc}^{-1}$ (for TT modes, with 1σ error bars) by the Planck collaboration [14], [56].

The lack of constraining data complicates the comparison between the wealth of inflationary models that exist in the literature. It has inspired authors to look for consistency relations (for instance [54]), encouraged meta studies (such as [57]), and statistical comparisons see for example [58]). The featurelessness of the CMB can be interpreted as a sign that inflation was driven by a very simple theory, with minimal field content. However, such an interpretation is mostly aesthetic, as the data is consistent with a plethora of (simple and less simple) models that reproduce the same phenomenology.

Spectral distortions

The late time anisotropy expresses itself in terms of distortions of the CMB spectrum. Such effects may occur when energy (in the form of matter, or as photons) is injected; or when energetic particles are produced. Interaction with the CMB photons will give rise to deviations from a perfect blackbody spectrum.

Spectral distortions can be parametrized in the y -type and the μ -type (and linear combinations). A y -distorted spectrum differs from a blackbody because of interactions with hot, isotropic, thermal electrons with particular Compton y -parameter; μ -type distortions can be captured by an effective chemical potential [59].

The type of distortion that is expected from an energy injection (or particle production) depends on the redshift at which the process occurs. At sufficiently high redshift, the photons can redistribute effectively to re-establish full thermodynamic equilibrium. Below this, the heating of CMB gives rise to a Bose-Einstein spectrum, and energy injections result in μ -distortions: of the form $n_x = 1/(e^{x+\mu(x)} - 1)$ where the chemical potential μ is a function of the frequency. At even lower redshift the thermalization cannot establish a Bose-Einstein spectrum, and energy injections contribute as $n_x = n_{x,0} + \Delta n_x(y)$ [60]. A measurement of a type of distortion may therefore place

¹⁸This is a model dependent measurement, with the strongest bound here corresponding to the "curvaton" scenario, in which the primordial perturbations are (in whole or in part) generated from isocurvature modes. That is, the adiabatic and isocurvature perturbations are fully (anti-) correlated.

limits on the time of the energy release, as μ -type can put a lower bound on the time of energy release, y -type distortions, an upper limit.

Thermalization of the CMB photons through processes like Bremsstrahlung and (double) Compton scattering may partially wash the spectral distortions out - but CMB constraints may still place tight limits on the Universe's thermal history. Recent experiments Planck and WMAP have been focussed on the angular distribution, such that the most recent measurements of the spectrum are from COBE/FIRAS [1]. Proposed experiments such as PIXIE and ASPERa are aimed at constraining the spectral distortions further and pose an interesting challenge for model building.

1.5 OUTLINE OF THIS THESIS

This thesis contains a collection of published work that was completed as part of my doctoral degree, which study pseudo-Goldstone Bosons as an answer to hierarchy problems in particle physics and cosmology. It is structured as follows:

- Chapter 2 contains [61], in which we argued that the flatness of the inflationary potential could be due to the inflaton's origin as a pGB,¹⁹ and tested a potential derived with EFT techniques against the CMB data. The merit of the paper was its generality: in particular, we included a variant of Extra-natural inflation [62] with bulk fermions, and its four dimensional duals, as well as a discussion of purely four dimensional models inspired by Composite Higgs physics. This later topic would be a first discussion of a class of natural inflation models that are sub-Planckian effective theories, in contrast to the original Natural Inflation.
- In [63], which is chapter 3, we further explored the symmetry arguments and the robustness against UV corrections of Goldstone Inflation (GI). Our setup involved a GB of the breaking $SO(5)/SO(4)$ which receives a potential from Coleman Weinberg contributions. Noticing that both bosonic and fermionic contributions are needed to build a successful inflationary model, we found that a potential flat enough for inflation implies that fermions have to be in a spinorial representation of the gauge group. This indicates that the symmetry breaking pattern giving rise to the Goldstone bosons is from an $SO(N)$ global group to its subgroup.

¹⁹This suggestion has priorly been made in different contexts, most notably in Natural Inflation, a model developed in the 90s [37].

As Goldstone bosons are expected to have strong momentum dependent self couplings, we noticed that the model may predict a low scale violation of perturbative unitarity or give rise to non-Gaussianities in the CMB. Upon confrontation with the data, we found that the model survives both these theoretical and experimental constraints. The information from inflationary constraints can be used to draw conclusions about the UV theory. The relevance of the discussion in this work reaches beyond the particular model considered here, and we included an outline of its application to both hybrid and multi-field GI.

- Building on the previous work, chapter 4 [64] can be seen as a proof-of-concept example, which can realize both inflation and populate the Universe with Higgs bosons directly after this era, via a perturbative decay. The Higgs then subsequently produces all other SM particles, primarily via decays to the top and massive vector bosons to which it couples most strongly. The Higgs mechanism, which gives rise to particle masses, finds a natural implementation in the setup, as does the hierarchy of the mass scales. Our model confronts CMB and collider data and is in agreement with both. This work is a first step in connecting the Early Universe to collider physics. As the inflationary scalar and the Higgs boson are both pGBs from the same symmetry breaking, they are connected. This allows for a simple scenario for reheating, the production of particles after inflation. The first analysis in this project focussed on a perturbative decay, but the framework also allows for richer reheating dynamics, which we are currently exploring.
- Chapter 5 is a lateral approach to GI. In [65] I considered a non-compact coset of the form $SO(n,1)/SO(n)$ and describe the GBs and their interactions using a geometric formalism. Of particular interest is the subset of models which can address the hierarchy problem of inflation: models in which large excursions in field space correspond to a very small change in potential energy. Such 'compactness' of the potential is found for specific transformation properties of the dynamics which explicitly breaks the symmetry. In this limit the potential is more successful than in the case with a compact coset (and residual discrete symmetry), and makes inflationary predictions compatible with the current Planck bounds.
- Models in which the Higgs is a pGB have been among the most popular explanations for its lightness. In chapter 6 [66] we explored such a scenario using higher dimensional (5D) techniques, instead of relying on 4D approximations as we have done for our remarks on UV completion of Goldstone Inflation models. 5D gauge invariance and locality are analogues of the Goldstone symmetry in the 4D theory. Along these lines one can construct a well defined "dictionary" between an "elementary" weak sector coupled to a strong sector in

4D and a gauge theory in the bulk of 5D. In this project we use this dictionary to extract information about the UV theory, in light of the current and future collider bounds.

- Finally, chapter 7 summarizes the main conclusions of the papers as well as describing possible directions for future research.

SAVING NATURAL INFLATION

Djuna Croon¹ and Verónica Sanz¹

¹Department of Physics and Astronomy, Pevensey II Building, University of Sussex, BN1 9RH,
UK

Slow-roll inflation requires the inflaton field to have an exceptionally flat potential, which combined with measurements of the scale of inflation demands some degree of fine-tuning. Alternatively, the flatness of the potential could be due to the inflaton's origin as a pseudo-Goldstone boson, as in Natural Inflation. Alas, consistency with Planck data places the original proposal of Natural Inflation in a tight spot, as it requires a trans-Planckian excursion of the inflaton. Although one can still tune the renormalizable potential to sub-Planckian values, higher order corrections from quantum gravity or sources of breaking of the Goldstone symmetry would ruin the predictivity of the model. In this paper we show how in more realistic models of Natural Inflation one could achieve inflation without a trans-Planckian excursion of the field. We show how a variant of Extra-natural inflation with bulk fermions can achieve the desired goal and discuss its four-dimensional duals. We also present a new type of four dimensional models inspired in Little Higgs and Composite Higgs models which can lead to sub-Planckian values of the inflaton field.

2.1 INTRODUCTION

The idea of Inflation [67] is a very successful paradigm, capable of explaining the cosmological data with the assumption that one field, the inflaton, dominates the evolution of the Universe in its early stage. Natural Inflation (NI) was first suggested in 1990 by Freese, Frieman and Olinto [37], [68], in answer to the hierarchy problem of inflation. This hierarchy problem addresses the fact that the condition for sufficient inflation combined with the amplitudes of the CMB anisotropy measurements imply that the width of the potential must be much larger than its height. Such a flat potential is generally considered unstable under radiative corrections, unless protected by some symmetry.

In Natural Inflation a shift symmetry is invoked to protect the flatness of the inflaton potential. The inflaton that possesses this shift symmetry is an axion, a Nambu Goldstone boson from a spontaneously broken Peccei-Quinn symmetry. But as the inflaton potential cannot be fully flat, the shift symmetry cannot be exact. An explicit symmetry breaking is introduced which generates a potential for the axion, now a pseudo-Nambu Goldstone boson (pNGB). In its simplest form, natural inflation has the potential [37], [68]

$$V(\phi) = \Lambda^4 \left(1 + \cos \left(\frac{\phi}{f} \right) \right). \quad (2.1)$$

Naturalness requires the spontaneous symmetry breaking scale (parametrized by the axion decay constant f) should be sub-Planckian, such that corrections from quantum gravity are suppressed.

Since the advent of the cosmological precision measurements by the WMAP [69] and Planck [70] satellite, the bounds on the spectral index n_s and the tensor to scalar ratio r have significantly improved. The original natural inflation model now needs trans-Planckian scales f to satisfy the most recent bounds, and therefore loses part of its motivation. A trans-Planckian decay constant f renders the out of the range of validity of the effective theory. Indeed, albeit the Natural inflation potential requires a well-behaved potential

$$V_{NI} \ll \tilde{M}_P^4, \quad (2.2)$$

this renormalizable potential will be corrected by non-renormalizable terms, e.g.

$$V_{NR} = \phi^4 \left(\frac{\phi}{\tilde{M}_P} \right)^n, \quad (2.3)$$

where \tilde{M}_P is the reduced Planck mass. Under these circumstances, the success of this inflationary model depends on the ultra-violet (UV) completion of the theory. The origin of these non-renormalizable terms could be sources of breaking of the quantum gravitational effects, such as wormholes [71] or any other source of breaking of the shift-symmetry at high-energies.

Models reconciling natural inflation with the CMB data should offer an explanation as to why the potential does not receive big gravitational corrections. Different efforts have been made to do so but strive to achieve sub-Planckian values of the field, for instance, by considering a hybrid axion model [72] [73], N-flation [74], and axion monodromy [75] and other pseudo-natural inflation models in Supersymmetry [76].

One of the proposals to improve Natural Inflation relies on a potential generated by a Wilson line in extra-dimensional models, also known as Extra-natural inflation [62]. In these models, the inflaton is the fifth component of a gauge field in the extra dimension, and is thus protected from both higher-order corrections and gravitational effects by its locality in the extra dimension. The potential is generated as

$$V(\phi) = \Lambda^4 \sum_I \left[(-1)^{F_I} \sum_{n=1}^{\infty} \frac{\cos\left(n q_I \frac{\phi}{f}\right)}{n^5} \right] \quad (2.4)$$

where $F_I = 1$ (0) for massless bosonic (fermionic) fields with charge q_I . Here f is the effective decay constant $f = 1/(2\pi g_4 R)$, with R the size of the extra-dimension and g_4 the four-dimensional (4D) gauge coupling defined by $g_4^2 = g_5^2/(2\pi R)$. The n^5 term in the denominator comes from the integration over the extra dimension, as shown explicitly in [77]. In this scenario, loops of gauge bosons lead to the same form of potential as in the original model of natural inflation but with a different interpretation of the decay constant. Nevertheless, cosmological data indicates that $f > M_p$, leading to the slow-roll conditions

$$2\pi g_4 M_p R \ll 1 \quad (2.5)$$

which requires a value of $g_{4D} \ll 1/2\pi$ for a compactification scale below the Planck mass.

In this case Extra-natural inflation makes predictions for n_s and r very similar from the predictions from Natural Inflation, as the higher terms in the sum are suppressed by $1/n^5$. These terms do become significant in the higher order slow-roll conditions, as was recently pointed out by [78], however, as both models predict values for the higher derivatives of the potential $V^{(III)}$ and $V^{(IV)}$ far below the current experimental limits, it is not possible to distinguish them yet.

Here we will propose a mechanism to keep Extra-natural inflation within the validity of the effective theory by adding bulk fermions in the effective potential. Besides gauge bosons (with charge $q = 1$) we also consider the effects of fermions of fractional charge: up-type fermions of charge $+2/3$, and down-type fermions of charge $-1/3$. We will show that for certain combinations of gauge bosons and fermions the model can be made compatible with the Planck data for $f \leq \tilde{M}_p$.

As a next example of a pNGB playing the role of the inflaton, we will consider a Coleman-Weinberg type potential generated by gauge and Yukawa couplings. We discuss its general struc-

ture, and study it numerically for the specific form

$$V(\phi) = \Lambda^4 \left(\cos \frac{\phi}{f} - \tilde{\beta} \sin^2 \frac{\phi}{f} \right) \quad (2.6)$$

This potential resembles the Minimal Composite Higgs model (MCHM) and the inflationary potential studied in [79] upon choosing $f_2 = f_1/2$ and $\Lambda_2/2 = \Lambda_1$. We show that this model can be made compatible with the data for particular values of $\tilde{\beta}$. In the interpretation of ϕ as a pNGB, this corresponds to a relation between its couplings to fermions and bosons.

Lastly we will consider the effects of quantum gravity and other UV breaking effects in the original model of Natural Inflation. We will consider effective higher order operators, which we parametrize these as

$$V(\phi) = \Lambda^4 \left[1 + \cos \left(\frac{\phi}{f} \right) + \sum_{n=5} c_n \phi^4 \left(\frac{\phi}{\tilde{M}_P} \right)^{n-4} \right]$$

We will investigate how these operators will affect the predictions of the model and show how the effect of tiny values of c_n is able to bring the model outside the Planck region. This is an illustration of how the predictions of inflationary models when $f > \tilde{M}_P$ are lost unless one specifies very precisely the UV structure of the model.

The paper is organized as follows. We present the general set-up for the inflaton as a pseudo-Goldstone boson in Sec. 2.2, moving to discuss the origin of the original Natural Inflation model, which we call *Vanilla Natural Inflation*, and its clash with Planck data in Sec. 3.2. We introduce a variant of the Natural Inflation scenario, namely Extra-Natural Inflation and explain how it leads to a similar clash unless one introduces bulk fermions, see Sec. 2.4. In Sec. 2.5 we finally move onto purely four-dimensional models inspired in the ideas of Little Higgs and Composite Higgs, where the pseudo-Goldstone is generated via Coleman-Weinberg with gauge and Yukawa contributions.

2.2 THE GENERAL SET-UP OF NATURAL INFLATION

The idea that the inflaton is a pseudo-Goldstone boson could explain the flatness of the potential required to generate enough inflation, without resorting to fine-tuning. The basic ingredient of all models of natural inflation is the existence of an approximate global symmetry, broken spontaneously at high energies. Hence, one expects a new degree of freedom, a pseudo-Goldstone boson (pGB).

$$\Phi \rightarrow \Phi + C \quad (2.7)$$

where C is a constant.

In this scenario, the pGB inflaton is originated by the breaking of a *global* symmetry G to a subgroup H . We will denote the generators of G as $T^a \in H$ and $T^{\hat{a}}$, where $T^{\hat{a}}$ are the broken generators. The resulting pNGBs are associated with these broken generators, and we will assume the inflaton field is one linear combination of them. The mass and couplings of the pGB would depend on how the global symmetry is explicitly broken.

Note that one can express the Goldstone boson as

$$\Sigma(x) = \Sigma_0 e^{i\Pi(x)/f} \text{ where } \Pi = T^{\hat{a}} \Phi^{\hat{a}} \quad (2.8)$$

As $\Phi^{\hat{a}}$ appears in exponential form, its potential will be forbidden by the shift symmetry, (2.7). The inflaton is then a linear combination of the pseudo-Goldstone bosons, and for large symmetry groups there could be more than one inflaton. In this paper, we will discuss a simple scenario with only one inflaton but it could be generalized to variants of hybrid inflation.

The potential for the inflaton could be generated in several ways, leading to different predictions for inflation. We will consider various options in this paper, namely

- A gauge group, external to G and H , breaks the symmetry G . The archetypical example is instanton effects and explicit breaking through quark mass terms, as in models for axions (QCD or hidden).
- An extra-dimensional gauge theory breaks down spontaneously via compactification, leading to extra-dimensional components of the gauge field exhibiting a shift symmetry. The potential is then generated as a non-zero expectation value of a Wilson line of the inflaton field, due the explicit breaking via Yukawa and new gauge couplings. This is the proposal of Extra-natural inflation. We will discuss how the extra-dimensional model has a dual description in terms of purely four-dimensional models.
- In theories where the inflaton is a 4D Goldstone boson, instead of relying on non-perturbative instanton effects to generate the potential, one could weakly gauge some of the global symmetries and also consider explicit breaking through Yukawa couplings. The potential is then generated as a Coleman-Weinberg contribution from fermions and gauge bosons. This is a popular mechanism to build Little Higgs and Composite Higgs models [24].

In this paper we will not consider the situation of the inflaton as a pseudo-Goldstone boson of the spontaneous breaking of a space-time symmetry, such as the dilaton or the radion in extra-dimensions, see Ref. [80], [81] for some work along these lines.

2.3 VANILLA NATURAL INFLATION: INSTANTON-LIKE POTENTIAL

In this section we introduce the basic idea of Natural Inflation, with a potential generated through instanton effects. We will then discuss the current situation of these models when confronted with cosmological data.

Consider a general non-abelian gauge theory X . Instantons are solutions to the gauge equations of motion

$$D_\mu F^{\mu\nu} = 0 \text{ at } |x| \rightarrow \infty \text{ with } A_\mu \rightarrow U \partial_\mu U^\dagger. \quad (2.9)$$

Instanton solutions can be found when there is a non-trivial element $U(x) \in \pi_3(G)$, the third homotopy group of X . These solutions are characterized by the size of the instanton ρ and the number of possible orientations under the gauge group, e.g. for $SU(N)$ there are $4N$ orientations [82]. The classical action of an instanton solution is given by

$$S_{inst} = \frac{8\pi^2}{g^2} = \frac{2\pi}{\alpha}. \quad (2.10)$$

Instanton effects are non-perturbative, the suppression $e^{-S_{inst}}$ selects gauge sectors with $\alpha \sim O(1)$. Note that instantons here are treated more generally than QCD instantons; they could be world-sheet, membrane instantons or supersymmetric instanton effects.

Assume that the inflaton is a singlet of the symmetry X and couples to the n -instanton solution through a term respecting the shift symmetry, (2.7). Then,

$$V_{n-\Phi} = -\Lambda^4 e^{-S_n} \Sigma^n \quad (2.11)$$

But as we must also consider the effect of n -anti-instanton solutions and sum over n ,

$$\sum_{n=1,\infty} V_{n-\Phi} + V_{\bar{n}-\Phi} \simeq -\Lambda^4 e^{-\frac{2\pi}{\alpha}} (\Sigma + \bar{\Sigma}) = -2\Lambda^4 e^{-\frac{2\pi}{\alpha}} \cos(\Phi/f) \quad (2.12)$$

the potential generated by instantons becomes of the familiar $\cos(\Phi/f)$ form. This form of the solution is independent of the origin of X , as all instanton solutions adopt the same form as a $SU(2)$ instanton [83].

Here we have taken Λ as the scale which allows the inflaton to couple to the instantons. For example, for QCD instantons, Λ is related to the QCD pion sector via the fermion trace anomaly, $\Lambda^4 \simeq f_\pi^2 m_\pi^2$.

Additional symmetries in the theory can make the instanton contributions to the inflaton in (2.14) vanish. For example, in Supersymmetry (SUSY) the coupling of instantons to the inflaton

appears through a superpotential W [84]

$$W_{SUSY} = M^3 e^{-S_n} \Sigma . \quad (2.13)$$

No contribution with $\bar{\Sigma}$ appears in the superpotential, as it is holomorphic in the chiral superfield Σ . Thus under these circumstances there is no dependence on Φ in the potential generated by F-terms ($|\partial W/\partial \Sigma|^2$) neither in supergravity contributions ($\propto |W|^2$). But this situation changes once SUSY is broken. For example, assume there is a non-zero F -SUSY breaking term, $F \sim M_{SUSY}^2$, then the interference of this source of SUSY breaking term and the inflaton's would lead again to a potential

$$V \simeq M_{SUSY}^2 \Lambda^2 e^{-\frac{2\pi}{\alpha}} \cos(\Phi/f) . \quad (2.14)$$

Finally we consider the situation that more than one instanton solution contributes to the inflaton potential. For example, if the gauge symmetry G is broken down to another non-abelian gauge symmetry H , instantons from both theories could contribute to the inflaton potential. This situation again leads to a $\cos \Phi/f$ potential [82].

We can use the invariance of the potential under a shift of Φ/f modulus 2π to rewrite the solution as a potential with a minimum at $\Phi = 0$, and we will do so in the next section.

2.3.1 THE PROBLEM WITH VANILLA NATURAL INFLATION

The vanilla natural inflation model (2.1) is an example of slow-roll inflation; that is, it satisfies the conditions $\epsilon \ll 1$ and $\eta \ll 1$, where ϵ and η are here given by

$$\epsilon = \frac{\tilde{M}_p^2}{2} \left(\frac{V'(\phi)}{V(\phi)} \right)^2 \quad \text{and} \quad \eta = \tilde{M}_p^2 \frac{V''(\phi)}{V(\phi)} . \quad (2.15)$$

To simplify our expressions, in this section we work in units of reduced Planck mass \tilde{M}_p ; that is, we will rescale our parameters $\phi \rightarrow \frac{\phi}{\tilde{M}_p}$ and $f \rightarrow \frac{f}{\tilde{M}_p}$.

The number of e-foldings in the slow-roll approximation is then given by

$$N = \frac{1}{\sqrt{2}} \int_{\phi_E}^{\phi_I} \frac{1}{\sqrt{\epsilon}} \quad (2.16)$$

where ϕ_E is fixed as the field value for which either $\epsilon = 1$ or $\eta = 1$, in other words, the field value for which the slow-roll approximation breaks down.

For a model with potential (2.1) we have

$$N = 2f^2 \left[\log \left(\sin \frac{\phi_E}{2f} \right) - \log \left(\sin \frac{\phi}{2f} \right) \right] \quad (2.17)$$

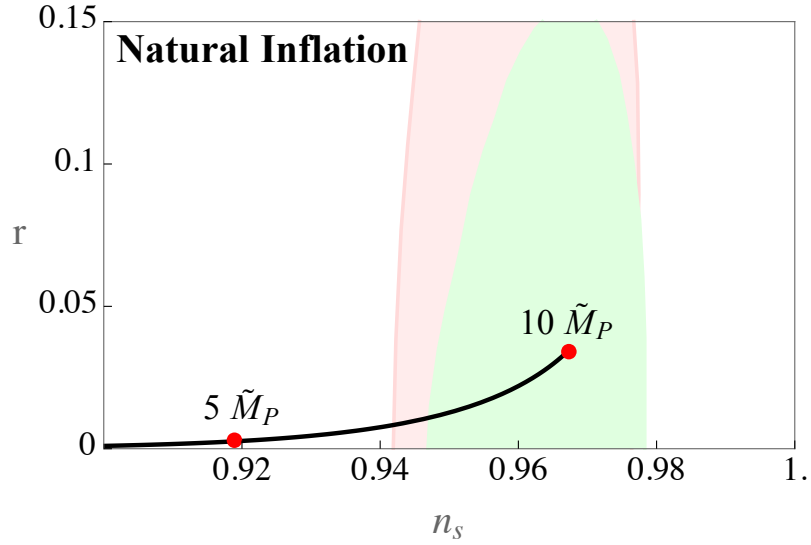


Figure 2.1: Values of cosmological parameters in the (n_s, r) plane with $N = 60$. The red points correspond to $f = M_P \approx 5\tilde{M}_P$, and $f = 2M_P \approx 10\tilde{M}_P$. The regions correspond to a combination of Planck, WP and BAO data, where the green (pink) region is the 95% CL assuming the Λ CDM hypothesis and r (and running of the spectral index).

where

$$\phi_E = f \tan^{-1} \left(\frac{1 - 2f^2}{2\sqrt{2}f} \right) \quad (2.18)$$

Now solving for the field in terms of the number of e-foldings, we obtain

$$\phi_{NI} = 2f \sin^{-1} \left[\exp \left(\frac{2f^2 \log \left(\sin \left(\frac{\phi_E}{2f} \right) \right) - N}{2f^2} \right) \right] \quad (2.19)$$

In Fig. 2.1 we show the values of n_s and r for this scenario, setting the number of e-foldings to $N = 60$. We do not show the line for $N = 50$, but it lies above the $N = 60$ with similar values of f , see for example Ref. [85], [86]. The pink and green regions correspond to a fit of Planck, WMAP and baryon acoustic oscillations (BAO) to n_s and r with and without running of the spectral index [70].

Successful vanilla natural inflation requires values of the decay constant $f \gg \tilde{M}_P$, hence any higher-dimensional operator of the type in (2.3), could dominate over the original renormalizable potential [71], [87]. In this situation, the inflationary theory ceases to be a good effective description, losing predictivity unless a complete understanding of the theory in the UV is achieved, including quantum gravity effects.

Nevertheless, as this term violates the discrete shift symmetry of the original Lagrangian, one could devise a UV completion which (approximately) respects the symmetry, parametrically suppressing the dangerous terms. Besides, one could envision taming quantum gravity effects by embedding the shift symmetry in a gauge symmetry at high-energies [71].

Also note that extending the axion-like inflationary scenario does not seem to circumvent the problem of trans-Planckian values of f . This is the case of axion monodromy [75], where one obtains $f \gg \tilde{M}_p$, or even N-flation [74], where one trades a large f by a large number ($\sim 10^3$) of axion-like inflatons [88].

Let us finish by discussing another way to study this inflationary scenario which does not rely on the n_s, r plane. One can couple the inflaton to gauge fields [89], [90],

$$\Delta\mathcal{L} = -\frac{1}{4}C(\phi)\epsilon^{\mu\nu\rho\sigma}F_{\mu\nu}F_{\rho\sigma} \quad (2.20)$$

as this transforms as a total derivative and therefore does not induce perturbative corrections to the inflaton potential: $E \cdot B \sim \epsilon^{\mu\nu\rho\sigma}F_{\mu\nu}F_{\rho\sigma} \sim \partial_\mu (\epsilon^{\mu\nu\rho\sigma}A_\nu F_{\rho\sigma})$; this is reminiscent of the original use of the axions to solve the strong CP problem. The term (2.20) may give rise non-Gaussianity and gravitational wave signals, and provides a decay channel for the inflaton.

Mild symmetry breaking effects may further give rise to the term [90]

$$\Delta\mathcal{L} = -\frac{1}{4}B(\phi)F^2 \quad (2.21)$$

However, slow-roll requires the effect to be very small, and thus $B(\phi)$ to be nearly constant.

It was shown in Refs. [90], [91] by using $H_{int} \sim E \cdot B$ in the mean field equations for ϕ that sufficiently large coupling to gauge fields causes a back-reaction. This is a purely classical effect, in which inhomogeneities in the inflaton field are sourced by those in the electromagnetic field. It increases the amount of inflation by about 10 e-foldings, or, equivalently, changes the spectral index n_s and the tensor to scalar ratio r with the same amount of efoldings. For sufficiently strong coupling to a large number of gauge fields one could accommodate $f < \tilde{M}_p$ within the experimental bounds. For such a coupling the model would also predict observable (but currently within the bound) non-Gaussianity from inverse decay.

2.4 EXTRA-NATURAL INFLATION: A 5D MODEL AND ITS DUALS

In this section we will explore a different route to generate a pNGB inflaton potential, which does not rely on instanton effects. The inflaton's shift symmetry could be the remnant of an extra-dimensional gauge symmetry broken down by compactification [62]. Moreover, we will discuss how this extra-dimensional mechanism has dual descriptions in terms of purely four-dimensional (4D) models.

To show how this mechanism works, let us discuss a simple example in a five-dimensional (5D) flat spacetime (the analysis can easily be generalized to warped space-times). Consider a gauge field in 5D,

$$S = -\frac{1}{4} \int d^5x F_{MN} F^{MN} \quad (2.22)$$

where M, N run over four-dimensional indexes $\mu = 0 - 3$ and over 5, the index along the fifth dimension. Before compactification, the 5D gauge invariance is given by

$$A_M(x) \rightarrow A_M(x) - \partial_M \alpha(x) . \quad (2.23)$$

The reduction from 5D to 4D can be done by compactifying the extra-dimension x_5 on an orbifold S^1/\mathbb{Z}_2 with $x_5 \in [0, L]$, by specifying the boundary conditions of the gauge field on the orbifold fixpoints at 0 and L . Let us consider two choices consistent with the orbifold,

$$\begin{aligned} \textbf{4D gauge:} \quad & \partial_5 A_\mu = 0 \text{ and } A_5 = 0 \text{ at } x_5 = 0, L \\ \textbf{Shift-symmetry:} \quad & A_\mu = 0 \text{ and } \partial_5 A_5 = 0 \text{ at } x_5 = 0, L, \end{aligned} \quad (2.24)$$

where ∂_5 denotes the derivative along the extra-dimension. In the first case, the low energy theory exhibits a 4D gauge symmetry, whereas in the second case all the gauge bosons become heavy except a massless A_5 4D zero-mode. The resulting low-energy theory of this zero-mode exhibits a shift symmetry, remnant of the 5D gauge symmetry. The A_5 can couple to any species charged under the 5D gauge group through a non-local gauge invariant Wilson line, $e^{i \oint_0^L A_5} = e^{i A_5 L}$.

Bulk fields propagating between the two orbifold fixed-points will radiatively generate a non-zero value for this Wilson line and hence provide a potential for A_5 , our inflaton candidate. Indeed, charged fermions and gauge bosons would have non-trivial boundary conditions in the presence of A_5 in the spectrum. For example, the equation of motion of a fermion coupled to A_5 would be solved with modified boundary conditions $\Psi(x_\mu, x_5) = \Psi(x_\mu, x_5 + L) e^{i e t \oint dx_5 A_5}$ [92]. We can then obtain the contribution to the inflaton potential from fermion and gauge degrees of freedom from the bulk as a closed loop of fields propagating in the bulk, with opposite sign fermionic and bosonic contributions. These contributions are periodic on the inflaton field and also proportional to the charge of the field under the extra-dimensional gauge symmetry. As announced in the introduction, the potential in Extra-natural inflation then takes the form,

$$V(\phi) = -\Lambda^4 \sum_i (-1)^{F_i} \sum_{n=1}^{\infty} \frac{1}{n^5} \cos \left(n q_i \frac{\phi}{f} \right) ,$$

where F_i is the fermionic number of species i , and q_i its charge. The inflationary potential scale is related to the size of the extra-dimension $L = 2\pi R$ by the expression [62]

$$\Lambda^4 = \frac{3}{4\pi^2} \frac{1}{L^4} , \quad (2.25)$$

and the inflaton's decay constant is given by $f = 1/(g_{4D}L)$, with g_{4D} the 4D gauge coupling of the gauge group which generated A_5 .

In the next section we will discuss viable models of inflation in this context. But before we move onto comparing with cosmological data, let us discuss the fact that these models can be viewed as four-dimensional models, dual versions of the extra-dimensional model. In the 5D picture, the spontaneous breaking of the gauge symmetry by compactification acts as a Higgsing mechanism. At low energies compared with the compactification scale (the mass of the Higgsed gauge bosons), the original gauge symmetry is realized as a global symmetry with A_5 a remaining Goldstone boson.

Deconstructed dual: One 4D dual of Extra-natural inflation is deconstruction [93], [94]. Instead of a 5D model, one could consider a set of N copies of the same 4D gauge group linked through bi-fundamental fields, called *links*. The role of the inflaton in this case is played by the Goldstone mode contained in the link field Σ_k system. Each link field is given by

$$\Sigma_k = e^{i \frac{\Pi_k}{\tilde{f}}} \quad (2.26)$$

and the inflaton is in this case

$$\Phi = \frac{1}{\sqrt{N}} \sum_{k=1}^N \Pi_k \quad (2.27)$$

Note that as the inflaton is a linear combination of N fields, its decay constant is $f = \sqrt{N}\tilde{f}$ with \tilde{f} the decay constant of each of the links Π_k . The potential generated in the deconstructed models is equivalent to the Extra-natural inflation but instead of a Wilson loop in 5D one computes a Coleman-Weinberg potential in this gauge configuration. For example, gauge contributions would lead to [95]

$$V(\Phi) = \frac{-9}{4\pi^2} \frac{g^2 f^4}{N^2} \sum_{n=1}^{\infty} \frac{\cos(2\pi n \Phi / f)}{n(n^2 N^2 - 1)(n^2 N^2 - 4)} . \quad (2.28)$$

4D Global symmetry dual: Another way to view the Extra-natural inflationary model is the use holographic methods, based on the AdS/CFT correspondence [96]. In this approach, 4D global symmetries correspond to 5D gauge equivalents. Therefore, the 4D dual of A_5 is a 4D Goldstone boson resulting from the spontaneous breaking of a global symmetry G down to H . This breaking is due to some new strongly coupled sector, and the 4D bound states from the strongly coupled sector are the duals of the Kaluza-Klein excitations in the Extra-natural inflationary model.

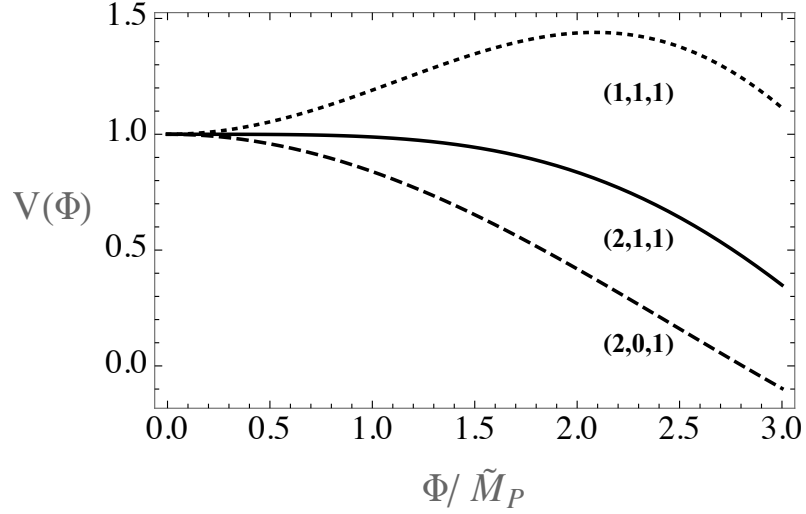


Figure 2.2: Shape of the inflationary potential for different choices of (N_U, N_D, N_V) . Models with more bosons than fermions do not generate inflation around $\phi=0$.

2.4.1 THE ISSUE WITH THE ORIGINAL EXTRA-NATURAL INFLATION MODEL, AND HOW TO SOLVE IT

The original model of Extra-natural inflation [62] considered an inflaton potential generated by bulk gauge bosons. In this case the model makes predictions for n_s and r very similar to Natural Inflation, and therefore suffers from the same issues. In the 5D picture $f > \tilde{M}_p$ may not be problematic (as long as (2.5) is satisfied; that is, for sufficiently small 4D gauge coupling g_4), but in deconstructing dimensions it implies the problematic relation $f_{link} \gg \tilde{M}_p$ [62].

Here we will investigate the effect of adding fermions to the original model. We consider gauge bosons (with charge $q = 1$) and fermions of fractional charge (up-type fermions of charge $+2/3$, and down-type fermions of charge $-1/3$). The potential becomes

$$V(\phi) = \Lambda^4 \left[N_U \cos\left(\frac{2\phi}{3f}\right) + N_D \cos\left(\frac{\phi}{3f}\right) - N_V \cos\left(\frac{\phi}{f}\right) \right] \quad (2.29)$$

We shall classify the different models using (N_U, N_D, N_V) . Considering non-integer charge fermions eludes the $\cos(\phi/f)$ form of the potential, which would lead to the same situation as in the vanilla inflation case discussed in the previous section.

We are specifically interested in the flat region around the origin of the potential: our setup (2.29) may be flatter than the vanilla model in this region. Close to $\phi = 0$ the second derivative of the potential is approximately given by

$$V''(\phi) \approx \left(N_V - \frac{N_D}{9} - \frac{4N_U}{9} \right) \phi, \quad (2.30)$$

hence when N_U and N_D are small compared to N_V , $V''(\phi)$ has the wrong sign at the origin, see Fig. 2.2. It is clear that one needs to consider models with fermions to render the inflationary

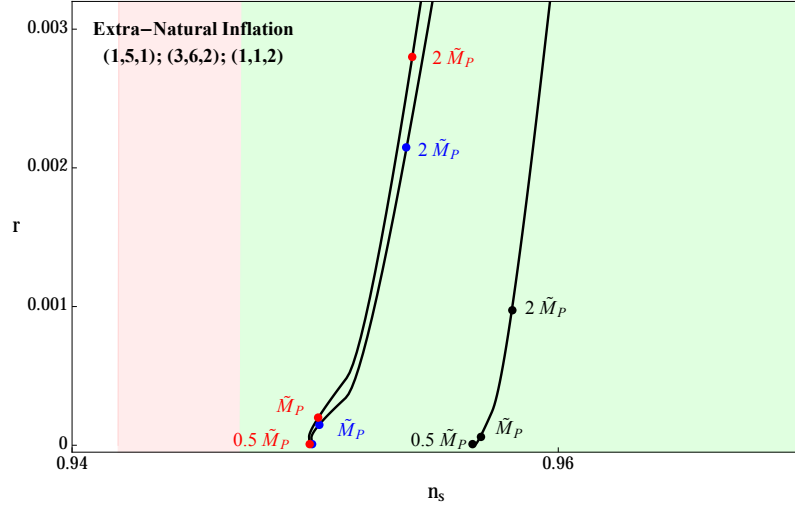


Figure 2.3: Values of cosmological parameters in the (n_s, r) plane with $N = 60$. The bullet points correspond to $f = 0.4M_P \simeq 2\tilde{M}_P$, $f = M_P/5 \simeq \tilde{M}_P$ and $f = M_P/10 \simeq \tilde{M}_P/2$. The regions correspond to a combination of Planck, WP and BAO data, where the green (pink) region is the 95% CL assuming the Λ CDM hypothesis and r (and running of the spectral index).

theory viable.

Therefore, one can classify configurations which could lead to successful inflation using the condition near the origin, e.g.

$$\begin{aligned}
 (N_U, N_D, N_V) = & (0, 9, 1), (1, 5, 1), (2, 1, 1), (2, 10, 2), (3, 6, 2), (4, 2, 2), \\
 & (5, 7, 3), (6, 3, 3), (7, 8, 4) \dots
 \end{aligned} \tag{2.31}$$

In the cases we consider, the flatness of the potential guarantees that $r < \mathcal{O}(0.1)$. Therefore we concentrate on compatibility of the spectral index when confronting the models with the cosmological data.

Not all these models would give successful inflation for a sub-Planckian decay constant f . Nonetheless, we do find successful inflation for a number of models, such as $(N_U, N_D, N_V) = (2, 1, 1), (1, 5, 1), (3, 6, 2), (0, 9, 2)$ and others, including any integer number of times the values of (N_U, N_D, N_V) mentioned above.

In Fig. 2.3 we show how for these solutions, successful inflation with sub-Planckian values for the field can be obtained with very little variation in the value of n_s . We have checked that the higher-derivatives of the potential satisfy the Planck bounds on V''' and V'''' .

2.5 REALISTIC 4D INFLATION: COLEMAN-WEINBERG INFLATION

In this section we consider a new type of inflationary model, with the inflaton a four-dimensional pseudo-Goldstone boson, and a potential generated via Coleman-Weinberg contributions from the explicit breaking of the global symmetry by weak gauging and Yukawa couplings, as mentioned in section 2.2. Indeed, loops of gauge bosons and fermions will generate a Coleman-Weinberg potential for the inflaton,

$$\begin{aligned} V_{CW}^g + V_{CW}^\Psi &= \frac{N_V}{2} \text{Tr} \int \frac{d^4 p}{(2\pi)^4} \log(p^2 + M_V^2(\Phi)) \\ &\quad - N_\psi \text{Tr} \int \frac{d^4 p}{(2\pi)^4} \log(p^2 + M_\Psi^\dagger(\Phi) M_\Psi(\Phi)) \end{aligned} \quad (2.32)$$

where $M_V(\Phi)$ ($M_\Psi(\Phi)$) is the mass term of the gauge bosons (fermions) in the presence of Φ as a background field. N_V is the number of vector degrees of freedom, $N_V = 2, 3$ for massless (massive) vector bosons and N_ψ is the number of Weyl fermions contributing to the potential. We will consider that our inflaton is a linear combination of the pseudo-Goldstone degrees of freedom in Φ and label it ϕ .

In theories where Φ is generated as a Goldstone boson, one can write the couplings to fermions and gauge fields in a general way as

$$\begin{aligned} \mathcal{L} &= \frac{1}{2} P^{\mu\nu} \left(\tilde{\Pi}_0(p^2) \text{Tr}(V_\mu V_\nu) + \tilde{\Pi}_1(p^2) \Sigma V_\mu V_\nu \Sigma^\dagger \right) \\ &\quad + \bar{\Psi} \not{p} (\Pi_0(p^2) + \Pi_1(p^2) \Gamma_i \Sigma_i) \Psi \end{aligned} \quad (2.33)$$

where Σ is given in (2.8), the fermion Ψ is written in a representation of the group G , and Γ_i are the fermionic Gamma matrices in this representation, and related to the broken generators $T^{\hat{a}}$. For example, see Sec. 2.40 for the explicit form of these matrices in the breaking $G/H = SO(5)/SO(4)$. $P^{\mu\nu}$ is the inverse propagator, namely for a gauge boson $P^{\mu\nu} = \eta^{\mu\nu} - p^\mu p^\nu / p^2$.

The form of the mass terms $M_\Psi(\Phi)$ and $M_V(\Phi)$ in (2.31) can be read from (2.32) after specifying the type of breaking responsible for the emergence of the Goldstone bosons. Generally speaking, the mass term is also a periodic function of the Goldstones, that is, a combination of

$$s_\Phi \equiv \sin \frac{\Phi}{f} \text{ and } c_\Phi \equiv \cos \frac{\Phi}{f}, \quad (2.34)$$

and therefore can be written in generality as

$$\begin{aligned} \mathcal{L} &= \bar{\psi}_i \not{p} \left(\Pi_0(p^2)_{ij} + \Pi_1^s(p^2)_{ij} s_\Phi + \Pi_1^c(p^2)_{ij} c_\Phi \right) \psi_j \\ &\quad + \frac{1}{2} P^{\mu\nu} \left(\tilde{\Pi}_0(p^2) \text{Tr}(V_\mu V_\nu) + (\tilde{\Pi}_1^{s^2} s_\Phi^2 + \tilde{\Pi}_1^{sc} s_\Phi c_\Phi + \tilde{\Pi}_1^{c^2} c_\Phi^2) V_\mu V_\nu \right) \end{aligned} \quad (2.35)$$

where the index i, j run over all Dirac fermions.

In the following we discuss in detail the fermion case, as the vector case is a simpler variation of the same mechanism.

2.5.1 FERMIONIC CONTRIBUTIONS

One can diagonalize $\Pi_0(p^2)_{ij}$ and bring the fermion fields to have a canonical kinetic terms. For diagonal $\Pi_0(p^2)_{ij} = \lambda_i^2 \delta_{ij}$, the scaling is simply $\psi_i \rightarrow \psi_i / \lambda_i$.

We can separate the contributions to the matrix $\Pi_{ij}^1 / \Pi_{ij}^0 = (\Pi^1 / \Pi^0)_{ij}$ for $i = j$ and $i \neq j$,

$$\Pi_{ij}^1 / \Pi_{ij}^0 = d_i \delta_{ij} + m_{ij} (1 - \delta_{ij}),$$

where no sum is implied and δ_{ij} is the Kronecker delta symbol. This leads to a Coleman-Weinberg potential

$$V(\Phi) = -2 \int \frac{d^4 p}{(2\pi)^4} \left(\sum_i \log(1 + d_i) + \sum_{ij} \log \left(1 - \frac{1}{p^2} \frac{m_{ij}^2}{d_j d_i} \frac{\Pi_i^0 \Pi_j^0}{\Pi_{ij}^0} \right) \right) \quad (2.36)$$

Note that, in general d_i and m_{ij} will contain s_Φ and c_Φ terms. Also, the form factors $\Pi(Q^2)$ need to satisfy a set of Weinberg sum rules to render the integral finite, i.e. $\lim_{Q^2 \rightarrow \infty} Q^{2n} \Pi(Q^2) = 0$. Whether these conditions are satisfied depends on the realization of the breaking. A common assumption is that the global symmetry G is a chiral symmetry of some UV fermionic sector. A new strong interaction, often called Technicolor (TC), is felt by the UV fermions, and causes fermion bilinears to condense. This condensation triggers the breaking of the global symmetry G to H . If the new strong force is of the type $SU(N_{TC})$, for large values of N_{TC} , one can write the form factors as a sum over an infinite set of resonances,

$$\Pi(Q^2) = \sum_{n=1}^{\infty} \frac{f_n^2}{Q^2 + m_n^2}, \quad (2.37)$$

with m_n and f_n their mass and decay constant, respectively. The Weinberg sum rules impose relations among these resonance parameters. For example, in extra-dimensional duals of this model, these resonances are identified with the Kaluza-Klein resonances, and one can then show that the form factors $\Pi(Q^2)$ do satisfy an infinite number of Weinberg sum rules due to non-locality in extra-dimensions [97]–[99].

Provided the Weinberg sum rules are satisfied, the logarithm term can be expanded. At leading and next-to-leading order,

$$V(\Phi) = \alpha_c c_\Phi + \alpha_s s_\Phi + \beta_c c_\Phi^2 + \beta_s s_\Phi^2 + \dots \quad (2.38)$$

where

$$\begin{aligned}\alpha_{c,s} &= -2 \sum_i \int \frac{d^4 p}{(2\pi)^4} d_i^{c,s} \\ \beta &= 2 \sum_{i,j} \int \frac{d^4 p}{(2\pi)^4} \frac{1}{p^2} \left(\frac{m_{ij}^2}{d_j d_i} \frac{\Pi_i^0 \Pi_j^0}{\Pi_{ij}^0} - d_i d_j \right)\end{aligned}\quad (2.39)$$

where i, j run over the Dirac fermions.

2.5.2 INFLATIONARY MODELS INPIRED ON THE HIGGS AS A PSEUDO-GOLDSTONE BOSON

There is an extensive literature on the Higgs as a pseudo-Goldstone boson. Popular examples of 4D set-ups are Little Higgs [26] and Composite Higgs models [24]. Among those, the minimal Composite Higgs model (MCHM) is relatively simple and is based on the breaking $\text{SO}(5) \rightarrow \text{SO}(4)$, but more elaborated models can be built with larger symmetry groups [21], [23].

In this section we introduce the structure of the MCHM and use it as a template for inflation instead of a candidate for Higgs phenomenology. We will then use cosmological data to obtain information about the structure of the UV model, namely to reconstruct the shape of the form factors $\Pi(Q^2)$ required to generate inflation. This is meant to serve as an illustration of the mechanism and it is by no means the only way to write a successful inflationary model. Inspecting (2.37), one sees that a variety of potentials involving periodic functions arise from different breaking patterns.

In the MCHM, right-handed and left-handed third generation fermions (top and bottom quarks) contribute to the potential and gauge bosons interactions gauge a sub-group of $\text{SO}(4)$. The spinorial representation of $\text{SO}(5)$ is as follows,

$$\Gamma^{\hat{a}} = \begin{bmatrix} 0 & \sigma^{\hat{a}} \\ \sigma^{\hat{a}\dagger} & 0 \end{bmatrix}, \quad \Gamma^5 = \begin{bmatrix} \mathbf{1} & 0 \\ 0 & -\mathbf{1} \end{bmatrix} \quad \text{where } \sigma^{\hat{a}} = \{\vec{\sigma}, -i\mathbf{1}\} \quad (2.40)$$

In this scenario, not all the possible form factors are generated. Indeed, if we inspect (2.35) and compare with the MCHM, the following relations are obtained,

$$d_i^s = 0, \quad m_{ij}^c = 0, \quad (2.41)$$

and the resulting potential is of the form

$$V = \alpha c_\Phi - \beta s_\Phi^2. \quad (2.42)$$

The relation between the parameters α, β and the resonances has been fleshed out in the previous section. If we consider contributions to the inflaton coming from vector resonances and N_F fermion flavors, one obtains [21], [23]

$$\frac{\beta}{\alpha} = -\frac{9}{16N_F} \frac{d_V}{d_F} \quad (2.43)$$

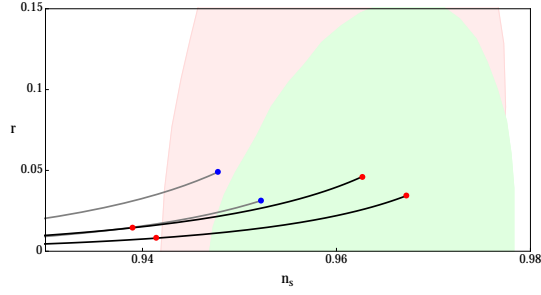


Figure 2.4: In grey $V(\phi) = \sin^2 \phi/f$, in black $V(\phi) = \cos \phi/f$ for $N = 60(50)$ for the lower (upper) line. The points $f = 10$ and $f = 7$ are marked.

where d is the ratio of form factors defined in (2.5.1), and the subscript V (F) means vector (fermion) contributions and N_F is the number of Dirac fermions.

In the next section we discuss the viability of this potential as a candidate for Natural Inflation and find that a specific relation between α and β is required. The interpretation in terms of resonances of a strongly coupled sector responsible for the breaking G/H can be done by noting that the ratio in (2.42) is related to a sum over bosonic and fermionic resonances.

2.5.3 INFLATING WITH A HIGGLIKE PNGB

We will consider inflation in the case (2.40), that is, a potential of the form

$$V(\phi) = \alpha \cos \frac{\phi}{f} - \beta \sin^2 \frac{\phi}{f} \quad (2.44)$$

It is clear that in the case $\alpha = 0$ ($\beta = 0$) the potential reduces to a simple $\sin^2 \phi/f$ ($\cos \phi/f$) potential. As discussed in depth for $\cos \phi/f$ and shown in the figure 2.4 for $\sin^2 \phi/f$, this can only be compatible with slow-roll if $f > M_p$.

Therefore we will explore the range of potentials with both $\alpha, \beta \neq 0$ as it would be the case in models where the explicit breaking of the global symmetry is carried by both gauge and Yukawa interactions. We re-parametrize the potential as

$$V(\phi) = \Lambda^4 \left(\cos \frac{\phi}{f} - \tilde{\beta} \sin^2 \frac{\phi}{f} \right), \quad (2.45)$$

where $\tilde{\beta} = \beta/\alpha$ in (2.43).

The potential has a very flat region around the origin for $-1/2 \lesssim \tilde{\beta} < 0$ as can be seen from Fig. 2.5. This range of $\tilde{\beta}$ can be translated into a region in the resonance parameter space using (2.42). In turn, it indicates a specific relation between the vector and fermionic masses and decay constants, using (2.36):

$$\tilde{\beta} = -1/2 \Rightarrow d_V = \frac{32}{9} N_F d_F. \quad (2.46)$$

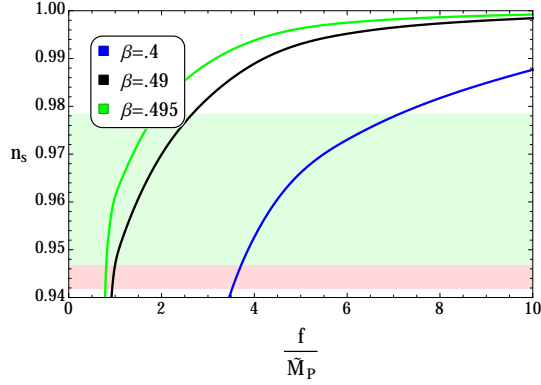


Figure 2.7: Predictions for $\tilde{\beta} = -0.4$, $\tilde{\beta} = -0.49$, $\tilde{\beta} = -0.495$ in the f - n_s plane.

At first sight, this relation may seem as unnatural, a partial conspiracy among the form factors of spin-one and spin one-half particles in the resonance sector. Yet these kind of relations among form factors can be obtained in models with extra symmetries. For example, these ideas were used to build technicolor/higgsless models consistent with electroweak precision tests, where a cancellation between bosonic resonances [99]–[101] or fermionic and bosonic resonances [102]–[104] was achieved in a walking theory.

This potential can indeed lead to sub-Planckian values for f and agree with Planck data. For example, we show the region for $f = \tilde{M}_P$ in figure 2.6 the sensitivity to the value of $\tilde{\beta}$. In Fig. 2.7 we show that for $\tilde{\beta}$ close to $-1/2$, $f < \tilde{M}_P$ and satisfy Planck's constraints on n_s .

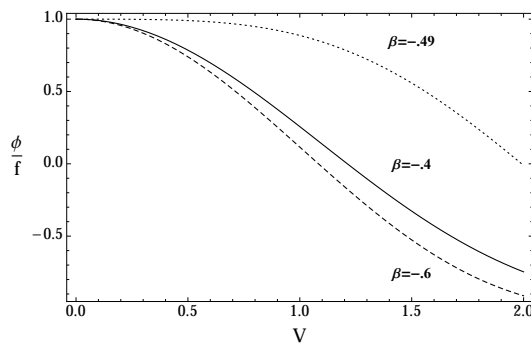


Figure 2.5: Shape of the potential for $f = 1\tilde{M}_P$ and $\tilde{\beta} = -0.49$, $\tilde{\beta} = -0.495$, $\tilde{\beta} = -0.497$

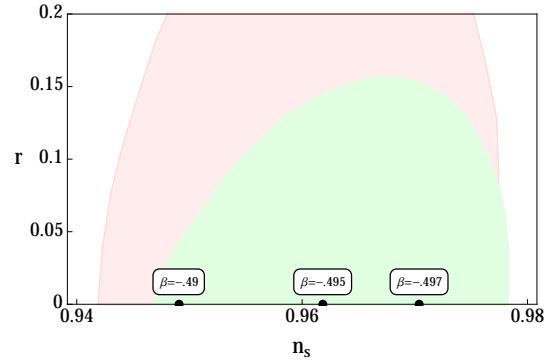


Figure 2.6: Predictions for $\tilde{\beta} = -0.49$, $\tilde{\beta} = -0.495$, $\tilde{\beta} = -0.497$ in the n_s - r plane

In the cases we consider, $r \ll O(1)$ (as sees clearly figure 2.6); this remains the case for different values of f . In figure 2.7 we compare predictions for n_s with different f .

To second order, the potential is

$$V(\phi) = \Lambda^4 \left(\cos \frac{\phi}{f} - \tilde{\alpha}_2 \cos^2 \frac{\phi}{f} + \tilde{\beta} \sin^2 \frac{\phi}{f} + \tilde{\beta}_2 \sin^2 \frac{\phi}{f} \left(1 + \cos \frac{2\phi}{f} \right) \right)$$

where

$$\tilde{\alpha}_2 = \frac{\alpha_q^2 + \alpha_u^2}{2(\alpha_q - \alpha_u)} = \frac{\alpha_q^2 + \alpha_u^2}{2\alpha}, \quad \tilde{\beta}_2 = \frac{\beta_f^2 + \beta_g^2}{4\alpha}$$

One then expects $\tilde{\alpha}_2$ and $\tilde{\beta}_2$ to be small, although larger if α_q and α_u are very close to each other.

2.6 THE EFFECT OF UV COMPLETIONS: HIGHER-DIMENSIONAL TERMS

Up to now we have discussed generation of the inflationary potential through infra-red (IR) effects, such as non-perturbative instanton, a Wilson line or a Coleman-Weinberg potential. As we discussed in the introduction, when $f > \tilde{M}_P$, the effect of UV corrections of the type in (2.3) is potentially dangerous. These would generate higher-dimensional operators (HDOs) which, for large values of the field, could dominate over the renormalizable terms. In this section we discuss the effects of non-renormalizable terms in the case of the Vanilla Natural Inflation discussed in Sec. 3.2 to show how sensitive these models are to HDOs in the regime of $f > \tilde{M}_P$.

We already mentioned wormhole terms in the Introduction, but there are other possible origins for HDOs. For example, graviton loop corrections [105], [106] would preserve the cosine form of the potential

$$\delta V = M^4 c_n \left[\cos \frac{n\phi}{f} \right]^m.$$

By choosing m and n appropriately, one can account for the terms we invoked in the Introduction, (2.1).

Also higher-order instanton effects could influence the HDOs. As explained in Sec. 3.2, instanton effects would maintain the periodicity of the potential. They thus will be of the form $(n > 1)$ ¹

$$\delta V = \Lambda^4 \tilde{c}_n \cos \frac{n\phi}{f} = \Lambda^4 \tilde{c}_n \sum_{k=0}^{\infty} \frac{(-1)^k \left(\frac{n\phi}{f} \right)^{2k}}{(2k)!} = \Lambda^4 c_n \sum_{k=0}^{\infty} (-1)^k \phi^{2k} \quad (2.47)$$

Of course, the expanded form masks the underlying shift symmetry, but it allows us to connect with the HDO language. It is clear that the coefficients c_n are growing with n , and will thus ruin slow-roll inflation unless the coefficients \tilde{c}_n decrease with n . The extra terms will not influence the slow-roll predictions from Natural Inflation much in the limits

$$\tilde{c}_n n^2 \ll 1 \text{ and } \frac{\phi}{f} \lesssim 2 \quad (2.48)$$

¹Note that this is the potential of Extra-natural Inflation, in which there is a sum over n . The term $n = 1$ gives the natural inflation model.

This is the case in Extra-natural inflation, in which $\tilde{c}_n \propto 1/n^5$. For non gravitational effects, \tilde{c}_n decreases with n as e^{-nS} where n is the number of instantons [105].

Finally, UV breaking of the inflaton's shift symmetry such as new fermion masses could generate new HDOs.

2.6.1 ADDING HIGHER-DIMENSIONAL OPERATORS TO VANILLA NATURAL INFLATION

Here we consider the effects of higher order operators added to the vanilla Natural Inflation model. We parametrise the effect as

$$V(\phi) = \Lambda^4 \left[1 + \cos\left(\frac{\phi}{f}\right) + \sum_{n=5}^{n=8} c_n \phi^n \right] \quad (2.49)$$

where c_n are dimensionless, as we have rescaled all dimensionful parameters by \tilde{M}_p . These non-renormalizable terms are higher-dimensional operators (HDOs). Note that the sensitivity of models with values of the field larger or close to the UV cutoff has been recently studied in, e.g. Refs. [87], [107] for quantum gravity and SUSY unification HDOs.

Since we assume that the HDO will give corrections to the leading order model, we solve for ϕ_N in this model perturbatively,

$$\phi_N = \phi_{NI} + \epsilon \phi_1 \quad (2.50)$$

using $N(\phi_{NI} + \epsilon \phi_1) = 60$. The zeroth order equation will be solved by (2.19).

In figure 2.8 we show the variation of the coefficients c_n (where $c_m = 0$ for $m \neq n$) in the $n_s - r$ plane for $f = 0.9M_p \simeq 4.5\tilde{M}_p$. All HDOs give contributions in a similar direction in the n_s, r plane.

The effect of tiny values of c_n could bring the model outside the Planck region. For example, the introduction of a small ϕ^6 term with a $c_6 \sim 10^{-7}$ does bring the model to unacceptable values of n_s and r . This is an illustration of how the predictions of inflationary models in the trans-Planckian region are questionable.

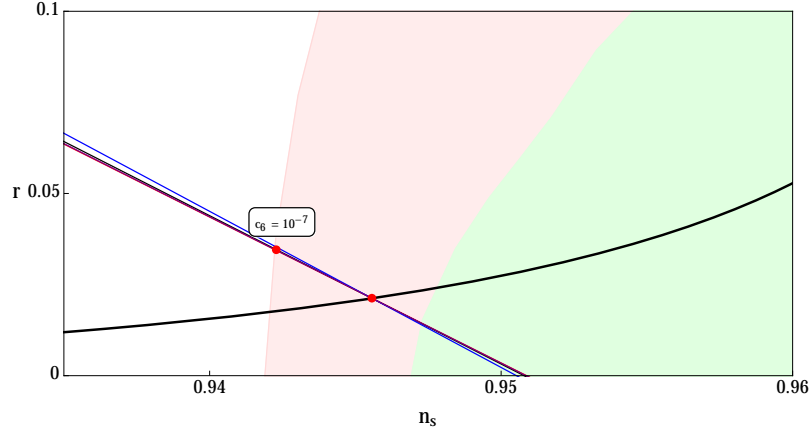


Figure 2.8: Varying the coefficients of HDOs in the $n_s - r$ plane for $f \simeq 4.5\tilde{M}_P$. With c_5, c_6, c_7, c_8 in blue, black, purple, and black respectively. At $r = 0$, $\Delta\phi \sim \phi_I = 0.21M_P$, $|\xi_V| < 4 \times 10^{-5}$ and $\varpi_V < 8 \times 10^{-7}$. At the Natural inflation reference point ($c_n = 0, \forall n$), $\Delta\phi \sim \phi_I = 0.24M_P$. The point at the edge of the pink region corresponds to $c_6 = 10^{-7}$.

Let us finish with some comments on the effect of HDOs in this model. Solving for the values of the dimensionless constants c_n at $r = 0$ ($c_m = 0, m \neq n$), we have

	$r = 0$
c_5	-1.85×10^{-6}
c_6	-1.58×10^{-7}
c_7	-1.32×10^{-8}
c_8	-1.10×10^{-9}

To make the perturbed natural inflation more compatible with the CMB data, the coefficients need to be small and negative, although the statement can be made less strong if a cancelation between them occurs.

For different values of f the contributions by the HDOs in the n_s, r plane will be similar. This allows us to find the maximal tensor to scalar ratio r as a function of f for which Natural Inflation can be made compatible with the Planck data (the green region in plot 2.1, as Natural Inflation predicts no running) with the aid of HDOs (Fig. 2.9). In particular it predicts a lower bound on f :

$$f \gtrsim 0.868M_P = 4.35\tilde{M}_P.$$

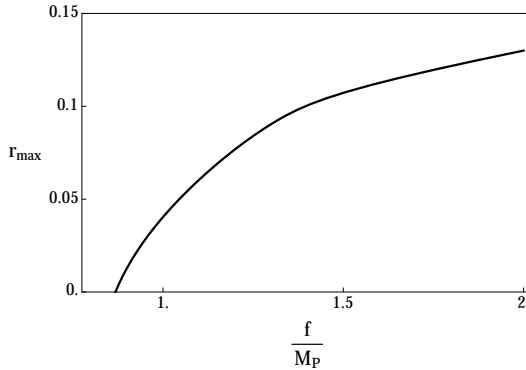


Figure 2.9: Maximal tensor to scalar ratio r as a function of f in vanilla Natural Inflation models and the operator $c_6\phi^6$.

2.7 CONCLUSIONS

The paradigm of slow-roll inflation after the Planck data, albeit very successful parametrization, requires a questionable field theory approach. The inflationary hierarchy problem, namely the tension between providing sufficient inflation yet satisfy the amplitude of the CMB anisotropy measurements, implies that the width of the potential must be much larger than its height. This tuning is generically unstable unless some symmetry protects the form of the potential. This is the idea of Natural Inflation [37], [68]: the inflationary potential is protected by a shift symmetry provided the inflaton is a pseudo-Goldstone boson.

The archetypical example of Natural Inflation is an axion-like inflaton with a potential generated by instantons. This specific form of the potential requires large values of the inflaton field to sustain sufficient inflation. Extra-natural inflation, based on an extra-dimensional realization of the same idea, suffers from the same problem. The unknown higher order corrections could easily upset the inflationary model predictions, implying that these models are not a good effective theory.

In this paper we aim at preserving the idea of Natural Inflation as a solution to the cosmological hierarchy problem in models with an adequate effective description, where the field does not undertakes any trans-Planckian excursion. We find that there are many of such models once we go beyond the original Natural Inflation model.

Indeed, in this paper we have explained how Extra-natural inflation can be generalized to encompass (more realistic) extra-dimensional models with bulk fermions. A large number of such bulk configurations do lead to a successful inflationary model with $f > \tilde{M}_P$ and a moderate amount of bulk matter content.

We have shown how four-dimensional models with Higgs-like potentials can also lead to successful inflation. We have presented the study of a specific such model based on the Minimal Composite Higgs model, but also developed a formalism to explore different breaking scenarios. We also showed how, once the inflationary conditions are set, one can obtain information about the sector of heavy resonances which accompanies the pseudo-Goldstone boson in these scenarios.

In the case of Vanilla Natural Inflation, we have studied the effect of higher-dimensional operators. In this case, as $f > \tilde{M}_p$, these higher-dimensional effects gives us a sense of how sensitive is the theory to the UV completion. We have found that moderate values of the operators do change drastically the cosmological predictions [87], [107], emphasizing once more the necessity of sub-Planckian field values to retain the predictivity of the model.

ACKNOWLEDGEMENTS

We would like to thank Xavier Calmet and Daniel Litim for discussions about quantum gravity corrections. The authors would like to acknowledge funding from grant STFC ST/L000504/1.

GOLDSTONE INFLATION

Djuna Croon¹, Verónica Sanz¹ and Jack Setford¹

¹Department of Physics and Astronomy, Pevensey II Building, University of Sussex, BN1 9RH,
UK

Identifying the inflaton with a pseudo-Goldstone boson explains the flatness of its potential. Successful Goldstone Inflation should also be robust against UV corrections, such as from quantum gravity: in the language of the effective field theory this implies that all scales are sub-Planckian. In this paper we present scenarios which realise both requirements by examining the structure of Goldstone potentials arising from Coleman-Weinberg contributions. We focus on single-field models, for which we notice that both bosonic and fermionic contributions are required and that spinorial fermion representations can generate the right potential shape. We then evaluate the constraints on non-Gaussianity from higher-derivative interactions, finding that axiomatic constraints on Goldstone boson scattering prevail over the current CMB measurements. The fit to CMB data can be connected to the UV completions for Goldstone Inflation, finding relations in the spectrum of new resonances. Finally, we show how hybrid inflation can be realised in the same context, where both the inflaton and the waterfall fields share a common origin as Goldstones.

3.1 INTRODUCTION

The empirically well supported paradigm of cosmic inflation [67] has a hierarchy problem from the perspective of particle physics. Parameterised in terms of a slowly rolling scalar field, the scale of inflation (from CMB data [14]) is exceeded by the field excursion (given by the Lyth bound [16], [108]) by roughly two orders of magnitude:

$$\Lambda^4 = (1.88 \times 10^{16} \text{ GeV})^4 \left(\frac{r}{.10} \right) \quad \text{and} \quad \Delta\phi \geq M_p \sqrt{\frac{r}{4\pi}} \quad (3.1)$$

where r is the ratio of the tensor to the scalar power spectrum, and where here $M_p = 2.435 \times 10^{18} \text{ GeV}$ is the reduced Planck mass. Meeting both these conditions implies an exceptionally flat potential for the inflaton, which generically is radiatively unstable.

Natural Inflation (NI) [37], [68] offers a solution to this hierarchy problem by imposing a symmetry on the inflaton: the inflaton potential exhibits a shift symmetry $\phi \rightarrow \phi + C$ with C a constant, and therefore could be protected from higher order corrections. The shift symmetry is realised by identifying the inflaton with the Goldstone boson (GB) ϕ of a broken global symmetry G to its subgroup H ($\phi \in G/H$). In turn, the GB obtains a potential through effects that render G inexact. The resulting degree of freedom is therefore not an exact Goldstone boson, but a *pseudo-Goldstone boson* (pGB). Different effects can lead to an inexact global symmetry; we reviewed the relevant mechanism in [61].

The original and most popular NI model has an axion as the inflaton, the GB of spontaneously broken Peccei-Quinn symmetry [37], [68]. The axion gets a potential through non-perturbative (instanton) effects. As shown in Ref. [84] these effects lead to the characteristic $\cos(\phi/f)$ potential across models, where f is the scale at which G is broken. To obtain the famous NI model one adds a cosmological constant term to impose the phenomenological constraint $V(\phi_{min}) = 0$, to obtain,

$$V(\phi) = \Lambda^4 (1 + \cos \phi/f) \quad (3.2)$$

Alas, the original NI model can only be successfully reconciled with the data from CMB missions for superplanckian scales of the decay constant: $f = O(10M_p)$. This is evidently a problem, because above the Planck scale one should expect a theory of Quantum Gravity (QG), and it is known that theories of QG in general do not conserve global symmetries [109]. Therefore one generically expects large contributions to the simple potential (3.2), as was shown recently in [110]. Thus, one may conclude that vanilla NI is not a good effective theory.¹

¹It is found that it is only possible to maintain control over the backreaction in very specific configurations, such as [111].

Different proposals have been made to explain the super-Planckian decay constant while maintaining the simple potential (3.2) and the explanatory power of the model. Among these are Extra-Natural inflation [62], hybrid axion models [72], [73], N-flation [74], [112], [113], axion monodromy [75] and other pseudo-natural inflation models in Supersymmetry [76]. These proposals usually focus on generating an effective decay constant f_{eff} in terms of model parameters, such that $f_{\text{eff}} = \mathcal{O}(10M_p)$ is no longer problematic. Some of these models rely on a large amount of tuning or on the existence of extra dimensions, as 4D dual theories suffer from the same problems as the vanilla model.

In [61] we recognised that pGB inflation does not have to have an axion as the inflaton. There are other models which generate a natural inflaton potential, protected from radiative corrections by the same mechanism. In particular, we focussed on compact group structures and showed that one can find models that fit the CMB constraints for a sub-Planckian symmetry breaking scale f^2 .

For example, if the pGB field is coupled to external gauge bosons and fermions, a Coleman-Weinberg potential is generated for the inflaton. We demonstrated the general mechanism and gave a specific successful example inspired by the minimal Composite Higgs model MCHM₅ [24].

Here we develop a comprehensive approach to Goldstone Inflaton. In Sec. 3.2, we give a full analysis of the potentials that can be generated, and motivate that the potential that is uniquely expected to give successful single-field inflation is given by

$$V(\phi) = \Lambda^4 \left(C_\Lambda + \alpha \cos(\phi/f) + \beta \sin^2(\phi/f) \right). \quad (3.3)$$

In Sec. 3.3, we compare its predictions against the CMB data and find that the latter singles out a specific region in the parameter space. We comment on the fine-tuning necessary and show that one obtains a successful model with $f < M_p$ at marginal tuning.

As the Goldstone inflaton is expected to have non-canonical kinetic terms, we give an analysis of the non-Gaussianity predictions. We show that the current bounds are comfortably evaded.

In Sec. 3.4, we further explore the region of parameter space that leads to successful inflation. The relations that we find by comparison with the Planck data give information about the form factors that parameterise the UV-theory. We comment on the scaling with momentum we expect from theoretical considerations. We finish with an analysis of the UV theory, in which we use QCD-tools to compute the relevant parameters and give a specific example in the approximation of light resonance dominance in Sec. 3.5. Finally, in the Appendices we give specific examples of single-field and hybrid inflation coming from Goldstone Inflation.

²One can also consider non-compact groups such as space time symmetries. In [80] the authors consider broken conformal symmetry and showed that a dilaton inflaton can generate inflation with strictly sub-Planckian scales.

3.2 A SUCCESSFUL COLEMAN-WEINBERG POTENTIAL

Our starting assumption is that the inflaton is a Goldstone boson, coming from the breaking of some global symmetry $G \rightarrow H$. We parameterise the Goldstone bosons using a non-linear sigma model

$$\Sigma(x) = \exp(iT^{\hat{a}}\phi^{\hat{a}}(x)/f), \quad (3.4)$$

where $T^{\hat{a}}$ are the broken G/H generators, $\phi^a(x)$ are the Goldstone fields, and f is the scale of spontaneous symmetry breaking [114]³. Under a G/H symmetry transformation the Goldstone bosons transform via a shift $\phi^a(x) \rightarrow \phi^a + f\alpha^a$, for some transformation parameters α^a . This non-linear shift symmetry prevents the Goldstone fields from acquiring a tree-level potential. The inflaton can only get a potential if there are sources of explicit symmetry-breaking that will render G inexact. We list two possibilities:

1. If the inflaton is a composite object formed of strongly-interacting UV fermions, then explicit fermion mass terms could break the symmetry and give the inflaton a non-zero mass. This would be analogous to the pions of QCD, which acquire a mass from the explicit breaking of chiral symmetry due to the small up and down quark masses.
2. If the inflaton sector has couplings to particles that do not form complete representations of G , then loops of these ‘external’ particles will generate a Coleman-Weinberg potential for the inflaton.

Although 1. is an interesting possibility, in this paper we will explore 2., since the Coleman-Weinberg potential can be computed perturbatively (up to coefficients determined by strongly interacting dynamics).

A point worth noting is that, as of yet, we have not fixed the scale at which inflation occurs. The ‘external’ particles relevant to our calculation are those with masses close to, but below the scale of symmetry breaking $\sim f$. If inflation occurs near the TeV scale, we would have to embed the SM gauge group and the heavy quarks into representations of G , since these particles would be expected to have the greatest contributions to the inflaton potential (just as in Composite Higgs models). If inflation occurs at the GUT scale $\sim 10^{16}$ GeV, then our lack of knowledge of the high-scale particle spectrum means we can be more open-minded. In the following treatment we leave this question open, considering generic possibilities for the particle content.

³Here we assume the CCZW formalism. A different proposal relying on quark seesaw has been made recently (see for instance [115] and references therein); however, in this setup the periodicity of the Goldstone field is disguised and therefore we will stick to CCZW.

That said, we will not consider the contribution from elementary scalars, our prime motivation being the unnaturalness of scalar masses much below the Planck scale. The only scalars appearing in our model will be those coming from the G/H breaking, with masses protected by the non-linear Goldstone symmetry.

We will work through in detail a scenario in which the strong sector has a global $SO(N)$ symmetry which breaks to $SO(N-1)$ ⁴. This symmetry breaking gives rise to $N-1$ massless Goldstone fields, one linear combination of which will play the role of the inflaton. We will assume that the symmetry-breaking VEV is in the fundamental representation:

$$\Sigma_0 = \langle \Sigma \rangle = \begin{pmatrix} 0 \\ 0 \\ \vdots \\ 1 \end{pmatrix}, \quad (3.5)$$

so that

$$\Sigma(x) = \exp(iT^{\hat{a}}\phi^{\hat{a}}(x)/f)\Sigma_0, \quad (3.6)$$

transforms as a fundamental of $SO(N)$.

If we take the unbroken symmetry $SO(N-1)$ to be a gauge symmetry, we can gauge away $N-2$ of the Goldstone fields (they give mass to $N-2$ gauge bosons), as we show pictorially in Fig. 3.1. This will leave us with one physical Goldstone field, which we identify with the inflaton. The same mechanism gives masses to the W^\pm and Z bosons in Composite Higgs models (see for example [19], [116]). We can gauge a smaller subgroup of $SO(N)$, although this will leave more than one Goldstone degree of freedom. Some possibilities are explored in Appendix 3.6.

We now attempt to write down an effective Lagrangian containing couplings of the Goldstone fields to the $SO(N-1)$ gauge bosons. A useful trick is to take the whole $SO(N)$ global symmetry to be gauged, and only at the end of the calculation setting the unphysical $SO(N)/SO(N-1)$ gauge fields to zero [21], [23]. The most general effective Lagrangian involving couplings between Σ and $SO(N)$ gauge bosons, in momentum space and up to quadratic order in the gauge fields, is

$$\mathcal{L}_{eff} = \frac{1}{2}(P_T)^{\mu\nu} \left[\Pi_0^A(p^2) \text{Tr}\{A_\mu A_\nu\} + \Pi_1^A(p^2) \Sigma^T A_\mu A_\nu \Sigma \right], \quad (3.7)$$

where $A_\mu = A_\mu^a T^a$ ($a = 1, \dots, N$) are the $SO(N)$ gauge fields, $P_T^{\mu\nu} = \eta^{\mu\nu} - q^\mu q^\nu / q^2$ is the transverse projector, and $\Pi_{0,1}^A(p^2)$ are scale-dependent form factors, parameterising the integrated-out dynamics of the strong sector.

⁴Many of the results of this section generalise straightforwardly to $SU(N) \rightarrow SU(N-1)$.

Taking an appropriate choice for the $SO(N)$ generators and expanding out the matrix exponential in (3.6), we obtain:

$$\Sigma = \frac{1}{\phi} \begin{pmatrix} \phi^1 \sin(\phi/f) \\ \vdots \\ \phi^{N-1} \sin(\phi/f) \\ \phi \cos(\phi/f) \end{pmatrix}, \quad (3.8)$$

where $\phi = \sqrt{\phi^{\tilde{a}} \phi^{\tilde{a}}}$. With an $SO(N-1)$ gauge transformation we can rotate the $\phi^{\tilde{a}}$ fields along the ϕ^1 direction, so that

$$\Sigma = \begin{pmatrix} \sin(\phi/f) \\ \vdots \\ 0 \\ \cos(\phi/f) \end{pmatrix}. \quad (3.9)$$

The remaining $N-2$ degrees of freedom give masses to as many gauge bosons. Expanding out all the terms in (3.7) and setting the $SO(N)/SO(N-1)$ gauge fields to zero as promised, we obtain:

$$\mathcal{L}_{\text{eff}} = \frac{1}{2} (P_T)^{\mu\nu} \left[\Pi_0^A(p^2) + \frac{1}{2} \Pi_1^A(p^2) \sin^2(\phi/f) \right] A_{\mu}^{\tilde{a}} A_{\nu}^{\tilde{a}}, \quad (3.10)$$

where $A_{\mu}^{\tilde{a}}$ are the $SO(N-1)/SO(N-2)$ gauge fields. The remaining (massless) $SO(N-2)$ gauge fields do not couple to the inflaton (See Fig. 3.1).

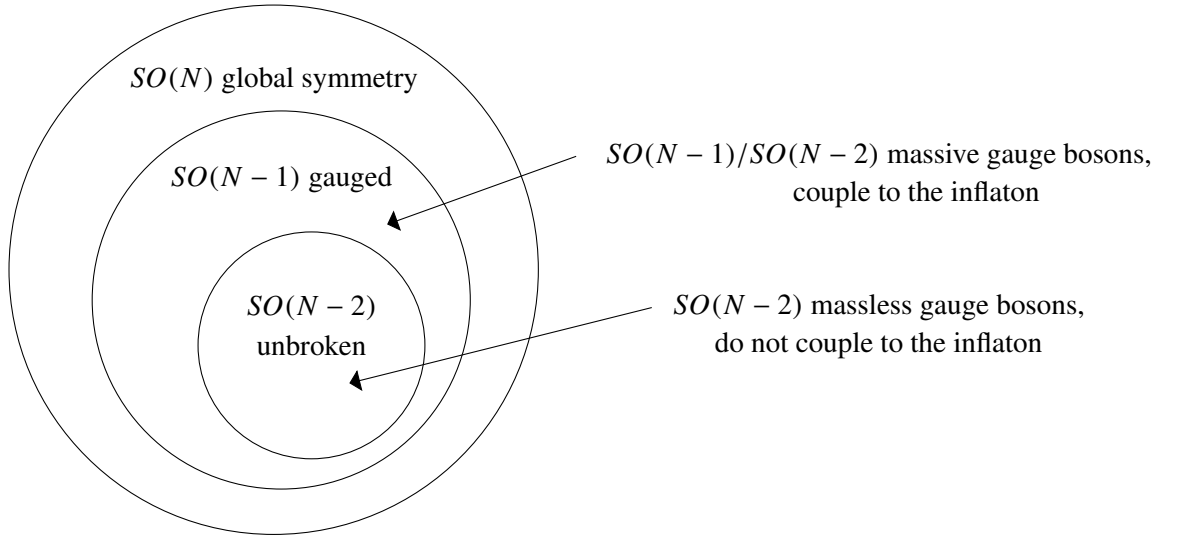


Figure 3.1: Subgroups of the global $SO(N)$ symmetry.

Using this Lagrangian we can derive a Coleman-Weinberg potential for the inflaton [22]:

$$V = \frac{3(N-2)}{2} \int \frac{d^4 p_E}{(2\pi)^4} \log \left[1 + \frac{1}{2} \frac{\Pi_1^A}{\Pi_0^A} \sin^2(\phi/f) \right], \quad (3.11)$$

where $p_E^2 = -p^2$ is the Wick-rotated Euclidean momentum. This result can be understood as the sum over the series of diagrams:

in which the inflaton field is treated as a constant, classical background. The factor of $3(N - 2)$ comes from the 3 degrees of freedom of each of the massive $SO(N - 1)/SO(N - 2)$ gauge bosons, any of which may propagate around the loop.

As discussed in [21], [23], Π_1 can be thought of as an order parameter, which goes to zero in the symmetry-preserving phase at high momenta. Provided the ratio Π_1^A/Π_0^A decreases fast enough, the integral in (3.11) will converge. We can approximate the potential by expanding the logarithm at leading order. This approximation is equivalent to assuming the dominant contribution comes from diagrams with one vertex, and that higher order diagrams are suppressed⁵. This gives

$$V(\phi) = \gamma \sin^2(\phi/f), \quad (3.14)$$

where

$$\gamma = \frac{3(N - 2)}{4} \int \frac{d^4 p_E}{(2\pi)^4} \left(\frac{\Pi_1^A}{\Pi_0^A} \right). \quad (3.15)$$

It is worth pointing out that gauge contributions generically lead to a \sin^2 type potential at leading order. A \sin^2 potential suffers from the same problems as the cosine of Natural Inflation – it is only flat enough for superplanckian values of f .

However, we should also include contributions from external fermions. Just as with the gauge case, the easiest way to write down a general effective Lagrangian is to assume that the fermions are embedded within representations of the full symmetry group $SO(N)$. First we try embedding two Dirac fermions (one left and one right handed) in fundamental $SO(N)$ representations:

$$\Psi_L = \begin{pmatrix} \psi_L \\ \vdots \\ 0 \end{pmatrix}, \quad \Psi_R = \begin{pmatrix} 0 \\ \vdots \\ \psi_R \end{pmatrix}. \quad (3.16)$$

The reader will note that fermions placed anywhere other than the first and N^{th} entries of these fundamentals will not contribute to the inflaton potential, since they will not couple to the rotated

⁵Equivalently

$$\int \frac{d^4 p_E}{(2\pi)^4} \left(\frac{\Pi_1^A}{\Pi_0^A} \right) \gg \int \frac{d^4 p_E}{(2\pi)^4} \frac{1}{2} \left(\frac{\Pi_1^A}{\Pi_0^A} \right)^2 \gg \int \frac{d^4 p_E}{(2\pi)^4} \frac{1}{3} \left(\frac{\Pi_1^A}{\Pi_0^A} \right)^3 \gg \dots \quad (3.13)$$

If the form factors behave as described in Section 3.5, then this is a reasonable approximation.

Σ (3.9). We place ψ_L and ψ_R in two separate fundamentals for the sake of generality – this arrangement will avoid cancellations between terms that would occur if we used the embedding

$$\begin{pmatrix} \psi_L \\ \vdots \\ \psi_R \end{pmatrix}. \quad (3.17)$$

The most general $SO(N)$ invariant effective Lagrangian we can write down, up to quadratic order in the fermion fields, is

$$\mathcal{L}_{eff} = \sum_{r=L,R} \bar{\Psi}_r^i \not{p} \left[\Pi_0^r(p) \delta_{ij} + \Pi_1^r(p) \Sigma_i \Sigma_j \right] \Psi_r^j + M(p) \bar{\Psi}_L^i \Sigma_i \Sigma_j \Psi_R^j + h.c., \quad (3.18)$$

which can be rewritten:

$$\begin{aligned} \mathcal{L}_{eff} = & \bar{\psi}_L \not{p} \left[\Pi_0^L(p) + \Pi_1^L(p) \sin^2(\phi/f) \right] \psi_L + \bar{\psi}_R \not{p} \left[\Pi_0^R(p) + \Pi_1^R(p) \cos^2(\phi/f) \right] \psi_R \\ & + M(p) \sin(\phi/f) \cos(\phi/f) \bar{\psi}_L \psi_R + h.c. \end{aligned} \quad (3.19)$$

We can derive the Coleman-Weinberg potential using the formula

$$V = -\frac{1}{2} N_c \int \frac{d^4 p_E}{(2\pi)^4} \text{Tr} \left[\log \left(\mathcal{M} \mathcal{M}^\dagger \right) \right], \quad (3.20)$$

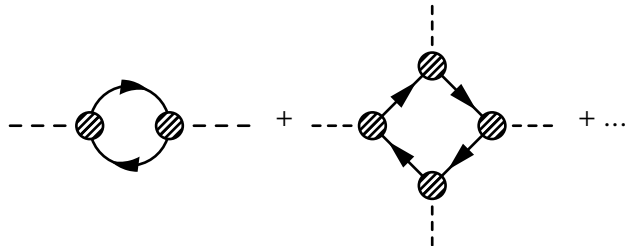
which is correct up to terms independent of ϕ . Here N_c is the number of fermion colours and

$$\mathcal{M}_{ij} = \frac{\partial^2 \mathcal{L}}{\partial \psi^i \partial \bar{\psi}^j}, \quad (3.21)$$

for all fermions ψ^i . We obtain, up to terms independent of ϕ :

$$\begin{aligned} V = -2N_c \int \frac{d^4 p_E}{(2\pi)^4} \log \left[1 + \frac{\Pi_1^L}{\Pi_0^L} \sin^2(\phi/f) + \frac{\Pi_1^R}{\Pi_0^R} \cos^2(\phi/f) + \frac{\Pi_1^L}{\Pi_0^L} \frac{\Pi_1^R}{\Pi_0^R} \sin^2(\phi/f) \cos^2(\phi/f) \right. \\ \left. + \frac{M^2}{p_E^2 \Pi_0^L \Pi_0^R} \sin^2(\phi/f) \cos^2(\phi/f) \right]. \end{aligned} \quad (3.22)$$

The presence of the $\sin^2 \cos^2$ function inside the logarithm is essentially due to the fact that there are loops in which both ψ_L and ψ_R propagate. We have, among other diagrams, the series:



$$+ \dots \quad (3.23)$$

This series includes diagrams with $2n$ vertices (compare to (3.12), which sums over diagrams with n vertices). Thus the resummation leads to a higher order term in the argument of the log. Again we can expand the logarithm at first order to get a potential of the form:

$$V(\phi) = \alpha \sin^2(\phi/f) + \beta \sin^2(\phi/f) \cos^2(\phi/f). \quad (3.24)$$

This potential has a very flat region for $\alpha \simeq \beta$, the flat region being a maximum (minimum) for $\beta > 0$ ($\beta < 0$). For realistic inflation we require the flat region to be a local maximum, so that the inflaton can roll slowly down the potential. However, since we expect the Π_0 form factors to be positive (see, for example [117]), the expansion of the log gives a *negative* value for β^6 . The gauge contribution – being of the form $\sin^2(\phi/f)$ – will not help matters.

Therefore we turn to the next simplest option: embedding the fermions in *spinorial* representations of $SO(N)$. Spinors of $SO(N)$, for odd N , have the same number of components as spinors of $SO(N-1)$. The extra gamma matrix Γ^N is the chiral matrix, which in the Weyl representation is the only diagonal gamma matrix. Spinors of $SO(N)$ are built from two spinors of $SO(N-2)$ in the same way that Dirac spinors are constructed using two Weyl spinors. We denote these $SO(N-2)$ spinors $\chi_{L,R}$, and embed the fermions as follows:

$$\chi_{L,R} = \begin{pmatrix} \psi_{L,R} \\ 0 \\ \vdots \end{pmatrix}, \quad (3.25)$$

and construct the full $SO(N)$ spinors thus:

$$\Psi_L = \begin{pmatrix} \chi_L \\ 0 \end{pmatrix}, \quad \Psi_R = \begin{pmatrix} 0 \\ \chi_R \end{pmatrix}. \quad (3.26)$$

This embedding is chosen so as to ultimately give a coupling between ψ_L and ψ_R – other embeddings that achieve this will lead to the same eventual result. The $SO(N)$ invariant effective Lagrangian takes the form

$$\mathcal{L}_{eff} = \sum_{r=L,R} \bar{\Psi}_r^i \not{p} \left[\Pi_0^r(p) \delta_{ij} + \Pi_1^r(p) \Gamma_{ij}^a \Sigma^a \right] \Psi_r^j + M(p) \bar{\Psi}_L^i \Gamma_{ij}^a \Sigma^a \Psi_R^j + h.c., \quad (3.27)$$

where Γ^a are the Gamma matrices of $SO(N)$. If we take

$$\Gamma^1 = \begin{pmatrix} 0 & I \\ I & 0 \end{pmatrix}, \quad \Gamma^N = \begin{pmatrix} I & 0 \\ 0 & -I \end{pmatrix} \quad (3.28)$$

this can be expanded to give:

$$\begin{aligned} \mathcal{L}_{eff} = & \bar{\Psi}_L \not{p} \left[\Pi_0^L(p) + \Pi_1^L(p) \cos(\phi/f) \right] \Psi_L + \bar{\Psi}_R \not{p} \left[\Pi_0^R(p) - \Pi_1^R(p) \cos(\phi/f) \right] \Psi_R \\ & + M(p) \sin(\phi/f) \bar{\Psi}_L \Psi_R + h.c. \end{aligned} \quad (3.29)$$

Combined with the gauge contribution, this will lead to the potential:

$$V(\phi) = \alpha \cos(\phi/f) + \beta \sin^2(\phi/f), \quad (3.30)$$

⁶Note that the $(\Pi_1^L \Pi_1^R)/(\Pi_0^L \Pi_0^R)$ term cancels other terms at next order in the expansion, so does not contribute to the potential.

where

$$\alpha = -2N_c \int \frac{d^4 p_E}{(2\pi)^4} \left(\frac{\Pi_1^L}{\Pi_0^L} - \frac{\Pi_1^R}{\Pi_0^R} \right), \quad \beta = \int \frac{d^4 p_E}{(2\pi)^4} \left(\frac{3(N-2)}{4} \frac{\Pi_1^A}{\Pi_0^A} - 2N_c \frac{M^2}{p_E^2 \Pi_0^L \Pi_0^R} \right). \quad (3.31)$$

This potential has a flat maximum for $\alpha \simeq 2\beta$, $\beta > 0$. The gauge contribution can now give us a positive value for β . Thus, for a region of parameter space, this is a viable inflationary potential.

Including more fermions in our model will lead to a wider class of diagrams contributing to the Coleman-Weinberg potential. If we expand consistently to first order in Π_1/Π_0 and $(M/\Pi_0)^2$ however, the only terms that appear at leading order will be those coming from diagrams in which only a single fermion, or an alternating pair of fermions, propagates around the loop. Equation (3.30) will therefore be the generic leading order result, although the coefficients will be modified. In particular, α will be given generally by

$$\alpha = -2N_c \int \frac{d^4 p_E}{(2\pi)^4} \left(\sum_i (-1)^{a_i} \frac{\Pi_1^i}{\Pi_0^i} \right), \quad (3.32)$$

where $a_i = 0$ if ψ_i is embedded in the upper half of an $SO(N)$ spinor, and $a_i = 1$ if ψ_i is embedded in the lower half.

We should also consider whether including NLO terms in the log expansion changes any of the above conclusions. Assuming that the log expansion is valid, we expect the NLO terms to be suppressed. A small $\sin^4(\phi/f)$ or $\cos(\phi/f) \sin^2(\phi/f)$ addition to the potential will only have the effect of changing slightly the conditions on the coefficients. For example, the potential

$$V(\phi) = \alpha \cos(\phi/f) + \beta \sin^2(\phi/f) + \delta \cos(\phi/f) \sin^2(\phi/f), \quad (3.33)$$

has the flatness condition $\alpha = 2(\beta + \delta)$.

To satisfy the phenomenological constraint that the inflaton potential should be zero at its minimum $V(\phi_{min}) = 0$, we now insert a constant term C_Λ by hand:

$$V(\phi) = C_\Lambda + \alpha \cos(\phi/f) + \beta \sin^2(\phi/f). \quad (3.34)$$

In this case, $C_\Lambda = \alpha$. As conventional when writing inflaton potentials we may factor out a scale Λ^4 to obtain (3.3), with a redefinition of the coefficients α and β .

The result that fermions in *fundamental* representations cannot induce a satisfactory inflation potential holds generically for any group, for precisely the reasons outlined above. It is for this reason that we did not consider $SU(N)$ symmetries, since the only single-index representations of $SU(N)$ are fundamental (or anti-fundamental) representations. Embedding fermions in spinorial representations will generally lead, at first order, to a potential of the form (3.30). Since spinorial representations only exist in $SO(N)$, we conclude that an $SO(N)$ symmetry of the strong sector is the simplest and most natural way to generate a realistic inflaton potential. Isomorphisms such

as $SO(6) \simeq SU(4)$ and $SO(4) \simeq SU(2) \times SU(2)$ allows us to extend this result a little further. For example, embedding fermions in a vector of $SO(4)$ should lead to the same result as fermions embedded in a $(2, 2)$ of $SU(2) \times SU(2)$.

3.3 CONSTRAINTS FROM INFLATION

After our discussion of the general structure of the inflaton potential, let us discuss the restrictions coming from inflation. We list some potentials that can give rise to inflation in Table 3.1.

We parameterise the flatness of the potential as usual in the slow roll approximation (SRA). That is, we require $\epsilon \ll 1$ and $\eta \ll 1$, where ϵ and η are here given by

$$\epsilon = \frac{M_P^2}{2} \left(\frac{V'(\phi)}{V(\phi)} \right)^2 \quad \text{and} \quad \eta = M_P^2 \frac{V''(\phi)}{V(\phi)}. \quad (3.35)$$

To simplify our expressions, in this section we work in units of reduced Planck mass M_P ; that is, we will rescale our parameters $\phi \rightarrow \frac{\phi}{M_P}$ and $f \rightarrow \frac{f}{M_P}$.

The number of e-foldings in the slow-roll approximation is then given by

$$N = \frac{1}{\sqrt{2}} \int_{\phi_E}^{\phi_I} \frac{1}{\sqrt{\epsilon}} \quad (3.36)$$

where ϕ_E is fixed as the field value for which either $\epsilon = 1$ or $\eta = 1$, in other words, the field value for which the SRA breaks down. In our models slow roll breaks down by the second condition. Here and in the following we conservatively choose $N = 60$ for our predictions, and this allows us to find the initial condition for ϕ .

We compare the predictions of our model and the CMB data for the spectral tilt and the tensor-to-scalar ratio, which can be expressed in the SRA as

$$n_s = 1 + 2\eta - 6\epsilon \quad (3.37)$$

$$r = 16\epsilon \quad (3.38)$$

respectively.

A generic potential for a pseudo-Goldstone boson would contain powers of periodic functions, $c_\phi = \cos \phi/f$ and $s_\phi = \sin \phi/f$, which we parametrize as

$$V(\phi) = \Lambda^4 (C_\Lambda + \sum_n \alpha_n c_\phi^n + \beta_n s_\phi^n) \quad (3.39)$$

The derivatives of this potential are again proportional to the same periodic functions. Roughly speaking, the flatness of the potential can be achieved in two ways. One possibility is setting

Model	$ \tilde{\beta} = \beta/\alpha $	$\beta/ \beta $	C_Λ (pheno)
$V = \Lambda^4 \left(C_\Lambda + \alpha \cos \frac{\phi}{f} + \beta \sin \frac{\phi}{f} \right)$	Like vanilla NI: no solution for $f \leq M_p$	+/-	$C_\Lambda = \sqrt{\alpha^2 + \beta^2}$
$V = \Lambda^4 \left(C_\Lambda + \alpha \cos \frac{\phi}{f} + \beta \sin^2 \frac{\phi}{f} \right)$ $= \Lambda^4 \left(\tilde{C}_\Lambda + \alpha \cos \frac{\phi}{f} - \beta \cos^2 \frac{\phi}{f} \right)$	$\lesssim 1/2$	+	$C_\Lambda = \alpha$ $\tilde{C}_\Lambda = \alpha + \beta$
$V = \Lambda^4 \left(C_\Lambda + \alpha \sin^2 \frac{\phi}{f} + \beta \sin^2 \frac{\phi}{f} \cos^2 \frac{\phi}{f} \right)$ $= \Lambda^4 \left(\bar{C}_\Lambda - \alpha \cos^2 \frac{\phi}{f} + \beta \sin^2 \frac{\phi}{f} \cos^2 \frac{\phi}{f} \right)$ $= \Lambda^4 \left(C_\Lambda + (\alpha + \beta) \sin^2 \frac{\phi}{f} - \beta \sin^4 \frac{\phi}{f} \right)$ $= \Lambda^4 \left(\bar{C}_\Lambda + (\beta - \alpha) \cos^2 \frac{\phi}{f} - \beta \cos^4 \frac{\phi}{f} \right)$	$\lesssim 1/2$	+	$C_\Lambda = \alpha$ $\bar{C}_\Lambda = 2\alpha$

Table 3.1: Goldstone models for inflation: Trigonometric inflationary potentials, grouped by equivalence upon a rotation in parameter space.

the argument, ϕ/f , to be very small (modulo 2π) as in the Natural Inflation scenario. As the fluctuations of the inflaton can be large, this condition typically implies $f \gtrsim M_p$, hence spoiling the predictivity of the model.

Another possibility, and that is what we pursue here, is to look for models with $f < M_p$, which in turn implies that two oscillating terms contribute to the flatness of the potential. This may seem like it would introduce fine-tuning in the model, but in the next section we quantify that tuning, finding it is milder than e.g. Supersymmetry with TeV scale superpartners.

Note that different models are equivalent from a cosmological perspective and can be transformed into each other by a rotation in parameter space. We list these redefinitions of the parameters and the cosmological constant in Table 3.1 as well.

In the limit that the ratio $\tilde{\beta} = \beta/\alpha$ is $\pm 1/2$, the potential is exactly flat at the origin and the spectrum is scale-invariant, i.e. $n_s = 1$ as shown in Fig. 4.2.

As the Planck data indicates a small deviation from scale invariance, we expect a small deviation of $\tilde{\beta}$ with respect to $1/2$. We find that the smaller f compared to M_p , the closer $\tilde{\beta}$ must be to the values in the table. The deviation $\delta\tilde{\beta} = 1/2 - \beta$ is then

$$1 \times 10^{-2} \left(\frac{f}{M_p} \right)^2 < \delta\tilde{\beta} < 2 \times 10^{-2} \left(\frac{f}{M_p} \right)^2 \quad (3.40)$$

for all models in the table, but most importantly the model motivated in the previous section (3.34).

This is the range of $\tilde{\beta}$ for which the model is compatible with the Planck data, as we plot in Fig. 3.3. for the well motivated example $V = \Lambda^4 \left(C_\Lambda + \alpha \cos \phi/f + \beta \sin^2 \phi/f \right)$. Our models

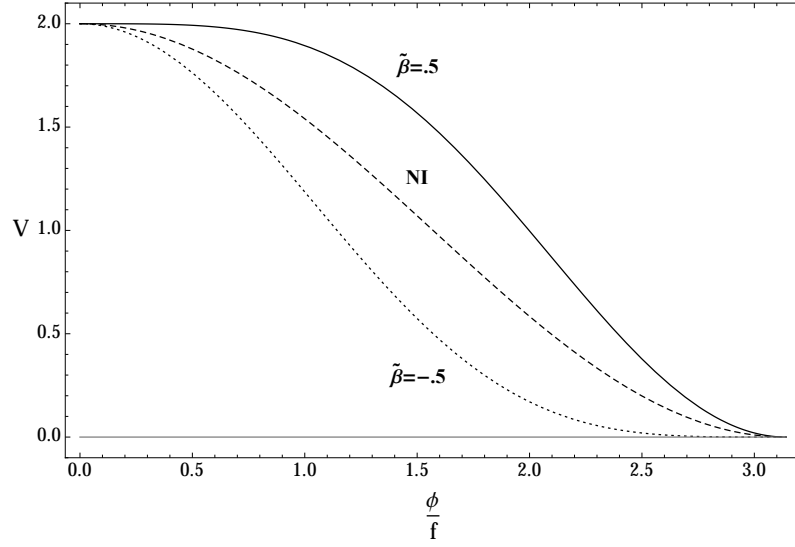


Figure 3.2: Shape of the potential for $\tilde{\beta} = \pm 1/2$ respectively. Different values will interpolate between these extreme cases. We show the shape of the vanilla NI (3.2) for comparison. The height of the potential is normalised to Λ .

predict negligible tensors, so the measurement of r imposes no constraint on $\tilde{\beta}$. In fact, the tensor to scalar ratio will scale as

$$r \propto \left(\frac{f}{M_p} \right)^4 \quad (3.41)$$

such that the lower the symmetry breaking scale, the smaller the predicted tensor modes are.

The scale of inflation can be found from the amplitude of the scalar power spectrum, as measured by Planck [14],

$$A_s = \frac{\Lambda^4}{24\pi^2 M_p^4 \epsilon} = \frac{e^{3.089}}{10^{10}} \quad (3.42)$$

where $\epsilon = r/16$ is the first slow roll parameter. For our case this implies

$$\Lambda_{inf} \approx 10^{15} \left(\frac{f}{M_p} \right) \text{ GeV}. \quad (3.43)$$

It is seen that Λ_{inf} is expected to be of order of the GUT scale, but can be lower if we allow for tuning. The symmetry breaking should occur before the onset of inflation, and therefore the scale f is expected to lie in the interval $\Lambda_{inf} < f < M_p$. Indeed, from the above relation, it is seen that $\Lambda_{inf} \approx 10^{-3} f$. Lowering the scale f as a result of more tuning thus directly results in lowering the scale inflation; for example, the model predicts $f \approx M_{GUT} \rightarrow \Lambda_{inf} \approx 10^{12} \text{ GeV}$ for $\delta\tilde{\beta} \approx 10^{-6}$. We will quantify the tuning in the model more precisely in the next section.

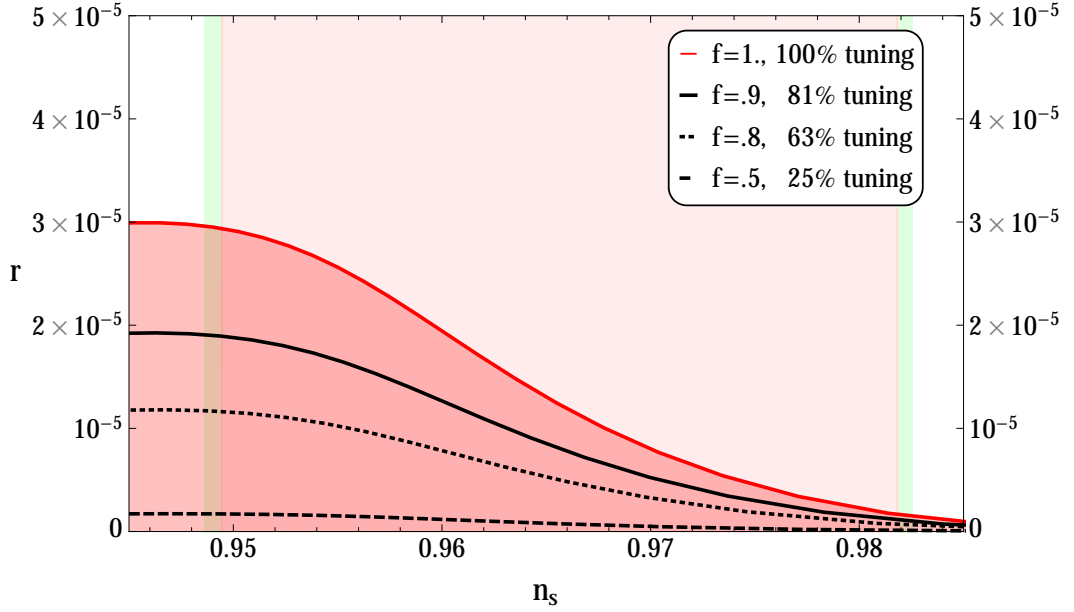


Figure 3.3: Parameters n_s and r plotted against the Planck 2015 data [14] for the model (3.34) for $f = M_p$ (red upper bound). For lower values $f < M_p$, $r \rightarrow 0$ (shaded region).

3.3.1 FINE-TUNING

One may note that the specific relationship between α and β in the model described above requires one to fine-tune it. Here we quantify the amount of fine-tuning that one will typically expect.

Defining tuning as is customary in Particle Physics [38], [118], we have⁷

$$\Delta = \left| \frac{\partial \log n_s}{\partial \log \tilde{\beta}} \right| = \left| \frac{\tilde{\beta}}{n_s} \frac{\partial n_s}{\partial \tilde{\beta}} \right| \approx [1.02 - 1.05] \left(\frac{f}{M_p} \right)^{-2} \quad (3.44)$$

This relation is not unexpected because for large $f > M_p$ the potential will very flat over a large field range $\Delta\phi$, and this flatness is not sensitive to the specific value of $\tilde{\beta}$. For $f < M_p$ one needs a (partial) cancelation in α and β , at the cost of fine-tuning.

Then we can define the percentage of tuning as

$$\text{Percentage tuning} = \frac{100}{\Delta} \% \approx 95 \left(\frac{f}{M_p} \right)^2 \%$$

It is seen in particular that if we take the upper bound $f = M_p$ seriously, the minimal tuning is at 95%. In Fig. 3.4 we plot the tuning Δ as defined in (4.35) for the model at hand, (3.3). It is seen that for $M_p/10 \lesssim f < M_p$ one expects no tuning below the percent level. One should note that $f < 10^{-2} M_p \approx M_{GUT}$ is not expected, as the symmetry breaking pattern should occur before the onset of inflation.

⁷Here we have chosen to measure tuning in terms of n_s , but one may instead be interested in the tuning of the combination $(n_s - 1)$. In this case one may use (4.35) to find $\Delta \approx [19.7 - 43.9] (f/M_p)^{-2}$. In both cases, the tuning in r is negligible compared to the tuning in the spectral index.

One can compare this amount of tuning with the one required to avoid the de-stabilization of the electroweak scale in Supersymmetry. For example, stops at 1 TeV require a much worse fine-tuning, at the level of 1% [119].

It is also noteworthy that the tuning necessary in the other models in Table 3.1 will be very similar to the tuning in $V = \Lambda^4 \left(C_\Lambda + \alpha \cos \phi/f + \beta \sin^2 \phi/f \right)$.

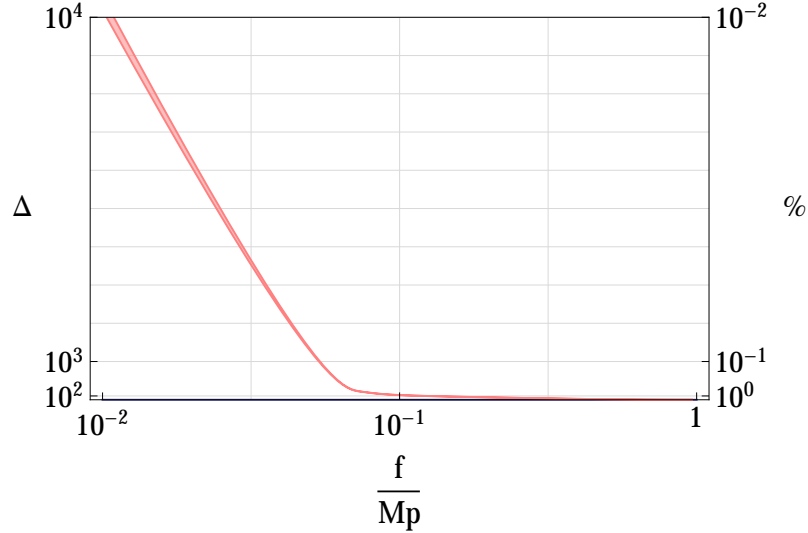


Figure 3.4: The parameter Δ as defined above for $V = \Lambda^4 \left(C_\Lambda + \alpha \cos \phi/f + \beta \sin^2 \phi/f \right)$. Outside of the pink zone the spectral index n_s predicted by the model is incompatible with the Planck data ($n_s < .948$ above the region, $n_s > .982$ below).

3.3.2 NON-GAUSSIANITY AND ITS RELATION TO GOLDSTONE SCATTERING

Even before switching on the Coleman Weinberg potential, Goldstone bosons interact with themselves through higher-order derivative terms. Indeed, consistent with the shift symmetry, one can write terms containing a number of derivatives of the field,

$$\mathcal{L} = \sum_n \frac{c_n}{f^{2n-4}} X^n, \text{ with } X = \frac{1}{2} \partial_\mu \Sigma \partial^\mu \Sigma^\dagger \quad (3.45)$$

The first order term ($n = 1$) is the usual kinetic term, whereas any other term ($n \geq 2$) would involve interactions of $2n$ pions. This expansion is called in the context of Chiral Perturbation Theory [120]–[122] as order $O(p^n)$ in reference to the number of derivatives involved. Goldstone self-interactions appear at order $O(p^4)$.

Alongside the Coleman-Weinberg potential we derived in the previous section, the derivative self-interactions are relevant for inflation as well, as a nontrivial speed of sound arises from a non-canonical kinetic term. Specifically, the sound speed is a parameterisation of the difference of the

coefficients of the spatial and temporal propagation terms for the Goldstone bosons ϕ :

$$\mathcal{L} \ni (\partial_t \phi)^2 - c_s^2 (\partial_i \phi)^2 \quad (3.46)$$

This difference arises from higher dimensional kinetic terms X^n and the fact that inflation breaks Lorentz invariance. This can of course already be seen from the metric,

$$ds^2 = (dt)^2 - a(t)^2 (dx_i)^2 \quad \rightarrow \quad g_{00} \neq g_{ii} \quad (3.47)$$

The speed of sound is then given by

$$c_s^2 = \left(1 + 2 \frac{X \mathcal{L}_{XX}}{\mathcal{L}_X} \right)^{-1} \quad (3.48)$$

where \mathcal{L}_X and \mathcal{L}_{XX} denote the first and the second derivative of the Lagrangian with respect to X respectively, and where c_s is expressed in units of the speed of light. It is immediately seen that models with a canonical kinetic term predict $c_s = 1$. The background equations of motion can be used to relate coefficients to the Hubble expansion parameter,

$$X \mathcal{L}_X = \dot{H} M_p^2 \approx c_1 f^4 \quad (3.49)$$

To second order, the kinetic term will have the form⁸

$$\mathcal{L}_2 = \frac{M_p^2 \dot{H} + M_p^2 \dot{H} (c_s - 1)}{f^4} (\partial_t \phi)^2 = \frac{M_p^2 \dot{H} c_s}{f^4} (\partial_t \phi)^2 \quad (3.50)$$

Canonically normalising the kinetic term thus implies,

$$f^4 = 2 \dot{H} M_p^2 c_s \quad (3.51)$$

These higher order derivatives are also constrained by arguments of unitarity, analyticity and crossing symmetry of Goldstone scattering amplitudes such as shown in Fig. 3.5,

$$\phi(p_1) \phi(p_2) \rightarrow \phi(p_3) \phi(p_4) . \quad (3.52)$$

This scattering amplitude must be a function of the Mandelstam parameters s , t and u , e.g. $s = (p_1 + p_2)^2 = (p_3 + p_4)^2$.⁹ This amplitude $A(s, t, u)$ must be analytical in the complex s plane, except for branch cuts (due to unitarity) and isolated points (due to the possible exchange of a resonance) [125]–[128]. Unitarity then implies the existence of a branch at some position $s \geq s_0$. Similarly, other branch crossings can be obtained by using crossing symmetry. Using these arguments, one can show that the amplitude would be non-analytical for $s > 4m_\phi^2$, where m_ϕ is the

⁸Here we use the expansions $\mathcal{L} \in (X \mathcal{L}_X + 2X^2 \mathcal{L}_{XX}) (\partial_t \phi)^2 / f^4$ and $c_s - 1 \approx \frac{X \mathcal{L}_{XX}}{\mathcal{L}_X}$

⁹In this simplified analysis we have neglected the curvature of space-time. Various issues related to the curvature, and the relevant assumptions one should make to obtain the positivity constraint were discussed in [123] and [124].

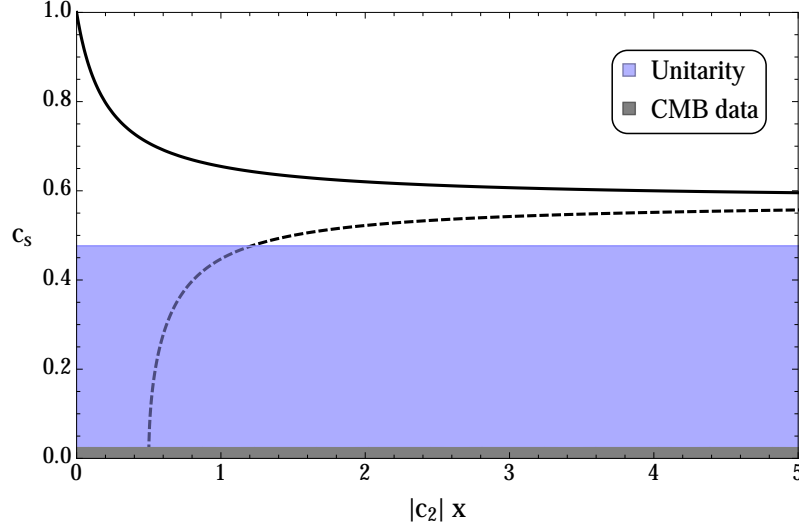


Figure 3.5: Predictions for $c_2 x$. In dark grey the Planck bound; the shaded region indicates the perturbativity bound. The continuous lines are the predictions for $c_2 > 0$, which is relevant for our model as discussed in the text. We also indicate the hypothetical situation $c_2 < 0$ with dashed curves. It is seen that the prediction approaches the asymptote $c_s = 1/\sqrt{3}$ for large c_2 , as expected from (3.55).

mass of the pseudo-Goldstone. Moreover, analyticity restricts the dependence of the amplitude on s , namely

$$\frac{d^2}{ds^2} A(s, t, u) \geq 0 \quad (3.53)$$

where s , t and u are restricted to the physical region, e.g. $s \leq 4m_\phi^2$. This translates into bounds for the coefficients of the Lagrangian in (3.45). At leading order in the Goldstone interactions,

$$\mathcal{L}^{(p^4)} = c_2 f^{-4} (\partial_\mu \phi^\dagger \partial^\mu \phi)^2 \quad (3.54)$$

the aforementioned conditions lead to a bound for c_2 . In particular, c_2 must be positive and larger than some function of the Goldstone mass.¹⁰

The positivity of c_2 constrains possible deviations from the speed of sound in the model with Goldstone inflatons. Indeed,

$$c_s = \left(1 + 2 \frac{2c_2 X}{f^2 + 2c_2 X} \right)^{-1/2} = \left(1 + 2 \frac{2c_2 x}{1 + 2c_2 x} \right)^{-1/2} \quad (3.55)$$

Where we have defined the dimensionless parameter $x = X/f^2$. As $X \sim p^2$, we expect the effective theory to be valid up to

$$X \leq (4\pi f)^2 \quad \text{or} \quad x \leq (4\pi)^2 \quad (3.56)$$

¹⁰Note that c_2 in the case of two- and three-flavour QCD have been computed, assuming that its dominant contribution comes from vector meson exchange [129], [130] or with the inclusion of scalar and pseudo-scalar resonances [131]

The current bound by Planck is $c_s > .024$ [14]. In Fig. 3.5 one can see how for positive c_2 the speed of sound is in agreement with Planck for any value of $c_2 x$.

As mentioned above, the sound speed is also constrained by arguments of (perturbative) unitarity. The scale at which violation of perturbative unitarity occurs was computed by Ref. [132] (and corrected in [133]) from imposing partial wave unitarity in the quartic interaction, and reads,

$$\Lambda_u^4 = \frac{24\pi}{5} \left(\frac{2M_p^2 |\dot{H}| c_s^5}{1 - c_s^2} \right) \quad (3.57)$$

We are in particular concerned with how Λ_u relates to the symmetry breaking scale f . If $\Lambda_u < f$, the action needs a completion below the symmetry breaking scale, possibly in terms of strongly coupled dynamics or new low-energy physics. The effective theory is therefore no longer a good description. One may thus consider a critical sound speed $(c_s)_*$, defined by [133]

$$\Lambda_u^4 = \frac{24\pi}{5} \left(\frac{2M_p^2 |\dot{H}| (c_s)_*^5}{1 - (c_s)_*^2} \right) = f^4 \quad (3.58)$$

For $c_s > (c_s)_*$ our model predicts $\Lambda_u > f$. Canonically normalising using (3.51), we have

$$\frac{24\pi}{5} \left(\frac{(c_s)_*^4}{1 - (c_s)_*^2} \right) > 1 \quad (3.59)$$

This theoretical lower bound is also shown in Fig. 3.5 for different values of x (subject to (3.56)). One can see how, once axiomatic conditions from Goldstone scattering are imposed, the inflaton evades both bounds.

The speed of sound is related to non-Gaussianity by

$$f_{NL}^{eq} \sim \frac{1}{c_s^2} \quad (3.60)$$

One does not expect significant contributions to non-Gaussianity from the non-derivative terms in the potential, as they will be slow-roll suppressed.

It is worth noting that a deviation from one in the speed of sound will modify the tensor to scalar ratio

$$r = 16\epsilon c_s \quad (3.61)$$

The predictions for r will in this case be lowered, but as the Planck bound is consistent with $r = 0$, this is only to the merit of models with a pGB inflaton.

3.4 LINK TO UV MODELS

We saw above that the model (3.3) gives inflation compatible with the CMB data for particular relations between the coefficients. Here we discuss what these relations indicate for the UV theory.

Firstly, we noticed that to have the right shape of the potential, we should require β to be positive, that is

$$\beta = \int \frac{d^4 p_E}{(2\pi\Lambda)^4} \left(\frac{3(N-2)}{4} \frac{\Pi_1^A}{\Pi_0^A} - 2N_c \frac{M^2}{p_E^2 \Pi_0^L \Pi_0^R} \right) > 0 \quad (3.62)$$

Then we saw in Table table that the requirement of a sufficiently flat potential gives the condition $\alpha \approx 2\beta$, which will give a relation between the form factors of the form

$$\begin{aligned} \alpha &= -2N_c \int \frac{d^4 p_E}{(2\pi\Lambda)^4} \left(\frac{\Pi_1^L}{\Pi_0^L} - \frac{\Pi_1^R}{\Pi_0^R} \right) \\ &= 2 \int \frac{d^4 p_E}{(2\pi\Lambda)^4} \left(\frac{3(N-2)}{4} \frac{\Pi_1^A}{\Pi_0^A} - 2N_c \frac{M^2}{p_E^2 \Pi_0^L \Pi_0^R} \right) = 2\beta \end{aligned} \quad (3.63)$$

Lastly we have that the phenomenological condition $V(\phi_{min}) = 0$ gives a preferred value of the constant C_Λ in terms of the model parameters. In explicit models this will give a condition of the form¹¹

$$\alpha = -2N_c \int \frac{d^4 p_E}{(2\pi\Lambda)^4} \left[\frac{\Pi_1^L}{\Pi_0^L} - \frac{\Pi_1^R}{\Pi_0^R} \right] = C_\Lambda \quad (3.64)$$

where C_Λ is a cosmological constant during inflation.

To obtain explicit expressions for the form factors Π_X one would need a UV-complete theory. However, using the relations above we can make some general remarks about their large momentum behaviour. First, we can use an operator product expansion to find the scaling of Π_1 . This implies that Π_1 scales as $\langle O \rangle / p^{d-2}$, where O is the lowest operator responsible for the breaking $G \rightarrow H$, with mass dimension d . In our case, we expect O to be a fermion condensate with $d = 6$. Secondly we can require finiteness of the fermion Lagrangian (3.27). The scaling of the other form factors can be found by consideration of the kinetic terms in the high momentum limit. We will discuss this in the next section. We summarise our conclusions in Table 3.2.

In the next section we will assume a light resonance connection to derive more specific conclusions in this approximation.

3.5 LIGHT RESONANCE CONNECTION

In this section we attempt to derive some of the properties of the UV theory, assuming that the integrated-out dynamics is dominated by the lightest resonances of the strong sector.

¹¹Note that in some models C_Λ will be related to $\alpha \pm \beta \approx 3/2 \alpha$, as is seen in Table 3.1.

Form factor	Large momentum behaviour	Argument
Π_1	$\sim \langle O \rangle / p^{d-2} = 1/p^4$	OPE coupling
Π_0	$\sim p^2$	Recovering the bosonic Lagrangian
Π_1^r	$\sim 1/p^6$	OPE coupling
Π_0^r	$\sim p^0$	Recovering the fermion Lagrangian
M^r	$\sim 1/p^2$	OPE coupling

Table 3.2: *Connection to the UV theory:* Scaling of the form factors derived from an operator product expansion and symmetry restoration at high energies.

To simplify what follows, we note that the form factor M in equation (3.29) is ‘naturally’ small in the ’t Hooft sense [13]. This is because in the limit $M \rightarrow 0$ we have an enhanced $U(1)_L \times U(1)_R$ global symmetry under which ψ_L and ψ_R transform with independent phase-rotations. Therefore in the following we will assume that the dominant contributions to α and β come from the $\Pi_{0,1}^i$ form factors. Note that this observation makes it very plausible that condition (3.62) is satisfied.

Note that to ensure a convergent behaviour of the form factors at high scales Q^2 , one would have to introduce a number of resonances to saturate the Weinberg sum rules. The minimum number of resonances depends on the behaviour of the form factor with Q . This behaviour is described in the previous section. The convergence of these form factors in the large- Q regime is not a necessary condition for a generic model of strong interactions, but rather helps on describing the interpolation between the low-energy regime of the theory with an asymptotically free UV theory (provided this is the case).

Irrespective of these issues of interpolation with the UV behaviour, one can consider a spectral decomposition of the form factor. A common description, valid for a $SU(N)$ gauge sector in the large- N limit is form factors as infinite sums over narrow resonances of the strong dynamics [134], [135]. In the following, we assume that the Π_1^i form factors can be well approximated by considering only the contribution from the lightest of these resonances.

We expect that Π_1^i has a pole at the mass of the lightest resonance m_i^2 , and that the residue of this pole is equal to the square of the amplitude to create the resonance from the vacuum. This amplitude, f_i , is equivalent to the decay constant of the resonance. This leads us to the following approximation for the fermionic Π_1^i :

$$\Pi_1^i(p^2) = \frac{f_i^2}{p^2 + m_i^2}. \quad (3.65)$$

In the gauge case, this expression is modified to

$$\frac{1}{p^2} \Pi_1^A(p^2) = \frac{f^2}{p^2} + \frac{f_A^2}{p^2 + m_A^2}, \quad (3.66)$$

which now has a pole at $p^2 = 0$, since the broken $SO(N)/SO(N-1)$ currents can excite the Goldstones from the vacuum [21], [23].

We approximate the Π_0 form factors with their tree level values. By inspecting (3.7) and (3.27), we see that to recover the tree level fermion and gauge Lagrangians we must have $\Pi_0 = 1$ in the fermionic case, and $\Pi_0 = p^2/g^2$ in the gauge case, where g is the gauge coupling.

Let us study the minimal model we can construct that leads to successful inflation. We will only need one external fermion – in this case we take the ψ_R of Sec. 3.2. Then α and β will be given by

$$\alpha = 2N_c \int \frac{d^4 p}{(2\pi\Lambda)^4} \left(\frac{\Pi_1^R}{\Pi_0^R} \right), \quad \beta = \frac{3(N-2)}{4} \int \frac{d^4 p}{(2\pi\Lambda)^4} \left(\frac{\Pi_1^A}{\Pi_0^A} \right). \quad (3.67)$$

Now we assume that Π_1^R and Π_1^A are given respectively by (3.65) and (3.66). With a single resonance, we cannot guarantee convergence of the integrals in (3.67) – generally this can be done by introducing more resonances and demanding that the form factors satisfy Weinberg sum rules [136], [137]. However we can argue that, since our effective theory is only expected to be valid up to a scale $\Lambda_{UV} = 4\pi f$, we should cut off the momentum integrals at $p^2 = \Lambda_{UV}^2$.

Putting all this together, we find:

$$\alpha = \frac{a}{8\pi^2\Lambda^4} \int_0^{\Lambda_{UV}^2} dp^2 \frac{p^2 f_R^2}{p^2 + m_R^2} = \frac{a f_R^2}{8\pi^2\Lambda^4} \left[\Lambda_{UV}^2 - m_R^2 \log \left(\frac{m_R^2 + \Lambda_{UV}^2}{m_R^2} \right) \right], \quad (3.68)$$

where $a = 2N_c$, and

$$\beta = \frac{b g^2}{8\pi^2\Lambda^4} \int_0^{\Lambda_{UV}^2} dp^2 f^2 = \frac{b g^2}{8\pi^2} \left[\Lambda_{UV}^2 f^2 + \Lambda_{UV}^2 f_A^2 - f_A^2 m_A^2 \log \left(\frac{m_A^2 + \Lambda_{UV}^2}{m_A^2} \right) \right], \quad (3.69)$$

where $b = 3(N-2)/4$.

The approximate relation $\alpha \simeq 2\beta$ then implies a relationship between the parameters of the UV theory. If we demand that the quadratic cutoff dependence cancels, we obtain the relation

$$a f_R^2 = 2b g^2 (f^2 + f_A^2), \quad (3.70)$$

and

$$a f_R^2 m_R^2 \log \left(\frac{m_R^2 + \Lambda_{UV}^2}{m_R^2} \right) = 2b g^2 f_A^2 m_A^2 \log \left(\frac{m_A^2 + \Lambda_{UV}^2}{m_A^2} \right). \quad (3.71)$$

Inserting (3.70) into (3.71) we obtain

$$\frac{2b g^2 f_A^2}{a f_R^2} = \frac{f_A^2}{f^2 + f_A^2} = \frac{m_R^2 \log[(m_R^2 + \Lambda_{UV}^2)/m_R^2]}{m_A^2 \log[(m_A^2 + \Lambda_{UV}^2)/m_A^2]}, \quad (3.72)$$

which implies that $m_R < m_A$.

If $f_A \gg f$, one finds that $m_R \simeq m_A$, i.e. there would be a degeneracy between fermionic and bosonic resonances. Note that this condition will be satisfied no matter the scale factor between α and β is, as long as they are proportional, $\alpha \propto \beta$. This kind of *mass-matching* situation [100],

[101], [138] where resonances from different sectors acquire the same mass is reminiscent of what had been found in trying to build successful Technicolor models, namely Cured Higgsless [103], [104] and Holographic Technicolor [98], [99] models.

3.6 DISCUSSION AND CONCLUSIONS

The framework of slow-roll inflation has been corroborated to a good precision by the Planck data. This framework, however, suffers from an *inflationary hierarchy problem*, namely the strain of providing sufficient inflation while still satisfying the amplitude of the CMB anisotropy measurements. This balancing act requires a specific type of potential, with a width much larger than its height.

This tuning is generically unstable unless some symmetry protects the form of the potential. In this paper we explored the idea that this potential could be related to the inflaton as a Goldstone boson, arising from the spontaneous breaking of a global symmetry.

Another issue for inflationary potentials, including Goldstone Inflation, is that they are only effective descriptions of the inflaton physics. With the inflationary scale relatively close to the scale of Quantum Gravity, one expects higher-dimensional corrections to the inflationary potential. These corrections would de-stabilise the inflationary potential unless the model is small-field [87], [105]. In other words, as the inflaton field value approaches M_p , the Effective Theory approach breaks down.

We found out that in Goldstone Inflation a predictive effective theory is indeed possible, and that the compatibility with data has specific implications for the theory. For example, in single-field inflation, we computed the most general Coleman-Weinberg inflaton potential and learnt that 1.) Only the breaking of $SO(N)$ groups provide successful inflation and 2.) fermionic and bosonic contributions to the potential must be present and 3.) for fermions in single-index representations, a successful inflaton potential is given uniquely by $V = \Lambda^4(C_\Lambda + \alpha \cos(\phi/f) + \beta \sin^2(\phi/f))$, with $\alpha \approx 2\beta$. When linking to UV completions of Goldstone Inflation, we have been able to show how relations among the fermionic and bosonic resonances are linked to the flatness of the potential.

As we have developed a specific model for inflation, we were able to address the amount of tuning required to make it work, and found that it is not dramatic. Indeed, we found that the tuning is milder than that found in Supersymmetric models nowadays.

Another advantage of this framework is the ability to examine the higher-order derivative terms in the Goldstone Lagrangian from several different points of view: modifications of the

CMB speed of sound, constraints from unitarity and also axiomatic principles from Goldstone scattering.

We have presented results in a rather generic fashion and for single-field inflation, and delegated to the appendices a discussion of a specific model of single-field inflation, and few examples of hybrid inflation which originate from this framework.

There are other aspects of Goldstone Inflation which deserve further study. For example, in these models, hybrid inflation and reheating are quite predictive as the inflaton and waterfall fields come from the same object and naturally the inflaton can decay to other, lighter pseudo-Goldstones. Moreover, there may be interesting features of the phase transition causing the spontaneous breaking of the global symmetry, which we plan to investigate.

ACKNOWLEDGEMENTS

We would like to thank Juanjo Sanz-Cillero for discussion on the Goldstone boson scattering, and Ewan Tarrant for explaining aspects of reheating. This work is supported by the Science Technology and Facilities Council (STFC) under grant number ST/L000504/1.

APPENDIX A: SUCCESSFUL PATTERNS OF BREAKING: AN EXAMPLE OF SINGLE FIELD

The simplest instance of the general model outlined in Section 3.2 takes the global symmetry of the strong sector to be $SO(3)$, breaking to $SO(2)$.¹² This gives rise to two Goldstone bosons, one of which is eaten when we gauge the remaining $SO(2)$ symmetry. We parameterise the Goldstones via:

$$\Sigma(x) = \exp(iT^{\hat{a}}\phi^{\hat{a}}/f)\Sigma_0, \quad (3.73)$$

with $\hat{a} = 1, 2$. We can take the generators of $SO(3)$ to be

$$T^1 = \frac{i}{\sqrt{2}} \begin{pmatrix} 0 & 0 & 0 \\ 0 & 0 & -1 \\ 0 & 1 & 0 \end{pmatrix}, \quad T^2 = \frac{i}{\sqrt{2}} \begin{pmatrix} 0 & 0 & 1 \\ 0 & 0 & 0 \\ -1 & 0 & 0 \end{pmatrix}, \quad T^3 = \frac{i}{\sqrt{2}} \begin{pmatrix} 0 & -1 & 0 \\ 1 & 0 & 0 \\ 0 & 0 & 0 \end{pmatrix}. \quad (3.74)$$

The broken generators satisfy $T^{\hat{a}}\Sigma_0 \neq 0$. If, following Sec. 3.2, we take Σ_0 to be

$$\Sigma_0 = \begin{pmatrix} 0 \\ 0 \\ 1 \end{pmatrix}, \quad (3.75)$$

then T^1 and T^2 are the broken generators. T^3 remains unbroken, and will generate the $SO(2)$ gauge symmetry. A suitable gauge transformation then allows us to set $\phi^1 = \phi$, $\phi^2 = 0$, and we can write

$$\Sigma = \begin{pmatrix} \sin(\phi/f) \\ 0 \\ \cos(\phi/f) \end{pmatrix}. \quad (3.76)$$

Following (3.7) the effective Lagrangian for the $SO(2)$ gauge boson is

$$\mathcal{L}_{eff} = \frac{1}{2}(P_T)^{\mu\nu} \left[\Pi_0^A(p^2) A_\mu^3 A_\nu^3 \text{Tr}\{T^3 T^3\} + \Pi_1^A(p^2) A_\mu^3 A_\nu^3 \Sigma^T T^3 T^3 \Sigma \right], \quad (3.77)$$

$$= \frac{1}{2}(P_T)^{\mu\nu} \left[\Pi_0^A(p^2) + \frac{1}{2}\Pi_1^A(p^2) \sin^2(\phi/f) \right] A_\mu^3 A_\nu^3. \quad (3.78)$$

This leads to the Coleman-Weinberg potential

$$V = \frac{3}{2} \int \frac{d^4 p}{(2\pi)^4} \log \left[1 + \frac{1}{2} \frac{\Pi_1^A}{\Pi_0^A} \sin^2(\phi/f) \right]. \quad (3.79)$$

Now we embed a fermion in an $SO(3)$ spinor:

$$\Psi_L = \begin{pmatrix} \psi_L \\ 0 \end{pmatrix}. \quad (3.80)$$

¹²This coset was also studied in the context of inflation in [139].

The gamma matrices of $SO(3)$ can be taken to be the Pauli matrices σ^a . Thus the most general effective Lagrangian for the fermion is

$$\mathcal{L}_{eff} = \bar{\Psi}_L \not{p} \left[\Pi_0^L(p) + \Pi_1^L(p) \sigma^a \Sigma^a \right] \Psi_L. \quad (3.81)$$

We find that

$$\sigma^a \Sigma^a = \begin{pmatrix} \cos(\phi/f) & \sin(\phi/f) \\ \sin(\phi/f) & -\cos(\phi/f) \end{pmatrix}, \quad (3.82)$$

so

$$\mathcal{L}_{eff} = \bar{\Psi}_L \not{p} \left[\Pi_0^L(p) + \Pi_1^L(p) \cos(\phi/f) \right] \Psi_L, \quad (3.83)$$

from which we derive the Coleman-Weinberg potential:

$$V = -2N_c \int \frac{d^4 p}{(2\pi)^4} \log \left[1 + \frac{\Pi_1^L}{\Pi_0^L} \cos(\phi/f) \right]. \quad (3.84)$$

Combining both gauge and fermion contributions, and expanding the logs at first order, we obtain

$$V(\phi) = \alpha \cos(\phi/f) + \beta \sin^2(\phi/f), \quad (3.85)$$

where

$$\alpha = -2N_c \int \frac{d^4 p}{(2\pi)^4} \left(\frac{\Pi_1^L}{\Pi_0^L} \right), \quad \beta = \frac{3}{4} \int \frac{d^4 p}{(2\pi)^4} \left(\frac{\Pi_1^A}{\Pi_0^A} \right). \quad (3.86)$$

APPENDIX B: SUCCESSFUL PATTERNS OF BREAKING: AN EXAMPLE OF HYBRID INFLATION

We can also construct models in which more than one physical Goldstone degree of freedom is left in the spectrum. This can be done by only gauging a subgroup of the unbroken $SO(N-1)$ symmetry. Let us look briefly at a simple example of such a model, in which we take the global symmetry breaking to be $SO(5) \rightarrow SO(4)$. In such a case we have four Goldstone bosons, and Σ is given by

$$\Sigma = \frac{\sin(\phi/f)}{\phi} \begin{pmatrix} \phi^1 \\ \phi^2 \\ \phi^3 \\ \phi^4 \\ \phi \cot(\phi/f) \end{pmatrix}, \quad (3.87)$$

where we have $\phi = \sqrt{\phi^{\hat{a}} \phi^{\hat{a}}}$, as before.

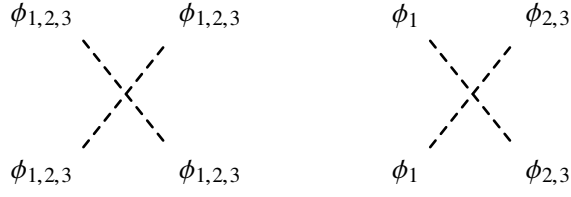


Figure 3.6: Goldstone quartic interactions

If we gauge only $SO(2) \in SO(4)$, taking for instance the gauged generator to be

$$T_g^1 = \frac{i}{\sqrt{2}} \begin{pmatrix} 0 & 0 & 0 & -1 & 0 \\ 0 & 0 & 0 & 0 & 0 \\ 0 & 0 & 0 & 0 & 0 \\ 1 & 0 & 0 & 0 & 0 \\ 0 & 0 & 0 & 0 & 0 \end{pmatrix}, \quad (3.88)$$

then the gauge freedom allows us to set $\phi^4 = 0$.

Following the same steps as before, the effective Lagrangian for the gauge field will be

$$\mathcal{L}_{eff} = \frac{1}{2} (P_T)^{\mu\nu} \left[\Pi_0^A(p^2) + \frac{1}{2} \Pi_1^A(p^2) \left(\frac{\phi^1}{\phi} \right)^2 \sin^2(\phi/f) \right] A_\mu A_\nu. \quad (3.89)$$

If we, as in Appendix 3.6, consider the contribution from a single left-handed fermion, now embedded in an $SO(5)$ spinor like so:

$$\Psi_L = \begin{pmatrix} \psi_L \\ 0 \\ 0 \\ 0 \end{pmatrix}, \quad (3.90)$$

then in fact the effective fermion Lagrangian will still be given by (3.83). Thus the Coleman-Weinberg potential will be given by

$$V(\phi) = \alpha \cos(\phi/f) + \beta \left(\frac{\phi_1}{\phi} \right)^2 \sin^2(\phi/f), \quad (3.91)$$

with α and β given by

$$\alpha = -2N_c \int \frac{d^4 p}{(2\pi)^4} \left(\frac{\Pi_1^L}{\Pi_0^L} \right), \quad \beta = \frac{3}{4} \int \frac{d^4 p}{(2\pi)^4} \left(\frac{\Pi_1^A}{\Pi_0^A} \right). \quad (3.92)$$

If we expand the trigonometric functions for small field excursions, we obtain, up to constant terms:

$$\begin{aligned} V(\phi_1, \phi_2, \phi_3) = & \frac{1}{f^2} \left(\beta - \frac{\alpha}{2} \right) \phi_1^2 - \frac{\alpha}{2f^2} (\phi_2^2 + \phi_3^2) + \frac{1}{f^4} \left(\frac{\alpha}{24} - \frac{\beta}{3} \right) \phi_1^4 \\ & + \frac{\alpha}{24f^4} (\phi_2^4 + \phi_3^4) + \frac{1}{f^4} \left(\frac{\alpha}{12} - \frac{\beta}{3} \right) (\phi_1^2 \phi_2^2 + \phi_1^2 \phi_3^2) + \frac{\alpha}{12f^4} \phi_2^2 \phi_3^2 + \mathcal{O} \left(\frac{\phi^6}{f^6} \right). \end{aligned} \quad (3.93)$$

We see that the three Goldstones have masses

$$m_1^2 = \beta - \alpha/2, \quad m_2^2 = m_3^2 = -\alpha/2, \quad (3.94)$$

and we have, among others, the quartic interactions shown in Fig. 3.6.

We can remove another of the Goldstone fields by gauging a further generator of $SO(2)$. For instance, if we gauge

$$T_g^2 = \frac{i}{\sqrt{2}} \begin{pmatrix} 0 & 0 & -1 & 0 & 0 \\ 0 & 0 & 0 & 0 & 0 \\ 1 & 0 & 0 & 0 & 0 \\ 0 & 0 & 0 & 0 & 0 \\ 0 & 0 & 0 & 0 & 0 \end{pmatrix}, \quad (3.95)$$

then the potential will be exactly as in (3.93), with ϕ_3 set to zero. We must also replace $\beta \rightarrow 2\beta$, since the potential now receives contributions from two gauge bosons.

We note further that if instead we gauged the generator

$$T_g^2 = \frac{i}{\sqrt{2}} \begin{pmatrix} 0 & 0 & 0 & 0 & 0 \\ 0 & 0 & -1 & 0 & 0 \\ 0 & 1 & 0 & 0 & 0 \\ 0 & 0 & 0 & 0 & 0 \\ 0 & 0 & 0 & 0 & 0 \end{pmatrix}, \quad (3.96)$$

then we obtain

$$V(\phi) = \alpha \cos(\phi/f) + \beta \left(\frac{\phi_1^2 + \phi_2^2}{\phi^2} \right) \sin^2(\phi/f) = \alpha \cos(\phi/f) + \beta \sin^2(\phi/f), \quad (3.97)$$

which is symmetric in ϕ_1 and ϕ_2 .

REHEATING WITH A COMPOSITE HIGGS

Djuna Croon¹, Verónica Sanz¹ and Ewan R. M. Tarrant¹

¹Department of Physics and Astronomy, Pevensey II Building, University of Sussex, BN1 9RH,
UK

The flatness of the inflaton potential and lightness of the Higgs could have the common origin of the breaking of a global symmetry. This scenario provides a unified framework of Goldstone Inflation and Composite Higgs, where the inflaton and the Higgs both have a pseudo-Goldstone boson nature. The inflaton reheats the Universe via decays to the Higgs and subsequent secondary production of other SM particles via the top and massive vector bosons. We find that inflationary predictions and perturbative reheating conditions are consistent with CMB data for sub-Planckian values of the fields, as well as opening up the possibility of inflation at the TeV scale. We explore this exciting possibility, leading to an interplay between collider data cosmological constraints.

4.1 INTRODUCTION

Scalar fields are popular protagonists in cosmological theories. They play chief roles in the leading paradigms for important events, such as inflation and electroweak symmetry breaking. However, it has been long known that fundamental scalars suffer radiative hierarchy problems: for theory to match observations, one requires an unnatural cancelation of UV corrections. In inflation, this radiative instability can be quantified by the tension between the Lyth bound [16] on the slow roll phase of the field, pushing towards $\Delta\phi > M_p$, and the measurement of CMB anisotropies, which indicate $\Lambda_{inf} \lesssim 10^{15}$ GeV. For electroweak symmetry breaking (EWSB), one usually considers the large separation of scales between the Higgs mass and the Planck scale as an illustration, as the latter is where the theory should be cut off for an elementary Higgs.

Here we will discuss the appeal of pseudo–Goldstone bosons (pGBs) for the dynamical generation of scales in both paradigms. The realisation that Goldstone bosons can solve hierarchy problems is not new: for EWSB, there is popular branch of model building that goes by Composite Higgs theory which postulates a new strongly coupled sector of which the Higgs is a bound state [19] (for a review see [23]). The effective theory then has a cut-off, such that the Higgs mass is not sensitive to effects above the compositeness scale.

Likewise, in inflationary model building “Natural Inflation” provides an inflaton candidate protected from UV corrections using essentially the same mechanism with an axionic GB [37]. Alas, vanilla Natural Inflation requires trans–Planckian scales to predict the measured Cosmic Microwave Background (CMB) spectrum and thus has questionable value as a valid effective theory.¹ In [61] the idea of a pGB inflaton was generalised, and it was shown there and in [63] that different models may realise inflation compatible with data from the Cosmic Microwave Background (CMB) without the issues that the original Natural Inflation has.

In this paper we will show how both mechanisms can be unified, thus realizing radiative stability for both models in a single simple set-up. We will explore the minimal symmetry breaking pattern that realises a Higgs $SU(2)$ doublet and an inflaton singlet. We discuss both the generation of an inflaton potential and reheating in this model. Interestingly, both can be fully perturbative processes. The inflationary predictions are shown to be compatible with the latest CMB data by Planck [14] without the necessity of introducing trans-Planckian scales in the effective theory. After inflation the inflaton decays into Higgs bosons, which subsequently decay into the Standard

¹There have been several proposals to explain the trans–Planckian decay constant while maintaining the simple potential and the explanatory power of the model. Among these are Extra–Natural inflation [62], hybrid axion models [72], [73], N-flation [74], [113], axion monodromy [75] and other pseudo-natural inflation models in Supersymmetry [76].

Model particles. Importantly, we find that the question if reheating can take place perturbatively crucially depends on the CP assignment in the model.

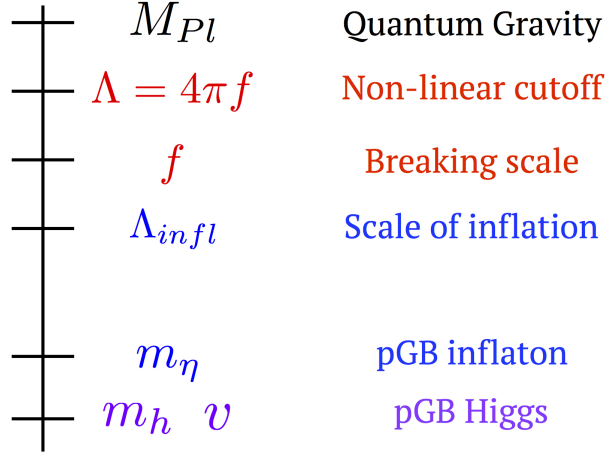


Figure 4.1: Pseudo-Goldstone bosons naturally realize mass hierarchies. CMB data and constraints on perturbative reheating allow us to relate the complete spectrum to the symmetry breaking scale f and the Planck scale M_P .

We will finish by showing how the model naturally connects to electroweak physics. The inflaton mass and couplings to the Higgs could be of the same order, leading to the possibility of looking for the inflaton through their mixing with the Higgs.

In Fig. 4.1 we show a graphic of the relevant scales in our model. The global symmetry is broken at the scale f , which is below the Planck scale at which we expect a UV completion in the form of a theory of quantum gravity. The scale of inflation is then expected to be parametrically smaller than f , as we will show. The Coleman Weinberg masses of the goldstone boson inflaton and Higgs are fixed by CMB and electroweak data respectively. Likewise, the values of the coefficients of the (self-) couplings in the potential can be fixed in light of the data, modulo the scale of inflation. This is a free parameter in our model. As usual for slow roll inflation, it is most naturally found around the GUT scale (10^{15} GeV), but can be as low as $\sim 10^5$ GeV if one allows for a degree of tuning.

Finally we would like to highlight some recent developments that may be of interest to the reader. In [17] a dynamical solution to the electroweak hierarchy problem was proposed, in terms of a Higgs boson coupling to an inflaton and an axion-like field. Although critics have pointed out several shortcomings, among which the necessity of a very large number of e-foldings and the low cut-off (which makes one arguably expect new physics around the EW scale) [140], the scanning mechanism is a new facet worth investigating. As the model behind the mechanism bears similarities with our set-up, it seems like a worthwhile exercise to look for a realisation in the

present context. A second recent result that is interesting in the present context is the observation in [141] that the Higgs-inflaton coupling $c_4 h^2 \eta^2$ may drastically alter the Higgs dynamics in the Early Universe, thereby stabilising the electroweak vacuum. As we will see the coupling c_4 will automatically be present in our model.

4.2 THE LAGRANGIAN OF THE HIGGS AND THE INFLATON

4.2.1 INFLATON–HIGGS COUPLINGS FOR PERTURBATIVE REHEATING

The condition that the inflaton field must decay completely into relativistic particles to complete the reheating process dictates the interaction structure in a successful theory of inflation. After the end of inflation, the inflaton field η begins to oscillate about the minimum of its potential with amplitude $\Phi(t)$. The universe is completely dominated by the zero-mode, $\langle \eta(t) \rangle$, which may be interpreted as a condensate of non-relativistic zero-momentum η -particles of mass m_η . The condensate oscillation amplitude decays as $\Phi(t) \sim t^{-1}$ due to the Hubble expansion and due to interactions with the higgs field. Trilinear couplings, $\frac{1}{2}\sigma\eta h^2$, and quartic couplings, $\frac{1}{2}g^2\eta^2 h^2$, with the higgs are to be expected on fairly general grounds, as we argue in the following section. As we will show in section 4.4, provided that the coupling constants σ, g^2 and the amplitude $\Phi(t)$ are small enough such that non-perturbative particle production processes are absent, the energy loss experienced by the condensate can be described by the Boltzmann equation

$$\frac{d}{dt} (a^3 \rho_\eta) = -\frac{\sigma^2 \Phi_0^2 m_\eta}{64\pi} - \frac{g^4 \Phi_0^4 m_\eta}{128\pi a^3}, \quad (4.1)$$

where a is the scale factor and Φ_0 is the initial amplitude of the inflaton oscillations at the start of reheating. The contribution from the quartic interaction decreases as $a^{-3} \sim t^{-2}$, which, as is well known [142]–[144], poses a major problem for theories which do not contain a trilinear interaction. Specifically, since the Hubble rate decreases as $H \sim a^{-3/2} \sim t^{-1}$, volume dilution due to the Hubble expansion takes place faster than the annihilation process $\phi\phi \rightarrow \chi\chi$ can drain energy from the condensate and so reheating never completes. In order to successfully reheat the universe, a trilinear coupling must be present. We will use this result as a guiding principle when constructing the Lagrangian for the composite Higgs model.

4.2.2 SYMMETRY BREAKING: THE MINIMAL COSET

The inflaton and Higgs corresponds to five scalar degrees of freedom which could come from the breaking of $SO(6)$ to $SO(5)$ or, equivalently $SU(4)$ to $Sp(4)$. This breaking pattern is very popular in building models of Composite Higgs, as it preserves custodial symmetry.

The breaking gives rise to five Goldstone bosons, transforming as a **5** of $SO(5)$. The most general vacuum which breaks $SO(6) \rightarrow SO(5) \sim SU(4) \rightarrow Sp(4)$ as shown in Ref. [145] is given by²

$$\Sigma_0 = \begin{pmatrix} 0 & e^{i\alpha} \cos(\theta) & \sin(\theta) & 0 \\ -e^{i\alpha} \cos(\theta) & 0 & 0 & \sin(\theta) \\ -\sin(\theta) & 0 & 0 & -e^{-i\alpha} \cos(\theta) \\ 0 & -\sin(\theta) & e^{-i\alpha} \cos(\theta) & 0 \end{pmatrix} \quad (4.2)$$

where α and θ are real angles. One recovers a well known choice of vacuum in Composite Higgs models [116] in the limit $\alpha \rightarrow \text{mod}(\pi)$ and $\theta \rightarrow \text{mod}(\pi)$.

In fact, the vacuum in which we have $\theta = \text{mod}(\pi)$ the vacuum has an enhanced custodial symmetry [145], as in this case the unbroken generators generate $SU(2) \times SU(2) \subset Sp(4)$. Likewise, the limit $\alpha = \text{mod}(\pi)$ parametrises the conservation of CP by the vacuum.

One can then parametrise the Goldstone bosons via the field $\Sigma(x)$,

$$\Sigma(x) = e^{i\Pi^a(x)T_\perp^a / \sqrt{2}f} \Sigma_0, \quad (4.3)$$

where $\Pi^a(x)$ are the Goldstone fields with decay constant f , corresponding to the broken $SO(6) \cong SU(4)$ generators T_\perp^a . A linear combination of three of the Goldstone fields is eaten by the Standard Model gauge fields such that the corresponding generators can be recognised as their longitudinal components. The two remaining Goldstone bosons remain in the spectrum as massless scalar fields and couple via the broken generators T_\perp^4 and T_\perp^5 :³

$$T_\perp^4 = \begin{pmatrix} 0 & \sigma_2 \\ \sigma_2 & 0 \end{pmatrix}, \quad T_\perp^5 = \begin{pmatrix} c_\theta e^{i\alpha} \mathbf{1}_2 & -is_\theta \sigma_2 \\ is_\theta \sigma_2 & c_\theta e^{i\alpha} \mathbf{1}_2 \end{pmatrix}. \quad (4.4)$$

²The discussion in Ref. [145] assumes the presence of CP conserving vacua, as well as CP breaking vacua, such that the Pfaffian of the inflaton is real.

³Here we use generalized expressions from Ref. [145]; obtained by assuming the general vacuum (Eq. A. 17) in the rotation Eq. B. 25.

Expanding the matrix exponential, we obtain

$$\Sigma(x) = \begin{pmatrix} c_\pi + \frac{\sqrt{2}f e^{i\alpha} c_\theta s_\pi \eta}{\sqrt{\pi_a^2}} & 0 & 0 & \frac{i\sqrt{2}f s_\pi (-ih - s_\theta \eta)}{\sqrt{\pi_a^2}} \\ 0 & c_\pi + \frac{\sqrt{2}f e^{i\alpha} c_\theta s_\pi \eta}{\sqrt{\pi_a^2}} & \frac{i\sqrt{2}f s_\pi (ih + s_\theta \eta)}{\sqrt{\pi_a^2}} & 0 \\ 0 & \frac{i\sqrt{2}f s_\pi (s_\theta \eta - ih)}{\sqrt{\pi_a^2}} & c_\pi - \frac{i\sqrt{2}f e^{i\alpha} c_\theta s_\pi \eta}{\sqrt{\pi_a^2}} & 0 \\ \frac{i\sqrt{2}f s_\pi (ih - s_\theta \eta)}{\sqrt{\pi_a^2}} & 0 & 0 & c_\pi - \frac{i\sqrt{2}f e^{i\alpha} c_\theta s_\pi \eta}{\sqrt{\pi_a^2}} \end{pmatrix} \Sigma_0(4.5)$$

where we have suppressed space-time dependence of the fields $h = h(x)$ and $\eta = \eta(x)$, and where we use the shorthands,

$$h(x)^2 + \eta(x)^2 = \pi_a^2 \quad \text{and} \quad s_\pi = \sin\left(\frac{\sqrt{\pi_a^2}}{\sqrt{2}f}\right), \quad c_\pi = \cos\left(\frac{\sqrt{\pi_a^2}}{\sqrt{2}f}\right) \\ s_\theta = \sin(\theta), \quad c_\theta = \cos(\theta) \quad . \quad (4.6)$$

We will further assume that gauging the theory breaks $SU(4)$ to the Standard Model group⁴ $SU(2)_L \times U(1)_Y$ and $U(1)_\eta$. This latter shift symmetry for η will assure that it does not get a potential from gauge bosons. Then the kinetic term becomes,

$$\frac{f^2}{8} \text{Tr}|D_\mu \Sigma|^2 = \frac{1}{2} \frac{(\eta \partial_\mu h - h \partial_\mu \eta)^2}{h^2 + \eta^2} + \frac{g^2}{4} h^2 \left(W_\mu^+ W^{-\mu} + \frac{1}{\cos^2 \theta_w} Z_\mu Z^\mu \right) \\ \approx \frac{1}{2} (\partial_\mu h)^2 + \frac{1}{2} (\partial_\mu \eta)^2 + \frac{1}{2} \frac{(h \partial_\mu h + \eta \partial_\mu \eta)^2}{1 - h^2 - \eta^2} + \frac{g^2}{4} h^2 \left(W_\mu^+ W^{-\mu} + \frac{1}{\cos^2 \theta_w} Z_\mu Z^\mu \right) \quad (4.7)$$

where the following field redefinitions are made:

$$h^2 s_\pi^2 f^2 / \pi_a^2 \rightarrow h^2 \quad \eta^2 s_\pi^2 f^2 / \pi_a^2 \rightarrow \eta^2 \\ (\partial_\mu h s_\pi f / \sqrt{\pi_a^2})^2 \rightarrow (\partial_\mu h)^2 \quad (\partial_\mu \eta s_\pi f / \sqrt{\pi_a^2})^2 \rightarrow (\partial_\mu \eta)^2 \quad (4.8)$$

corresponding to dropping the operators with more than four powers in the field (they will be effectively suppressed by f). For the sigma model, there is an equivalence between the original and rotated fields. However, the rotated fields couple to gauge bosons as in (4.7) and are as such the physically relevant choice.

At this level, the η and h fields are true Goldstone bosons. (Small) explicit breaking of the symmetry will generate a Coleman-Weinberg contributions to the scalar potential, via gauge and Yukawa interactions. This potential accounts, then, for resummations of loops of gauge bosons and fermions. Rather than considering the fully generic case, we can use the information from the previous section as prior information about what a Lagrangian which gives perturbative reheating will look like. In particular, the necessity of terms with odd powers of the singlet η in the scalar

⁴Here we do not address the colour group $SU(3)_c$.

potential implies that the singlet η has specific transformation properties under CP that differ from the Composite Higgs model. This can be understood in the following way: if we for a moment assume that CP is unbroken, we can set $\alpha = 0$. As we will see, the way we parametrise the coupling between η and (Dirac) fermions can schematically be written as

$$\eta \bar{F}(c_{even} + ic_{odd}\gamma_5)F \quad (4.9)$$

Clearly, for $c_{odd} = 0$, η behaves as a scalar, such that the trilinear interaction ηh^2 is allowed by the symmetry. However in the Composite Higgs case ($c_{odd} \neq 0$) where η behaves as a (partial) pseudo-scalar, the term ηh^2 breaks CP.

In contrast, the breaking of the enhanced custodial symmetry by taking $\theta \neq 0$ does not have such a direct impact on the predictions for perturbative reheating. It is expected to give rise to mass mixing, i.e. terms of the form $V \ni c_i \eta h$. Deviations from custodial symmetry in the Higgs sector are rather constrained by low-energy data and it will therefore be practical to assume $\theta = 0$ in the following. This choice corresponds to identifying the Higgs with the bi-doublet under the subgroup $SO(4) \cong SU(2)_L \times SU(2)_R$, and η with the singlet: $\mathbf{1} \oplus \mathbf{4} = (\mathbf{1}, \mathbf{1}) \oplus (\mathbf{2}, \mathbf{2})$.

As the scalar η does not couple to the $SU(2)_L$ gauge group, see (4.7), couplings to gauge bosons do not help with generating a cubic term. The difference in dynamics between the different vacua has to come from the couplings to fermions.

As an example, we implement the fermions in a $\mathbf{6}$ of $SU(4)$ (corresponding to the vector representation of $SO(6)$). Other options for fermion representations, such $\mathbf{4}$ and the $\mathbf{10}$, have their own difficulties to address [116].

The $\mathbf{6}$ of $SU(4)$ decomposes as $(\mathbf{2}, \mathbf{2}) \oplus (\mathbf{1}, \mathbf{1}) \oplus (\mathbf{1}, \mathbf{1})$ under $SU(2)_L \times SU(2)_R$, such that we can implement the fermions as [116]

$$\Psi_q = \frac{1}{2} \begin{pmatrix} 0 & Q \\ -Q^T & 0 \end{pmatrix} \quad \Psi_u = \Psi_u^+ + \epsilon_u \Psi_u^- \quad \Psi_u^\pm = \frac{1}{2} \begin{pmatrix} \pm U & 0 \\ 0 & U \end{pmatrix} \quad (4.10a)$$

$$\Psi_{q'} = \frac{1}{2} \begin{pmatrix} 0 & Q' \\ -Q'^T & 0 \end{pmatrix} \quad \Psi_d = \Psi_d^+ + \epsilon_d \Psi_d^- \quad \Psi_d^\pm = \frac{1}{2} \begin{pmatrix} \pm D & 0 \\ 0 & D \end{pmatrix} \quad (4.10b)$$

where $Q = (0, q_L)$, $Q' = (q_L, 0)$, $U = u_R i \sigma_2$ and $D = d_R i \sigma_2$. The $\epsilon_{u,d}$ are complex free parameters defining the embedding of the quarks into the singlets, and consecutively the CP-assignment of η . In the limit $|\epsilon_{u,d}| = 1$ the fermions have definite charges under $U(1)_\eta$ and it is therefore expected that η is massless.

The coupling of Σ to fermions will be of the form

$$\begin{aligned} \mathcal{L}_{eff} = & \sum_{r=q,u,q',d} \left[\Pi_0' \text{Tr}[\bar{\Psi}_r \not{p} \Psi_r] + \Pi_1' \text{Tr}[\bar{\Psi}_r \Sigma] \not{p} \text{Tr}[\Psi_r \Sigma^\dagger] \right] \\ & + M_u \text{Tr}[\bar{\Psi}_q \Sigma] \text{Tr}[\Psi_u \Sigma^\dagger] + M_d \text{Tr}[\bar{\Psi}_{q'} \Sigma] \text{Tr}[\Psi_d \Sigma^\dagger] \end{aligned} \quad (4.11)$$

4.2.3 COMPOSITE HIGGS LIMIT: CP ASSIGNMENT IN THE FERMION SECTOR

As we show in the Appendix, loops of fermions and gauge bosons will generate a Coleman Weinberg potential at one loop, which will be of the form [116]

$$V(\kappa, h) = a_1 h^2 + \lambda h^4 + |\kappa|^2 (a_2 + a_3 h^2 + a_4 |\kappa|^2) \quad \text{where} \quad \kappa = \sqrt{f^2 - \eta^2 - h^2 + i\epsilon_t \eta} \quad (4.12)$$

where a_i are dimensionful constants dependent on the form factors of the UV theory as given in the Appendix. Here ϵ_t is the parameter that defines the embedding of the up-type fermion in the global symmetry and determines the mass and CP assignment of η , as we demonstrated above. It is easy to see that the scenario in which ϵ_t is real is distinctly different from the case in which it can be complex. For $\epsilon_t \in \mathbb{R}$, we find that η behaves like a pseudoscalar ($c_{odd} \neq 0$ and $c_{even} = 0$ in (4.9)), and we can expand (4.12) to obtain the following CP and custodially symmetric potential:

$$V(\eta, h) = m_h^2 h^2 + \lambda_h h^4 + m_\eta^2 \eta^2 + \lambda_\eta \eta^4 + c_4 \eta^2 h^2 \quad (4.13)$$

Here, in terms of the parameters above we have defined

$$m_h^2 = (a_1 + a_3 - a_2 - a_4) \quad (4.14a)$$

$$\lambda_h = (\lambda - a_3 + a_4) \quad (4.14b)$$

$$m_\eta^2 = (1 - \epsilon_t^2)(-a_2 - a_4) \quad (4.14c)$$

$$\lambda_\eta = (1 - \epsilon_t^2)^2 a_4 \quad (4.14d)$$

$$c_4 = (1 - \epsilon_t^2)(-a_3 + 2a_4) \quad (4.14e)$$

And as announced the trilinear term is absent. If we allow for complex coupling to fermions,

$$\epsilon_t = \epsilon_t^{RE} + i\epsilon_t^{IM} \quad (4.15)$$

where $\epsilon_t^{IM} \neq 0$, we will find η has $c_{even} \neq 0$ in (4.9).⁵ In this case the scalar potential will include a trilinear interaction and a tadpole for η , both of which multiply ϵ_t^{IM} ,

$$V = c_{tad} \eta + m_\eta^2 \eta^2 + \tilde{c}_\eta \eta^3 + \lambda_\eta \eta^4 + m_h^2 h^2 + \lambda_h h^4 + c_3 \eta h^2 + c_4 \eta^2 h^2 \quad (4.16)$$

⁵In the boundary case $\epsilon_t^{RE} = 0, \epsilon_t^{IM} \neq 0$ η behaves like a scalar.

where

$$\tilde{c}_\eta = 4a_4\epsilon_t^{IM} \left(1 - (\epsilon_t^{RE})^2\right) \sqrt{f^2 - \eta^2 - h^2} \quad (4.17a)$$

$$c_3 = (4a_4 - 2a_3)(\epsilon_t^{IM}) \sqrt{f^2 - \eta^2 - h^2} \quad (4.17b)$$

$$c_4 = (a_3 - 2a_4)(\epsilon_t^{RE})^2 - 4a_4(\epsilon_t^{IM})^2 + 2a_4 - a_3 \quad (4.17c)$$

and the other coefficients remain as above. The tadpole and trilinear interaction term violate CP for $\epsilon_t^{RE} \neq 0$. We may shift away the tadpole $c_{tad}\eta$ by an appropriate vacuum expectation value v_η , which solves,

$$c_{tad} + 2m_\eta^2 v_\eta + 3\tilde{c}_\eta v_\eta^2 + 4\lambda_\eta v_\eta^3 = 0 \quad (4.18)$$

this will also shift the parameters,

$$m_\eta^2 \rightarrow m_\eta^2 + 3\tilde{c}_\eta v_\eta + 6\lambda_\eta v_\eta^2 \quad (4.19a)$$

$$\tilde{c}_\eta \rightarrow \tilde{c}_\eta + 4v_\eta \lambda_\eta \quad (4.19b)$$

$$m_h^2 \rightarrow m_h^2 + c_3 v_\eta + c_4 v_\eta^2 \quad (4.19c)$$

$$c_3 \rightarrow c_3 + 2c_4 v_\eta \quad (4.19d)$$

In terms of the shifted parameters the potential becomes

$$\boxed{V = m_\eta^2 \eta^2 + \tilde{c}_\eta \eta^3 + \lambda_\eta \eta^4 + m_h^2 h^2 + \lambda_h h^4 + c_3 \eta h^2 + c_4 \eta^2 h^2} \quad (4.20)$$

This potential has the required form to be a suitable candidate for inflation followed by perturbative reheating.

4.2.4 SPONTANEOUSLY BROKEN CP BY THE INFLATON ($\alpha \neq 0$)

For the Composite Higgs vacuum discussed above $\alpha = 0$ and CP is unbroken by the vacuum. Here we relax this constraint we introduce CP breaking in the model to

$$0 < \alpha \leq 1/2\pi \quad (4.21)$$

For $\alpha = 1/2\pi$ both fields have a quadratic term and do not interact. For the open interval, $0 < \alpha < 1/2\pi$, we indeed find the same potential as at the end of the previous sector, to fourth order in the fields:

$$V(\eta, h) = m_\eta^2 \eta^2 + \tilde{c}_\eta \eta^3 + \lambda_\eta \eta^4 + m_h^2 h^2 + \lambda_h h^4 + c_3 \eta h^2 + c_4 \eta^2 h^2. \quad (4.22)$$

The coefficients are in general nonzero, except for at $\alpha = 1/4\pi$. We refer the reader to the Appendix for a discussion, and an example computation. Importantly, in these vacua we are not required to introduce explicit CP breaking by a complex fermion representation to get the η -odd terms as we were for $\alpha = 0$, that is, we may have either $\in \mathbb{R}$ or $\in \mathbb{C}$.

In these vacua the η field couples directly to fermions as

$$(\eta \bar{u}_R \not{p} u_R) \in \mathcal{L}, \quad (4.23)$$

an effect proportional to $(1 - \epsilon_u^2)$. Indeed, is seen that the odd powers of η in the potential (which includes the trilinear coupling) are multiplied by $(1 - \epsilon_u^2)$ and $(b_1 - b_2 \epsilon_u^2)$ for some constants b_i (from the linear and the second order expansion of the logarithm respectively). This combination plays the role that ϵ_t^{IM} played in the previous section, as an order parameter of CP breaking.

As expected from periodicity, the two quadrants $0 < \alpha < 1/2\pi$ and $1/2\pi < \alpha < \pi$ are equivalent, modulo a redefinition of the fields:⁶

$$\eta \rightarrow -\eta \quad \text{and} \quad h \rightarrow -h \quad (4.24)$$

We demonstrate this explicitly in the appendix.

We will finish this section with a comment on the appearance domain walls [146]. As we introduced the possibility of breaking CP spontaneously, one may be worried that these will be present, and become energetically important. However, if the vacuum breaks CP spontaneously, it does it at the scale of symmetry breaking f . But, as we will see in the next section, we expect inflation to occur below this scale, $\Lambda_{inf} < f$, hence the domain walls will be diluted during inflation.

4.3 INFLATION

In this section we study inflation due to the field η . As the scale of inflation will turn out to be much larger than the electroweak scale, the Higgs field would be stabilized at the minimum of its potential during inflation, and so we set $h = 0$. Hence, we neglect the dynamics of the Higgs field during inflation, and the model is effectively single field. We can canonically normalise the inflationary sector via the field redefinition

$$\phi = f \arcsin(\eta/f), \quad (4.25)$$

⁶Because of custodial symmetry, which shows up here as a Z_2 symmetry for h , $h \rightarrow -h$ is a symmetry over the whole range. The latter substitution is therefore made for free.

such that the scalar potential becomes, in the unbroken CP limit,

$$V_{CP}(\phi) = m_\eta^2 f^2 \sin^2(\phi/f) + \lambda_\eta f^4 \sin^4(\phi/f) . \quad (4.26)$$

This is equivalent to the Goldstone Inflation [63] potential

$$V(\phi) = \Lambda^4 \left(\sin^2(\phi/f) - \tilde{\beta} \sin^4(\phi/f) \right) , \quad (4.27)$$

if we identify

$$\lambda_\eta f^4 = -\tilde{\beta} \Lambda^4 \quad \text{and} \quad m_\eta^2 f^2 = \Lambda^4 .$$

In figure 4.2 we show a plot of the form of the potential, for the moment with $\tilde{c}_\eta/m_\eta^2 = 0$. This model would lead to inflation with $f < M_p$ (where M_p is the reduced planck mass) and spectral index within the bounds allowed by Planck (at 2σ) [14],⁷

$$n_s = [.948 - .982] \quad \text{for} \quad \tilde{\beta} \lesssim 1/2 \rightarrow \lambda_\eta f^2 \gtrsim -1/2 m_\eta^2$$

As in Goldstone Inflation, the sensitivity to the exact value of $\tilde{\beta}$ that predicts the right spectral

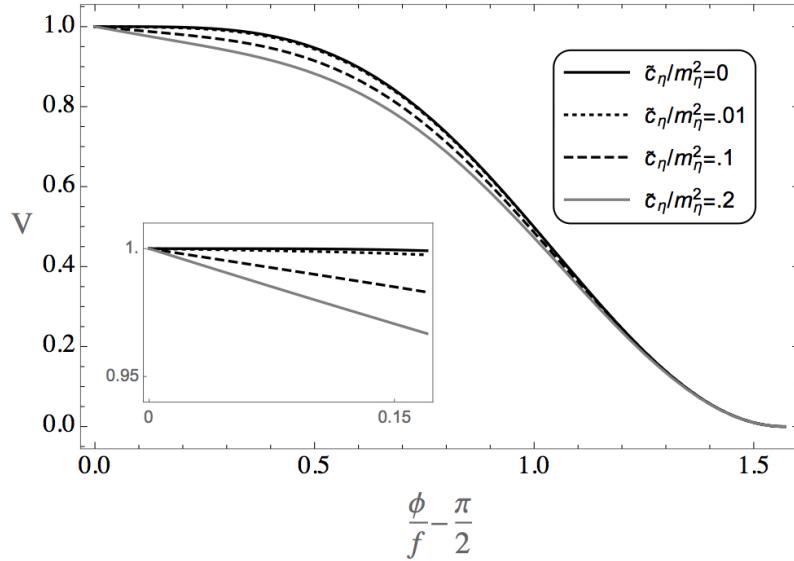


Figure 4.2: Form of the potential for $\lambda_\eta f^2 \gtrsim -1/2 m_\eta^2$.

index is a function of $(f/M_p)^2$:

$$4 \times 10^{-4} \left(\frac{f}{M_p} \right)^2 < \delta \tilde{\beta} < 3 \times 10^{-3} \left(\frac{f}{M_p} \right)^2 \quad \text{where} \quad \delta \tilde{\beta} = 1/2 - \tilde{\beta} \quad (4.28)$$

As in [63], this feeds into the amount of tuning needed in the model, which we will discuss below.

⁷Of course, the factor in the relation between the parameters m_η and λ_η depends on their normalization chosen in the scalar potential. In particular, a canonical mass term would eliminate the factor $1/2$.

Likewise, the model has the initial condition for the start of slow roll as a function of $(f/M_p)^2$,

$$\phi_i - 1/2\pi f = (0.020 - 0.025) \left(\frac{f}{M_p} \right)^2 M_p. \quad (4.29)$$

As in all models of Goldstone Inflation, the tensor to scalar ratio will also be subject to fine tuning, but its value is generically very small:

$$r \approx 10^{-6} (f/M_p)^4. \quad (4.30)$$

A measurement of CMB tensor modes would fix the symmetry breaking scale f (as well as the scale of inflation, as usual) in our model.

In the CP breaking fermion implementation described above there is an additional term

$$V_{\mathcal{CP}}(\phi) = \tilde{c}_\eta \sin^3(\phi/f) \sqrt{1 - \sin^2(\phi/f)} = \tilde{c}_\eta \sin^3(\phi/f) \cos(\phi/f). \quad (4.31)$$

This term imposes modulations on the potential with period πf , as seen from Fig. 4.2. Increasing the CP breaking in the model corresponds to increasing the value of the tensor to scalar ratio r . The bound $r < 0.1$ gives

$$\tilde{c}_\eta \leq O(10^{-1}) m_\eta^2 f^2. \quad (4.32)$$

The effect of the CP breaking term is illustrated for an order of magnitude below this bound in Fig. 4.3.

The scale of inflation is related to the amplitude of the scalar power spectrum, as measured by Planck [14],

$$A_s = \frac{\Lambda^4}{24\pi^2 M_p^4 \epsilon} = \frac{e^{3.089}}{10^{10}} \quad (4.33)$$

where ϵ is the first slow roll parameter. For our case (Eq. ((4.30)), where $r = 16\epsilon$ in the slow roll approximation) this implies

$$\Lambda \approx 10^{15} \left(\frac{f}{M_p} \right) \text{GeV}. \quad (4.34)$$

Interestingly, we can see from this relation that the onset of inflation is related to the scale of the symmetry breaking: $\Lambda \sim 10^{-3} f$. That is, fitting to the CMB data implies a mass gap of roughly three orders of magnitude between the two scales.

4.3.1 TUNING

Following convention, tuning can be expressed numerically using the Barbieri-Giudice [38] parametrization as follows

$$\Delta = \left| \frac{\partial \log n_s}{\partial \log \tilde{\beta}} \right| = \left| \frac{\tilde{\beta}}{n_s} \frac{\partial n_s}{\partial \tilde{\beta}} \right| \approx [8.1 - 8.5] \left(\frac{f}{M_p} \right)^{-2} \quad (4.35)$$

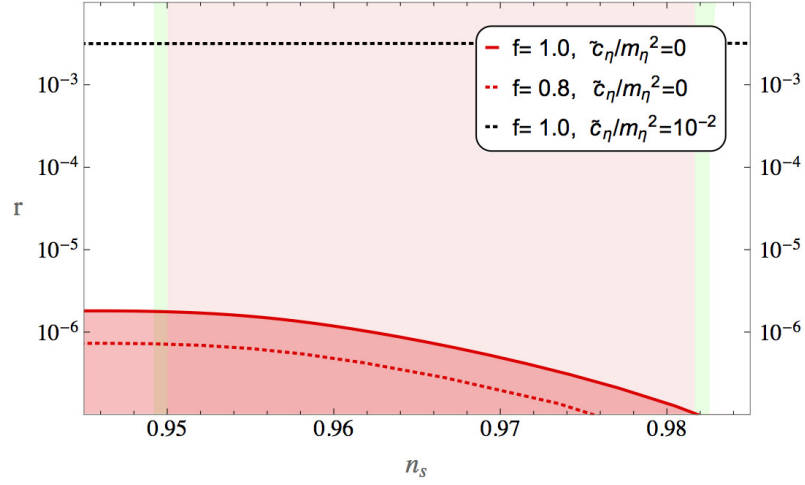


Figure 4.3: Model predictions against the Planck 2015 2σ bounds [14]. For convenience, we have set $M_p = 1$ here. In green: the TT spectrum and polarisation data at low- ℓ (lowP); in pink the combined spectra TT, TE, EE +lowP.

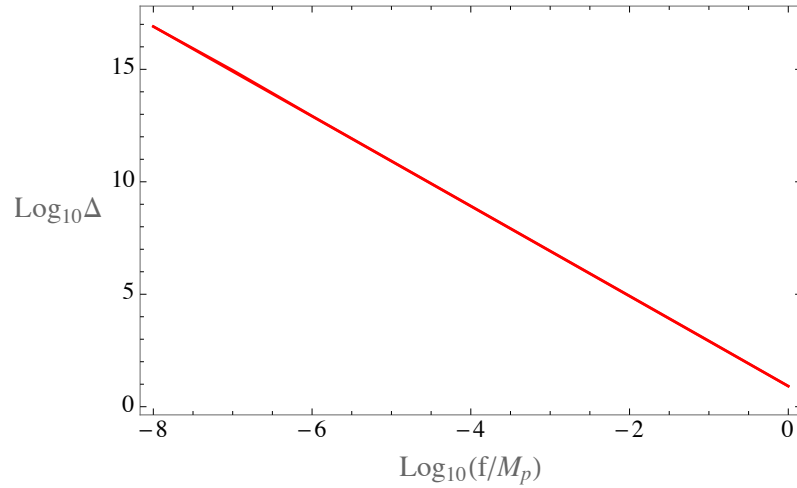


Figure 4.4: Fine-tuning, numerically defined as in (4.35).

See Fig. 4.4 below. It is seen that the parameters are sensitive to the square of the ratio of scales.

However, the relation $\tilde{\beta} \approx .5$ can be seen as a consequence of a symmetry in the sector responsible for the breaking of the global symmetry $SO(6)/SO(5)$.⁸ This would agree with naturalness in the 't Hooft interpretation. In this case the fact that the small deviation $\delta\tilde{\beta}$ is sensitive to the relation of the scales f and M_p implies that a symmetry in the sector is broken at the same time as $SO(6)/SO(5)$. In [63] we related this symmetry to the spectrum of resonances in the composite sector.

When we identify the other scalar resonance with the Higgs, we introduce a second source of tuning, between the electroweak scale v and the symmetry breaking scale f . This source of

⁸This would lead to a *mass-matching* situation [100], [101], [138], in which resonances from different sectors acquire degenerate masses, such as in Cured Higgsless [103], [104] and Holographic Technicolor [98], [99] models.

tuning coincides with the tuning in the Minimal and the Next to Minimal Composite Higgs model, and is a function of $(v/f)^2$, see for instance [19]. As this is a tuning of the parameters in the Higgs potential, which are independent combinations of the input parameters (the form factors, vacuum angles, and fermion representation), this tuning is independent and additive. The Barbieri-Giudice function will then take the form $\Delta_{\text{total}} = c_1 (M_p/f)^2 + c_2 (f/v)^2$, where c_1 and c_2 are $\mathcal{O}(1)$ constants. This suggests that the Barbieri-Giudice function is minimized for $\Delta_{\text{total}}(f^2 = \sqrt[4]{c_1/c_2} M_p v) \sim 10^{16}$, which is a large, but technically natural fine-tuning.

4.4 REHEATING

At the end of inflation, the inflation field approaches, overshoots and begins to oscillate about the minimum of its potential. At this stage, the universe is completely dominated by the zero-mode of the oscillating inflaton field $\langle\phi(t)\rangle$. Interactions with the higgs field, which we have so far neglected, lead to dissipation which drains energy from $\langle\phi(t)\rangle$, and excites relativistic higgs particles. We refer to these collective processes as reheating (see e.g., [142], [147] for reviews). The calculation that we present below section is semi-classical: we treat the inflaton condensate as a classical source in the mode equations for the quantum fluctuations of the higgs field. This treatment neglects many of the complicated processes which are present during the reheating phase, such as thermal corrections, re-scatterings of the produced higgs particles on the inflaton condensate, and the thermalisation process. As we discuss at the end of this section, these effects can in general modify the rate of decay of the condensate. Our approach does however provide an estimate for the perturbative decay rate of $\langle\phi(t)\rangle$ into higgs particles, and allows us to estimate the reheating temperature T_R .

4.4.1 EQUATIONS OF MOTION

To begin, we study the classical inflaton background. As a first approximation, we neglect interactions with the higgs field and set $h = 0$. As before, the inflaton sector can be canonically normalised through the field redefinition $\eta(t) = f \sin(\phi(t)/f)$. We neglect excitations of the inflaton field, $\delta\phi$, and so for simplicity label the zero-mode $\phi(t) \equiv \langle\phi(t)\rangle$ which obeys the usual Klein Gordon equation:

$$\ddot{\phi} + 3H\dot{\phi} + \frac{\partial V}{\partial \phi}|_{h=0} = 0, \quad (4.36)$$

where the potential is given by (4.27). After inflation, the inflaton field approaches, overshoots and begins to oscillate about its minimum. This region of the potential, where $\phi/f \ll 1$, is essentially quadratic:

$$V_{h=0}(\phi) \approx \frac{1}{2} m_\phi^2 \phi^2, \quad m_\phi^2 \equiv 2m_\eta^2 \approx 2 \times 10^{-14} \left(\frac{f}{M_P} \right)^2 M_P^2, \quad (4.37)$$

where we have used the Planck constraint on the amplitude of scalar power spectrum (4.34) to determine the mass m_ϕ in terms of the scale f . To describe the oscillations, notice that (4.36) can be written as

$$\frac{d^2}{dt^2} (a^{3/2} \phi) + \left[m_\phi^2 - \left(\frac{9}{4} H^2 + \frac{3}{2} \dot{H} \right) \right] (a^{3/2} \phi) = 0. \quad (4.38)$$

At the onset of oscillation, $m_\phi^2 \gg H^2, \dot{H}$ and under this condition, (4.38) has the damped sinusoidal solution:

$$\phi(t) = \frac{\Phi_0}{a^{3/2}(t)} \sin(m_\phi t + \vartheta), \quad \Phi_0 \approx 0.6 \left(\frac{f}{M_P} \right) M_P. \quad (4.39)$$

The numerical value for the initial amplitude, Φ_0 , was obtained by matching the above solution with an exact numerical integration of Eq.(4.36) – see the left hand panel of Fig. 4.5 for illustration. Subscript zero denotes evaluation at the onset of oscillations (start of reheating), and we set $a_0 = 1$. The scale factor, averaged over many oscillations, grows as $a(t) \sim t^{2/3}$, while the energy density of the field decreases as:

$$\rho_\phi(t) = \frac{1}{2} \dot{\phi}^2(t) + \frac{1}{2} m_\phi^2 \phi^2(t) \simeq \frac{m_\phi^2 \Phi_0^2}{2a^3}. \quad (4.40)$$

We see that the vacuum energy of the inflaton field exists as spatially coherent oscillations, which can be interpreted as a condensate of non-relativistic zero-momentum ϕ -particles. The amplitude of the oscillations decay due to the Hubble expansion and also due production of higgs particles. We can obtain an estimate for this particle production rate by considering propagation of higgs fluctuations, h_k , in the background of the classical inflaton condensate.

We begin by canonically normalising the higgs kinetic sector (given by (4.7)) by performing the following field redefinition:

$$\partial_\mu \chi(x) = \sqrt{\frac{f^2 - \eta^2(t)}{f^2 - \eta^2(t) - h^2(x)}} \partial_\mu h(x), \quad (4.41)$$

such that

$$h(x) = f \cos(\phi(t)/f) \sin \hat{\chi}(x), \quad \hat{\chi}(x) \equiv \frac{\chi(x)}{f \cos^2(\phi(t)/f)}. \quad (4.42)$$

We will henceforth drop the space-time labels and write $\chi = \chi(x)$, $\phi = \phi(t)$: it is to be understood that the higgs is inhomogeneous, whilst the inflaton condensate is homogeneous, and described by

(4.39). Under these field redefinitions we obtain:

$$\mathcal{L} = -\frac{1}{2}\partial_\mu\chi\partial^\mu\chi - \frac{1}{2}\left[1 + \sin^2(\phi/f)\tan^2\hat{\chi}\right]\partial_\mu\phi\partial^\mu\phi - [\sin(\phi/f)\tan\hat{\chi}]\partial_\mu\chi\partial^\mu\phi - V(\phi,\chi), \quad (4.43)$$

where the potential is given by (4.22). The canonically normalised higgs equation of motion is obtained by varying the action with respect to χ :

$$\ddot{\chi} - \frac{\nabla^2}{a^2}\chi + 3H\dot{\chi} = -\frac{\partial V(\phi,\chi)}{\partial\chi} + \sin(\phi/f)\tan\hat{\chi}\frac{\partial V(\phi)}{\partial\phi}|_{h=0} - \frac{\dot{\phi}^2}{f^2}K(\phi,\chi), \quad (4.44)$$

where

$$K(\phi,\chi) \equiv \frac{f\sin\hat{\chi}\cos^2\hat{\chi}\cos^4(\phi/f) + 2\chi\cos\hat{\chi}\sin^2(\phi/f) - f\sin\hat{\chi}\cos(\phi/f) + f\sin\hat{\chi}\cos^3(\phi/f)}{\cos^3(\phi/f)\cos^3\hat{\chi}} \quad (4.45)$$

In deriving (4.44), we have used (4.36) to eliminate $\ddot{\phi}$ which arises from the variation of the action. The task at hand is to solve (4.44) given the inflaton background (4.39). This is made tractable by expanding the RHS of (4.44) about $\phi/f = 0$, and about $\chi/f = 0$:

$$\ddot{\chi} - \frac{\nabla^2}{a^2}\chi + 3H\dot{\chi} \approx -\left[m_\chi^2 + \sigma\phi + g^2\phi^2 + \frac{\dot{\phi}^2}{f^2}\right]\chi + \dots, \quad (4.46)$$

where we have defined

$$m_\chi^2 \equiv 2m_h^2, \quad \sigma \equiv 2c_3, \quad g^2 \equiv 2\left[m_h^2/f^2 - m_\eta^2/f^2 + c_4\right]. \quad (4.47)$$

The expansion in ϕ/f is permitted since the amplitude of the inflaton oscillations are small with respect to the scale f : $\Phi_0/a^{3/2}(t) \sim 0.6f/a^{3/2}(t)$. The expansion in χ/f is permitted since we assume that the higgs field is stabilised at the minimum of its potential throughout inflation, $\langle\chi(\mathbf{x},t)\rangle = 0$. Furthermore we consider perturbative reheating only: we restrict ourselves to regions of parameter space where the coupling constants σ and g^2 are small enough such that resonant enhancement of higgs modes is not possible. This ensures that $\chi \ll f$ throughout reheating. We will discuss the conditions for perturbative reheating shortly. Notice that inflaton mass, m_η^2 , and the higgs mass, m_h^2 , enter the definition of the coupling g^2 : their presence may be traced back to canonical normalisation of the higgs kinetic term.

For the analysis of (4.46) it is convenient to define a co-moving field

$$\mu_k(\tau) \equiv a(\tau)\chi_k(\tau), \quad (4.48)$$

and to work in conformal time, which is related to cosmic time by an integral over the scale factor:

$$t(\tau) = \int_{\tau_0}^{\tau} d\tau' a(\tau'). \quad (4.49)$$

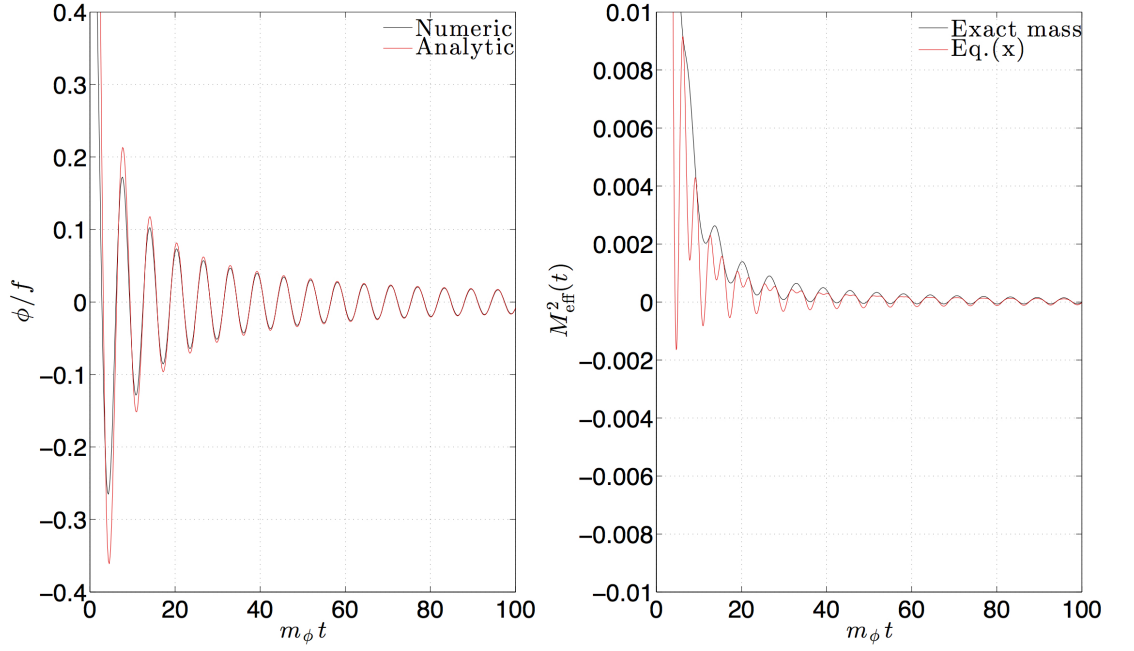


Figure 4.5: Left panel: Comparison between the exact numerical solution of (4.36) and the approximate analytic solution (4.39).

Right panel: Comparison between the exact ‘mass’ (the coefficient of the term linear in χ of (4.44)) and $M_{\text{eff}}^2(t)$ as defined in (4.53).

According to standard arguments, we may decompose this field into creation and annihilation operators:

$$\mu(\tau, \mathbf{x}) = \int \frac{d^3k}{(2\pi)^{3/2}} \left[a_{\mathbf{k}} \mu_k(\tau) + a_{-\mathbf{k}}^\dagger \mu_k^*(\tau) \right] e^{i\mathbf{k} \cdot \mathbf{x}}, \quad (4.50)$$

where the mode functions obey

$$\mu_k''(\tau) + \omega_k^2(\tau) \mu_k(\tau) = 0, \quad (4.51)$$

and where a prime denotes differentiation with respect to conformal time. The time dependent frequency is given by

$$\omega_k^2(\tau) \equiv k^2 + a^2 M_{\text{eff}}^2(\tau) - \frac{a''}{a}, \quad \frac{a''}{a} = \frac{a^2}{6M_{\text{p}}^2} (\rho_\phi - 3P_\phi), \quad (4.52)$$

where $P_\phi \simeq 0$ is the pressure of the field, and we have defined the effective mass:

$$M_{\text{eff}}^2(t) \equiv m_\chi^2 + \frac{\sigma \Phi_0}{a^{3/2}(t)} \sin(m_\phi t + \vartheta) + \frac{g^2 \Phi_0^2}{a^3(t)} \sin^2(m_\phi t + \vartheta) + \frac{\Phi_0^2 m_\phi^2}{f^2 a^3(t)} \cos^2(m_\phi t + \vartheta). \quad (4.53)$$

The final term on the RHS of $M_{\text{eff}}^2(t)$ is the leading contribution from $\dot{\phi}^2/f^2$: we have neglected terms which decay faster than a^{-3} . In the right panel of Fig. 4.5, we plot the effective mass against the coefficient of the term linear in χ of (4.44), which demonstrates the accuracy of this expansion. Equations of the type (4.51), with time dependent mass (4.53) have been extensively studied in

the context of (p)reheating after inflation. For certain regions of $\{\sigma, g^2, \Phi_0\}$ parameter space, the mode functions experience exponential growth as parametric instability develops, a phenomenon known as parametric resonance [142], [144], [148], [149]. To be specific, when any one of the three terms in $M_{\text{eff}}^2(t)$ is dominant, the oscillator equation (4.51) may be written

$$\frac{d^2 \mu_k}{dz^2} + [A_k - 2q_i \cos(2z)] \mu_k = 0, \quad (4.54)$$

$$q_0 \equiv \frac{\Phi_0^2}{4f^2 a^3}, \quad q_3 \equiv \frac{\sigma \Phi_0}{m_\phi^2 a^{3/2}}, \quad q_4 \equiv \frac{g^2 \Phi_0^2}{4m_\phi^2 a^3}, \quad A_k \equiv \frac{k^2 + m_\chi^2}{m_\phi^2 a^2} + 2q_{(0,4)}, \quad (4.55)$$

following a time redefinition of the form $z \equiv m_\phi t + \text{const.}$ Here we have ignored terms proportional to H/m_ϕ (recall that $H \ll m_\phi$ during reheating). (4.54) is known as the Mathieu equation, which is known to possess instability bands for certain values of A_k and q_i . For $q_i \gg 1$, a large region of parameter space is unstable and broad parametric resonance can develop. Throughout this paper we restrict ourselves to regions of parameter space where $q_i \ll 1$, such that non-perturbative preheating processes are negligible. With $\Phi_0 \approx 0.6f$, we find $q_0 = 0.09$, and so parametric instability cannot be triggered by this term. Meanwhile, $q_{3,4} \ll 1$ requires:

$$\sigma \ll \frac{m_\phi^2}{\Phi_0}, \quad g^2 \ll \left(\frac{m_\phi}{\Phi_0} \right)^2, \quad (4.56)$$

or, in terms of the original parameters of the potential (4.22):

$$c_3 \ll m_\eta^2/f, \quad m_h^2/f^2 + c_4 \ll 10m_\eta^2/f^2. \quad (4.57)$$

This relation for the smallness of the CP breaking term c_3 in terms of the inflaton mass is consistent with the similar relation for c_η found in the previous section. Likewise, the constraint on c_4 is consistent with our expectations from the computation of the potential, as can be verified with the appendix. We always ensure that the above bounds are respected, and do not consider parametric resonance in this paper.

If we regard the inflaton condensate ϕ to be a collection of zero-momentum inflaton ‘particles’, then the effective mass $M_{\text{eff}}^2(t)$ has a physical interpretation in terms of Feynman diagrams:

These diagrams describe the three-leg, $-\frac{1}{2}\sigma\phi\chi^2$, and four-leg, $-\frac{1}{2}g^2\phi^2\chi^2$, interaction terms which reside in the canonically normalised Lagrangian – (4.43). Since we have not quantised the inflaton, there are no ϕ -propagators, which allows for tree-level diagrams only. These diagrams describe the perturbative decay of a single inflaton ‘particle’ with mass m_ϕ into two higgs particles of comoving momentum $k \sim am_\phi/2$, and the annihilation of a pair of ϕ ‘particles’ into pair of χ particles with comoving momentum $k \sim am_\phi$ respectively. We use the term inflaton ‘particle’

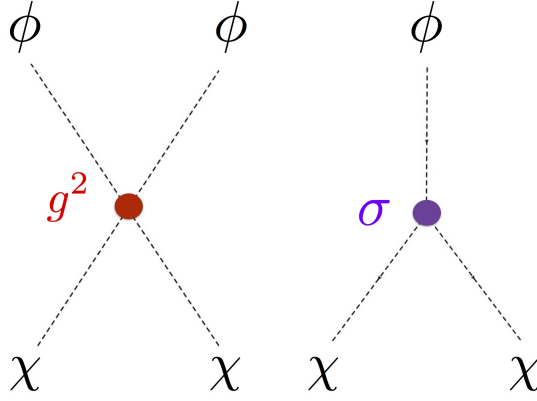


Figure 4.6: Inflaton-Higgs couplings in $SO(6)/SO(5)$.

rather loosely here, since what we are really describing is creation of higgs particles from a classical inflaton condensate. This diagrammatic representation does however offer intuition for the physical processes at work.

4.4.2 BOGOLIUBOV CALCULATION

We wish to solve (4.51) with frequency (4.52). Our calculation closely follows that of Ref. [144]. First, we notice that since the inflaton condensate behaves like a collection of non-relativistic particles with zero pressure, $P_\phi \approx 0$, and so we have $a''/a \approx 2a^2H^2$. Therefore, for the modes $k^2 \sim a^2m_\phi^2$ which we expect to be produced, we can safely neglect a''/a , given that $H \ll m_\phi$ during reheating. In the adiabatic representation, the solution to the mode equation (4.51) may be written in the WKB form (see eg. [142], [144]):

$$\mu_k(\tau) = \frac{\alpha_k(\tau)}{\sqrt{2\omega_k(\tau)}} e^{-i\Psi_k(\tau)} + \frac{\beta_k(\tau)}{\sqrt{2\omega_k(\tau)}} e^{+i\Psi_k(\tau)}, \quad (4.58)$$

where the accumulated phase is given by

$$\Psi_k(\tau') \equiv \int_{\tau_0}^{\tau'} d\tau'' \omega_k(\tau''). \quad (4.59)$$

(4.58) is a solution of (4.51) provided that the Bogoliubov coefficients satisfy the following coupled equations:

$$\alpha'_k(\tau) = \beta_k(\tau) \frac{w'_k(\tau)}{2w_k(\tau)} e^{+2i\Psi_k(\tau)}, \quad \beta'_k(\tau) = \alpha_k(\tau) \frac{w'_k(\tau)}{2w_k(\tau)} e^{-2i\Psi_k(\tau)}, \quad (4.60)$$

which also implies that:

$$\mu'_k(\tau) = -i\alpha_k(\tau) \sqrt{\frac{w_k(\tau)}{2}} e^{-i\Psi_k(\tau)} + i\beta_k(\tau) \sqrt{\frac{w_k(\tau)}{2}} e^{+i\Psi_k(\tau)}. \quad (4.61)$$

The wronskian condition, $W[\mu_k(t), \mu_k^*(t)] = i$, demands that the Bogoliubov coefficients are normalised as $|\alpha_k(t)|^2 - |\beta_k(t)|^2 = 1$. In this basis, the Hamiltonian of the χ field is instantaneously diagonalised. The single particle mode occupation number n_k , is defined as the energy of the mode, $\frac{1}{2}|\mu'_k|^2 + \frac{1}{2}\omega_k^2|\mu_k|^2$, divided by the frequency of the mode:

$$n_k(\tau) = \frac{|\mu'_k(\tau)|^2 + \omega_k^2(\tau)|\mu_k(\tau)|^2}{2\omega_k(\tau)} - \frac{1}{2} = |\beta_k(\tau)|^2. \quad (4.62)$$

The $-1/2$ corresponds to subtraction of the zero-point energy, and the last equality is obtained via substitution of the WKB solution (4.58). In terms of the classical mode functions, creation of higgs particles occurs due to departure from the initial positive-frequency solution: the initial conditions therefore at $\tau = \tau_0$ (the start of reheating) are then $\alpha_k = 1$, $\beta_k = 0$, and so $n_k(\tau_0) = 0$. Since we work in the perturbative regime specified by (4.56) the mode occupation numbers remain small, $|\beta_k(\tau)|^2 \ll 1$, and so we can iterate (4.60) to obtain

$$\beta_k(\tau) \approx \int_{\tau_0}^{\tau} d\tau' \frac{\omega'_k(\tau')}{2\omega_k(\tau')} e^{-2i\Psi_k(\tau')}. \quad (4.63)$$

In the perturbative regime we can approximate

$$\Psi_k(\tau') \approx k \int_{\tau_0}^{\tau'} d\tau'' \sqrt{1 + \left(\frac{a(\tau'')m_\chi}{k}\right)^2}, \quad (4.64)$$

whilst for the frequency we have

$$\frac{\omega'_k}{2\omega_k} \approx \frac{a^{3/2}(\tau')\Phi_0 m_\phi}{4k^2} \left[\frac{\sigma + 2\Phi_0(g^2 - m_\phi^2/f^2)a^{-3/2}(\tau')\sin(m_\phi t(\tau') + \vartheta)}{1 + a^2(\tau')m_\chi^2/k^2} \right] \cos(m_\phi t(\tau') + \vartheta), \quad (4.65)$$

where we have neglected terms containing derivatives of the scale factor. Inserting these results into (4.63) gives:

$$\begin{aligned} \beta_k(\tau) &= \frac{\sigma\Phi_0 m_\phi}{8k^2} \int_{\tau_0}^{\tau} \frac{d\tau' a^{3/2}(\tau')}{1 + a^2(\tau')m_\chi^2/k^2} \left[e^{+i\psi_{3,k}^-(\tau')} + e^{-i\psi_{3,k}^+(\tau')} \right] \\ &+ \frac{(g^2 - m_\phi^2/f^2)\Phi_0^2 m_\phi}{8ik^2} \int_{\tau_0}^{\tau} \frac{d\tau'}{1 + a^2(\tau')m_\chi^2/k^2} \left[e^{+i\psi_{4,k}^-(\tau')} - e^{-i\psi_{4,k}^+(\tau')} \right], \end{aligned} \quad (4.66)$$

where we have defined the phases

$$\psi_{3,k}^\pm(\tau) \equiv \pm 2\Psi_k(\tau) + m_\phi t(\tau) + \vartheta, \quad \psi_{4,k}^\pm(\tau) \equiv \pm 2\Psi_k(\tau) + 2(m_\phi t(\tau) + \vartheta). \quad (4.67)$$

As discussed in Ref. [144], (see also [142]), the integrals in (4.66) can be evaluated using the method of stationary phase: they are dominated near the instants $\tau_{3,k}$ and $\tau_{4,k}$ where

$$\begin{aligned} \frac{d}{d\tau} \psi_{3,k}^-(\tau)|_{\tau_{3,k}} &= 0, \quad \Rightarrow \quad k = \frac{1}{2}m_\phi a(\tau_{3,k}) \sqrt{1 - 4\delta_M^2}, \\ \frac{d}{d\tau} \psi_{4,k}^-(\tau)|_{\tau_{4,k}} &= 0, \quad \Rightarrow \quad k = m_\phi a(\tau_{4,k}) \sqrt{1 - \delta_M^2}, \end{aligned} \quad (4.68)$$

where we have defined $\delta_M \equiv m_\chi/m_\phi$. For the 3-leg interaction, the above result corresponds to the creation of pair of higgs particles with momentum $k \sim am_\phi/2$ from an inflaton with mass m_ϕ at the instant $\tau_{3,k}$ of the resonance between the mode k and the inflaton condensate. A similar interpretation may be given for the 4-leg interaction. Upon performing the integrals, we find:

$$n_k(\tau) = \frac{\pi\sigma^2\Phi_0^2m_\phi}{32k^4} (1 - 4\delta_M^2) \frac{a^3(\tau_{3,k})}{a'(\tau_{3,k})} + \frac{\pi(g^2 - m_\phi^2/f^2)^4\Phi_0^2m_\phi}{64k^4} \frac{(1 - \delta_M^2)}{a'(\tau_{4,k})} \\ + \frac{\pi\sigma(g^2 - m_\phi^2/f^2)\Phi_0^3m_\phi}{32k^4} \sqrt{2(1 - 4\delta_M^2)(1 - \delta_M^2)} \mathcal{I}(\tau_{3,k} \tau_{4,k}), \quad (4.69)$$

where we have defined

$$\mathcal{I}(\tau_{3,k} \tau_{4,k}) \equiv \sqrt{\frac{a^3(\tau_{3,k})}{a'(\tau_{3,k})a'(\tau_{4,k})}} \sin \left[\psi_{4,k}^-(\tau_{4,k}) - \psi_{3,k}^-(\tau_{3,k}) \right]. \quad (4.70)$$

As discussed in [144], the oscillatory term $\mathcal{I}(\tau_{3,k} \tau_{4,k})$ represents the interference between the two decay channels ($\phi \rightarrow \chi\chi$ and $\phi\phi \rightarrow \chi\chi$) of the inflaton. It is present because we have treated the inflaton as a classical oscillating source, and not an honest collection of particles.

4.4.3 BOLTZMANN EQUATIONS

Since $m_\phi \gg m_\chi$ the higgs particles are relativistic when produced. This means we can effectively treat them as a bath of radiation with g_* number of degrees of freedom. We define the co-moving energy density in the higgs field as

$$a^4\rho_\chi \equiv \int_0^\infty \frac{d^3k}{(2\pi)^3} \omega_k n_k \\ = \frac{\sigma^2\Phi_0^2m_\phi}{64\pi} (1 - 4\delta_M^2) \int_0^\infty \frac{dk}{k^2} \sqrt{k^2 + a^2(\tau)m_\chi^2} \frac{a^3(\tau_{3,k})}{a'(\tau_{3,k})} \\ + \frac{(g^2 - m_\phi^2/f^2)^2\Phi_0^4m_\phi}{128\pi} (1 - \delta_M^2) \int_0^\infty \frac{dk}{k^2} \sqrt{k^2 + a^2(\tau)m_\chi^2} \frac{1}{a'(\tau_{4,k})} \\ + \frac{\sigma(g^2 - m_\phi^2/f^2)\Phi_0^3m_\phi}{64\pi} \sqrt{2(1 - 4\delta_M^2)(1 - \delta_M^2)} \int_0^\infty \frac{dk}{k^2} \sqrt{k^2 + a^2(\tau)m_\chi^2} \mathcal{I}(\tau_{3,k} \tau_{4,k}). \quad (4.71)$$

At first glance these integrals appear divergent. This however is not the case, as can be seen from the requirement that the higgs particles be produced perturbatively. (4.68) enforces:

$$\frac{1}{2}m_\phi a_0 \sqrt{1 - 4\delta_M^2} < k < \frac{1}{2}m_\phi a(\tau) \sqrt{1 - 4\delta_M^2}, \quad \text{for } \phi \rightarrow \chi\chi \quad (4.72)$$

$$m_\phi a_0 \sqrt{1 - \delta_M^2} < k < m_\phi a(\tau) \sqrt{1 - \delta_M^2}, \quad \text{for } \phi\phi \rightarrow \chi\chi. \quad (4.73)$$

Hence, the limits of the first and the third integrals on the RHS of (4.71) should be replaced by the limits of (4.72), whilst those of the second integral should be replaced by (4.73). Once again

neglecting derivatives of a , we obtain

$$\frac{d}{d\tau} (a^4 \rho_\chi) \approx a^2 \frac{\sigma^2 \Phi_0^2 m_\phi}{64\pi} \sqrt{1 - 4\delta_M^2} + a^{-1} \frac{(g^2 - m_\phi^2/f^2)^2 \Phi_0^4 m_\phi}{128\pi} \sqrt{1 - \delta_M^2}, \quad (4.74)$$

where we have discarded the interference term since it vanishes when averaged over time. Replacing factors of a using $\rho_\phi \approx m_\phi^2 \Phi_0^2 / (2a^3)$, we are left with the familiar Boltzmann equation:

$$a^{-4} \frac{d}{dt} (a^4 \rho_\chi) \approx \Gamma_{\phi \rightarrow \chi\chi} \rho_\phi + 2 \frac{[\sigma_{\phi\phi \rightarrow \chi\chi} v]_{v=0}}{m_\phi} \rho_\phi^2, \quad (4.75)$$

where

$$\Gamma_{\phi \rightarrow \chi\chi} = \frac{\sigma^2}{32\pi m_\phi} \sqrt{1 - 4 \frac{m_\chi^2}{m_\phi^2}}, \quad [\sigma_{\phi\phi \rightarrow \chi\chi} v]_{v=0} = \frac{(g^2 - m_\phi^2/f^2)^2}{64\pi m_\phi^2} \sqrt{1 - \frac{m_\chi^2}{m_\phi^2}}. \quad (4.76)$$

The decay rate $\Gamma_{\phi \rightarrow \chi\chi}$ agrees with the tree-level result obtained from QFT. The cross section $\sigma_{\phi\phi \rightarrow \chi\chi}$ also agrees with QFT so long as the Feynman amplitude is evaluated at zero relative velocity, $v = 0$.

Note that ϕ , as a CP odd particle, could have couplings to vector bosons as an axion. For example, it could have couplings to gluons and photons as

$$\mathcal{L}_{CP} = \frac{c_{\gamma\alpha}}{f} \phi F_{\mu\nu} \tilde{F}^{\mu\nu} + \frac{c_{\gamma\alpha_s}}{f} \phi \text{Tr} G_{\mu\nu} \tilde{G}^{\mu\nu} \quad (4.77)$$

as well as to W and Z bosons. These couplings could be generated by triangle diagrams involving fermionic degrees of freedom coupled to SM gauge interactions. Whether these are present or not is a highly-model dependent question, whereas we have focused in this paper on interactions between the Goldstone bosons (the Higgs and the inflaton). We refer the reader to Refs. [150], [151] for a thorough analysis of preheating due to non-zero couplings to gauge bosons.

Conservation of energy demands $a^{-3} \frac{d}{dt} (a^3 \rho_\phi) = -a^{-4} \frac{d}{dt} (a^4 \rho_\chi)$, which gives

$$\frac{d}{dt} (a^3 \rho_\phi) = -\Gamma_{\phi \rightarrow \chi\chi} (a^3 \rho_\phi) - 2 \frac{[\sigma_{\phi\phi \rightarrow \chi\chi} v]_{v=0}}{m_\phi a^3} (a^3 \rho_\phi)^2. \quad (4.78)$$

If the trilinear interaction is absent ($\sigma = 0$) we can integrate (4.78) to show that $a^3 \rho_\phi \rightarrow \text{const}$ as $t \rightarrow \infty$. This means that the inflaton does not completely decay: volume dilution due to the Hubble expansion takes place faster than the annihilation process $\phi\phi \rightarrow \chi\chi$ can drain energy from the inflaton condensate. In order to successfully reheat the universe, the trilinear coupling must be present. Indeed, in the absence of $\phi\phi \rightarrow \chi\chi$ annihilations, (if $g^2 = m_\phi^2/f^2$) we can integrate (4.78) to show that $a^3 \rho_\phi \sim e^{-\Gamma t}$: in a time of order $\Gamma_{\phi \rightarrow \chi\chi}^{-1}$ the inflaton has decayed completely. For the remainder of this section we set $g^2 = m_\phi^2/f^2$ in order to place order-of-magnitude bounds on the model parameters.

Up to this point we have neglected the decay of the higgs to the SM. The dominant channel is $\chi \rightarrow b\bar{b}$, with width

$$\Gamma_{\chi \rightarrow b\bar{b}} = \frac{3m_\chi}{8\pi} \left(\frac{m_b}{v_\chi} \right)^2 \left(1 - \frac{4m_b^2}{m_\chi^2} \right)^{3/2} \sim 5 \text{ MeV}. \quad (4.79)$$

Since $m_\chi \gg m_b$, the $b\bar{b}$ decay products are produced relativistically:

$$a^{-4} \frac{d}{dt} (a^4 \rho_b) = \Gamma_{\chi \rightarrow b\bar{b}} \rho_b. \quad (4.80)$$

With $\phi\phi \rightarrow \chi\chi$ processes absent, energy conservation demands:

$$a^{-4} \frac{d}{dt} (a^4 \rho_\chi) \approx \Gamma_{\phi \rightarrow \chi\chi} \rho_\phi - \Gamma_{\chi \rightarrow b\bar{b}} \rho_b, \quad a^{-3} \frac{d}{dt} (a^3 \rho_\phi) = -\Gamma_{\phi \rightarrow \chi\chi} \rho_\phi. \quad (4.81)$$

(4.80) and (4.81) are the final Boltzmann equations describing perturbative reheating in the composite higgs model. The approximations involved in their derivation will begin to break down when the energy density of the decay products becomes comparable to the energy density of the inflaton condensate. Furthermore, as pointed out in [152], and discussed in detail in [153], [154], $\Gamma_{\phi \rightarrow \chi\chi}$ develops a temperature dependence due to interactions (which we have not accounted for) between the decay products and the condensate. Indeed, as the decay products thermalise via scatterings and further decays, they acquire a temperature dependent ‘plasma’ mass $m_p(T)$ of the order $\sim \lambda T^2$, where λ is a typical coupling constant for a particle in the plasma. The presence of these ‘thermal’ masses prevent decay of the condensate if $m_\phi^2 \approx \lambda T^2$: the decay process becomes kinematically forbidden. An important consequence of these finite temperature corrections is that the reheating temperature, T_R (the temperature at the onset of the radiation dominated phase) is generally higher compared to the naive estimate obtained via setting $\Gamma = H$ (see the following section).

In addition to the effect of thermal masses, the produced χ particles can ‘rescatter’ off the oscillating condensate $\langle \phi \rangle$ to excite $\delta\phi$ particles. This opens another possible channel for decay of the condensate. We illustrate this schematically in Fig. 4.7 for the case of the 4-leg interaction. In the language of our Bogoliubov calculation, this process corresponds to the term $\chi^2 \phi \delta\phi$ which results from expanding ϕ about the mean field: $\phi(x) = \phi(t) + \delta\phi(x)$. There is also a sub-dominant process of the type $\chi\chi \rightarrow \delta\phi\delta\phi$, which is phase space suppressed. Such processes, which we have neglected in this work, will promote the decay rate $\Gamma_{\phi \rightarrow \chi\chi}$ from a constant to a function of time and temperature. To include these processes would require recourse to non-equilibrium thermal field theory, which is beyond the scope of this paper. Having acknowledged these caveats, we use the Boltzmann Equations (4.80) and (4.81) to place rough bounds on our model parameters only.

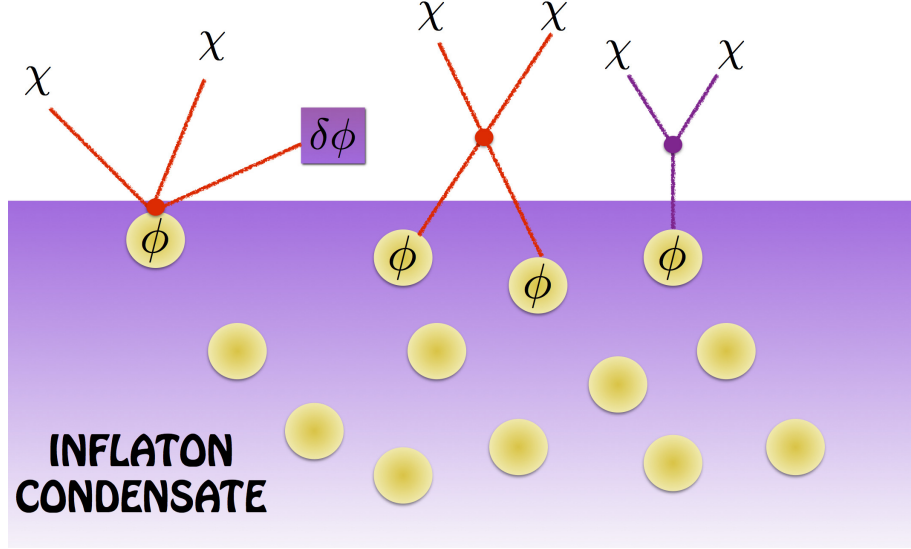


Figure 4.7: The vacuum energy of the inflaton field exists as spatially coherent oscillations, which can be interpreted as a condensate of non-relativistic zero momentum ϕ particles. The condensate decays via three-leg, $-\frac{1}{2}\sigma\phi\chi^2$, and four-leg, $-\frac{1}{2}g^2\phi^2\chi^2$ interactions. The Bogoliubov calculation presented in section 4.4.2 treats the condensate as a classical source, and so 'rescattering' processes between the produced Higgs particles and the condensate which excite $\delta\phi$ particles are ignored.

4.4.4 PARAMETER CONSTRAINTS FROM REHEATING

Combining the Planck constraint on the inflaton mass, (4.37), with the bound (4.56), we find that for reheating to proceed perturbatively:

$$\left(\frac{\sigma}{M_{\text{P}}}\right)^2 \ll 10^{-27} \left(\frac{f}{M_{\text{P}}}\right)^2, \quad (4.82)$$

where we have used $\Phi_0 \sim 0.6f$. This provides an upper bound on the trilinear coupling σ in terms of the scale f . A lower bound on σ can be obtained from the condition that the universe be totally radiation dominated before the BBN epoch. This requires knowledge of the reheating temperature T_R , which may be estimated as follows: Reheating completes at time t_c , when the Hubble rate $H^2 = \rho/3M_{\text{P}}^2 \sim t_c^{-2}$ drops below the decay rate $\Gamma_{\phi \rightarrow \chi\chi}$. The density of the universe at this moment is then

$$\rho(t_c) \simeq 3M_{\text{P}}^2 H^2(t_c) = 3M_{\text{P}}^2 \Gamma_{\phi \rightarrow \chi\chi}^2. \quad (4.83)$$

Provided that the higgs particles are produced in thermal and chemical equilibrium, the temperature of the higgs plasma is T_R . Treating this ultrarelativistic gas of particles with Bose–Einstein

statistics, the energy density of the universe in thermal equilibrium is then

$$\rho(T_R) \simeq \left(\frac{\pi^2}{30}\right) g_* T_R^4, \quad (4.84)$$

where the factor $g_*(T_R) \sim 10^2 - 10^3$ depends on the number of ultrarelativistic degrees of freedom. Comparing Eqs. (4.83) and (4.84) we arrive at

$$T_R \approx 0.1 \sqrt{\Gamma_{\phi \rightarrow \chi\chi} M_{\text{P}}} \quad (4.85)$$

In order not to spoil the success of BBN, the universe must be completely dominated by relativistic particles before the BBN epoch. This constrains the reheating temperature to be $T_R \gtrsim 5 \text{ MeV}$ [155], [156], which in turn implies⁹:

$$\Gamma_{\phi \rightarrow \chi\chi} \gtrsim 10^{-40} M_{\text{P}}. \quad (4.86)$$

Combining Eqs. (4.37), (4.76), (4.86) we find:

$$\left(\frac{\sigma}{M_{\text{P}}}\right)^2 \gtrsim 10^{-45} \left(\frac{f}{M_{\text{P}}}\right). \quad (4.87)$$

Finally, combining this temperature bound with the bound for perturbative reheating Eq. (4.82), we find:

$$f \gg 10^{-18} M_{\text{P}}. \quad (4.88)$$

4.5 TeV INFLATON AND ITS CONSEQUENCES

With the inflaton and Higgs doublet originated by the breaking of the same global symmetry, the Coleman-Weinberg contributions to their potential are naturally of the same order. Therefore, we would expect the mass of both particles to be not far from each other, $m_\eta \sim m_h$, as well as similar size couplings. From perturbative reheating we require $m_\eta > 2m_h$ as well as a condition on the cubic coupling Eq. (4.57), namely

$$\frac{c_3}{f} \ll \left(\frac{m_\eta}{f}\right)^2, \quad (4.89)$$

which is technically natural as the parameter c_3 breaks the symmetry $\eta \rightarrow -\eta$.

Inflation would also impose a bound on the mass of the inflaton respect to the scale of breaking, see (4.34) and (4.3), $m_\eta/f \simeq 10^{-6}$, a hierarchy which is again technically natural. On the other

⁹We note that since T_R also enters expressions for the primordial observables, the lower bound on $\Gamma_{\phi \rightarrow \chi\chi}$ given by (4.86) may be tightened if our model were to be confronted with CMB data – see for example Ref. [157].

hand, in our inflationary potential we could have added a constant term, a *phenomenological* cosmological constant which could change this condition and allow closer values of f and m_η .

One should also keep in mind that inflation cannot last to reach energies around the MeV when the very predictive theory of Big-Bang Nucleosynthesis takes on [158]. Another constraint to keep in mind is the generation of baryon asymmetry in the Universe, which in the context of Electroweak Baryogenesis (see Ref. [159] and references therein) would require inflation to end some time before the electroweak scale. One additional attractive feature of this model is that the conditions for reheating, which in turn require CP violation, could be helpful for baryogenesis, e.g. see Ref. [160] for a study of electroweak baryogenesis in a similar model.

If the inflaton is heavier than the Higgs doublet, one can integrate it out leading to an Effective Field Theory (EFT). In Ref. [161] one can find a more general discussion on the EFT due the presence of a singlet like η , and its phenomenology.

Interestingly, the cubic term c_3 is the main player in the reheating discussion as well as the collider phenomenology. The cubic term, when the Higgs acquires a vacuum expectation value v , would lead to a mixing of the singlet with the Higgs, resulting in two mass eigenstates with an admixture of η and h . The mixing angle is given by

$$s_\theta \simeq \frac{c_3 v}{m_\eta^2} \quad (4.90)$$

The mixing, then, changes the way the physical SM-like Higgs behaves, as well as induces new couplings of the heavy η -like state to vector bosons and fermions. Detailed studies from Electroweak Precision Tests (EWPT) at LEP, as well as current constraints from the measurement of the Higgs properties imposes strong bounds on this mixing. Moreover, the heavier state can be searched for directly and the reach for these searches is related to the amount of mixing.

In Figure 4.8, we show current and future constraints on these parameters. They include 1.) a χ^2 fit to Higgs coupling measurements [162]–[171], 2.) The 95% C.L. exclusion prospects for LHC at 14 TeV with $\mathcal{L} = 300 \text{ fb}^{-1}$ and $\mathcal{L} = 3000 \text{ fb}^{-1}$, by assuming that future measurements of Higgs signal strengths will be centered at the SM value, and use the projected CMS sensitivities, 3.) A fit to the oblique parameters S, T, U using the best-fit values and standard deviations from the global analysis of the GFitter Group [172], and finally 4.) Future limits on EW precision observables from e^+e^- colliders (see e.g. [173]), ILC and FCC-ee.

The corrections to S and T from the inflaton-Higgs mixing given by

$$\begin{aligned} \Delta S &= \frac{1}{\pi} s_\theta^2 \left[-H_S \left(\frac{m_h^2}{m_Z^2} \right) + H_S \left(\frac{m_\eta^2}{m_Z^2} \right) \right] \\ \Delta T &= \frac{g^2}{16 \pi^2 c_W^2 \alpha_{\text{EM}}} s_\theta^2 \left[-H_T \left(\frac{m_h^2}{m_Z^2} \right) + H_T \left(\frac{m_\eta^2}{m_Z^2} \right) \right] \end{aligned} \quad (4.91)$$

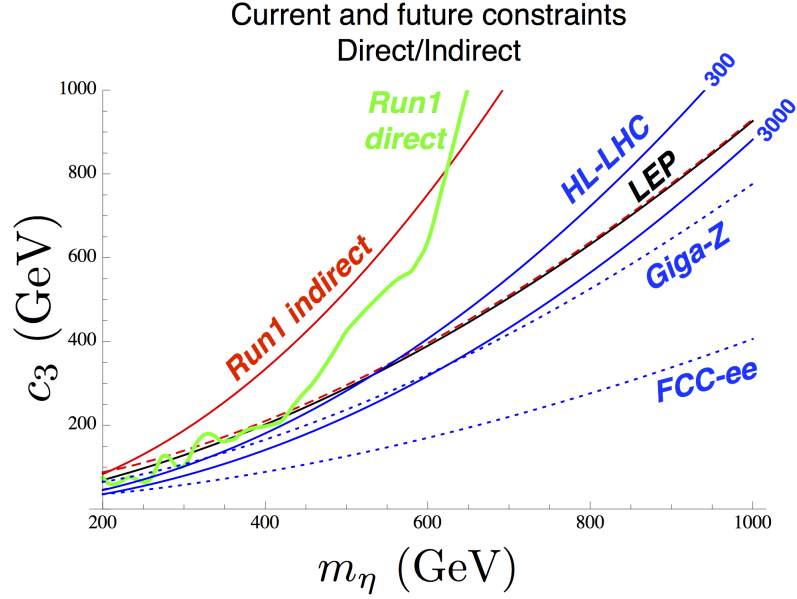


Figure 4.8: Present and future 95% C.L. exclusion limits in the (m_η, c_3) plane from ATLAS and CMS measurements of Higgs signal strengths (denoted by Run1 indirect) and from EWPT (denoted by LEP). Values above the red-dashed line are excluded at 95% C.L. by the combination (EWPT and Higgs signal strength). Above the green line may also be excluded by constraints from heavy scalar searches at LHC, although these limits could be evaded in the presence of new decay modes for η . Also shown is the projected exclusion reach from Higgs signal strengths at the 14 TeV run of LHC with $\mathcal{L} = 300 \text{ fb}^{-1}$ and at HL-LHC with $\mathcal{L} = 3000 \text{ fb}^{-1}$ in blue, as well as projections from measurements of the S and T oblique parameters with ILC-*GigaZ* and FCC-ee in dashed-blue.

with the functions $H_S(x)$ and $H_T(x)$ defined in Appendix C of [174].

Regarding future colliders, we assumed a SM best-fit value, and interpreted the ILC *GigaZ* program's expected precision is $\sigma_S = 0.017$ and $\sigma_T = 0.022$ [172], [175] and the FCC-ee prospects of $\sigma_S = 0.007$ and $\sigma_T = 0.004$ [176]. As one can see, colliders are sensitive to relatively large values of the triple coupling, whereas perturbative reheating is sensitive to lower values of the coupling.

Finally, note that in the explicit CP breaking scenario, there would be direct couplings of the inflaton to SM fermions (ϵ_f) and these would be proportional to c_3 , see (4.17b).

4.6 CONCLUSIONS

We have presented a single model that can realise inflation, perturbative reheating, and electroweak symmetry breaking in a natural way. In the minimal model the five Goldstone bosons from the global symmetry breaking $SO(6) \sim SU(4) \rightarrow SO(5) \sim Sp(4)$ play the role of a Higgs doublet and

an inflaton singlet. We have argued that a trilinear coupling between the latter (η) and two Higgs bosons (h) is necessary for successful reheating, and shown under which condition this term can be present. In particular, the model needs to have broken CP, which can be realised spontaneously or explicitly. A detailed derivation of the scalar potential for h and η arising from loops of $SU(2)$ gauge bosons and fermions in the **6** of $SU(4)$ was given in the first section.

The CMB results [14] allow us relate the parameters in our model, and explain mass hierarchies. A range of energy scales for inflation, or equivalently for the mass of the inflaton was presented in the second section. To the merit of the model, none of the relevant scales are expected to be affected by quantum gravity.

The motive of perturbative reheating further fixes the parameters in the potential. For a particular range of parameter space (given by Eq. (4.57)) parametric instability is not triggered and non-perturbative effects are subdominant. With a Bogoliubov calculation [144] we find the single particle occupation numbers, and as usual the evolution of the fields is established using Boltzmann equations. We finished this section by an exposition of the numerical constraints on the reheating temperature and the model parameters from perturbativity (4.86)-(4.88).

We have also explored the possibility of TeV values of the inflaton mass and coupling to the Higgs. As an effective theory, the inflaton's effect at low energies is inducing a mixing effect in the Higgs particle properties, an effect which is constrained by precise electroweak data as well as the LHC. We discussed the future reach for colliders on the inflaton-Higgs parameter space, finding that while perturbative reheating explores a region of small mixing, colliders are most sensitive to large values of this parameter.

The model building presented in this paper hints at interesting opportunities for further studies. The fact that the model is able to address and connect normally unrelated cosmological events in a natural way makes that the considerations here may indeed tempt the reader to further inquiry, in the light of recent developments. As mentioned in the introduction, the discussion of cosmological relaxation by an interplay between the Higgs and a pGB [17] offers an attractive example. Other directions include an investigation of the changed evolution of the Higgs dynamics and its implications on electroweak stability [141], possible UV completions for which the present theory is a boundary condition at low energy (on which we commented in [63]), as well as the implications of CP violation and the inflaton degree of freedom for electroweak baryogenesis.

ACKNOWLEDGEMENTS

We would like to thank Marco Drewes, Hitoshi Murayama and Josemi No for discussions. This work is supported by the Science Technology and Facilities Council (STFC) under grant number ST/L000504/1.

APPENDIX A: COMPUTATION OF THE SCALAR POTENTIAL

COMPOSITE HIGGS VACUUM

At one loop, the Coleman-Weinberg potential due to up-type quarks coupling to Σ as in (4.11) is given by¹⁰

$$V(h, \eta) = -2N_c \int \frac{d^4 p}{(2\pi)^4} \log \left(p^2 \Pi_{u_L} \Pi_{u_R} - |\Pi_{u_L u_R}|^2 \right) \quad (4.92)$$

where we have used new form factors for simplicity, which are just rotations of the original parameters in the Lagrangian (4.11):

$$\Pi_{u_L} = \frac{\Pi_0^q + \Pi_0^{q'}}{2} - \Pi_1^q \frac{\text{Tr}[\bar{\Psi}_q \Sigma] \not{p} \text{Tr}[\Psi_q \Sigma^\dagger]}{\bar{u}_L \not{p} u_L} \quad (4.93a)$$

$$\Pi_{u_R} = \Pi_0^u - \Pi_1^u \frac{\text{Tr}[\bar{\Psi}_u \Sigma] \not{p} \text{Tr}[\Psi_u \Sigma^\dagger]}{\bar{u}_R \not{p} u_R} \quad (4.93b)$$

$$\Pi_{u_L u_R} = M_1^u \frac{\text{Tr}[\bar{\Psi}_q \Sigma] \text{Tr}[\Psi_u \Sigma^\dagger]}{\bar{u}_L u_R} \quad (4.93c)$$

as explained in the main text, we refer to Ψ as the fermion multiplets in the 6 of SU(4).

If we assume the ratios form factors fall off rapidly enough with momentum to make the integrals converge, we may expand the logarithms to find the following Lagrangian to fourth order in the fields:¹¹

$$V(\phi, h) = a_1 h^2 + \lambda h^4 + |\kappa|^2 \left(a_2 + a_3 h^2 + a_4 |\kappa|^2 \right) \quad (4.94)$$

¹⁰In general there will be contributions from down type quarks and gauge bosons as well. In fact, it should be noted that at least one other fermion generation is needed to make the CP assignment physical [177]. However, these will not lead to different couplings in the scalar potential, and here we take them to be sub-leading corrections to the coefficients.

¹¹This is a common assumption, motivated by the fact that higher order terms are expected to be suppressed by squares of ratios of form factors. In other words, this falls under the same assumption as the convergence of the integrals.

where $\kappa = \sqrt{f^2 - h^2 - \eta^2} + i\epsilon_t \eta$. The coefficients are given by integrals over the form factors of the fields contributing to the CW potential: the gauge bosons, and the up-type and down-type fermions. If we assume the contributions are dominated by the heaviest up-type quark, which we will call the top as in the Standard Model (while this quark is not necessarily identified with the Standard Model top), the coefficients are given by:

$$a_1 = -2f^2 N_c \int \frac{d^4 p}{(2\pi)^4} \frac{1}{\Pi_0} (-4\Pi_1^q \Pi_0^t) \quad (4.95a)$$

$$a_2 = -2f^2 N_c \int \frac{d^4 p}{(2\pi)^4} \frac{1}{\Pi_0} (-2\Pi_0^q \Pi_1^t - 2\Pi_1^{q'} \Pi_1^t) \quad (4.95b)$$

$$a_3 = -2N_c \int \frac{d^4 p}{(2\pi)^4} \frac{1}{\Pi_0} \left(-\frac{4|M_t^1|^2}{p^2} + \frac{8\Pi_0^q \Pi_1^q \Pi_0^t \Pi_1^t}{\Pi_0} + \frac{8\Pi_1^q \Pi_1^{q'} \Pi_0^t \Pi_1^t}{\Pi_0} + 16\Pi_1^q \Pi_1^t \right) \quad (4.95c)$$

$$a_4 = -2N_c \int \frac{d^4 p}{(2\pi)^4} \frac{1}{\Pi_0} \left(\frac{2(\Pi_0^q)^2 (\Pi_1^t)^2}{\Pi_0} + \frac{4\Pi_0^q \Pi_1^q (\Pi_1^t)^2}{\Pi_0} + \frac{2(\Pi_1^{q'})^2 (\Pi_1^t)^2}{\Pi_0} \right) \quad (4.95d)$$

$$\lambda = -2N_c \int \frac{d^4 p}{(2\pi)^4} \frac{1}{\Pi_0} \left(\frac{8(\Pi_1^q)^2 (\Pi_0^t)^2}{\Pi_0} \right) \quad (4.95e)$$

where Π_0 is the relevant field independent factor:

$$\Pi_0 = \frac{1}{2} \Pi_0^t (\Pi_0^q + \Pi_0^{q'}) \quad (4.96)$$

i.e., a function of the different propagation terms for the fermions, the first terms in the fermion Lagrangian (4.11). Also, note we have defined

$$p \rightarrow p/f \quad (4.97)$$

for simplicity.

CP BREAKING VACUUM

Here we repeat the exercise in the previous section to compute the coefficients of the CP breaking vacuum potential,

$$V(\eta, h) = c_{tad}\eta + m_\eta^2 \eta^2 + \tilde{c}_\eta \eta^3 + \lambda_\eta \eta^4 + m_h^2 h^2 + \lambda_h h^4 + c_3 \eta h^2 + c_4 \eta^2 h^2 \quad (4.98)$$

The coefficients c_i are in general nonzero, except for at $\alpha = 1/4\pi$. Below we compute the parameters in an example with $\alpha = 1/3\pi$ case. As argued in the main text, the $\alpha = 2/3\pi$ case can be

obtained from this by making the substitution $\eta \rightarrow -\eta$ in the potential:¹²

$$c_{tad} = -2N_c f^3 \int \frac{d^4 p}{(2\pi)^4} \frac{1}{2\Pi_0} \sqrt{3}\eta \Pi_1^t ((\epsilon_u - 4)\epsilon_u - 1)(\Pi_0^q + \Pi_0^{q'}) \quad (4.99a)$$

$$m_\eta^2 = -2N_c f^2 \int \frac{d^4 p}{(2\pi)^4} \frac{1}{\Pi_0} \left(\frac{3\Pi_1^t ((\epsilon_u - 4)\epsilon_u - 1)^2 (\Pi_0^q + \Pi_0^{q'})^2}{8\Pi_0} - \Pi_1^t (\epsilon_u^2 - 1) (\Pi_0^q + \Pi_0^{q'}) \right) \quad (4.99b)$$

$$\tilde{c}_\eta = -2N_c f \int \frac{d^4 p}{(2\pi)^4} \left(-\frac{\sqrt{3}\eta^3 (\Pi_1^t)^2 (\epsilon_u^2 - 1) ((\epsilon_u - 4)\epsilon_u - 1) (\Pi_0^q + \Pi_0^{q'}) (\Pi_0^q + \Pi_0^{q'})}{2\Pi_0^2} \right) \quad (4.99c)$$

$$\lambda_\eta = -2N_c \int \frac{d^4 p}{(2\pi)^4} \frac{(\Pi_1^t)^2 (\epsilon_u^2 - 1)^2 (\Pi_0^q + \Pi_0^{q'})^2}{2\Pi_0^2} \quad (4.99d)$$

$$m_h^2 = -2N_c \int \frac{d^4 p}{(2\pi)^4} \frac{(p^2 (\Pi_1^t (\epsilon_u^2 + 3) (\Pi_0^q + 2\Pi_1^q + \Pi_0^{q'}) - 2\Pi_1^q \Pi_0^t) - 2M_t^2 (\epsilon_u^2 + 3))}{2p^2 \Pi_0} \quad (4.99e)$$

$$\lambda_h = -2N_c f^2 \int \frac{d^4 p}{(2\pi)^4} \frac{(\epsilon_u^2 + 3) (M_q^2 - p^2 \Pi_1^q \Pi_1^t)}{p^2 \Pi_0} + \frac{(\Pi_1^t (\epsilon_u^2 + 3) (\Pi_0^q + 2\Pi_1^q + \Pi_0^{q'}) - 2\Pi_1^q \Pi_0^t)^2}{8\Pi_0^2} \quad (4.99f)$$

$$c_3 = -2N_c f \int \frac{d^4 p}{(2\pi)^4} \left(\frac{\sqrt{3}((\epsilon_u - 4)\epsilon_u - 1) (M_t^2 - p^2 \Pi_1^q \Pi_1^t)}{p^2 \Pi_0} \right) \quad (4.99g)$$

$$+ \frac{\sqrt{3}\Pi_1^t ((\epsilon_u - 4)\epsilon_u - 1)(\Pi_0^q + \Pi_0^{q'}) (\Pi_1^t (\epsilon_u^2 + 3) (\Pi_0^q + 2\Pi_1^q + \Pi_0^{q'}) - 2\Pi_1^q \Pi_0^t)}{4\Pi_0^2} \quad (4.99h)$$

$$c_4 = -2N_c \int \frac{d^4 p}{(2\pi)^4} \left(\frac{2(\epsilon_u^2 - 1) (p^2 \Pi_1^q \Pi_1^t - M_t^2)}{p^2 \Pi_0} \right) \quad (4.99i)$$

$$- \frac{\eta^2 h^2 \Pi_1^t (\epsilon_u^2 - 1) (\Pi_0^q + \Pi_0^{q'}) (\Pi_1^t (\epsilon_u^2 + 3) (\Pi_0^q + 2\Pi_1^q + \Pi_0^{q'}) - 2\Pi_1^q \Pi_0^t)}{2\Pi_0^2} \quad (4.99j)$$

where again Π_0 is the relevant field independent factor, here given by:

$$\Pi_0 = \frac{1}{2} (\Pi_0^q + \Pi_0^{q'}) (\Pi_0^t - 2\Pi_1^t (\epsilon_u^2 + 1)) \quad (4.100)$$

As explained in the main text, the tadpole term can be shifted away by an appropriate shift in the other parameters, corresponding to a vev for η :

$$c_{tad} + 2m_\eta^2 v_\eta + 3\tilde{c}_\eta v_\eta^2 + 4\lambda_\eta v_\eta^3 = 0$$

¹²These are again the parameters before shifting away the tadpole term, in exactly the same way as above.

The new parameters will then be given in terms of the quoted parameters as

$$m_\eta^2 \rightarrow m_\eta^2 + 3\tilde{c}_\eta v_\eta + 6\lambda_\eta v_\eta^2 \quad (4.101a)$$

$$\tilde{c}_\eta \rightarrow \tilde{c}_\eta + 4v_\eta \lambda_\eta \quad (4.101b)$$

$$m_h^2 \rightarrow c_3 v_\eta + c_4 v_\eta^2 \quad (4.101c)$$

$$c_3 \rightarrow c_3 + 2c_4 v_\eta \quad (4.101d)$$

MODEL BUILDING WITH NON-COMPACT COSETS

Djuna Croon¹

¹Department of Physics and Astronomy, Pevensey II Building, University of Sussex, BN1 9RH,
UK

We explore Goldstone boson potentials in non-compact cosets of the form $SO(n,1)/SO(n)$. We employ a geometric approach to find the scalar potential, and focus on the conditions under which it is compact in the large field limit. We show that such a potential is found for a specific misalignment of the vacuum. This result has applications in different contexts, such as in Composite Higgs scenarios and theories for the Early Universe. We work out an example of inflation based on a non-compact coset which makes predictions which are consistent with the current observational data.

5.1 INTRODUCTION

Goldstone bosons are popular actors in theories beyond the Standard Model of Particle Physics. They resolve the dichotomy between the aptness of scalars in cosmological theories and the theoretical hierarchy problems that fundamental scalars suffer. The study of their Effective Field Theory is further motivated by their omnipresence in UV theories with global symmetries, such as models for axions [178]–[180], and supersymmetry [181]–[183].

There is a vast body of literature which focuses on Goldstone bosons in compact cosets, that is, on theories in which a compact global symmetry breaks spontaneously to its compact subgroup. An example is the Minimal Composite Higgs Model MCHM₅, in which $SO(5) \rightarrow SO(4)$. In theories of this kind the Goldstone bosons lie on a compact manifold, such as the hypersphere $S^4 \simeq SO(5)/SO(4)$. Their interactions are invariant under a shift symmetry, such that a potential is forbidden at all orders in perturbation theory.

In the presence of a source of explicit breaking of the global group the shift symmetry is broken, and a potential for the pseudo-Goldstone Bosons (pGBs) may be generated. Such an explicit breaking can be mediated by external gauge bosons which gauge part of the global group, as is common in Composite Higgs models, or by couplings to instantons which do not respect the symmetry, as is the case with axions. The resulting potential will have a remnant periodic shift symmetry, stabilizing it against quantum corrections. Examples which employ such a scenario are Composite Higgs models [19], Natural Inflation [37], Goldstone Inflation [63], [64], and composite dark matter [184].

Goldstone bosons in non-compact cosets have received far less attention. Of particular interest are models in which a non-compact group breaks to its compact subgroup. There are indications that such cosets could give promising models of inflation [185] and electroweak symmetry breaking [186]. Like in the compact case, these cosets may address hierarchy problems by giving rise to stable scalar potentials.

Here we will explore the idea that scalar sectors can be studied in a coordinate-invariant way, something that has recently attracted some attention in the context of Higgs Effective Field Theory [186]–[188]. It has been observed [189] that results in non-compact cosets may be extrapolated from corresponding compact cosets by considering imaginary parameters, such that the corresponding manifold undergoes a Wick rotation. Here we instead follow a more general, geometric approach to study the potential of the Goldstone bosons of the hyperbolic space $SO(n,1)/SO(n)$. In section 5.2 we describe the different models for hyperboloids that are of interest to this analysis.

The shift symmetry in the non-compact case will also be broken in the presence of explicit

symmetry breaking effects, misaligned with the original breaking. For $SO(n,1)/SO(n)$ the remnant symmetry takes the form of a discrete scaling symmetry. We will parametrize the explicit breaking without choosing a particular particle physics interpretation, bearing in mind the different ways of breaking the shift symmetry. Our approach generalizes the analysis of [185] in the context of inflation, and provides an alternative description of the discussion of Goldstone bosons in non-compact cosets in [188]. The models are intimately related to models with a negatively curved field space resulting from a non-minimal coupling to gravity, such as Starobinsky inflation [190], supergravity models with particular Kähler potentials [191], and (more generally) the α -attractor models [192]–[194].

The focus of this paper will be on the conditions under which the Goldstone boson potential is bounded, i.e. confined to lie in a specific region in the limit in which the field excursion of the scalars is large. This is of particular interest for inflationary model building, as in typical scenarios one has to explain the gap between the magnitude of the scalar potential ($V^{1/4} \sim 10^{15}$ GeV) and the large field excursion ($\Delta\phi \sim M_p$), highlighted by the familiar Lyth bound [16]. In section 5.3 we will show that a bounded potential is generated when the symmetry breaking parameters transform as a null vector of the hyperbolic space.

In the last section we will discuss the application of this class of models to inflation. We will explore the inflationary predictions, and compare them to data from the Planck collaboration [14].

5.2 MODELS OF HYPERBOLIC SPACE

Below the scale of the spontaneous breaking $SO(n,1) \rightarrow SO(n)$, the relevant degrees of freedom are a set of Goldstone bosons which lie on the non-compact, n -dimensional hyperbolic sheet given by $SO(n,1)/SO(n)$. In the absence of any additional sources of breaking, the Goldstone bosons respect a shift symmetry which forbids a scalar potential. They will obtain a potential when they couple to a source of explicit breaking. This is for instance the case if a smaller group is gauged by external bosons such as in Composite Higgs models. This case is well studied; it has for instance recently been discussed in [186] in the context of Higgs Effective Field Theory. Here we use a less restrictive approach, in which we focus on the transformation properties of the symmetry breaking parameters which couple to the Goldstone bosons.

The coset $SO(n,1)/SO(n)$ can be described as a sheet of a space-like hyperbola,¹ defined by the

¹The terminology in this chapter is adopted often in analogy with space-time symmetries, however, the reader is assured that we consider internal symmetries only in this paper.

interval

$$L = \{(x_1, \dots, x_{n+1}) : x_{n+1}^2 - x_n^2 - x_{n-1}^2 - \dots - x_1^2 = \ell^2 \text{ and } x_{n+1} > 0\} \quad (5.1)$$

$$ds_L^2 = \eta_{\alpha\beta} dx^\alpha dx^\beta = dx_{n+1}^2 - \sum_{i=1}^n dx_i^2 \quad (5.2)$$

where $x_{n+1} > 0$. This space is associated with the Hermitian form or dot product with the signature $(n, 1)$,

$$g_{\mu\nu} x^\mu y^\nu = x_\mu y^\mu = -x_1 y_1 + x_2 y_2 + \dots + x_n y_n \quad (5.3)$$

It has constant negative curvature,

$$\mathcal{R}_{fieldspace} = -n(1+n) < 0. \quad (5.4)$$

As we will see in the following, the model "L" is not always the most transparent choice to describe the features of the Goldstone potential. An alternative choice is the Poincare disk model, which is defined by

$$J = \{(x_1, \dots, x_{n+1}) : x_1^2 + \dots + x_{n+1}^2 = \ell^2 \text{ and } x_{n+1} > 0\} \quad (5.5)$$

$$ds_J^2 = \frac{dx_{n+1}^2 + \sum_{i=1}^n dx_i^2}{x_{n+1}^2} \quad (5.6)$$

This model is related to "L" by a central projection from the point $(-\ell, 0, \dots, 0)$,

$$L \rightarrow J, \quad (x_1, \dots, x_n, x_{n+1}) \mapsto (x_1 \ell / x_{n+1}, \dots, x_n \ell / x_{n+1}, \ell^2 / x_{n+1}) \quad (5.7)$$

Another choice is the Poincare Half plane model, which reduces to the well known complex projective coordinates often employed in supersymmetry for $n = 2$. The Half plane model is defined by

$$H = \{(1, x_2, \dots, x_{n+1}) : x_{n+1} > 0\} \quad (5.8)$$

$$ds_H^2 = \frac{dx_{n+1}^2 + \sum_{i=2}^n dx_i^2}{x_{n+1}^2} \quad (5.9)$$

The Half plane model can in turn be related to J by a central projection from the point $(0, \dots, 0, \ell)$, i.e. the mapping

$$J \rightarrow H, \quad (x_1, \dots, x_n, x_{n+1}) \mapsto (-\ell, 2\ell x_2 / (x_1 - \ell), \dots, 2\ell x_{n+1} / (x_1 - \ell)) \quad (5.10)$$

From this, it follows that "H" and "L" are related by the mapping,

$$L \rightarrow H, \quad (x_1, \dots, x_n, x_{n+1}) \mapsto (-\ell, 2\ell x_2 / (x_1 - x_{n+1}), \dots, 2\ell^2 / (x_1 - x_{n+1})) \quad (5.11)$$

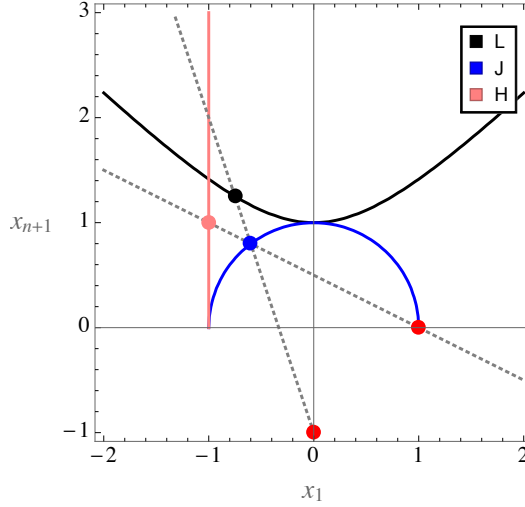


Figure 5.1: Models of the coset in two dimensions. An arbitrary point on the hyperbola, $\{x_1^L, x_{n+1}^L\}$ (in black), can be projected it unto the sphere $x_1^2 + x_{n+1}^2 = 1$ from the point $\{-1, 0\}$. This gives the coordinates in the Disk model, $\{x_1^J, x_{n+1}^J\} = \left\{ \frac{x_1^L}{x_{n+1}^L}, \frac{1}{x_{n+1}^L} \right\}$ (in blue). A further projection from the point $\{1, 0\}$ onto the line $x_1 = -1$ gives the coordinates in "H" $\{x_1^H, x_{n+1}^H\} = \left\{ -1, 2 / \left(x_{n+1}^L \left(1 - \frac{x_1^L}{x_{n+1}^L} \right) \right) \right\}$ (in pink).

5.3 COMPACT POTENTIALS FROM NON-COMPACT COSETS

Before the second symmetry breaking, the Goldstone bosons are massless and their target metric is described by the hyperboloid $SO(n,1)/SO(n)$. In the previous section we have shown different ways to describe such a field space.

A potential for the Goldstone bosons of the coset $SO(n,1)/SO(n)$ is generated in the presence of symmetry breaking effects, misaligned from the original vacuum. We use a very minimal description, based on particular choices for the transformation properties of the symmetry breaking parameters under the higher dimensional Lorentz group. Here we derive which transformation properties lead to a compact potential, i.e., a potential that does not diverge in the large field limit.

First we observe the following,

$$x_{n+1}^L - x_1^L = 2\ell^2/x_{n+1}^H \quad (5.12)$$

(and as we saw above $x_{n+1}^H > 0$). This combination corresponds to an $(n+1)$ dimensional null vector of $SO(n,1)$. Notice that the symmetry always allows one to rotate the spacelike components of a vector into the x_1 direction. Thus if the symmetry breaking parameters transform as a null vector, that is,

$$V_L = \frac{V_\mu x^\mu}{\ell} = V \left(\frac{x_{n+1}^L - x_1^L}{\ell} \right) \quad (5.13)$$

where V is just the normalization of the vector, we recover compactness in the “H” coordinates,

$$V_H = \frac{2\ell V}{x_{n+1}^H}. \quad (5.14)$$

The theory is then defined by this potential and the target metric in “H”, such that (dropping the superscripts)

$$\mathcal{L} = \mathcal{L}_{kin} - V = \frac{f^2}{4} \frac{dx_2^2 + \dots + dx_{n+1}^2}{x_{n+1}^2} - \frac{V_1}{x_{n+1}} \quad (5.15)$$

As this Lagrangian is invariant under a shift symmetry for all x_k ($k \neq n+1$), it is seen that one can always find stationary points where x_k is constant. In particular, it is always possible to find a field space trajectory for which only x_{n+1} evolves. In that light, we may canonically normalize x_{n+1} in terms of the field ϕ ,

$$\phi = \frac{f}{\sqrt{2}} \log x_{n+1} \quad (5.16)$$

such that we arrive at the negative exponential potential

$$\mathcal{L} = \frac{1}{2}(\partial\phi)^2 - V_1 e^{-\sqrt{2}\phi/f} \quad (5.17)$$

Note that the positivity of x_{n+1} guarantees that ϕ is a real direction and that $-\infty < \phi \leq \infty$.

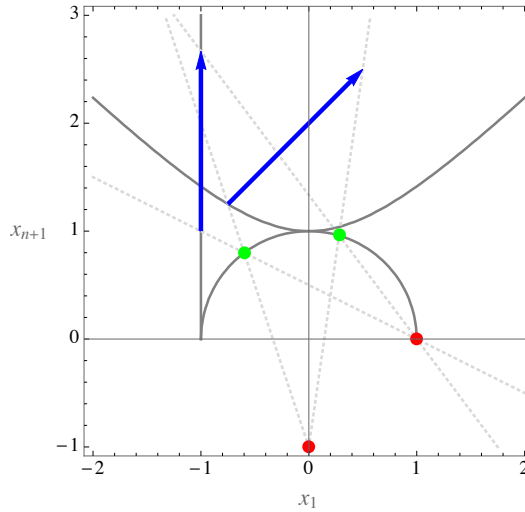


Figure 5.2: Mapping of a transformation in two dimensions. It is seen that a time-like vector from an arbitrary point on the hyperbolic manifold will map to a finite projection in the model “H”.

Similarly, a timelike vector is mapped to its inverse by $L \rightarrow J$,

$$x_{n+1}^L = \ell^2 / x_{n+1}^J \quad (5.18)$$

Following similar steps in this simpler example we arrive at the same result

$$\mathcal{L} = \frac{1}{2}(\partial\phi)^2 - V_1 e^{-\sqrt{2}\phi/f} \quad (5.19)$$

Note that this exponential potential respects a classical scale invariance, under which

$$\phi \rightarrow \phi + \epsilon, \quad x^\mu \rightarrow x^\mu e^{\epsilon/\sqrt{2}f}. \quad (5.20)$$

and the action is just rescaled by $e^{\sqrt{2}\epsilon/f}$.

In general, the transformation rule of the symmetry breaking parameters allows for a constant term and higher order terms as well, suppressed by the relevant scale Λ . If the symmetry breaking effects can be parametrized in terms of a single vector V_μ which couples linearly to the Goldstones, higher order terms can be built from invariants of the form $V_\mu x^\mu$, such that,

$$V_L = V_0 + \sum_{j=1}^{\infty} g_j \frac{(V_\mu x^\mu)^j}{\Lambda^{4(j-1)}} = V_0 + \sum_{j=1}^{\infty} \tilde{g}_j \Lambda^4 \left(\frac{x_{n+1} - x_1}{\ell} \right)^j \quad (5.21)$$

where $\tilde{g}_j = g_j (V_1/\Lambda^4)^j$. The above steps will generate the exponential potential

$$V = V_0 - V_1 e^{-\sqrt{2}\phi/f} + \sum_{j=2}^{\infty} (-1)^j \tilde{g}_j \Lambda^4 e^{-j\sqrt{2}\phi/f} \quad (5.22)$$

which also respects the scaling symmetry, as it must. Generically one expects the higher harmonics to be of the size $(V_1/\Lambda^4)^j$ [74]. In this limit ($g_j = 1$), the potential can be resummed,

$$V = V_0 + V_1 \sum_{j=1}^{\infty} \left(\frac{V_1}{\Lambda^4} \right)^{j-1} (-e^{-\sqrt{2}\phi/f})^j = V_0 - V_1 \frac{e^{-\sqrt{2}\phi/f}}{1 + (V_1/\Lambda^4)e^{-\sqrt{2}\phi/f}} \quad (5.23)$$

We have seen that one may recover a bounded single field potential for any n , when the symmetry breaking dynamics transforms as a vector of $\text{SO}(n,1)$. The field space dimensionality of the potential is unsurprising when one considers that an $\text{SO}(n)$ transformation may always rotate the spacelike components along one direction, such that the only distinct cases are timelike, spacelike, and null.

In the limit of exactly massless, non-interacting spectator fields, we do not expect the phenomenology to be altered with respect to the single field case. Let us consider the massless Goldstone fields in (5.15), with the field redefinition

$$\chi_i = x_i f / \sqrt{2} \quad i \neq n+1 \quad (5.24)$$

such that GBs have mass dimension 1. As only derivative interactions respect the shift symmetry for the $(n-1)$ massless Goldstones, the lowest dimension couplings to fermions are dimension $d = 5$ and of the form $\partial_\mu \chi_i \bar{\psi} \gamma^\mu \psi$.

Another possibility is that the $(n-1)$ massless Goldstones are "eaten" to become the longitudinal components of gauge bosons, if the misalignment of the vacuum is due to gauging a subgroup of $\text{SO}(n,1)$. Examples of such subgroups are given in Table 5.1. The effective mass of these gauge bosons will be set by the field ϕ , which may develop a vacuum expectation value, reminiscent of

the Higgs mechanism. This vev is dependent on the form of the scalar potential, which is sensitive to deviations from $g_j = 1$, but is expected to be at least of the order of the symmetry breaking scale f .

n	Subgroup
9	SU(3)
8	SU(2)xSU(2)xU(1)
7	SU(2)xSU(2) or SO(4)
6	SU(2)xU(1)xU(1)
5	SU(2)xU(1)
4	SU(2) or SO(3)
3	U(1)xU(1)
2	U(1)

Table 5.1: Gauged subgroups such that n-1 Goldstone Bosons are "eaten".

5.4 INFLATION ALONG THE COMPACT DIRECTION

We have successfully constructed a compact potential in the large field limit based on the non-compact cosets $SO(n,1)/SO(n)$. This is a promising candidate for an inflationary theory, in which one typically considers a large field excursion $\Delta\phi \sim M_p$, while measurements of the density perturbations forces the magnitude of the scalar potential to be orders of magnitude lower $V^{1/4}/\epsilon \sim 10^{15}$ GeV (where $\epsilon \ll 1$ is the first slow roll parameter).

To interpret the pGB as the inflaton, consider the potential (5.23),

$$V = V_0 + V_1 \sum_{j=1}^{\infty} g_j \left(\frac{V_1}{\Lambda^4} \right)^{j-1} (-e^{-\sqrt{2}\phi/f})^j \quad (5.25)$$

where here we phenomenologically impose $V_0 = \Lambda^4$ to render the potential positive definite. We will work out an example with $g_j = 1$ such that the potential is bounded from below, however, as we will find below, the inflationary results only depend strongly on the first term in the sum and are therefore insensitive to this assumption. With these assumptions, the potential can be rewritten as

$$V = \frac{\Lambda^4}{\alpha e^{-\sqrt{2}\phi/f} + 1} \quad (5.26)$$

where $\alpha = V_1/\Lambda^4$. This model can reproduce the inflationary predictions from the Planck data [14]. It is, to a first approximation, a single field model, with slow roll parameters given by

$$\epsilon = \frac{M_p^2}{2} \left(\frac{V'(\phi)}{V(\phi)} \right)^2 = \frac{M_p^2}{f^2} \frac{\alpha^2}{(\alpha + e^{\sqrt{2}\phi/f})^2} \quad (5.27)$$

$$\eta = M_p^2 \left(\frac{V''(\phi)}{V(\phi)} \right) - \frac{M_p^2}{2} \left(\frac{V'(\phi)}{V(\phi)} \right)^2 = \frac{M_p^2}{f^2} \frac{\alpha (\alpha - 2e^{\sqrt{2}\phi/f})}{(\alpha + e^{\sqrt{2}\phi/f})^2} \quad (5.28)$$

where M_p is the reduced Planck mass. It is seen that for a slow roll scenario to take place below the Planck scale ($f < M_p$), one has to be in the regime $\alpha \ll e^{\sqrt{2}\phi/f}$. Thus, to study inflation it would have been sufficient to only consider the first term in the series expansion; we have considered the resummed potential here to show that it is bounded from below.

Slow roll ends when $\epsilon \rightarrow 1$. We use this relation to estimate

$$\phi_E = \frac{\log(\alpha(\beta - 1))}{\sqrt{2}\beta} \quad (5.29)$$

where $\beta = (f/M_p)^{-1}$. The number of e-foldings is then given by

$$N = \frac{1}{M_p^2} \int_{\phi_i}^{\phi_e} \frac{V(\phi)}{V'(\phi)} d\phi \quad (5.30)$$

In figure 5.3 we show the inflationary predictions of the model in terms of the spectral index n_s and the tensor- to scalar ratio r . The values that fall are allowed by the Planck data, and satisfy

$$\frac{f}{M_p} < 1 \quad (5.31)$$

lowering this ratio implies reducing the prediction for the tensor to scalar ratio, as is common to Goldstone Inflation models [63], [64]. For comparison, we have also shown the predictions of the Starobinsky model [190], in which the negative field space curvature results from a non-minimal coupling to gravity.

As shown in the previous section, the other GB fields ($\chi_i = x_i f / \sqrt{2}$, $i \neq n+1$) are exactly massless in this model, and the inflationary dynamics is therefore completely dominated by the inflaton field ϕ . It is well known that for light spectator fields with $V''(\chi_i)/H^2 \ll 1$ the non-Gaussianity parameter f_{NL} is suppressed and there is no observable effect on the inflationary power spectrum. This effect can be checked explicitly for the current model (with a non-trivial field space metric) using the methodology described in [195].

However, the effects of the massless GB fields may become manifest during reheating after the slow-roll phase. The leading couplings between the massive field ϕ and other fields carry at least dimension five. A two-body decay to Standard Model gauge bosons from a coupling to the field

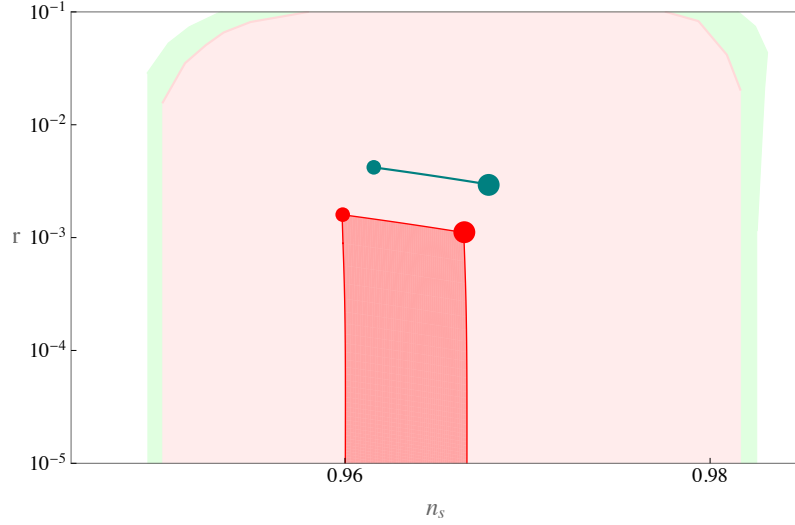


Figure 5.3: Inflationary predictions of n_s versus r . The biggest dot marks the point $N = 60, f \approx M_p$, the smaller dot marks $N = 50, f \approx M_p$. Lowering the scale f corresponds to lowering the tensor to scalar ratio, as indicated by the sweeping lines in the plot. The teal dots represent the predictions of the Starobinsky model for $N = 60, 50$ respectively. In green the TT spectrum and polarisation data at low- ℓ (lowP) from [14]; in pink the combined spectra TT, TE, EE + lowP.

strength would for instance be given by the decay rate $\Gamma_{\phi F^2} = 1/(8\pi)|\mathcal{M}|^2/m_\phi \approx 1/(8\pi)m_\phi^3/M_p^2$. When ϕ is interpreted as the inflaton, this may lower the reheat temperature, typically given by $T_r = \sqrt{\Gamma_{\phi F^2} M_p}$.

The coupled kinetic term (5.15) mixes the evolution of the scalar fields. As we will see, the curved field-space metric may give rise to a backreaction on the inflaton dynamics that forms the background for reheating. This effect is distinct from the usual Hubble induced mass for spectator fields (for instance such as described in [196]). From the equations (5.15), (5.16), (5.24), the equation of motion for the ϕ and χ_i fields are given by (conform [89])

$$\ddot{\chi}_i + 3H\dot{\chi}_i - \frac{2\sqrt{2}}{f}\dot{\chi}_i\dot{\phi} = 0 \quad (5.32)$$

$$\ddot{\phi} + 3H\dot{\phi} + \frac{2\sqrt{2}}{f}e^{-\frac{2\sqrt{2}\phi}{f}}(\dot{\chi}_i)^2 + \frac{\sqrt{2}V_1}{f}e^{-\frac{\sqrt{2}\phi}{f}} = 0 \quad (5.33)$$

Here the Hubble parameter is given by

$$H^2 = \frac{1}{3M_p^2} \left[\frac{1}{2} \left(\dot{\phi}^2 + e^{-\frac{2\sqrt{2}\phi}{f}} \dot{\chi}_i^2 \right) + V(\phi) \right] \quad (5.34)$$

where summation over the field index i is implied in both (5.33) and (5.34). The curved metric becomes important in the regime $H \ll \dot{\phi}/f$, for which the last term in (5.32) dominates. In this limit the equation is solved by

$$\dot{\chi}_i = c_1 f^2 e^{\frac{2\sqrt{2}\phi}{f}} \quad (5.35)$$

Inserting this result to solve the equation of motion for the inflaton, we find

$$\ddot{\phi} + 3H\dot{\phi} + 2\sqrt{2}(n-1)f^3 e^{\frac{2\sqrt{2}\phi}{f}} + \frac{\sqrt{2}V_1}{f}e^{-\frac{\sqrt{2}\phi}{f}} = 0 \quad (5.36)$$

For instance, in the limit $\phi/f \ll 1$, this is solved by

$$\phi/f \approx c_1 e^{i\tilde{f}_n^2 \frac{t}{f}} + c_2 e^{-i\tilde{f}_n^2 \frac{t}{f}} - \sqrt{2} \frac{\hat{f}_n^4}{\tilde{f}_n^4} \quad (5.37)$$

where we have defined

$$\tilde{f}_n^4 = 2(n-1)f^4 - V_1/2 \quad (5.38)$$

$$\hat{f}_n^4 = 2(n-1)f^4 + V_1. \quad (5.39)$$

The coefficients c_1 and c_2 are set by the value of the field when inflation ends, usually estimated as $\phi/f|_{\epsilon=1} = c_1 + c_2 - \sqrt{2}$. For $V_1 \ll f^4$ the oscillation simplifies to

$$\phi/f \approx c_1 e^{i\sqrt{2(n-1)}ft} + c_2 e^{-i\sqrt{2(n-1)}ft} - \sqrt{2} \quad (5.40)$$

Thus we can see that the dimension of the symmetry breaking can play a role in the oscillation period of the inflaton after inflation, and thus affect timescale of reheating.

5.5 CONCLUSIONS

Here we have considered a geometric approach to describe Goldstone bosons in the non-compact coset $SO(n,1)/SO(n)$, by considering different models to describe the hyperbolic field space. Since the dynamics of the Goldstone bosons is specified by the target metric of this manifold, this approach lends itself to simple visualizations. The Goldstone bosons obtain a potential when their shift symmetry is broken by terms that explicitly break $SO(n,1)$ and couple to the Goldstone bosons. This can also be described geometrically, and without choosing a specific model, in terms of symmetry breaking parameters.

It was well known that pGB potentials based on compact cosets are compact, that is, the resulting potential is bounded in the large field limit. Here we have shown for cosets describing hyperbolic manifolds (in arbitrary dimensions) that the pGB potential can be compact as well. We have shown two examples, in which the parameters that break the global symmetry transform like a time-like or null vector of the hyperbolic space. This result is promising for models of inflation, and gives predictions compatible with the data from Planck [14] as shown in Fig.5.3.

Our result cannot in general be extrapolated to the breaking of different non compact cosets. For example, if one would consider the breaking of an indefinite orthogonal group to its maximal compact subgroup, i.e. the coset $SO(p,q)/SO(p)$, one will encounter ghost fields.

The geometric approach may also be applied in other contexts. The negative exponential potential is reminiscent of the first ekpyrotic models [197], though this case which has one effective

degree of freedom does not reproduce a (nearly) scale invariant spectrum of perturbations. It remains an open question whether a similar result can be found for an effectively multifield model.

The techniques described here may also find an application in Higgs physics, complimentary to recent HEFT studies in spaces with negative curvature [186]–[188]. Such a study may allow a unified understanding of the dynamics in an arbitrary number of dimensions.

ACKNOWLEDGEMENT

DC would like to thank C. Burgess for useful discussions and the Perimeter Institute for the support and hospitality during the development of this work.

EXPLORING HOLOGRAPHIC COMPOSITE HIGGS MODELS

Djuna Croon¹, Barry Dillon¹, Stephan Huber¹, Verónica Sanz¹

¹Department of Physics and Astronomy, Pevensey II Building, University of Sussex, BN1 9RH,
UK

Simple Composite Higgs models predict new vector-like fermions not too far from the electroweak scale, yet LHC limits are now sensitive to the TeV scale. Motivated by this tension, we explore the holographic dual of the minimal model, MCHM₅, to try and alleviate this tension without increasing the fine-tuning in the Higgs potential. Interestingly, we find that lowering the UV cutoff in the 5D picture allows for heavier top partners and less fine-tuning. In the 4D dual this corresponds to increasing the number of “colours” N , thus increasing the decay constant of the Goldstone Higgs. This is essentially a ‘Little Randall-Sundrum Model’, which is known to reduce some flavour and electroweak constraints. Furthermore, in anticipation of the ongoing efforts at the LHC to put bounds on the top Yukawa, we demonstrate that deviations from the SM can be suppressed or enhanced with respect to what is expected from mere symmetry arguments in 4D. We conclude that the 5D holographic realisation of the MCHM₅ with a small UV cutoff is not in tension with the current experimental data.

6.1 INTRODUCTION

The discovery of the Higgs boson at LHC [5], [6], which so-far appears to be very Standard Model-like, and the non observation of new physics raises the question of the origin of the electroweak scale. Among some well motivated explanations of this scale, such as supersymmetry or extra dimensions, is Higgs compositeness. In this framework the Higgs field is composed of some particles interacting via a strongly interacting gauge theory which confines at the TeV scale. A “little hierarchy” between the electroweak scale and the new physics scale can arise naturally if the Higgs bound state is a pseudo-Goldstone boson of this new strongly interacting sector.

Despite difficulties in extracting predictions from strongly coupled gauge theories, several methods have been developed. The most basic of these makes use of large N approximations in $SU(N)$ gauge theories, and of the global symmetry structure in the low energy effective theory [117], [198]–[204]. These methods, although useful, can be rather limited since precise calculations of form factors are impracticable. This means that one is unable to extract precise values of physical quantities, such as the mass spectrum of particles and their couplings. For these reasons it is difficult to constrain the models using experimental data.

It is possible to make progress beyond this using computational tools such as lattice simulations, and while determining baryon states is still challenging, some studies in non-minimal Composite Higgs models have been done regarding the structure of the meson states [131], [205], [206]. In this paper we adopt another popular method, namely holography, which has been proven useful to describe another strongly coupled theory, QCD at low energies [97], [207]–[210] as well as a way to develop new, non-QCD like, models of Technicolor [98], [99], [211], [212]. In the context of Composite Higgses, the pioneer papers of Contino et al. [19], [21], followed an intense exploration of the Higgs as a holographic pseudo-Goldstone boson in warped extra-dimensions, see e.g. [24]. Holography is a method based on the conjectured duality between strongly interacting gauge theories in 4D and weakly coupled gravitational theories on a 5D AdS space. Since the dual theory is weakly coupled, we are able to extract precise predictions for the form factors and all masses and couplings in the model. Here the word *precision* comes from the determination of 4D observables in terms of the 5D model parameters after dimensional reduction, yet the relation with the target strongly coupled 4D theory is still a conjecture and hence bound to an inherent uncertainty.

The physics of 5D AdS spaces [213]–[216] was studied independently of its application to composite Higgs models, and many of the results and constraints are the same in both cases. The most important of these are the constraints imposed by the electroweak precision observables. In

the absence of additional symmetries, large corrections to the T parameter imply a lower bound on the spin-1 resonances of ~ 8 TeV [217], [218]. Some ways of improving this bound are to account for incalculable contributions to the operators in the 5D bulk [217], consider modifications to the AdS geometry [218], employ models with more than one extra dimension [219], or introduce large brane kinetic terms for gauge fields [220]. The most natural way to protect larger contributions to the T parameter however, is to extend the gauge sector in the bulk to include a custodial symmetry [221], [222]. This mechanism is employed in most realistic composite Higgs models, and allows for spin-1 resonances with masses as low as about 2.5 TeV.

The space of composite Higgs models is parametrised by the global symmetry structure of the low energy effective theory, and the embedding of the quarks and leptons into this global symmetry. A large literature exists on the simplest composite Higgs models. We will focus on what is known as the Minimal Composite Higgs Model (MCHM) [19], [21] with the quarks and leptons embedded in fundamental representations of the global symmetry (MCHM₅) [20], [223]. This model has a global $SO(5)$ symmetry broken to $SO(4)$ at the TeV scale, thus employing the custodial protection of the T parameter. A detailed discussion of this model is reserved for section 2. For further details on the model-building approaches in Composite Higgs models see [46], [115], [224]–[232].

Using the holographic approach it has been shown that it is possible to reproduce the correct top mass, Higgs vev and Higgs mass quite naturally. However it is found that this usually requires light top partners [20], [223]. Typically top partners below about 700 GeV are required, and this is already in tension with bounds on vector-like quarks at the LHC [233], [234] which, for single channel final states, already reach 900 GeV. For specific information on top partner phenomenology we refer the reader to [48], [235]–[246] and for general LHC phenomenology of the MCHM to [177], [247]–[257].

There have been some attempts to alleviate the need for the light top partners in holographic models. It has been shown that by embedding the leptons in larger representations, their contributions to the Higgs potential can help alleviate the need for light top partners [220]. Also using the holographic realisations (although with a flat background), authors in [258] use larger embeddings for the third generation to reduce the fine-tuning in the Higgs potential and allow for heavier top-partners. More recently, models of composite Higgs with more than one breaking scale have been studied in a 4D realisation, and it was found that this also allows for heavier top partners [259].

In general, tension from light top partners is not as much of a problem in the 4D explicit realisations as it is in the holographic models. In [199], [260] it has been demonstrated that one can achieve heavy top partners while having a light Higgs and keeping the fine-tuning at acceptable

values. The correspondence between the 4D and 5D models can be described in terms of a dictionary from which one can relate the 4D and 5D parameters. One entry in this relates the number of “colours” in the strongly coupled 4D gauge theory to the UV cutoff in the 5D AdS theory. In this work we investigate how the top partner spectrum changes as we vary this parameter. The effects of lowering this UV cutoff has been studied previously in 5D AdS scenarios in which the Higgs is not a pseudo-Goldstone boson, these models are referred to as “Little Randall-Sundrum” (LRS) models [261], [262]. It has been shown that these models reduce bounds on some flavour and electroweak observables. In models of gauge-Higgs unification, lowering the UV cutoff allows for lower values of v/f_π while keeping the Kaluza-Klein (KK) scale constant. In the dual theory this is related to an increase in the number of colours “ N ”. In doing this we find that, while keeping the KK scale and the Higgs and top quark masses at the observed values, we can increase the mass of the lightest top resonance. This is easily understood in the KK picture, where lowering the UV scale modifies the couplings of the KK modes. The LRS models have also found use in recent attempts to explain the di-photon excess detected at ATLAS [263] and CMS [264] in terms of a KK graviton or a radion [265], [266], where the KK graviton interpretation requires some extra brane kinetic terms to explain its relatively small mass [267], [268]. One important aspect of these LRS models is that there must be some dynamics which kills the graviton zero mode arising from fluctuations of the background metric. Since we only use these holographic models as tools for calculating effective theories for Composite Higgs models, this simply means that there is no massless spin-2 composite state arising from the strongly coupled field theory which gives us the Higgs.

Having constructed a MCHM without light top partners, we investigate deviations in the top Yukawa coupling, motivated by the ongoing experimental effort at LHC to put bounds on deviations from the SM prediction. In composite Higgs models the top Yukawa is generally suppressed compared to the SM. If this effect is too large, it could lead to a potential conflict with current or future data. We study the top Yukawa coupling in the 5D realisation and find that in some regions of parameter space the deviations to the SM can be suppressed relative to what is expected from pure (4D) symmetry arguments. This will be very relevant once the experimental precision on the top Yukawa increases.

Overall, we find that our 5D holographic realisation of the MCHM₅ with a smaller UV cutoff is not in tension with current experimental data (both on the top partner spectrum and the top Yukawa coupling). In fact, we find that having a lower 5D cut-off allows for a better comparison between the holographic and 4D explicit realisations, and we find good agreement between the results. The mechanisms we study that allow for heavier top partners and suppressed Yukawa deviations are

very general, and in particular do not rely on any specific coset or fermion embedding. Therefore, we expect that these results will generalise to non-minimal versions of composite Higgs, and it will be interesting and fruitful to study this in detail in the future.

6.2 OVERVIEW OF THE MCHM₅

Composite Higgs models posit a new strong sector with a global symmetry ($SO(5) \times U(1)_X$ in the MCHM) which spontaneously breaks to its subgroup ($SO(4) \times U(1)_X$), below its confinement scale. The resulting four Goldstone bosons, transforming in the fundamental representation of $SO(4)$ (or equivalently as a bi-doublet of $SU(2)_L \times SU(2)_R$), are identified with the Higgs doublet. A tree-level potential for the Goldstone bosons is forbidden by shift-symmetry, but a potential is generated radiatively if we introduce a further explicit breaking. This is done by gauging the subgroup $SU(2)_L \times U(1)_Y$ of $SO(4) \times U(1)_X$ and by choice of the fermion interaction structure.

The new strong sector adds heavy bound states, with masses around the breaking scale, to the Standard Model field content. Mixing between the new states and the SM results in modified couplings; constraints can be placed on these modifications normalised to the SM prediction. Most stringently, electroweak precision tests put bounds the gauge boson self-energy parametrised by the oblique parameters. In the MCHM the T -parameter is protected from large corrections due to the custodial symmetry. However, as we will see, the S -parameter bounds form an important constraint on the scale of new spin-1 resonances.

The spectrum of the spin-1 states is fixed by the symmetry breaking pattern, but there is some freedom for the new spin- $\frac{1}{2}$ states. One has to choose how to embed the standard model quarks and leptons into the $SO(5) \times U(1)_X$ symmetry, and how to introduce an explicit breaking. As the third generation of the SM couples most strongly to the Higgs, we will focus on that for our present work, as is customary.

Embedding the standard model $SU(2)_L$ doublets in bi-doublets of $SU(2)_L \times SU(2)_R$ protects the $Zb\bar{b}$ from large corrections. A simple way to do this is to embed each standard model quark generation into two fundamentals of $SO(5) \times U(1)_X$,

$$\xi_{q1} = \begin{bmatrix} \psi'_{q1,(L,R)} \\ \psi_{q1,(L,R)} \\ \eta_{q1,(L,R)} \end{bmatrix}_{\frac{2}{3}}, \quad \xi_{q2} = \begin{bmatrix} \psi_{q2,(L,R)} \\ \psi'_{q2,(L,R)} \\ \eta_{q2,(L,R)} \end{bmatrix}_{-\frac{1}{3}} \quad (6.1)$$

where the ψ fields transform as a bi-doublet of $SU(2)_L \times SU(2)_R$ and the η fields transform as singlets. The elements of each multiplet have left and right-handed components such that the new

fermionic states couple to the gauge fields in a vector-like way. The Standard Model left-handed doublets are identified with one linear combination of $\psi_{q1,L}$ and $\psi_{q2,L}$, while the other linear combination is made massive. The right-handed fields are identified with $\eta_{q1,R}$ and $\eta_{q2,R}$. The charge under $U(1)_X$ is assigned such that the fields carry the correct hypercharge, $Y = T_R^3 + X$.

As the SM is the low energy limit of the theory, the non-SM fields are assumed to have masses of the order of the breaking scale. The SM fields have heavy spin- $\frac{1}{2}$ partners with the same quantum numbers. The spurious fields give rise to additional exotic multiplets with charges $Y = \frac{7}{6}$ and $Y = -\frac{5}{3}$.

Fermionic contributions to the Higgs potential are introduced via linear $SO(5)$ violating couplings to heavy composite fermionic degrees of freedom. This mechanism is known as partial compositeness. The same couplings are also responsible for generating the masses and Yukawa couplings of the SM fields.

It has long been known that the 4D model described here has a dual in 5D gauge-Higgs unification. The strong coupling in the 4D action makes it impossible to compute the form factors perturbatively, but the weak coupling in the dual allows one to calculate them explicitly. 5D methods therefore provide very useful analytical tools for studying strongly coupled 4D gauge theories. In the next section we will describe in more detail a 5D model leading to the low energy physics as the MCHM₅ described in this section.

6.3 A HOLOGRAPHIC MODEL

In this section we follow closely the calculational procedure of [223]. We will consider a 5D AdS bulk space bounded by two 3-branes,

$$ds^2 = \frac{R^2}{r^2}(\eta^{\mu\nu} dx_\mu dx_\nu - dr^2), \quad (6.2)$$

where r is a conformal co-ordinate related to the fifth spatial co-ordinate, y , by $r = \frac{1}{k}e^{ky}$, in which k is the curvature of the 5D space. The branes are located at $r = R = 1/k$ (the UV) and $r = R' = \frac{1}{M_{KK}} \sim O(\text{TeV}^{-1})$ (the IR). The position of the IR brane is related to the scale of spontaneous symmetry breaking in 4D.

In the MCHM dual, the 5D bulk has a local $SO(5) \times U(1)_X$ gauge symmetry. To describe the third quark generation, we require four fermion multiplets living in the 5D bulk, transforming as fundamentals of $SO(5)$. Two of these correspond to ξ_{q1} and ξ_{q2} , with $U(1)_X$ charges $\frac{2}{3}$ and $-\frac{1}{3}$. And the other two, ξ_u and ξ_d , correspond to the composite states required by the partial

compositeness mechanism. The boundary conditions of the 5D fields are assigned as follows,

$$\begin{aligned}
 & A^a(++), \quad A^{\hat{a}}(+-) \\
 & \xi_{q1} = \begin{bmatrix} \psi'_{q1}(-+) \\ \psi_{q1}(++) \\ \eta_{q1}(--) \end{bmatrix}_{\frac{2}{3}}, \quad \xi_{q2} = \begin{bmatrix} \psi_{q2}(++) \\ \psi'_{q2}(-+) \\ \eta_{q2}(--) \end{bmatrix}_{-\frac{1}{3}} \\
 & \xi_u = \begin{bmatrix} \psi'_u(+-) \\ \psi_u(+-) \\ \eta_u(-+) \end{bmatrix}_{\frac{2}{3}}, \quad \xi_d = \begin{bmatrix} \psi_d(+-) \\ \psi'_d(+-) \\ \eta_d(-+) \end{bmatrix}_{-\frac{1}{3}}
 \end{aligned} \tag{6.3}$$

where A^a and $A^{\hat{a}}$ are the $SO(4) \times U(1)_X$ and broken generators, respectively. Here the $+$ ($-$) represents a Neumann (Dirichlet) boundary condition, and the order of these is to be understood as (UV, IR). For the gauge fields we denote the boundary condition on the (μ, ν) component, while the A^5 components will have the opposite boundary conditions. For the fermion fields we denote the boundary condition on the left-handed mode, while the right-handed modes will also have the opposite boundary conditions. It follows that fermion fields with $(++)$ will have a massless left-handed component, while those with $(--)$ have a massless right-handed component, and fields with $(+-)$ or $(-+)$ have no massless components. For the gauge fields, components with $(++)$ boundary conditions will have a massless A^μ mode, while components with $(--)$ will have a massless A^5 scalar mode, and again the components with $(+-)$ or $(-+)$ will not have any massless component.

The $SO(5) \times U(1)_X$ symmetry on the UV brane should be broken to the SM electroweak group in such a way that $Y = T_R^3 + X$. In addition to this, the linear combination $(\psi_{q1,L} - \psi_{q2,L})$ should be given a mass on the UV brane so that only $(\psi_{q1,L} + \psi_{q2,L})$ has a massless component. We then identify the SM left-handed doublet as $\psi_q = (\psi_{q1,L} + \psi_{q2,L})$. Taking all of this into account, the low energy theory now looks very much like the SM before electroweak symmetry breaking.

6.3.1 THE 5D GAUGE SECTOR

In the 5D models the composite Higgs can be identified with the zero mode of the fifth component of the 5D gauge fields, i.e. A_5^0 . The only A_5 fields which have a massless zero mode are those with $(--)$ boundary conditions. From eq. 6.3 it can be seen that these precisely correspond to the $SO(5)/SO(4)$ generators, as expected. With the description of the model given so far, the dynamics of the 5D gauge sector is fixed. The only free parameters being the scale M_{KK} and the

ratio of UV/IR scales, $\ln(\Omega)$. In principle we could also include brane kinetic terms, but these are expected to be radiatively induced and we assume their effects to be negligible.

From the 5D model one can derive expressions for observables in the 4D composite Higgs model. Firstly, the decay constant of the Goldstone fields is found to be,

$$f_\pi^2 = \frac{4M_{KK}^2}{g^2 \ln \Omega} \quad (6.4)$$

where g is the EW gauge coupling ~ 0.65 and $\Omega = \frac{R'}{R}$ is the ratio of scales in the model. This expression can be generalized to non-AdS warped metrics as in Refs. [100], [269], [270].

Since the Higgs doublet is a Goldstone field, its couplings are of the form $\sin(h/f_\pi)$. Once electroweak symmetry is broken, obtaining the correct W and Z boson masses requires that

$$\sin^2\left(\frac{h}{f_\pi}\right) \equiv s_h^2 = \frac{v^2}{f_\pi^2} = \frac{m_W^2}{M_{KK}^2} \ln(\Omega). \quad (6.5)$$

Thus deviations in the Higgs boson couplings can depend as much on the UV scale as they do the IR. The holographic picture relates the $1/N$ (large number of “colours”) expansion in a 4D strongly coupled gauge theory to an expansion in a small 5D gauge coupling g_5 in AdS space. From this picture the following correspondence arises,

$$\frac{1}{N} = \frac{g_5^2 k}{16\pi^2}, \quad (6.6)$$

where $g_5^2 k = g^2 \ln(\Omega)$. This allows us to think of the ratio of scales in the 5D theory as dual to the number of colours in the 4D picture: larger N implies a smaller $\ln(\Omega)$, which is also related to the cutoff of the theory [270]. Note that there is no reason to keep $\Omega \sim 10^{15}$, as is done in some warped extra dimensional models to solve the Planck-electroweak hierarchy problem. We should remember that the 5D NDA condition for calculability requires that $\frac{g^2 \ln(\Omega)}{24\pi^2} \ll 1$, but even with $\ln(\Omega) = 40$ this is ~ 0.07 . Lastly, an important bound on these models comes in the form of the electroweak S -parameter, which can be expressed as,

$$S \simeq \frac{3}{8} \frac{N}{\pi} s_h^2 = \frac{6\pi}{g^2 \ln \Omega} s_h^2 = \frac{3\pi v^2}{2M_{KK}^2}. \quad (6.7)$$

The constraints for S are correlated with the T parameter: for an exact custodial symmetry, $T = 0$, the bound is $S < 0.02$ (implying $M_{KK} > 3.8$ TeV), allowing for maximal contribution to T it relaxes to $S < 0.3$ (which is saturated for $M_{KK} \simeq 1$ TeV). In this latter case the lightest gauge KK modes are approximately at $\frac{3\pi}{4} M_{KK} \sim 2.35$ TeV. Note that as long as some hierarchy exists between the IR and UV scales, the S -parameter only depends on the IR scale.

6.3.2 THE 5D QUARK SECTOR

In the quark sector, to familiarise ourselves with the parameters of the model, it is instructive to look at the 5D action for the fields,

$$S_\Phi = \int d^4x \int_R^{R'} dr \sqrt{|g|} \sum_{i=q,u} \left(\frac{1}{2} \left(\bar{\xi}_i \gamma^M D_M \xi_i - D_M \bar{\xi}_i \gamma^M \xi_i \right) - c_i k \bar{\xi}_i \xi_i \right), \quad (6.8)$$

$$+ \int d^4x \left(m_u \bar{\xi}_q^b \xi_u^b + M_u \bar{\xi}_q^s \xi_u^s + h.c. \right)_{r=R'}$$

where E_a^M is the fünfbein, $E_a^M \gamma^a = \gamma^M$, $\gamma^a = (\gamma^\mu, i\gamma^5)$ are the gamma matrices in flat space, and ω_M is the spin connection. The b and s superscripts in the brane mixing terms denote the bi-doublet and singlet components of the fermion multiplets. The IR brane masses control the breaking of $SO(5)$: for $m_u \neq 1/M_u$ it is broken explicitly, preserving the $SO(4)$ subgroup.

Varying the 5D mass parameters (c_q and c_u) determines the degree of compositeness of the fermionic operators. The field ξ_q has a left-handed zero mode and hence becomes more composite as c_q moves in a negative direction. Whereas ξ_u has a right-handed zero mode so becomes more composite as c_u moves in a positive direction. For $c_q = -c_u$ the fields have the same degree of compositeness. In the Kaluza-Klein picture these mass parameters control the localisation of any massless zero modes in the spectrum: a greater composite component corresponds to more IR localisation.

We have defined $\psi_q = (\psi_{q1,L} + \psi_{q2,L})$, but when calculating the Higgs potential the state with the most composite mixing will contribute the most. Thus when calculating the top quark contribution to the Higgs potential we will assume $\psi_{q1,L}$ to be most composite and take $\psi_q \simeq \psi_{q1,L}$.

6.3.3 THE EFFECTIVE ACTION

Once the model is defined, one can write down the most general effective Lagrangian compatible with the symmetry structure. In the case of the MCHM₅ this is,

$$\mathcal{L}_{\text{eff}} = -\frac{P_t^{\mu\mu}}{2} \left[\frac{2}{g_5^2} W_\mu^+ \left(\Pi_0 + \frac{s_h^2}{2} \Pi_1 \right) W_\nu^- + A_\mu \left(\frac{1}{g_5^2} \Pi_0 + \frac{c_w^2 - s_x^2}{g_{5,X}^2} \Pi_0^X \right) A_\nu \right.$$

$$+ Z_\mu \left(\frac{c_w^2 + s_x^2 s_w^2}{g_5^2} \Pi_0 + \frac{c_x^2 s_w^2}{g_{5,X}^2} \Pi_0^X + \frac{s_h^2}{2c_w^2 g_5^2} \Pi_1 \right) Z_\nu \left. \right] + \bar{q}_L \left(\Pi_0^q + \frac{s_h^2}{2} \Pi_1^q H^c H^{c\dagger} \right) \not{p} q_L$$

$$+ \bar{u}_R \left(\Pi_0^u + \frac{s_h^2}{2} \Pi_1^u \right) \not{p} u_R + \frac{s_h c_h}{\sqrt{2}} M_1^u \bar{q}_L H^c u_R + h.c. \quad (6.9)$$

The form factors Π_0^X are associated with the $U(1)_X$ gauge field, and the mixing angles s_x and c_x arise via the breaking to the SM subgroup on the UV brane. For more details on the how this effective action is derived we refer the reader to [223]. In a 4D approach one can only estimate the momentum dependence of these form factors based on sum-rules and Large- N gauge theory results. But in the 5D holographic approach they can be explicitly calculated, the results of these calculations are presented in the appendix. It is expected that the form factors will contain poles corresponding to massive composite resonances at $p^2 \sim M_{KK}^2$. In the 5D approach these are simply the Kaluza-Klein states one obtains from the 5D gauge and fermion fields. While the masses of the spin-1 resonances are solely determined by M_{KK} , the masses of the spin- $\frac{1}{2}$ resonances depend also on c_q , c_u , m_u and M_u . Before EWSB, when $s_h = 0$, they can be expressed in terms of the above form factors as,

$$\begin{aligned} m_{1/6} &= \text{zeros}\{\not{p}\Pi_0^q\} \\ m_{2/3} &= \text{zeros}\{\not{p}\Pi_0^u\} \\ m_{7/6} &= \text{poles}\{\not{p}(\Pi_0^u + \Pi_1^u)\}. \end{aligned} \quad (6.10)$$

After EWSB the (1/6) and (2/3) states mix resulting in a tower of top partners with (2/3) charge and masses determined by the zeros of,

$$\left[p^2 \left(\Pi_0^q + \frac{s_h^2}{2} \Pi_1^q \right) \left(\Pi_0^u + \frac{s_h^2}{2} \Pi_1^u \right) - \frac{s_h^2 c_h^2}{2} (M_1^u)^2 \right]. \quad (6.11)$$

There will also be a tower of states with hypercharge (5/3) and mass equal to $m_{7/6}$. It is generally found that when one or both of the multiplets has a large composite mixing, there will generally be relatively light fermionic states in the model. This large compositeness also generally implies a large gap in the masses of the lightest (1/6), (2/3) and (7/6) top partners. Thus, by varying the 5D mass parameters, we can significantly alter the spectrum of top partners we expect to observe. Summarising, from the 5D description of the model we have six parameters,

$$M_{KK} \quad \ln \Omega \quad c_q \quad c_u \quad m_u \quad M_u. \quad (6.12)$$

We can use three observables to fit to: v , m_h and m_t , leaving us with three free parameters. Here we will demonstrate the freedom that these parameters give in the top sector. In particular, there are three aspects we wish to study,

- How the 5D parameters are related to the top partner masses;
- How the top partner masses are related to s_h , and;
- How much 5D contributions alter the top Yukawa deviation expected from 4D composite Higgs models.

6.4 HIGGS POTENTIAL AND EWSB

From the effective action for the gauge fields and the top quark it is a simple exercise to write down the Coleman-Weinberg expression for the one-loop Higgs potential. After a Wick rotation we arrive at the following field-dependent potential,

$$V(h) = \int \frac{d^4 p_E}{(2\pi)^4} \left(\frac{3}{2} \log \left[1 + \frac{3}{2} \frac{\Pi_1}{\Pi_0} \right] - 6 \log \left[\left(1 + \frac{s_h^2}{2} \frac{\Pi_1^q}{\Pi_0^q} \right) \left(1 + \frac{s_h^2}{2} \frac{\Pi_1^u}{\Pi_0^u} \right) + \frac{s_h^2 c_h^2}{2} \frac{(M_1^u)^2}{p_E^2 \Pi_0^q \Pi_0^u} \right] \right) \quad (6.13)$$

where we have neglected the effects of the $U(1)_X$ field. Expanding these logs, it is found that the potential has the following form,

$$V(h) \simeq (\alpha_G + \alpha_F) s_h^2 - \beta_F s_h^2 c_h^2 \quad (6.14)$$

where the F and G subscripts refer to gauge and fermion contributions. Notice that without the fermion contribution one cannot achieve EWSB at all. Minimising this we find that the Higgs potential has a non-trivial ground state when $\beta_F > 0$ and $\beta_F > |\alpha_F + \alpha_G|$, situated at

$$s_h^2 = \frac{1}{2} - \frac{\alpha_G + \alpha_F}{2\beta_F}. \quad (6.15)$$

Taking the second derivative of $V(h)$ we find,

$$m_H^2 = \frac{8\beta_F}{f_\pi^2} s_h^2 c_h^2. \quad (6.16)$$

After EWSB it is found that the mass of the top is given by,

$$m_t^2 \simeq \frac{s_h^2 c_h^2}{2} \frac{(M_1^u)^2}{(\Pi_0^q + \frac{s_h^2}{2} \Pi_1^q)(\Pi_0^u + \frac{s_h^2}{2} \Pi_1^u)} \Big|_{p^2=(174\text{GeV})^2}. \quad (6.17)$$

Since the top quark gives by far the most dominant contribution to the potential, we should expect a lot of correlation between the top partner spectrum and the Higgs mass. Approximating the form factors by their limiting expressions for vanishing momentum, we can write this in terms of the 5D parameters as

$$m_t^2 \simeq \frac{M_u v \sqrt{(\tilde{c}_q - 2)\tilde{c}_q(\tilde{c}_u - 2)\tilde{c}_u} \sqrt{1 - \frac{v^2}{f_\pi^2}(1 - m_u M_u)}}{f_\pi L_1 \sqrt{-(\tilde{c}_q - 2)M_u^2 + \frac{\tilde{c}_u v^2(m_u^2 M_u^2 - 1)}{f_\pi^2}} + \tilde{c}_u \sqrt{M_u^2 \left(\tilde{c}_q m_u^2 \left(2 - \frac{v^2}{f_\pi^2} \right) - 2\tilde{c}_u + 4 \right) + \frac{\tilde{c}_q v^2}{f_\pi^2}}}, \quad (6.18)$$

where we have defined

$$c_u = \frac{\tilde{c}_u - 1}{2} \quad \text{and} \quad c_q = \frac{1 - \tilde{c}_q}{2}, \quad (6.19)$$

such that $0 \leq \tilde{c}_q$, and $\tilde{c}_u \leq 2$, and the profiles are flat ($c_{q,u} = \pm 1/2$) for $\tilde{c}_{q,u} = 0$.

6.4.1 YUKAWA COUPLINGS IN THE HOLOGRAPHIC MCHM₅

From the discussion above it is seen that the Yukawa coupling of the top quark in MCHM₅ deviates from its Standard Model value. Following the definition of the effective Yukawa coupling by [247],

$$y_\psi^{(0)} \simeq \frac{dm_\psi^{(0)}}{dv}, \quad (6.20)$$

we will be interested in the quantity

$$\kappa_t = \frac{y_t^{(0)}}{y_{t,SM}^{(0)}} = \frac{y_t^{(0)}v}{m_t^{(0)}}. \quad (6.21)$$

The current LHC ATLAS bounds are $\kappa_t = 0.94 \pm 0.21$ at 2σ [271]. This bound is expected to be strengthened to the ten percent level after the current run.

From (6.17) we may calculate κ_t in terms of the 5D form factors. To quartic order in $s_h = v/f_\pi$, we have

$$\kappa_t = 1 - \frac{s_h^2}{c_h^2} - s_h^2 \left(\frac{\Pi_1^q}{2\Pi_0^q} + \frac{\Pi_1^u}{2\Pi_0^u} \right) + s_h^4 \left(\frac{(\Pi_1^q)^2}{4(\Pi_0^q)^2} + \frac{(\Pi_1^u)^2}{4(\Pi_0^u)^2} \right) + O(s_h^5). \quad (6.22)$$

As by definition, the Standard Model result ($\kappa_t = 1$) is recovered in the limit $s_h \rightarrow 0$. Also, as we have noted above, if the IR brane masses are related as $M_u = -1/m_u$, the fermion form factors vanish ($\Pi_1^q = \Pi_1^u = 0$). In this case the BSM Yukawa corrections are universal and equal to $-s_h^2/c_h^2$ (to all orders in s_h). From (6.18), in terms of the fermion profiles we have,

$$\frac{y_\psi^{(0)}v}{m_\psi^{(0)}} = 1 - \frac{s_h^2}{c_h^2} - s_h^2 \left(\frac{(m_u^2 M_u^2 - 1) (M_u^2 (\tilde{c}_q ((2 - \tilde{c}_q) - 2\tilde{c}_u m_u^2) - 2(2 - \tilde{c}_u)\tilde{c}_u) + \tilde{c}_q \tilde{c}_u)}{2M_u^2 (-\tilde{c}_q m_u^2 - (2 - \tilde{c}_u)) ((2 - \tilde{c}_q)M_u^2 + \tilde{c}_u)} \right) + O(s_h^4). \quad (6.23)$$

In section 6 we will study how these additional contributions proportional to $(m_u^2 M_u^2 - 1)$ can play a role in alleviating tensions with bounds from the LHC.

6.5 TOP PARTNERS IN HOLOGRAPHIC MCHM₅

Taking the values of s_h and c_h at the minimum of $V(h)$, we can re-write the Higgs mass term from eq. 6.16 as,

$$m_H^2 = \frac{2}{f_\pi^2} \frac{\beta^2 - \alpha^2}{\beta}. \quad (6.24)$$

The α and β terms are of dimension four and we can expect them to be $\sim M_{KK}^4$. Thus to obtain a light Higgs we require a degree of cancellation among the terms in the Higgs potential. A similar

cancellation is also required to obtain a light vacuum expectation value. Due to the required cancellation among these terms, the precise value of s_h alone is only a crude estimate of the fine-tuning of the model.

It has been shown that if $M_{KK} \sim 1$ TeV, and $f_\pi \sim 500$ GeV, one requires the ξ_u multiplet to have a large composite mixing in order to get the correct degree of cancellation in α and β , and thus obtain the correct values of m_H , $m_{t,pole}$ and v [20]. This implies that light top partners are expected in models with a large mass gap among the different charged states. Similar results have been observed in the 4D realisations, however in these cases there is more freedom with the model and light top partners can be avoided more easily. Currently, the prediction of light top partners from holographic models is in tension with observations at the LHC.

The obvious way to avoid these constraints is to push up M_{KK} , but in doing one severely increases the fine-tuning of the model and it becomes “un-natural”. There have been several attempts at alleviating the need for light top partners without increasing the fine-tuning, in both the purely 4D and the holographic picture. An example of the former is [117], [260], in which the authors show that by embedding the third generation in different representations of $SO(5)$, the structure of the Higgs mass term can be altered. For particular cases a light Higgs could be obtained with top partners ~ 1 TeV in this way. The authors point out that to achieve a light Higgs with moderate fine-tuning, it is preferred to have $m_T/f_\pi \sim 1$, where m_T is the scale of the top partner masses. To highlight an example of a holographic approach, in [220] the realisation of the model includes leptonic contributions to the Higgs potential, which allow the authors to show that a light Higgs can be achieved while having top partners ~ 1 TeV, with only moderate fine-tuning.

In this paper we wish to investigate an alternative method of reducing the need for light top partners in the holographic realisation of the model. Moving the top zero mode wave functions away from the IR brane increases the mass of the top partners, but simultaneously results in an increase in the Higgs mass. However, by lowering the UV scale (i.e. lowering $\ln(\Omega)$) we increase f_π and suppress the Higgs mass. Using this mechanism we can push the top zero mode wave functions further from the IR, pushing up the top partner masses, while keeping the Higgs mass at the observed value. In the 4D dual, lowering the UV scale should correspond to an increase in the number of colours “N” of the strongly coupled gauge theory [20], [262].

To illustrate this idea we perform a scan in which we fix $M_{KK} = 1.1$ TeV and vary the other parameters in the ranges $0.2 < c_q < 0.4$, $-0.4 < c_u < 0.4$, $-2 < m_u M_u < -0.5$ and $20 < \ln(\Omega) < 50$. For $c_q = 0.5$ ($c_u = -0.5$) the 5D profile of the left-handed (right-handed) zero mode will be flat. So the choices of fermion localisations ensure that the composite mixing for q_L is small, whereas the mixing of the t_R state is allowed to be large or small. We find two distinct

cases in the results, $|m_u| < 1.4$ and $|m_u| > 1.4$. In figures 6.1 and 6.2 below we show how c_u and $\ln(\Omega)$ are correlated after we fix $m_{t,pole}$, m_H , and v to their observed values.

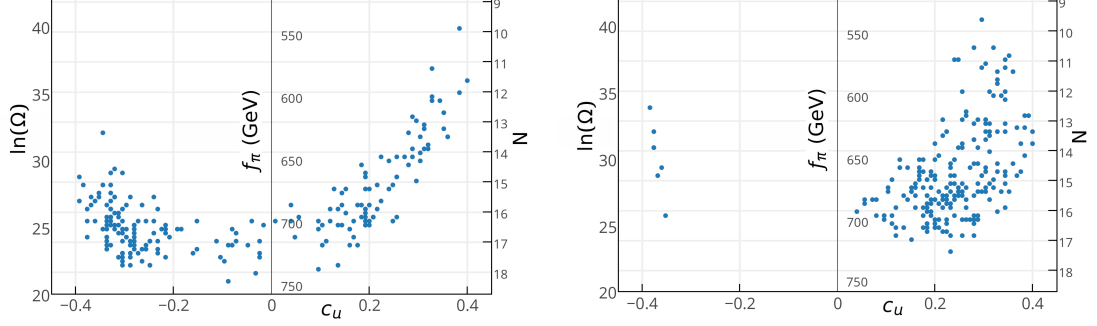


Figure 6.1: Correlation between c_u and $\ln(\Omega)$ when $|m_u| < 1.4$. **Figure 6.2:** Correlation between c_u and $\ln(\Omega)$ when $|m_u| > 1.4$.

From these plots it is clear that for a large value of $\ln(\Omega)$ ($\gtrsim 35$), a light Higgs requires the spurious multiplet to have large positive values of c_u . However by allowing for smaller values of $\ln(\Omega)$ we can have significantly different values for this c_u parameter. The effects of this on the top partner spectrum are shown below in figures 6.3 and 6.4.

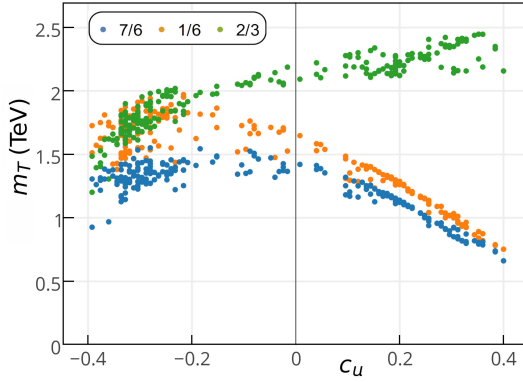


Figure 6.3: Correlation between c_u and the top partner masses when $|m_u| < 1.4$. Here the green points correspond to the top partner with hypercharge (2/3), the orange with (1/6), and the blue with (7/6).

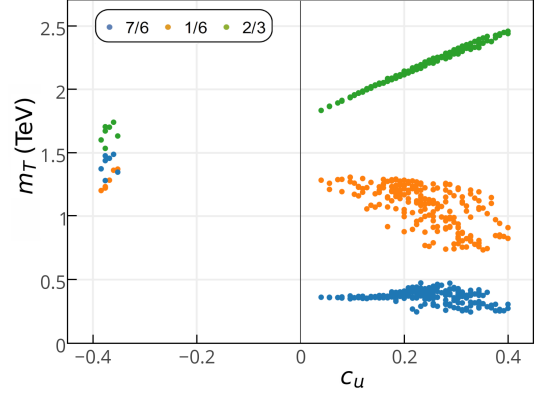


Figure 6.4: Correlation between c_u and the top partner masses when $|m_u| > 1.4$. As in the left panel, the different coloured points correspond to top partners with different hypercharge.

If we were to fix $\ln(\Omega)$ to be > 35 , we would be forced to have $c_u \gtrsim 0.3$. This results in a distinct top partner spectrum in which the left-handed top partner and exotic top partners are $\lesssim 1$ TeV while the right-handed top partner is ~ 2 TeV. However, by lowering the value of $\ln(\Omega)$ we can move c_u to regions with less composite mixing in which the top partner spectrum is remarkably different. We can easily have scenarios where all the top partners have masses $\gtrsim 1$ TeV, and where the mass gap among the different charged states is very small. Note that, in the

4D picture, having $\ln(\Omega) \sim 37$ means having the number of colours at ~ 10 . Lowering $\ln(\Omega)$ to ~ 25 means that $N \sim 15$. In the case of figure 6.3, we can say that the mass gap between the top partners is strongly related to their degree of compositeness.

Since we fix $M_{KK} = 1.1$ TeV and fix the vev, varying $\ln(\Omega)$ is analogous to varying s_h . In figures 6.5 and 6.6 we see the correlation between top partner masses and s_h explicitly.

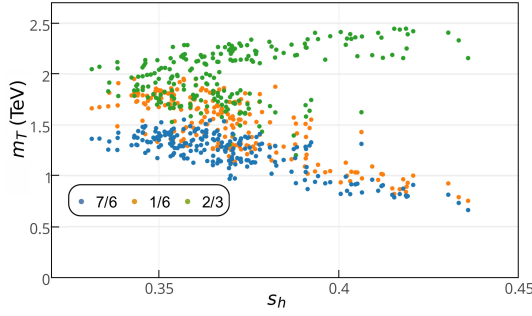


Figure 6.5: Correlation between s_h and the top partner masses when $|m_u| < 1.4$. As above, the different coloured points correspond to top partners with different hypercharge.

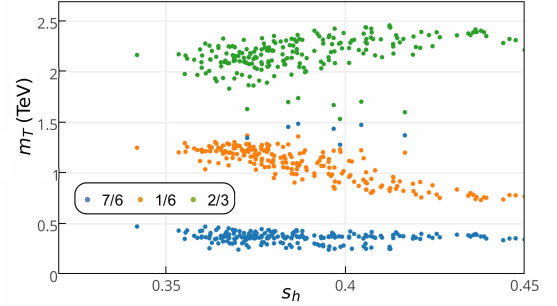


Figure 6.6: Correlation between s_h and the top partner masses when $|m_u| > 1.4$.

From figure 6.5 it appears that reducing the mass gap between the top partners is strongly correlated with a reduction in s_h . However we do not see this behaviour in figure 6.6. Thus from the above figures we can conclude that, when $|m_u| \lesssim 1.4$ we can have less composite mixing and a smaller s_h is correlated with a smaller mass gap among the top partners, and an increase in the mass of the lightest top partner. Whereas for $|m_u| \gtrsim 1.4$, we are forced to have a larger composite mixing, and lowering s_h doesn't alter the top partner spectrum very much.

Taking the case where $|m_u| < 1.4$, it is useful to plot the masses of the 7/6 partners against the masses of the 2/3 partners and to look at how s_h varies here. From figure 6.7 we see that lower values of s_h are not necessarily correlated with a smaller mass gap, but with heavier 7/6 partners.

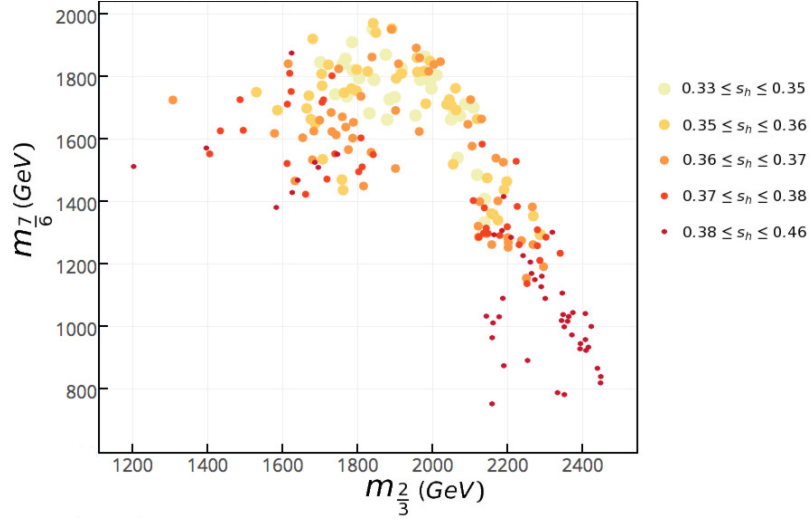


Figure 6.7: Here we plot the masses of the hypercharge 7/6 multiplet against the hypercharge 2/3 singlet and show how the value of s_h depends on these masses.

In figures 6.8 and 6.9 we perform similar scans, except we allow M_{KK} to vary. In one case, we have a very light top partner with a large mass gap, and in the other we have no light top partners and a small mass gap.

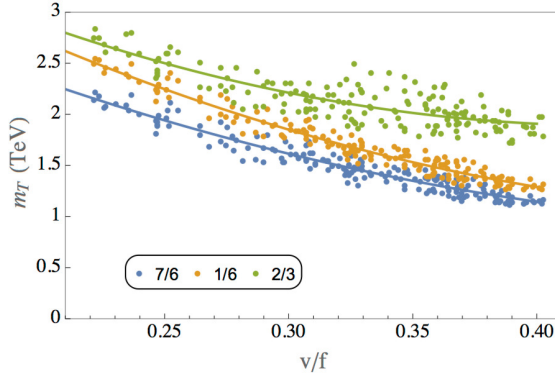


Figure 6.8: $c_q = 0.4$, $0 \leq -c_u \leq 0.4$, $1 \leq M_{KK}(\text{TeV}) \leq 2$ TeV, $20 \leq \ln(\Omega) \leq 30$ and $m_u = -1/M_u$. As above, the different coloured points correspond to top partners with different hypercharge.

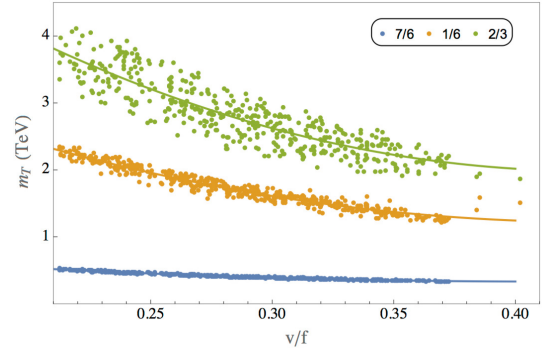


Figure 6.9: $c_q = 0.2$, $0 \leq c_u \leq 0.4$, $1 \leq M_{KK}(\text{TeV}) \leq 2$ TeV, $20 \leq \ln(\Omega) \leq 30$ and $m_u = -1/M_u$.

One would naturally expect that by reducing s_h , the mass of the top partners increase. What we show here is that this is only true in the case that $0 \leq -c_u \leq 0.4$, i.e. when there is less composite mixing for ξ_u . When $0 \leq c_u \leq 0.4$, i.e. large composite mixing, we clearly show that lowering s_h does not result in an increase in the mass of the lightest state. This is hinted at in figure 6.6, and re-enforced by the data in figure 6.9.

In studying composite Higgs models in 4D it is found that one expects the following approximate relation to hold,

$$m_H^2 \sim \frac{3}{16\pi^2} \left(\frac{v}{f_\pi} \right)^2 m_T^2 \quad (6.25)$$

where m_T is the mass of the top partners. Since we fix v to its SM value, this implies a linear relation between the Higgs mass and both the top partner masses and the ratio v/f . In the figures 6.10 and 6.11 test we test the latter relation, finding that this relation receives $O(1)$ corrections in the dual model.

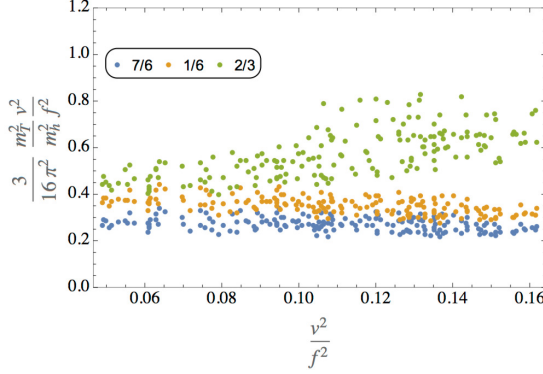


Figure 6.10: $c_q = 0.4$, $0 \leq c_u \leq 0.4$, $1 \leq M_{KK}(\text{TeV}) \leq 2$ TeV, $20 \leq \ln(\Omega) \leq 30$ and $m_u = -1/M_u$. As above, the different coloured points correspond to top partners with different hypercharge.

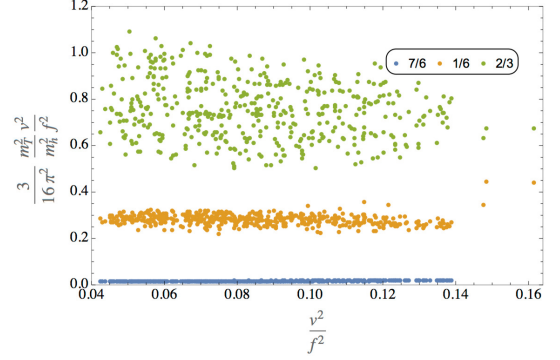


Figure 6.11: $c_q = 0.2$, $0 \leq -c_u \leq 0.4$, $1 \leq M_{KK}(\text{TeV}) \leq 2$ TeV, $20 \leq \ln(\Omega) \leq 30$ and $m_u = -1/M_u$.

It is useful at this point to compare our results to those obtained in explicit 4D realisations. Although varying $\ln(\Omega)$ produces results which differ from what is usually expected in the holographic models, it appears that doing this allows for a better comparison to the 4D models. In fact, the results we have obtained here, with the mass gap among the top partners varying, agree quite well with the explicit 4D realisations in [199], [203]. In these works they show that $m_H^2 \sim \ln(m_{7/6}/m_{2/3})$, implying that a smaller mass gap results in a lighter Higgs, which is exactly what we find here.

In [223] it was shown that increasing the scale M_{KK} in this 5D realisation leads to heavier top partners and lower values of s_h , but also a larger fine-tuning. It is now interesting to ask what effect lowering $\ln(\Omega)$ has on the fine-tuning in this model, since it also leads to heavier top partners and lower values of s_h , one might expect an increase in the fine-tuning. To quantify the fine-tuning in our model, in accordance with what was done in [223], we use the Barbieri-Giudici parameterisation,

$$\Delta_{BG} = \sqrt{\sum_i \left(\frac{\partial \log s_h^2}{\partial \log k_i} \right)^2} \quad (6.26)$$

where k_i are our input parameters M_{KK} , c_u , c_q , m_u , M_u , and $\ln(\Omega)$. The Δ_{BG} parameter measures the sensitivity of s_h^2 to changes in the input parameters. In figure 6.12 we plot the values of this parameter for the data we have with $|m_u| < 1.4$ as a function of the 5D localisation c_u and $\ln(\Omega)$. On the same plots we include the values of $1/s_h^2$ for each point to show how s_h and Δ_{BG} are correlated. Other observables for these data points have been shown in figures 6.1, 6.3, 6.5, and

6.7.

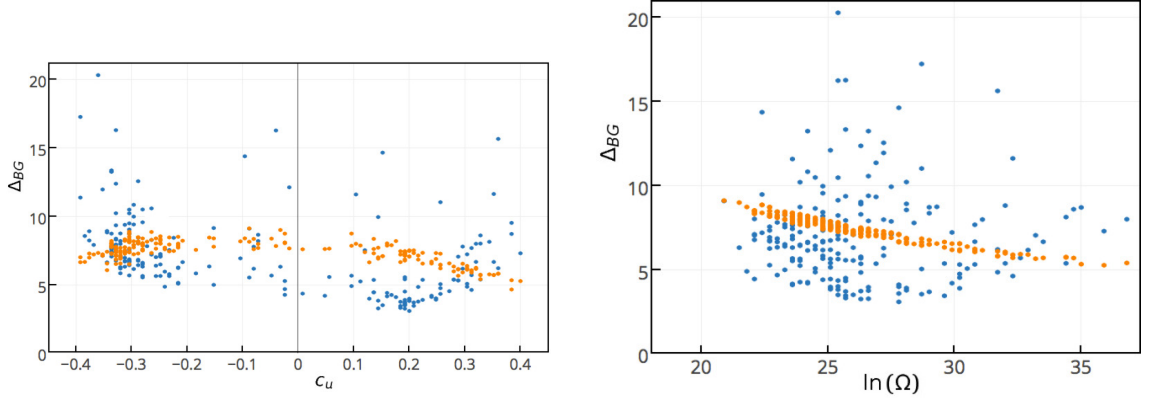


Figure 6.12: The blue points are the values of Δ_{BG} calculated from eq. 6.26, while the orange points are the values of $1/s_h^2$ for each point.

These plots show us something very interesting, that is, lowering $\ln(\Omega)$ allows for a reduced fine-tuning in the Higgs potential and heavier top partners. This result should not be too surprising since varying $\ln(\Omega)$ in the 5D models results in changes to the effective couplings between KK states and the Higgs in the effective theory, and it has been shown using an explicit 4D realisation in [260] that the fine-tuning in Composite Higgs models depends strongly on these couplings. We can see from the plots that the fine-tuning is minimised for $c_u \sim 0.2$ and $25 < \ln(\Omega) < 30$, which is slightly IR localised, and corresponds to the lightest top partner being just above 1 TeV (7/6 partner), with the next top partner laying just above 2 TeV (2/3 partner).

6.6 HIGGS COUPLINGS TO THE TOP SECTOR

In this section we study deviations to the top Yukawa coupling and possible future measurements of the Higgs in association with a hard object (vector boson, jet) as a probe for the Higgs-top-antitop form factor. First of all, we look at the top Yukawa coupling. We expect an inverse scaling between M_u and (the negative of) m_u . We will take a mildly more general relation

$$M_u = -\frac{a_1}{m_u} \quad (6.27)$$

with a_1 a real constant. In this case our expression simplifies to

$$\frac{y_\psi^{(0)} v}{m_\psi^{(0)}} = 1 - \frac{s_h^2}{c_h^2} - s_h^2 (a_1^2 - 1) \left(\frac{\tilde{c}_q}{2a_1^2 \tilde{c}_q + 2(2 - \tilde{c}_u)M_u^2} - \frac{\tilde{c}_u}{(2 - \tilde{c}_q)M_u^2 + \tilde{c}_u} \right) + O(s_h^4) \quad (6.28)$$

It is now obvious that the additional Yukawa correction due to 5D effects vanishes for either $a_1 = \pm 1$, and for flat profiles. It is also seen that the contribution switches sign for $a_1^2 = 1$ and for

$$a_1^2 = \frac{1}{2} + \frac{M_u^2 \left((2 - \tilde{c}_q)\tilde{c}_q - 2(2 - \tilde{c}_u)\tilde{c}_u \right)}{2\tilde{c}_q\tilde{c}_u}$$

In other words, in the region

$$\frac{1}{2} + \frac{M_u^2 \left((2 - \tilde{c}_q)\tilde{c}_q - 2(2 - \tilde{c}_u)\tilde{c}_u \right)}{2\tilde{c}_q\tilde{c}_u} < a_1^2 < 1$$

there can be an effective cancelation between the universal contribution and the Yukawa contribution.

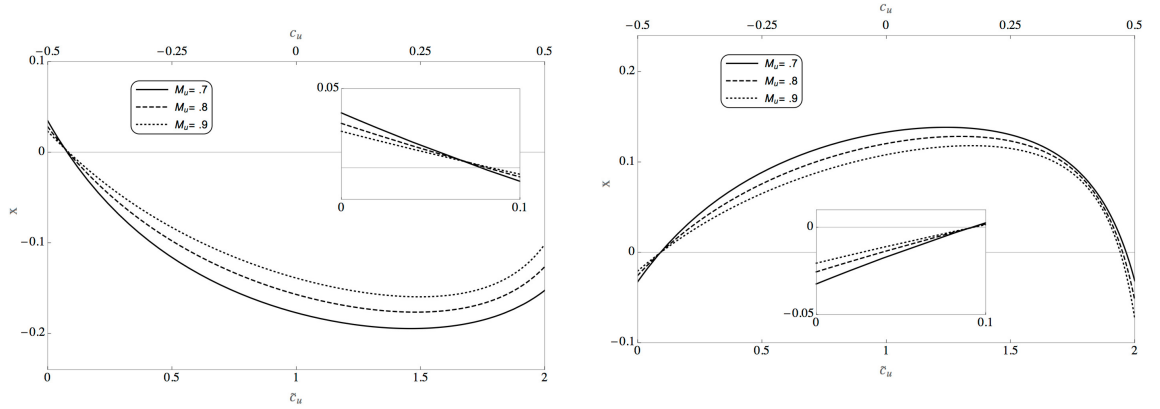


Figure 6.13: Profile contribution to the Yukawa coupling: on the left, $c_q = 0.4$ ($\tilde{c}_q = 0.2$) and $a_1 = 1.2$; on the right, $c_q = 0.4$ ($\tilde{c}_q = 0.2$) and $a_1 = 0.8$. It is seen that the contribution is larger for IR localised fermions, and that the sign is dependent on the sign of $(a_1 - 1)$. The values of M_u are chosen such that the scan results will map between the curves.

We can see this explicitly for two benchmark scenarios, $a_1 = 0.8$ and $a_1 = 1.2$. Writing

$$\frac{y_\psi^{(0)} v}{m_\psi^{(0)}} = 1 - s_h^2 \left(\frac{1}{c_h^2} - x \right) + O(s_h^4) \quad (6.29)$$

where x is the Yukawa correction (modulo s_h^{-2}),

$$x = (1 - a_1^2) \left(\frac{\tilde{c}_q}{2a_1^2\tilde{c}_q + 2(2 - \tilde{c}_u)M_u^2} - \frac{\tilde{c}_u}{(2 - \tilde{c}_q)M_u^2 + \tilde{c}_u} \right).$$

We plot this isolated mode contribution for the benchmarks in figure 6.13. Here we see indeed that the sign of the correction is dependent on the sign of $a_1 - 1$, that is, on the relation between the brane masses M_u and m_u . It is also seen that the correction is expected to be out of experimental reach for a small departure of $a_1 = 1$. However, the contribution can be made more sizeable values of a_1 . For instance, in the case in which $a_1 = 1.5$, one finds a maximum of $x = 0.6$ for $\tilde{c}_u \approx 1.7$. We use this large case to plot the range of imaginable contributions in the $\kappa_V - \kappa_t$ plane in figure 6.14.

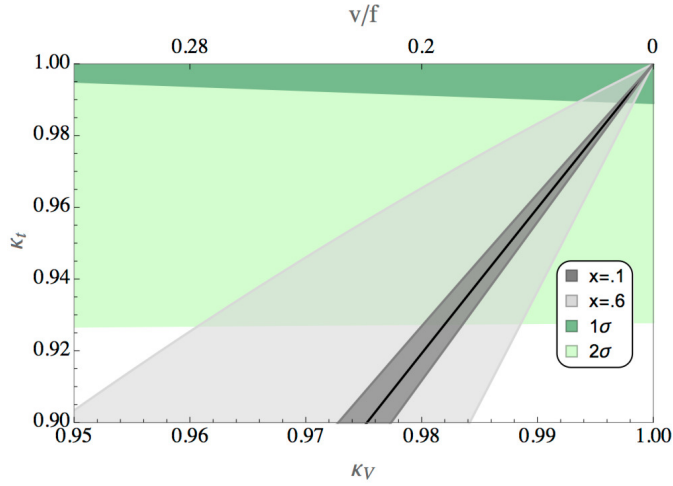


Figure 6.14: Profile contribution to the Yukawa coupling: in terms of the experimental variables κ_t and κ_V . In light and dark green the ATLAS 1σ and 2σ limits from [272].

6.6.1 HIGGS DIFFERENTIAL DISTRIBUTIONS AS A TEST OF COMPOSITENESS

In equations 6.10 and 6.11 we see the combinations of form factors whose zeros correspond to the top partner masses. The expressions also contain information on the two point functions for these fields away from $p^2 = m_n^2$, where n denotes the n^{th} resonance. In principle, one should be able to see the effect of these resonances in the form factor of the coupling of the Higgs to tops and top-partners. To produce the Higgs with some inherent momentum, we can produce the Higgs in, e.g., association with a vector boson or with a hard jet,

$$pp \rightarrow VH \text{ where } V = Z, W^\pm \text{ or } pp \rightarrow H + j \quad (6.30)$$

Differential distributions of, e.g., the Higgs p_T would be a good proxy to understand this form factor. In [246], [273], [274] the authors have studied, using 4D realisations of Composite Higgs models, the effects of the top partners in the differential distribution of the Higgs p_T for the process $pp \rightarrow H + j$. In these studies the authors only include the effects of one top-partner, with the Yukawa couplings fixed by a mixing between the top and top-partner. This cross-section is proportional to the Yukawa couplings and is suppressed at high energies by the PDFs of the initial state gluons. They find that the presence of top partners has a visible effect in this differential distribution, and that this technique can be used to probe a large range of top partner masses. The method outlined there is useful for studying the effects of new heavy states on the Higgs production, but it does not include effects arising in the Higgs couplings due to the compositeness of the fields. This can only be done if one can determine the momentum dependence of the Higgs couplings, and one advantage of the 5D holographic realisations is that they allow us to do this. The

momentum dependence is encoded in the form factors we discussed in section 3, and the effects of all top-partners are accounted for in these terms.

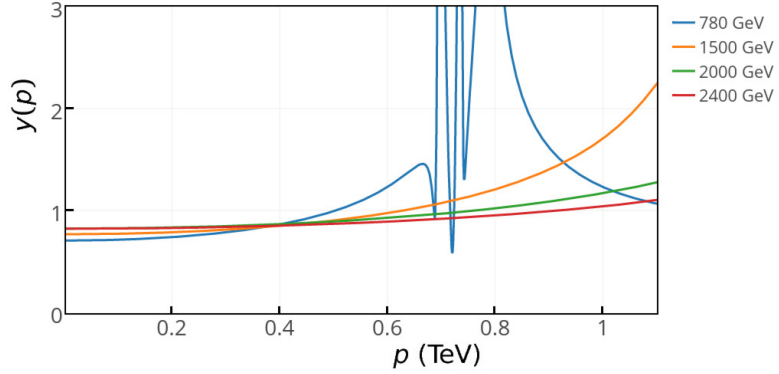


Figure 6.15: Here we plot the momentum dependence of the form factor for the $Ht_L t_R$ coupling. The masses quoted in the legend are for the hypercharge-1/6 top-partners, however the effects of other top-partners are also seen in the coupling.

In figure 6.15 we plot the momentum dependence of the $Ht_L t_R$ form factor. We look at cases where the lightest hypercharge-1/6 top partner ranges from ~ 780 GeV to ~ 2400 GeV, while reproducing the correct Higgs mass, top mass and v.e.v.. At low momenta we see the coupling settles at a constant value close to one, as expected. However at larger momenta, near the top-partner masses, we see that the resonances are actually visible in the momentum dependence of this coupling. Thus, one would imagine that this effect could be seen in the differential distribution of the Higgs p_T for $gg \rightarrow H + j$.

In another work [275] we are using these form factor techniques to perform a similar analysis as done in the previous works. The purpose of this is two-fold; firstly we will be able to include the effects of the whole tower of top-partners and the momentum dependence of the coupling in the calculation, and secondly, this will allow us to directly compare collider predictions from the 4D and 5D realisations of Composite Higgs models.

6.7 CONCLUSIONS

In this paper we addressed the question of whether or not a light Higgs implies light top partners in the Minimal Composite Higgs Model (MCHM₅). The experimental constraints on the detection of top partners can be avoided by increasing the scale M_{KK} , but this is at the cost of a severe fine-tuning. Attempts at realising the MCHM₅ model without light top partners and large fine-tuning

have been primarily focussed on the fermion sector: 4D approaches include a different embedding of the third generation of quarks in representations of $SO(5)$; holographic realisations include leptonic contributions to the Higgs potential. Here we propose an alternative method to alleviate the tension: we show that if the degree of composite mixing in the multiplets is reduced, the mass of the lightest top partners can be increased, without increasing the compositeness scale M_{KK} . To maintain a light Higgs, the cutoff in the 5D model (measured by $\ln \Omega$) is reduced. Interestingly, we find that the Higgs mass is proportional to the mass gap between the $7/6$ and $2/3$ charged top partners, in agreement with what is found in 4D explicit models [199], [203].

Since heavier top partners might naively lead one to expect more fine-tuning, we calculated this and found that as we lower $\ln(\Omega)$ the minimum value of the Barbieri-Giudici parameter tends to decrease. This is particularly nice, since we now know that increasing M_{KK} and lowering $\ln(\Omega)$ both allow for heavier top partners and lower values of s_h , however only lowering $\ln(\Omega)$ does not lead to an increased fine-tuning. This result also correlates well with the 4D explicit realisations, where the Higgs mass and the fine-tuning are proportional to the coupling between the top partners and the Higgs, a quantity which is controlled by $\ln(\Omega)$ in the holographic models. We find that, with spin-1 states at ~ 2.5 TeV and the left-handed top localised away from the IR, the fine-tuning is reduced when the lightest top partner is above 1 TeV.

With an eye to the next LHC run we discuss the phenomenology of this version of the MCHM₅. In anticipation of improved LHC constraints on the lightest top Yukawa coupling, we show that a deviation from the relation between IR brane masses $m_u = -1/M_u$ can reduce or enhance the Composite Higgs prediction for y_t as derived from symmetry arguments alone. The deviation from the Standard Model is captured in the parameters κ_V and κ_T , which allow for a comparison with the ATLAS data. In particular, it is seen that relaxing the brane mass relation may relieve the tension slightly by increasing the predicted coupling.

We further discussed the expected phenomenology of the top partner states in future searches. Testing the relation between the Higgs and top partner masses as a function of s_h , we find that the masses scale approximately linearly, as expected, with a slight deviation for the $(2/3)$ exotic state.

The form factors computed in the 5D dual contain qualitative information about the spectrum of top partners. In particular, in the last section we show the momentum dependence of the form factor encoding the $Ht_L t_R$ coupling, upon which the differential distribution of Higgs p_T in $pp \rightarrow H + j$ will strongly depend. Future searches at the LHC are expected to contain decisive information about the state of the MCHM₅, both through measurements of the top yukawa coupling and through differential distributions of the Higgs momentum.

APPENDIX A: FORM FACTORS IN THE HOLOGRAPHIC MCHM₅

In this appendix we present the explicit forms of the form factors introduced in section 3.3, we follow a similar procedure as in [223]. Neglecting brane kinetic terms, the form factors for the gauge interactions can be written as,

$$\Pi^{(+)}(p) = p \frac{\mathbf{Y}_0(pR')\mathbf{J}_0(pR) - \mathbf{J}_0(pR')\mathbf{Y}_0(pR)}{\mathbf{Y}_0(pR')\mathbf{J}_1(pR) - \mathbf{J}_0(pR')\mathbf{Y}_1(pR)} \quad (6.31)$$

$$\Pi^{(-)}(p) = p \frac{\mathbf{Y}_1(pR')\mathbf{J}_0(pR) - \mathbf{J}_1(pR')\mathbf{Y}_0(pR)}{\mathbf{Y}_1(pR')\mathbf{J}_1(pR) - \mathbf{J}_1(pR')\mathbf{Y}_1(pR)}, \quad (6.32)$$

and are sometimes written in terms of $\Pi_0 = \Pi^{(+)}$ and $\Pi_1 = (\Pi^{(-)} - \Pi^{(+)})$.

The fermionic form factors are more complicated due to the brane mixings in the IR. We use the following holographic profiles as building blocks,

$$G^+(r, c) = \sqrt{r} \left(\mathbf{Y}_{c-\frac{1}{2}}(pR')\mathbf{J}_{c+\frac{1}{2}}(pr) - \mathbf{J}_{c-\frac{1}{2}}(pR')\mathbf{Y}_{c+\frac{1}{2}}(pr) \right) \quad (6.33)$$

$$G^-(r, c) = \sqrt{r} \left(\mathbf{Y}_{c-\frac{1}{2}}(pR')\mathbf{J}_{c-\frac{1}{2}}(pr) - \mathbf{J}_{c-\frac{1}{2}}(pR')\mathbf{Y}_{c-\frac{1}{2}}(pr) \right), \quad (6.34)$$

where $c = \pm c_{q,u}$ represents the 5D fermion mass parameter, and q and u represent the appropriate fermion multiplets. From now on we denote $G^\pm(R, c)$ simply as $G^\pm(c)$. Assuming no brane kinetic terms, and only two quark multiplets with real mixings, we can write the form factors as,

$$\Pi_0^q(p) = \frac{1}{p} \frac{G^+(-c_u)G^-(c_q) + m_u^2 G^-(c_u)G^+(-c_q)}{G^+(c_q)G^+(-c_u) - m_u^2 G^-(c_q)G^-(c_u)} \quad (6.35)$$

$$\Pi_0^u(p) = -\frac{1}{p} \frac{G^+(c_u)G^-(c_q) + M_u^2 G^-(c_u)G^+(c_q)}{G^-(c_q)G^-(c_u) - M_u^2 G^+(c_q)G^+(-c_u)} \quad (6.36)$$

$$M_0^u(p) = \frac{1}{2} \frac{m_u}{p} \frac{G^+(c_q)G^+(-c_q) + G^-(c_q)G^-(c_u) + G^+(c_u)G^+(-c_u) + G^-(c_u)G^-(c_u)}{G^+(c_q)G^+(-c_u) - m_u^2 G^-(c_q)G^-(c_u)} \quad (6.37)$$

$$\Pi_1^q(p) = \Pi_0^q \left(m_u \rightarrow \frac{1}{M_u} \right) - \Pi_0^q \quad (6.38)$$

$$\Pi_1^u(p) = \Pi_0^u \left(M_u \rightarrow \frac{1}{m_u} \right) - \Pi_0^u \quad (6.39)$$

$$M_1^u(p) = M_0^u - M_0^u \left(m_u \rightarrow \frac{1}{M_u} \right). \quad (6.40)$$

It is clear now that $\Pi_1^{q,u} \rightarrow 0$ when $m_u \rightarrow \pm \frac{1}{M_u}$ and $M_1^u \rightarrow 0$ when $m_u \rightarrow \frac{1}{M_u}$. To get the Wick rotated form factors one simply has to rotate $p \rightarrow ip_E$, the resulting form factors are expressed in terms of modified Bessel functions \mathbf{I}_α and \mathbf{K}_α .

CONCLUSION

7.1 SUMMARY OF THE THESIS

This thesis has studied aspects of dynamical symmetry breaking as an answer to hierarchy problems in particle physics and cosmology. This thesis has considered the flatness of the inflation potential through the lens of Composite Higgs models, and shown that a similar framework could stabilize it from radiative corrections, which spoil its inflationary predictions.

The first paper included in this thesis, chapter 2, can be seen as a first exploration into mechanisms to evade the problems of the vanilla Natural Inflation, which are set out in detail, while maintaining its merits. It includes an example of an extra-dimensional model as well as a four dimensional dual which succeed in this objective.

Chapter 3 includes a more detailed study of an inflation model based on cosets of the form $SO(n)/SO(n-1)$ ($n \geq 3$) and fermions in spinorial representations of $SO(n)$. The model's inflationary predictions are compared to experimental data, and the paper briefly alludes to boundary conditions for a UV completion that the data suggest for this model.

From this setup chapter 4 considers the possibility that the dynamical generation of scales in the inflaton and Higgs sector are related, by proposing that both scalars are pseudo-Goldstone Bosons of the same global symmetry breaking. This connection also suggests a reheating mechanism, of which a proof-of-concept calculation in the perturbative regime has been performed. Combining the Higgs and the inflation sector allows the model to be tested at colliders; this work illustrates that the collider bounds on the model parameters of the present model are consistent with successful reheating.

Chapter 5 includes an excursion from the compact cosets on which the rest of the thesis is based, to the non-compact groups $SO(n,1)/SO(n)$. It is shown in this chapter that a successful inflationary model can be realized in such a setup. It also surveys the implications from the field space curvature on the reheating mechanism.

Lastly, chapter 6 presents a study of the near-future prospects of holographic Composite Higgs models at colliders, focussing in particular on the minimal $SO(5)/SO(4)$. This paper finds relations between parameters of the 5D and 4D duals, and discussed the phenomenological prospects for top partner searches.

7.2 DIRECTIONS FOR FURTHER STUDY

The treatise of Goldstone fields in cosmology in this thesis has been far from complete; and moreover, it has opened up new avenues for further studies. Here I give a few examples.

7.2.1 A FULL CLASSIFICATION OF PGB POTENTIALS FOR INFLATION

This work has proposed proof-of-concept models of inflation and EWSB linked via a single global symmetry breaking. A full classification of such models which links to UV completion would be a logical next step. This would include geometric approaches to the effective theory of symmetry breaking, and the applicability of the results for Goldstone potentials in different group theoretic structures, such as I explored recently [65] for non-compact groups.

7.2.2 A CONCLUSIVE ANALYSIS OF SPECTATOR FIELDS DURING INFLATION

Given the strong constraints on primordial isocurvature modes [56], in particular when (anti-) correlated with adiabatic perturbations, the status of any light fields during inflation is presently uncertain. Moreover, unlike in single field models, the curvature fluctuations are not automatically conserved on super-horizon scales by conservation of energy-momentum.

After inflaton decay, the decay products will inherit its perturbation. It has been suggested [276] that the isocurvature modes from a light field, which is subdominant in energy, are "swamped" by the adiabatic contributions of the inflaton and its decay products. The model in chapter 4, in which the inflaton decays into the (lighter) Higgs, could lead to an interesting scenario for the relative importance of adiabatic and isocurvature modes.

7.2.3 TACHYONIC REHEATING AFTER GOLDSTONE INFLATION

A full analysis of the parameter space of the model in chapter 4, which allows for non-perturbative processes, besides the perturbative reheating channels that provide the proof of concept in our work. Allowing for the non-perturbative decay is expected to open up a larger range of parameter space in the model. In particular, a trilinear coupling between an inflaton and the Standard Model Higgs boson opens up an exponentially enhanced decay channel. Such a coupling is generically present in a combined Goldstone Inflation and Composite Higgs scenario.

An analysis of the tachyonic reheating channel for the effective Lagrangian in 4 has been done analytically in [277] and more recently on the lattice [278]. A new bound on the trilinear coupling is derived from vacuum stability of the Higgs field; as the variance of the Higgs field grows the model becomes susceptible to vacuum decay.

Interestingly, the studies [277], [278] both indicate¹ that the tachyonic enhancement does not have the capacity to drain all energy from the inflaton field, before the growth of the Higgs variances shuts it off. It therefore seems that a successful model necessarily contains a perturbative decay channel through which some of the inflaton energy dissipates.

7.2.4 ELECTROWEAK BARYOGENESIS AFTER GOLDSTONE INFLATION

The possibility of electroweak baryogenesis in the context of Goldstone Inflation and reheating. The model we have used as a proof of concept suggests the presence of CP-violating couplings in the scalar sector. In fact, this CP breaking may both be explicit and spontaneous, as a nonzero vacuum expectation value for a pseudo-scalar may be generated. Therefore, there may be a region in the parameter space in which electroweak baryogenesis occurs.

As was recently discussed in [279], electroweak baryogenesis with a singlet scalar coupling to the Higgs in a CP violating way can lead to a strongly first order phase transition due to a tree-level barrier and baryogenesis, without the fine-tuning that is usually expected in two Higgs doublet models.

¹In agreement with early studies of the authors of chapter 4.

BIBLIOGRAPHY

- [1] D. J. Fixsen, E. S. Cheng, J. M. Gales, J. C. Mather, R. A. Shafer and E. L. Wright, The Cosmic Microwave Background spectrum from the full COBE FIRAS data set, *Astrophys. J.*, vol. 473, p. 576, 1996. arXiv: astro-ph/9605054 [astro-ph] (cit. on pp. 1, 19).
- [2] G. Hinshaw *et al.*, Nine-Year Wilkinson Microwave Anisotropy Probe (WMAP) Observations: Cosmological Parameter Results, *Astrophys. J. Suppl.*, vol. 208, p. 19, 2013. arXiv: 1212.5226 [astro-ph.CO] (cit. on p. 1).
- [3] P. A. R. Ade *et al.*, Planck 2015 results. XIII. Cosmological parameters, *Astron. Astrophys.*, vol. 594, A13, 2016. arXiv: 1502.01589 [astro-ph.CO] (cit. on p. 1).
- [4] J. Martin, C. Ringeval, R. Trotta and V. Vennin, The Best Inflationary Models After Planck, *JCAP*, vol. 1403, p. 039, 2014. arXiv: 1312.3529 [astro-ph.CO] (cit. on p. 1).
- [5] G. Aad *et al.*, Observation of a new particle in the search for the Standard Model Higgs boson with the ATLAS detector at the LHC, *Phys. Lett.*, vol. B716, pp. 1–29, 2012. arXiv: 1207.7214 [hep-ex] (cit. on pp. 1, 117).
- [6] S. Chatrchyan *et al.*, Observation of a new boson at a mass of 125 GeV with the CMS experiment at the LHC, *Phys. Lett.*, vol. B716, pp. 30–61, 2012. arXiv: 1207.7235 [hep-ex] (cit. on pp. 1, 117).
- [7] K. A. Olive *et al.*, Review of Particle Physics, *Chin. Phys.*, vol. C38, p. 090001, 2014 (cit. on p. 1).
- [8] H. Georgi, H. R. Quinn and S. Weinberg, Hierarchy of Interactions in Unified Gauge Theories, *Phys. Rev. Lett.*, vol. 33, pp. 451–454, 1974 (cit. on p. 1).
- [9] L. Susskind, Dynamics of Spontaneous Symmetry Breaking in the Weinberg-Salam Theory, *Phys. Rev.*, vol. D20, pp. 2619–2625, 1979 (cit. on pp. 1, 3).
- [10] D. H. Lyth, A Bound on Inflationary Energy Density From the Isotropy of the Microwave Background, *Phys. Lett.*, vol. B147, p. 403, 1984, [Erratum: *Phys. Lett.* B150, 465 (1985)] (cit. on p. 1).

- [11] Y. B. Zeldovich, Cosmological Constant and Elementary Particles, *JETP Lett.*, vol. 6, p. 316, 1967, [Pisma Zh. Eksp. Teor. Fiz.6,883(1967)] (cit. on p. 1).
- [12] C. D. Froggatt and H. B. Nielsen, Statistical Analysis of Quark and Lepton Masses, *Nucl. Phys.*, vol. B164, pp. 114–140, 1980 (cit. on p. 1).
- [13] G. 't Hooft, Naturalness, chiral symmetry, and spontaneous chiral symmetry breaking, *NATO Sci. Ser. B*, vol. 59, pp. 135–157, 1980 (cit. on pp. 2, 3, 64).
- [14] P. A. R. Ade *et al.*, Planck 2015 results. XX. Constraints on inflation, *Astron. Astrophys.*, vol. 594, A20, 2016. arXiv: 1502.02114 [astro-ph.CO] (cit. on pp. 3, 4, 17, 18, 46, 57, 58, 62, 73, 82–84, 99, 106, 112–114).
- [15] M. P. Hobson, G. P. Efstathiou and A. N. Lasenby, General relativity: An introduction for physicists. Cambridge University Press, 2006 (cit. on p. 4).
- [16] D. H. Lyth, What would we learn by detecting a gravitational wave signal in the cosmic microwave background anisotropy?, *Phys. Rev. Lett.*, vol. 78, pp. 1861–1863, 1997. arXiv: hep-ph/9606387 [hep-ph] (cit. on pp. 4, 46, 73, 106).
- [17] P. W. Graham, D. E. Kaplan and S. Rajendran, Cosmological Relaxation of the Electroweak Scale, *Phys. Rev. Lett.*, vol. 115, no. 22, p. 221 801, 2015. arXiv: 1504.07551 [hep-ph] (cit. on pp. 5, 74, 99).
- [18] V. V. Khoze and M. Spannowsky, Higgsplosion: Solving the Hierarchy Problem via rapid decays of heavy states into multiple Higgs bosons, 2017. arXiv: 1704.03447 [hep-ph] (cit. on p. 5).
- [19] K. Agashe, R. Contino and A. Pomarol, The Minimal composite Higgs model, *Nucl. Phys.*, vol. B719, pp. 165–187, 2005. arXiv: hep-ph/0412089 [hep-ph] (cit. on pp. 8, 9, 49, 73, 85, 105, 117, 118).
- [20] R. Contino, L. Da Rold and A. Pomarol, Light custodians in natural composite Higgs models, *Phys. Rev.*, vol. D75, p. 055 014, 2007. arXiv: hep-ph/0612048 [hep-ph] (cit. on pp. 8, 118, 128).
- [21] R. Contino, The Higgs as a Composite Nambu-Goldstone Boson, in *Physics of the large and the small, TASI 09, proceedings of the Theoretical Advanced Study Institute in Elementary Particle Physics, Boulder, Colorado, USA, 1-26 June 2009*, 2011, pp. 235–306. arXiv: 1005.4269 [hep-ph]. [Online]. Available: <https://inspirehep.net/record/856065/files/arXiv:1005.4269.pdf> (cit. on pp. 8, 37, 49, 51, 65, 117, 118).
- [22] S. Coleman and E. Weinberg, Radiative corrections as the origin of spontaneous symmetry breaking, *Physical Review D*, vol. 7, no. 6, p. 1888, 1973 (cit. on pp. 9, 50).

- [23] B. Bellazzini, C. Csáki and J. Serra, Composite Higgses, *Eur. Phys. J.*, vol. C74, no. 5, p. 2766, 2014. arXiv: 1401.2457 [hep-ph] (cit. on pp. 9, 37, 49, 51, 65, 73).
- [24] R. Contino, Y. Nomura and A. Pomarol, Higgs as a holographic pseudoGoldstone boson, *Nucl. Phys.*, vol. B671, pp. 148–174, 2003. arXiv: hep-ph/0306259 [hep-ph] (cit. on pp. 9, 26, 37, 47, 117).
- [25] N. Arkani-Hamed, A. G. Cohen, E. Katz and A. E. Nelson, The Littlest Higgs, *JHEP*, vol. 07, p. 034, 2002. arXiv: hep-ph/0206021 [hep-ph] (cit. on p. 9).
- [26] N. Arkani-Hamed, A. G. Cohen, E. Katz, A. E. Nelson, T. Gregoire and J. G. Wacker, The Minimal moose for a little Higgs, *JHEP*, vol. 08, p. 021, 2002. arXiv: hep-ph/0206020 [hep-ph] (cit. on pp. 9, 37).
- [27] I. Low, W. Skiba and D. Tucker-Smith, Little Higgses from an antisymmetric condensate, *Phys. Rev.*, vol. D66, p. 072 001, 2002. arXiv: hep-ph/0207243 [hep-ph] (cit. on p. 9).
- [28] D. E. Kaplan and M. Schmaltz, The Little Higgs from a simple group, *JHEP*, vol. 10, p. 039, 2003. arXiv: hep-ph/0302049 [hep-ph] (cit. on p. 9).
- [29] S. Chang and J. G. Wacker, Little Higgs models and custodial SU(2), *Physical Review D*, vol. 69, no. 3, p. 035 002, 2004 (cit. on p. 9).
- [30] W. Skiba and J. Terning, A Simple model of two little Higgses, *Phys. Rev.*, vol. D68, p. 075 001, 2003. arXiv: hep-ph/0305302 [hep-ph] (cit. on p. 9).
- [31] M. Schmaltz, The Simplest little Higgs, *JHEP*, vol. 08, p. 056, 2004. arXiv: hep-ph/0407143 [hep-ph] (cit. on p. 9).
- [32] M. Schmaltz, D. Stolarski and J. Thaler, The bestest little Higgs, *Journal of High Energy Physics*, vol. 2010, no. 9, pp. 1–40, 2010 (cit. on p. 9).
- [33] J. Reuter and M. Tonini, Can the 125 GeV Higgs be the Little Higgs?, *JHEP*, vol. 02, p. 077, 2013. arXiv: 1212.5930 [hep-ph] (cit. on p. 10).
- [34] M. Crisostomi, R. Klein and D. Roest, Higher Derivative Field Theories: Degeneracy Conditions and Classes, 2017. arXiv: 1703.01623 [hep-th] (cit. on p. 10).
- [35] M. Ostrogradsky, Mémoires sur les équations différentielles, relatives au problème des isopérimètres, *Mem. Acad. St. Petersburg*, vol. 6, no. 4, pp. 385–517, 1850 (cit. on p. 10).
- [36] J. R. Ellis, M. K. Gaillard, M. Gunaydin and B. Zumino, Supersymmetry and Noncompact Groups in Supergravity, *Nucl. Phys.*, vol. B224, pp. 427–450, 1983 (cit. on p. 11).

- [37] K. Freese, J. A. Frieman and A. V. Olinto, Natural inflation with pseudo - Nambu-Goldstone bosons, *Phys. Rev. Lett.*, vol. 65, pp. 3233–3236, 1990 (cit. on pp. 11, 19, 23, 43, 46, 73, 105).
- [38] R. Barbieri and G. F. Giudice, Upper Bounds on Supersymmetric Particle Masses, *Nucl. Phys.*, vol. B306, pp. 63–76, 1988 (cit. on pp. 12, 58, 83).
- [39] V. Vennin, K. Koyama and D. Wands, Inflation with an extra light scalar field after Planck, *JCAP*, vol. 1603, no. 03, p. 024, 2016. arXiv: 1512.03403 [astro-ph.CO] (cit. on p. 12).
- [40] Y. Ali-Haïmoud, J. Chluba and M. Kamionkowski, Constraints on Dark Matter Interactions with Standard Model Particles from Cosmic Microwave Background Spectral Distortions, *Phys. Rev. Lett.*, vol. 115, no. 7, p. 071 304, 2015. arXiv: 1506.04745 [astro-ph.CO] (cit. on p. 12).
- [41] T. Marrodán Undagoitia and L. Rauch, Dark matter direct-detection experiments, *J. Phys.*, vol. G43, no. 1, p. 013 001, 2016. arXiv: 1509.08767 [physics.ins-det] (cit. on p. 12).
- [42] M. Persic, P. Salucci and F. Stel, The Universal rotation curve of spiral galaxies: 1. The Dark matter connection, *Mon. Not. Roy. Astron. Soc.*, vol. 281, p. 27, 1996. arXiv: astro-ph/9506004 [astro-ph] (cit. on p. 12).
- [43] J. Berger, K. Jedamzik and D. G. E. Walker, Cosmological Constraints on Decoupled Dark Photons and Dark Higgs, *JCAP*, vol. 1611, p. 032, 2016. arXiv: 1605.07195 [hep-ph] (cit. on p. 12).
- [44] S. Weinberg, Implications of dynamical symmetry breaking: an addendum, *Physical Review D*, vol. 19, no. 4, p. 1277, 1979 (cit. on p. 13).
- [45] M. E. Peskin and T. Takeuchi, Estimation of oblique electroweak corrections, *Phys. Rev.*, vol. D46, pp. 381–409, 1992 (cit. on p. 13).
- [46] K. Agashe and R. Contino, The Minimal composite Higgs model and electroweak precision tests, *Nucl. Phys.*, vol. B742, pp. 59–85, 2006. arXiv: hep-ph/0510164 [hep-ph] (cit. on pp. 13, 118).
- [47] P. Sikivie, L. Susskind, M. B. Voloshin and V. I. Zakharov, Isospin Breaking in Technicolor Models, *Nucl. Phys.*, vol. B173, pp. 189–207, 1980 (cit. on p. 14).
- [48] A. De Simone, O. Matsedonskyi, R. Rattazzi and A. Wulzer, A First Top Partner Hunter’s Guide, *JHEP*, vol. 04, p. 004, 2013. arXiv: 1211.5663 [hep-ph] (cit. on pp. 14, 118).

- [49] V. Sanz and J. Setford, Composite Higgs models after Run2, 2017. arXiv: 1703.10190 [hep-ph] (cit. on p. 15).
- [50] S. Dawson *et al.*, Working Group Report: Higgs Boson, in *Proceedings, 2013 Community Summer Study on the Future of U.S. Particle Physics: Snowmass on the Mississippi (CSS2013): Minneapolis, MN, USA, July 29-August 6, 2013*, 2013. arXiv: 1310.8361 [hep-ex]. [Online]. Available: <https://inspirehep.net/record/1262795/files/arXiv:1310.8361.pdf> (cit. on p. 15).
- [51] N. Craig and S. Thomas, Exclusive Signals of an Extended Higgs Sector, *JHEP*, vol. 11, p. 083, 2012. arXiv: 1207.4835 [hep-ph] (cit. on p. 15).
- [52] A. A. Penzias and R. W. Wilson, A measurement of excess antenna temperature at 4080 mc/s. *The Astrophysical Journal*, vol. 142, pp. 419–421, 1965 (cit. on p. 15).
- [53] C. L. Bennett *et al.*, Nine-Year Wilkinson Microwave Anisotropy Probe (WMAP) Observations: Final Maps and Results, *Astrophys. J. Suppl.*, vol. 208, p. 20, 2013. arXiv: 1212.5225 [astro-ph.CO] (cit. on p. 15).
- [54] R. Gobetti, E. Pajer and D. Roest, On the Three Primordial Numbers, *JCAP*, vol. 1509, no. 09, p. 058, 2015. arXiv: 1505.00968 [astro-ph.CO] (cit. on pp. 16, 18).
- [55] N. Bartolo, E. Komatsu, S. Matarrese and A. Riotto, Non-Gaussianity from inflation: Theory and observations, *Phys. Rept.*, vol. 402, pp. 103–266, 2004. arXiv: astro-ph/0406398 [astro-ph] (cit. on p. 17).
- [56] P. A. R. Ade *et al.*, Planck 2015 results. XVII. Constraints on primordial non-Gaussianity, *Astron. Astrophys.*, vol. 594, A17, 2016. arXiv: 1502.01592 [astro-ph.CO] (cit. on pp. 18, 140).
- [57] J. Martin, C. Ringeval and V. Vennin, Encyclopædia Inflationaris, *Phys. Dark Univ.*, vol. 5-6, pp. 75–235, 2014. arXiv: 1303.3787 [astro-ph.CO] (cit. on p. 18).
- [58] V. Vennin, J. Martin and C. Ringeval, Cosmic Inflation and Model Comparison, *Comptes Rendus Physique*, vol. 16, no. 10, pp. 960–968, 2015 (cit. on p. 18).
- [59] J. Chluba, Science with CMB spectral distortions, in *Proceedings, 49th Rencontres de Moriond on Cosmology: La Thuile, Italy, March 15-22, 2014*, 2014, pp. 327–334. arXiv: 1405.6938 [astro-ph.CO]. [Online]. Available: <http://inspirehep.net/record/1298250/files/arXiv:1405.6938.pdf> (cit. on p. 18).
- [60] Ya. B. Zeldovich and R. A. Sunyaev, The Interaction of Matter and Radiation in a Hot-Model Universe, *Astrophys. Space Sci.*, vol. 4, pp. 301–316, 1969 (cit. on p. 18).

- [61] D. Croon and V. Sanz, Saving Natural Inflation, *JCAP*, vol. 1502, no. 02, p. 008, 2015. arXiv: 1411.7809 [hep-ph] (cit. on pp. 19, 46, 47, 73).
- [62] N. Arkani-Hamed, H.-C. Cheng, P. Creminelli and L. Randall, Extra natural inflation, *Phys. Rev. Lett.*, vol. 90, p. 221 302, 2003. arXiv: hep-th/0301218 [hep-th] (cit. on pp. 19, 24, 30, 31, 33, 47, 73).
- [63] D. Croon, V. Sanz and J. Setford, Goldstone Inflation, *JHEP*, vol. 10, p. 020, 2015. arXiv: 1503.08097 [hep-ph] (cit. on pp. 19, 73, 82, 84, 99, 105, 112).
- [64] D. Croon, V. Sanz and E. R. M. Tarrant, Reheating with a composite Higgs boson, *Phys. Rev.*, vol. D94, no. 4, p. 045 010, 2016. arXiv: 1507.04653 [hep-ph] (cit. on pp. 20, 105, 112).
- [65] D. Croon, Model Building with Non-Compact Cosets, *Phys. Lett.*, vol. B762, pp. 543–548, 2016. arXiv: 1605.06772 [hep-ph] (cit. on pp. 20, 140).
- [66] D. Croon, B. M. Dillon, S. J. Huber and V. Sanz, Exploring holographic Composite Higgs models, *JHEP*, vol. 07, p. 072, 2016. arXiv: 1510.08482 [hep-ph] (cit. on p. 20).
- [67] A. H. Guth, The Inflationary Universe: A Possible Solution to the Horizon and Flatness Problems, *Phys. Rev.*, vol. D23, pp. 347–356, 1981 (cit. on pp. 23, 46).
- [68] F. C. Adams, J. R. Bond, K. Freese, J. A. Frieman and A. V. Olinto, Natural inflation: Particle physics models, power law spectra for large scale structure, and constraints from COBE, *Phys. Rev.*, vol. D47, pp. 426–455, 1993. arXiv: hep-ph/9207245 [hep-ph] (cit. on pp. 23, 43, 46).
- [69] E. Komatsu *et al.*, Seven-Year Wilkinson Microwave Anisotropy Probe (WMAP) Observations: Cosmological Interpretation, *Astrophys. J. Suppl.*, vol. 192, p. 18, 2011. arXiv: 1001.4538 [astro-ph.CO] (cit. on p. 23).
- [70] P. A. R. Ade *et al.*, Planck 2013 results. XVI. Cosmological parameters, *Astron. Astrophys.*, vol. 571, A16, 2014. arXiv: 1303.5076 [astro-ph.CO] (cit. on pp. 23, 29).
- [71] R. Kallosh, A. D. Linde, S. Prokushkin and M. Shmakova, Gauged supergravities, de Sitter space and cosmology, *Phys. Rev.*, vol. D65, p. 105 016, 2002. arXiv: hep-th/0110089 [hep-th] (cit. on pp. 23, 29).
- [72] A. D. Linde, Hybrid inflation, *Phys. Rev.*, vol. D49, pp. 748–754, 1994. arXiv: astro-ph/9307002 [astro-ph] (cit. on pp. 24, 47, 73).
- [73] J. E. Kim, H. P. Nilles and M. Peloso, Completing natural inflation, *JCAP*, vol. 0501, p. 005, 2005. arXiv: hep-ph/0409138 [hep-ph] (cit. on pp. 24, 47, 73).

- [74] S. Dimopoulos, S. Kachru, J. McGreevy and J. G. Wacker, N-flation, *JCAP*, vol. 0808, p. 003, 2008. arXiv: [hep-th/0507205](#) [[hep-th](#)] (cit. on pp. 24, 30, 47, 73, 110).
- [75] E. Silverstein and A. Westphal, Monodromy in the CMB: Gravity Waves and String Inflation, *Phys. Rev.*, vol. D78, p. 106 003, 2008. arXiv: [0803.3085](#) [[hep-th](#)] (cit. on pp. 24, 30, 47, 73).
- [76] N. Arkani-Hamed, H.-C. Cheng, P. Creminelli and L. Randall, Pseudonatural inflation, *JCAP*, vol. 0307, p. 003, 2003. arXiv: [hep-th/0302034](#) [[hep-th](#)] (cit. on pp. 24, 47, 73).
- [77] I. Antoniadis, K. Benakli and M. Quiros, Finite Higgs mass without supersymmetry, *New J. Phys.*, vol. 3, p. 20, 2001. arXiv: [hep-th/0108005](#) [[hep-th](#)] (cit. on p. 24).
- [78] K. Kohri, C. S. Lim and C.-M. Lin, Distinguishing between Extra Natural Inflation and Natural Inflation after BICEP2, *JCAP*, vol. 1408, p. 001, 2014. arXiv: [1405.0772](#) [[hep-ph](#)] (cit. on p. 24).
- [79] M. Czerny and F. Takahashi, Multi-Natural Inflation, *Phys. Lett.*, vol. B733, pp. 241–246, 2014. arXiv: [1401.5212](#) [[hep-ph](#)] (cit. on p. 25).
- [80] C. Csaki, N. Kaloper, J. Serra and J. Terning, Inflation from Broken Scale Invariance, *Phys. Rev. Lett.*, vol. 113, p. 161 302, 2014. arXiv: [1406.5192](#) [[hep-th](#)] (cit. on pp. 26, 47).
- [81] J. Ellis, N. E. Mavromatos and D. V. Nanopoulos, Starobinsky-Like Inflation in Dilaton-Brane Cosmology, *Phys. Lett.*, vol. B732, pp. 380–384, 2014. arXiv: [1402.5075](#) [[hep-th](#)] (cit. on p. 26).
- [82] C. Csaki and H. Murayama, Instantons in partially broken gauge groups, *Nucl. Phys.*, vol. B532, pp. 498–526, 1998. arXiv: [hep-th/9804061](#) [[hep-th](#)] (cit. on pp. 27, 28).
- [83] S. Coleman, Aspects of symmetry: selected Erice lectures. Cambridge University Press, 1988 (cit. on p. 27).
- [84] P. Svrcek and E. Witten, Axions In String Theory, *JHEP*, vol. 06, p. 051, 2006. arXiv: [hep-th/0605206](#) [[hep-th](#)] (cit. on pp. 28, 46).
- [85] K. Freese and W. H. Kinney, Natural Inflation: Consistency with Cosmic Microwave Background Observations of Planck and BICEP2, *JCAP*, vol. 1503, p. 044, 2015. arXiv: [1403.5277](#) [[astro-ph.CO](#)] (cit. on p. 29).

- [86] K. Freese, C. Savage and W. H. Kinney, Natural Inflation: The Status after WMAP 3-year data, *Int. J. Mod. Phys.*, vol. D16, pp. 2573–2585, 2008. arXiv: 0802.0227 [hep-ph] (cit. on p. 29).
- [87] X. Calmet and V. Sanz, Excursion into Quantum Gravity via Inflation, *Phys. Lett.*, vol. B737, pp. 12–15, 2014. arXiv: 1403.5100 [hep-ph] (cit. on pp. 29, 41, 44, 66).
- [88] C. P. Burgess, M. Cicoli and F. Quevedo, String Inflation After Planck 2013, *JCAP*, vol. 1311, p. 003, 2013. arXiv: 1306.3512 [hep-th] (cit. on p. 30).
- [89] M. A. Amin, M. P. Hertzberg, D. I. Kaiser and J. Karouby, Nonperturbative Dynamics Of Reheating After Inflation: A Review, *Int. J. Mod. Phys.*, vol. D24, p. 1530003, 2014. arXiv: 1410.3808 [hep-ph] (cit. on pp. 30, 113).
- [90] N. Barnaby, E. Pajer and M. Peloso, Gauge Field Production in Axion Inflation: Consequences for Monodromy, non-Gaussianity in the CMB, and Gravitational Waves at Interferometers, *Phys. Rev.*, vol. D85, p. 023525, 2012. arXiv: 1110.3327 [astro-ph.CO] (cit. on p. 30).
- [91] M. M. Anber and L. Sorbo, Naturally inflating on steep potentials through electromagnetic dissipation, *Phys. Rev.*, vol. D81, p. 043534, 2010. arXiv: 0908.4089 [hep-th] (cit. on p. 30).
- [92] H. Hatanaka, T. Inami and C. S. Lim, The Gauge hierarchy problem and higher dimensional gauge theories, *Mod. Phys. Lett.*, vol. A13, pp. 2601–2612, 1998. arXiv: hep-th/9805067 [hep-th] (cit. on p. 31).
- [93] N. Arkani-Hamed, A. G. Cohen and H. Georgi, (De)constructing dimensions, *Phys. Rev. Lett.*, vol. 86, pp. 4757–4761, 2001. arXiv: hep-th/0104005 [hep-th] (cit. on p. 32).
- [94] C. T. Hill, S. Pokorski and J. Wang, Gauge invariant effective Lagrangian for Kaluza-Klein modes, *Phys. Rev.*, vol. D64, p. 105005, 2001. arXiv: hep-th/0104035 [hep-th] (cit. on p. 32).
- [95] N. Arkani-Hamed, A. G. Cohen and H. Georgi, Electroweak symmetry breaking from dimensional deconstruction, *Phys. Lett.*, vol. B513, pp. 232–240, 2001. arXiv: hep-ph/0105239 [hep-ph] (cit. on p. 32).
- [96] O. Aharony, S. S. Gubser, J. M. Maldacena, H. Ooguri and Y. Oz, Large N field theories, string theory and gravity, *Phys. Rept.*, vol. 323, pp. 183–386, 2000. arXiv: hep-th/9905111 [hep-th] (cit. on p. 32).

- [97] J. Hirn and V. Sanz, Interpolating between low and high energy QCD via a 5-D Yang-Mills model, *JHEP*, vol. 12, p. 030, 2005. arXiv: hep-ph/0507049 [hep-ph] (cit. on pp. 36, 117).
- [98] J. Hirn and V. Sanz, A Negative S parameter from holographic technicolor, *Phys. Rev. Lett.*, vol. 97, p. 121 803, 2006. arXiv: hep-ph/0606086 [hep-ph] (cit. on pp. 36, 66, 84, 117).
- [99] J. Hirn and V. Sanz, The Fifth dimension as an analogue computer for strong interactions at the LHC, *JHEP*, vol. 03, p. 100, 2007. arXiv: hep-ph/0612239 [hep-ph] (cit. on pp. 36, 39, 66, 84, 117).
- [100] J. Hirn, A. Martin and V. Sanz, Benchmarks for new strong interactions at the LHC, *JHEP*, vol. 05, p. 084, 2008. arXiv: 0712.3783 [hep-ph] (cit. on pp. 39, 65, 84, 123).
- [101] J. Hirn, A. Martin and V. Sanz, Describing viable technicolor scenarios, *Phys. Rev.*, vol. D78, p. 075 026, 2008. arXiv: 0807.2465 [hep-ph] (cit. on pp. 39, 65, 84).
- [102] G. Cacciapaglia, C. Csaki, C. Grojean and J. Terning, Higgsless electroweak symmetry breaking, *eConf*, vol. C040802, FRT004, 2004, [,259(2004)] (cit. on p. 39).
- [103] G. Cacciapaglia, C. Csaki, C. Grojean and J. Terning, Curing the Ills of Higgsless models: The S parameter and unitarity, *Phys. Rev.*, vol. D71, p. 035 015, 2005. arXiv: hep-ph/0409126 [hep-ph] (cit. on pp. 39, 66, 84).
- [104] K. Agashe, C. Csaki, C. Grojean and M. Reece, The S-parameter in holographic technicolor models, *JHEP*, vol. 12, p. 003, 2007. arXiv: 0704.1821 [hep-ph] (cit. on pp. 39, 66, 84).
- [105] N. Kaloper, A. Lawrence and L. Sorbo, An Ignoble Approach to Large Field Inflation, *JCAP*, vol. 1103, p. 023, 2011. arXiv: 1101.0026 [hep-th] (cit. on pp. 40, 41, 66).
- [106] L. Smolin, Gravitational Radiative Corrections as the Origin of Spontaneous Symmetry Breaking!, *Phys. Lett.*, vol. B93, pp. 95–100, 1980 (cit. on p. 40).
- [107] F. Brummer, V. Domcke and V. Sanz, GUT-scale inflation with sizeable tensor modes, *JCAP*, vol. 1408, p. 066, 2014. arXiv: 1405.4868 [hep-ph] (cit. on pp. 41, 44).
- [108] D. H. Lyth, BICEP2, the curvature perturbation and supersymmetry, *JCAP*, vol. 1411, no. 11, p. 003, 2014. arXiv: 1403.7323 [hep-ph] (cit. on p. 46).
- [109] R. Kallosh, A. D. Linde, D. A. Linde and L. Susskind, Gravity and global symmetries, *Phys. Rev.*, vol. D52, pp. 912–935, 1995. arXiv: hep-th/9502069 [hep-th] (cit. on p. 46).

- [110] M. Montero, A. M. Uranga and I. Valenzuela, Transplanckian axions!?, *JHEP*, vol. 08, p. 032, 2015. arXiv: 1503.03886 [hep-th] (cit. on p. 46).
- [111] Z. Kenton and S. Thomas, D-brane Potentials in the Warped Resolved Conifold and Natural Inflation, *JHEP*, vol. 02, p. 127, 2015. arXiv: 1409.1221 [hep-th] (cit. on p. 46).
- [112] A. R. Liddle, A. Mazumdar and F. E. Schunck, Assisted inflation, *Phys. Rev.*, vol. D58, p. 061 301, 1998. arXiv: astro-ph/9804177 [astro-ph] (cit. on p. 47).
- [113] E. J. Copeland, A. Mazumdar and N. J. Nunes, Generalized assisted inflation, *Phys. Rev.*, vol. D60, p. 083 506, 1999. arXiv: astro-ph/9904309 [astro-ph] (cit. on pp. 47, 73).
- [114] C. G. Callan Jr., S. R. Coleman, J. Wess and B. Zumino, Structure of phenomenological Lagrangians. 2. *Phys. Rev.*, vol. 177, pp. 2247–2250, 1969 (cit. on p. 48).
- [115] G. von Gersdorff, E. Pontón and R. Rosenfeld, The Dynamical Composite Higgs, *JHEP*, vol. 06, p. 119, 2015. arXiv: 1502.07340 [hep-ph] (cit. on pp. 48, 118).
- [116] B. Gripaios, A. Pomarol, F. Riva and J. Serra, Beyond the Minimal Composite Higgs Model, *JHEP*, vol. 04, p. 070, 2009. arXiv: 0902.1483 [hep-ph] (cit. on pp. 49, 76, 78, 79).
- [117] A. Pomarol and F. Riva, The Composite Higgs and Light Resonance Connection, *JHEP*, vol. 08, p. 135, 2012. arXiv: 1205.6434 [hep-ph] (cit. on pp. 53, 117, 128).
- [118] J. R. Ellis, K. Enqvist, D. V. Nanopoulos and F. Zwirner, Observables in Low-Energy Superstring Models, *Mod. Phys. Lett.*, vol. A1, p. 57, 1986 (cit. on p. 58).
- [119] J. R. Espinosa, C. Grojean, V. Sanz and M. Trott, NSUSY fits, *JHEP*, vol. 12, p. 077, 2012. arXiv: 1207.7355 [hep-ph] (cit. on p. 59).
- [120] J. Gasser and A. Zepeda, Approaching the Chiral Limit in QCD, *Nucl. Phys.*, vol. B174, p. 445, 1980 (cit. on p. 59).
- [121] J. Gasser and H. Leutwyler, Chiral Perturbation Theory to One Loop, *Annals Phys.*, vol. 158, p. 142, 1984 (cit. on p. 59).
- [122] ———, Chiral Perturbation Theory: Expansions in the Mass of the Strange Quark, *Nucl. Phys.*, vol. B250, pp. 465–516, 1985 (cit. on p. 59).
- [123] D. Baumann, D. Green, H. Lee and R. A. Porto, Signs of Analyticity in Single-Field Inflation, *Phys. Rev.*, vol. D93, no. 2, p. 023 523, 2016. arXiv: 1502.07304 [hep-th] (cit. on p. 60).

- [124] B. Bellazzini, L. Martucci and R. Torre, Symmetries, Sum Rules and Constraints on Effective Field Theories, *JHEP*, vol. 09, p. 100, 2014. arXiv: 1405.2960 [hep-th] (cit. on p. 60).
- [125] A. V. Manohar and V. Mateu, Dispersion Relation Bounds for $\pi\pi$ Scattering, *Phys. Rev.*, vol. D77, p. 094019, 2008. arXiv: 0801.3222 [hep-ph] (cit. on p. 60).
- [126] V. Mateu, Universal Bounds for SU(3) Low Energy Constants, *Phys. Rev.*, vol. D77, p. 094020, 2008. arXiv: 0801.3627 [hep-ph] (cit. on p. 60).
- [127] A. Filipuzzi, J. Portoles and P. Ruiz-Femenia, Zeros of the $W_L Z_L \rightarrow W_L Z_L$ Amplitude: Where Vector Resonances Stand, *JHEP*, vol. 08, p. 080, 2012. arXiv: 1205.4682 [hep-ph] (cit. on p. 60).
- [128] J. J. Sanz-Cillero, D.-L. Yao and H.-Q. Zheng, Positivity constraints on the low-energy constants of the chiral pion-nucleon Lagrangian, *Eur. Phys. J.*, vol. C74, p. 2763, 2014. arXiv: 1312.0664 [hep-ph] (cit. on p. 60).
- [129] G. Ecker, J. Gasser, A. Pich and E. de Rafael, The Role of Resonances in Chiral Perturbation Theory, *Nucl. Phys.*, vol. B321, pp. 311–342, 1989 (cit. on p. 61).
- [130] G. Ecker, J. Gasser, H. Leutwyler, A. Pich and E. de Rafael, Chiral Lagrangians for Massive Spin 1 Fields, *Phys. Lett.*, vol. B223, pp. 425–432, 1989 (cit. on p. 61).
- [131] R. Lewis, C. Pica and F. Sannino, Light Asymmetric Dark Matter on the Lattice: SU(2) Technicolor with Two Fundamental Flavors, *Phys. Rev.*, vol. D85, p. 014504, 2012. arXiv: 1109.3513 [hep-ph] (cit. on pp. 61, 117).
- [132] D. Baumann and D. Green, Equilateral Non-Gaussianity and New Physics on the Horizon, *JCAP*, vol. 1109, p. 014, 2011. arXiv: 1102.5343 [hep-th] (cit. on p. 62).
- [133] D. Baumann, D. Green and R. A. Porto, B-modes and the Nature of Inflation, *JCAP*, vol. 1501, no. 01, p. 016, 2015. arXiv: 1407.2621 [hep-th] (cit. on p. 62).
- [134] G. Hooft, A planar diagram theory for strong interactions, *Nuclear Physics B*, vol. 72, no. 3, pp. 461–473, 1974 (cit. on p. 64).
- [135] E. Witten, Baryons in the $1/n$ Expansion, *Nucl. Phys.*, vol. B160, pp. 57–115, 1979 (cit. on p. 64).
- [136] S. Weinberg, Precise relations between the spectra of vector and axial vector mesons, *Phys. Rev. Lett.*, vol. 18, pp. 507–509, 1967 (cit. on p. 65).

- [137] M. Knecht and E. de Rafael, Patterns of spontaneous chiral symmetry breaking in the large $N(c)$ limit of QCD - like theories, *Phys. Lett.*, vol. B424, pp. 335–342, 1998. arXiv: hep-ph/9712457 [hep-ph] (cit. on p. 65).
- [138] A. Martin and V. Sanz, Mass-Matching in Higgsless, *JHEP*, vol. 01, p. 075, 2010. arXiv: 0907.3931 [hep-ph] (cit. on pp. 65, 84).
- [139] W. H. Kinney and K. T. Mahanthappa, Inflation at low scales: General analysis and a detailed model, *Phys. Rev.*, vol. D53, pp. 5455–5467, 1996. arXiv: hep-ph/9512241 [hep-ph] (cit. on p. 68).
- [140] J. R. Espinosa, C. Grojean, G. Panico, J. R. Espinosa, C. Grojean, G. Panico, A. Pomarol, O. Pujolàs and G. Servant, Cosmological Higgs-Axion Interplay for a Naturally Small Electroweak Scale, 2015. arXiv: 1506.09217 [hep-ph] (cit. on p. 74).
- [141] C. Gross, O. Lebedev and M. Zatta, Higgs-inflaton coupling from reheating and the meta-stable Universe, 2015. arXiv: 1506.05106 [hep-ph] (cit. on pp. 75, 99).
- [142] L. Kofman, A. D. Linde and A. A. Starobinsky, Towards the theory of reheating after inflation, *Phys. Rev.*, vol. D56, pp. 3258–3295, 1997. arXiv: hep-ph/9704452 [hep-ph] (cit. on pp. 75, 85, 89–91).
- [143] D. I. Podolsky, G. N. Felder, L. Kofman and M. Peloso, Equation of state and beginning of thermalization after preheating, *Phys. Rev.*, vol. D73, p. 023 501, 2006. arXiv: hep-ph/0507096 [hep-ph] (cit. on p. 75).
- [144] J. Braden, L. Kofman and N. Barnaby, Reheating the Universe After Multi-Field Inflation, *JCAP*, vol. 1007, p. 016, 2010. arXiv: 1005.2196 [hep-th] (cit. on pp. 75, 89–92, 99).
- [145] J. Galloway, J. A. Evans, M. A. Luty and R. A. Tacchi, Minimal Conformal Technicolor and Precision Electroweak Tests, *JHEP*, vol. 10, p. 086, 2010. arXiv: 1001.1361 [hep-ph] (cit. on p. 76).
- [146] V. A. Rubakov and M. E. Shaposhnikov, Do We Live Inside a Domain Wall?, *Phys. Lett.*, vol. B125, pp. 136–138, 1983 (cit. on p. 81).
- [147] R. Allahverdi, R. Brandenberger, F.-Y. Cyr-Racine and A. Mazumdar, Reheating in Inflationary Cosmology: Theory and Applications, *Ann.Rev.Nucl.Part.Sci.*, vol. 60, pp. 27–51, 2010. arXiv: 1001.2600 [hep-th] (cit. on p. 85).
- [148] J. H. Traschen and R. H. Brandenberger, Particle Production During Out-of-equilibrium Phase Transitions, *Phys.Rev.*, vol. D42, pp. 2491–2504, 1990 (cit. on p. 89).

- [149] Y. Shtanov, J. H. Traschen and R. H. Brandenberger, Universe reheating after inflation, *Phys. Rev.*, vol. D51, pp. 5438–5455, 1995. arXiv: hep-ph/9407247 [hep-ph] (cit. on p. 89).
- [150] A. Linde, S. Mooij and E. Pajer, Gauge field production in supergravity inflation: Local non-Gaussianity and primordial black holes, *Phys. Rev.*, vol. D87, no. 10, p. 103 506, 2013. arXiv: 1212.1693 [hep-th] (cit. on p. 93).
- [151] P. Adshead, J. T. Giblin, T. R. Scully and E. I. Sfakianakis, Gauge-preheating and the end of axion inflation, 2015. arXiv: 1502.06506 [astro-ph.CO] (cit. on p. 93).
- [152] E. W. Kolb, A. Notari and A. Riotto, On the reheating stage after inflation, *Phys. Rev.*, vol. D68, p. 123 505, 2003. arXiv: hep-ph/0307241 [hep-ph] (cit. on p. 94).
- [153] M. Drewes, On finite density effects on cosmic reheating and moduli decay and implications for Dark Matter production, *JCAP*, vol. 1411, no. 11, p. 020, 2014. arXiv: 1406.6243 [hep-ph] (cit. on p. 94).
- [154] M. Drewes and J. U. Kang, The Kinematics of Cosmic Reheating, *Nucl. Phys.*, vol. B875, pp. 315–350, 2013. arXiv: 1305.0267 [hep-ph] (cit. on p. 94).
- [155] M. Kawasaki, K. Kohri and N. Sugiyama, Cosmological constraints on late time entropy production, *Phys. Rev. Lett.*, vol. 82, p. 4168, 1999. arXiv: astro-ph/9811437 [astro-ph] (cit. on p. 96).
- [156] K. Ichikawa, M. Kawasaki and F. Takahashi, The Oscillation effects on thermalization of the neutrinos in the Universe with low reheating temperature, *Phys. Rev.*, vol. D72, p. 043 522, 2005. arXiv: astro-ph/0505395 [astro-ph] (cit. on p. 96).
- [157] J. Martin, C. Ringeval and V. Vennin, Observing Inflationary Reheating, *Phys. Rev. Lett.*, vol. 114, no. 8, p. 081 303, 2015. arXiv: 1410.7958 [astro-ph.CO] (cit. on p. 96).
- [158] S. Hannestad, What is the lowest possible reheating temperature?, *Phys. Rev.*, vol. D70, p. 043 506, 2004. arXiv: astro-ph/0403291 [astro-ph] (cit. on p. 97).
- [159] A. G. Cohen, D. B. Kaplan and A. E. Nelson, Progress in electroweak baryogenesis, *Ann. Rev. Nucl. Part. Sci.*, vol. 43, pp. 27–70, 1993. arXiv: hep-ph/9302210 [hep-ph] (cit. on p. 97).
- [160] J. R. Espinosa, B. Gripaios, T. Konstandin and F. Riva, Electroweak Baryogenesis in Non-minimal Composite Higgs Models, *JCAP*, vol. 1201, p. 012, 2012. arXiv: 1110.2876 [hep-ph] (cit. on p. 97).

- [161] M. Gorbahn, J. M. No and V. Sanz, Benchmarks for Higgs Effective Theory: Extended Higgs Sectors, 2015. arXiv: 1502.07352 [hep-ph] (cit. on p. 97).
- [162] G. Aad *et al.*, Measurement of Higgs boson production in the diphoton decay channel in pp collisions at center-of-mass energies of 7 and 8 TeV with the ATLAS detector, *Phys. Rev.*, vol. D90, no. 11, p. 112015, 2014. arXiv: 1408.7084 [hep-ex] (cit. on p. 97).
- [163] V. Khachatryan *et al.*, Observation of the diphoton decay of the Higgs boson and measurement of its properties, *Eur. Phys. J.*, vol. C74, no. 10, p. 3076, 2014. arXiv: 1407.0558 [hep-ex] (cit. on p. 97).
- [164] G. Aad *et al.*, Measurements of Higgs boson production and couplings in the four-lepton channel in pp collisions at center-of-mass energies of 7 and 8 TeV with the ATLAS detector, *Phys. Rev.*, vol. D91, no. 1, p. 012006, 2015. arXiv: 1408.5191 [hep-ex] (cit. on p. 97).
- [165] S. Chatrchyan *et al.*, Measurement of the properties of a Higgs boson in the four-lepton final state, *Phys. Rev.*, vol. D89, no. 9, p. 092007, 2014. arXiv: 1312.5353 [hep-ex] (cit. on p. 97).
- [166] G. Aad *et al.*, Measurements of the properties of the Higgs-like boson in the $WW^{(*)} \rightarrow \ell\nu\ell\nu$ decay channel with the ATLAS detector using 25 fb^{-1} of proton-proton collision data, 2013 (cit. on p. 97).
- [167] S. Chatrchyan *et al.*, Measurement of Higgs boson production and properties in the WW decay channel with leptonic final states, *JHEP*, vol. 01, p. 096, 2014. arXiv: 1312.1129 [hep-ex] (cit. on p. 97).
- [168] T. A. collaboration, Search for the bb decay of the Standard Model Higgs boson in associated W/ZH production with the ATLAS detector, 2013 (cit. on p. 97).
- [169] S. Chatrchyan *et al.*, Search for the standard model Higgs boson produced in association with a W or a Z boson and decaying to bottom quarks, *Phys. Rev.*, vol. D89, no. 1, p. 012003, 2014. arXiv: 1310.3687 [hep-ex] (cit. on p. 97).
- [170] T. A. collaboration, Evidence for Higgs Boson Decays to the $\tau^+\tau^-$ Final State with the ATLAS Detector, 2013 (cit. on p. 97).
- [171] S. Chatrchyan *et al.*, Evidence for the 125 GeV Higgs boson decaying to a pair of τ leptons, *JHEP*, vol. 05, p. 104, 2014. arXiv: 1401.5041 [hep-ex] (cit. on p. 97).
- [172] M. Baak, J. Cth, J. Haller, A. Hoecker, R. Kogler, K. Mnig, M. Schott and J. Stelzer, The global electroweak fit at NNLO and prospects for the LHC and ILC, *Eur. Phys. J.*, vol. C74, p. 3046, 2014. arXiv: 1407.3792 [hep-ph] (cit. on pp. 97, 98).

- [173] J. Fan, M. Reece and L.-T. Wang, Possible Futures of Electroweak Precision: ILC, FCC-ee, and CEPC, 2014. arXiv: 1411.1054 [hep-ph] (cit. on p. 97).
- [174] K. Hagiwara, S. Matsumoto, D. Haidt and C. S. Kim, A Novel approach to confront electroweak data and theory, *Z. Phys.*, vol. C64, pp. 559–620, 1994, [Erratum: *Z. Phys.*C68,352(1995)]. arXiv: hep-ph/9409380 [hep-ph] (cit. on p. 98).
- [175] D. M. Asner *et al.*, ILC Higgs White Paper, in *Community Summer Study 2013: Snowmass on the Mississippi (CSS2013) Minneapolis, MN, USA, July 29-August 6, 2013*, 2013. arXiv: 1310.0763 [hep-ph]. [Online]. Available: <https://inspirehep.net/record/1256491/files/arXiv:1310.0763.pdf> (cit. on p. 98).
- [176] M. Bicer *et al.*, First Look at the Physics Case of TLEP, *JHEP*, vol. 01, p. 164, 2014. arXiv: 1308.6176 [hep-ex] (cit. on p. 98).
- [177] M. Redi and A. Tesi, Implications of a Light Higgs in Composite Models, *JHEP*, vol. 10, p. 166, 2012. arXiv: 1205.0232 [hep-ph] (cit. on pp. 100, 118).
- [178] R. D. Peccei and H. R. Quinn, CP Conservation in the Presence of Instantons, *Phys. Rev. Lett.*, vol. 38, pp. 1440–1443, 1977 (cit. on p. 105).
- [179] S. Weinberg, A New Light Boson?, *Phys. Rev. Lett.*, vol. 40, pp. 223–226, 1978 (cit. on p. 105).
- [180] F. Wilczek, Problem of Strong p and t Invariance in the Presence of Instantons, *Phys. Rev. Lett.*, vol. 40, pp. 279–282, 1978 (cit. on p. 105).
- [181] J. Iliopoulos and B. Zumino, Broken Supergauge Symmetry and Renormalization, *Nucl. Phys.*, vol. B76, p. 310, 1974 (cit. on p. 105).
- [182] P. Fayet and J. Iliopoulos, Spontaneously Broken Supergauge Symmetries and Goldstone Spinors, *Phys. Lett.*, vol. B51, pp. 461–464, 1974 (cit. on p. 105).
- [183] L. O’Raifeartaigh, Spontaneous Symmetry Breaking for Chiral Scalar Superfields, *Nucl. Phys.*, vol. B96, pp. 331–352, 1975 (cit. on p. 105).
- [184] M. Frigerio, A. Pomarol, F. Riva and A. Urbano, Composite Scalar Dark Matter, *JHEP*, vol. 07, p. 015, 2012. arXiv: 1204.2808 [hep-ph] (cit. on p. 105).
- [185] C. P. Burgess, M. Cicoli, F. Quevedo and M. Williams, Inflating with Large Effective Fields, *JCAP*, vol. 1411, p. 045, 2014. arXiv: 1404.6236 [hep-th] (cit. on pp. 105, 106).

- [186] R. Alonso, E. E. Jenkins and A. V. Manohar, Sigma Models with Negative Curvature, *Phys. Lett.*, vol. B756, pp. 358–364, 2016. arXiv: 1602.00706 [hep-ph] (cit. on pp. 105, 106, 115).
- [187] —, A Geometric Formulation of Higgs Effective Field Theory: Measuring the Curvature of Scalar Field Space, *Phys. Lett.*, vol. B754, pp. 335–342, 2016. arXiv: 1511.00724 [hep-ph] (cit. on pp. 105, 115).
- [188] —, Geometry of the Scalar Sector, *JHEP*, vol. 08, p. 101, 2016. arXiv: 1605.03602 [hep-ph] (cit. on pp. 105, 106, 115).
- [189] I. Low, Minimally symmetric Higgs boson, *Phys. Rev.*, vol. D91, no. 11, p. 116 005, 2015. arXiv: 1412.2146 [hep-ph] (cit. on p. 105).
- [190] A. A. Starobinsky, Spectrum of relict gravitational radiation and the early state of the universe, *JETP Lett.*, vol. 30, pp. 682–685, 1979, [Pisma Zh. Eksp. Teor. Fiz.30,719(1979)] (cit. on pp. 106, 112).
- [191] S. Ferrara, R. Kallosh, A. Linde and M. Porrati, Minimal Supergravity Models of Inflation, *Phys. Rev.*, vol. D88, no. 8, p. 085 038, 2013. arXiv: 1307.7696 [hep-th] (cit. on p. 106).
- [192] R. Kallosh, A. Linde and D. Roest, Superconformal Inflationary α -Attractors, *JHEP*, vol. 11, p. 198, 2013. arXiv: 1311.0472 [hep-th] (cit. on p. 106).
- [193] R. Kallosh and A. Linde, Multi-field Conformal Cosmological Attractors, *JCAP*, vol. 1312, p. 006, 2013. arXiv: 1309.2015 [hep-th] (cit. on p. 106).
- [194] —, Universality Class in Conformal Inflation, *JCAP*, vol. 1307, p. 002, 2013. arXiv: 1306.5220 [hep-th] (cit. on p. 106).
- [195] K.-Y. Choi, L. M. H. Hall and C. van de Bruck, Spectral Running and Non-Gaussianity from Slow-Roll Inflation in Generalised Two-Field Models, *JCAP*, vol. 0702, p. 029, 2007. arXiv: astro-ph/0701247 [astro-ph] (cit. on p. 112).
- [196] T. Fujita and K. Harigaya, Hubble induced mass after inflation in spectator field models, *JCAP*, vol. 1612, no. 12, p. 014, 2016. arXiv: 1607.07058 [astro-ph.CO] (cit. on p. 113).
- [197] J.-L. Lehners, P. McFadden, N. Turok and P. J. Steinhardt, Generating ekpyrotic curvature perturbations before the big bang, *Phys. Rev.*, vol. D76, p. 103 501, 2007. arXiv: hep-th/0702153 [HEP-TH] (cit. on p. 114).
- [198] S. De Curtis, M. Redi and A. Tesi, The 4D Composite Higgs, *JHEP*, vol. 04, p. 042, 2012. arXiv: 1110.1613 [hep-ph] (cit. on p. 117).

- [199] O. Matsedonskyi, G. Panico and A. Wulzer, Light Top Partners for a Light Composite Higgs, *JHEP*, vol. 01, p. 164, 2013. arXiv: 1204.6333 [hep-ph] (cit. on pp. 117, 118, 132, 137).
- [200] D. Marzocca, M. Serone and J. Shu, General Composite Higgs Models, *JHEP*, vol. 08, p. 013, 2012. arXiv: 1205.0770 [hep-ph] (cit. on p. 117).
- [201] G. F. Giudice, C. Grojean, A. Pomarol and R. Rattazzi, The Strongly-Interacting Light Higgs, *JHEP*, vol. 06, p. 045, 2007. arXiv: hep-ph/0703164 [hep-ph] (cit. on p. 117).
- [202] C. Anastasiou, E. Furlan and J. Santiago, Realistic Composite Higgs Models, *Phys. Rev.*, vol. D79, p. 075 003, 2009. arXiv: 0901.2117 [hep-ph] (cit. on p. 117).
- [203] G. Panico and A. Wulzer, The Discrete Composite Higgs Model, *JHEP*, vol. 09, p. 135, 2011. arXiv: 1106.2719 [hep-ph] (cit. on pp. 117, 132, 137).
- [204] A. Azatov and J. Galloway, Light Custodians and Higgs Physics in Composite Models, *Phys. Rev.*, vol. D85, p. 055 013, 2012. arXiv: 1110.5646 [hep-ph] (cit. on p. 117).
- [205] A. Hietanen, R. Lewis, C. Pica and F. Sannino, Composite Goldstone Dark Matter: Experimental Predictions from the Lattice, *JHEP*, vol. 12, p. 130, 2014. arXiv: 1308.4130 [hep-ph] (cit. on p. 117).
- [206] A. Hietanen, R. Lewis, C. Pica and F. Sannino, Fundamental Composite Higgs Dynamics on the Lattice: SU(2) with Two Flavors, *JHEP*, vol. 07, p. 116, 2014. arXiv: 1404.2794 [hep-lat] (cit. on p. 117).
- [207] D. T. Son and M. A. Stephanov, QCD and dimensional deconstruction, *Phys. Rev.*, vol. D69, p. 065 020, 2004. arXiv: hep-ph/0304182 [hep-ph] (cit. on p. 117).
- [208] J. Erlich, E. Katz, D. T. Son and M. A. Stephanov, QCD and a holographic model of hadrons, *Phys. Rev. Lett.*, vol. 95, p. 261 602, 2005. arXiv: hep-ph/0501128 [hep-ph] (cit. on p. 117).
- [209] L. Da Rold and A. Pomarol, Chiral symmetry breaking from five dimensional spaces, *Nucl. Phys.*, vol. B721, pp. 79–97, 2005. arXiv: hep-ph/0501218 [hep-ph] (cit. on p. 117).
- [210] J. Hirn, N. Rius and V. Sanz, Geometric approach to condensates in holographic QCD, *Phys. Rev.*, vol. D73, p. 085 005, 2006. arXiv: hep-ph/0512240 [hep-ph] (cit. on p. 117).

- [211] C. Csaki, C. Grojean, L. Pilo and J. Terning, Towards a realistic model of Higgsless electroweak symmetry breaking, *Phys. Rev. Lett.*, vol. 92, p. 101 802, 2004. arXiv: hep-ph/0308038 [hep-ph] (cit. on p. 117).
- [212] G. Cacciapaglia, C. Csaki, C. Grojean and J. Terning, Oblique corrections from Higgsless models in warped space, *Phys. Rev.*, vol. D70, p. 075 014, 2004. arXiv: hep-ph/0401160 [hep-ph] (cit. on p. 117).
- [213] L. Randall and R. Sundrum, A Large mass hierarchy from a small extra dimension, *Phys. Rev. Lett.*, vol. 83, pp. 3370–3373, 1999. arXiv: hep-ph/9905221 [hep-ph] (cit. on p. 117).
- [214] N. Arkani-Hamed and M. Schmaltz, Hierarchies without symmetries from extra dimensions, *Phys. Rev.*, vol. D61, p. 033 005, 2000. arXiv: hep-ph/9903417 [hep-ph] (cit. on p. 117).
- [215] S. J. Huber and Q. Shafi, Fermion masses, mixings and proton decay in a Randall-Sundrum model, *Phys. Lett.*, vol. B498, pp. 256–262, 2001. arXiv: hep-ph/0010195 [hep-ph] (cit. on p. 117).
- [216] S. J. Huber and Q. Shafi, Higgs mechanism and bulk gauge boson masses in the Randall-Sundrum model, *Phys. Rev.*, vol. D63, p. 045 010, 2001. arXiv: hep-ph/0005286 [hep-ph] (cit. on p. 117).
- [217] B. M. Dillon and S. J. Huber, Non-Custodial Warped Extra Dimensions at the LHC?, *JHEP*, vol. 06, p. 066, 2015. arXiv: 1410.7345 [hep-ph] (cit. on p. 118).
- [218] J. A. Cabrer, G. von Gersdorff and M. Quiros, Suppressing Electroweak Precision Observables in 5D Warped Models, *JHEP*, vol. 05, p. 083, 2011. arXiv: 1103.1388 [hep-ph] (cit. on p. 118).
- [219] P. R. Archer and S. J. Huber, Electroweak Constraints on Warped Geometry in Five Dimensions and Beyond, *JHEP*, vol. 10, p. 032, 2010. arXiv: 1004.1159 [hep-ph] (cit. on p. 118).
- [220] A. Carmona and F. Goertz, A naturally light Higgs without light Top Partners, *JHEP*, vol. 05, p. 002, 2015. arXiv: 1410.8555 [hep-ph] (cit. on pp. 118, 128).
- [221] K. Agashe, A. Delgado, M. J. May and R. Sundrum, RS1, custodial isospin and precision tests, *JHEP*, vol. 08, p. 050, 2003. arXiv: hep-ph/0308036 [hep-ph] (cit. on p. 118).
- [222] M. Carena, E. Ponton, J. Santiago and C. E. M. Wagner, Electroweak constraints on warped models with custodial symmetry, *Phys. Rev.*, vol. D76, p. 035 006, 2007. arXiv: hep-ph/0701055 [hep-ph] (cit. on p. 118).

- [223] P. R. Archer, Fine Tuning in the Holographic Minimal Composite Higgs Model, 2014. arXiv: 1403.8048 [hep-ph] (cit. on pp. 118, 121, 125, 132, 138).
- [224] G. Panico and A. Wulzer, The Composite Nambu-Goldstone Higgs, *Lect. Notes Phys.*, vol. 913, pp.1–316, 2016. arXiv: 1506.01961 [hep-ph] (cit. on p. 118).
- [225] M. Low, A. Tesi and L.-T. Wang, Twin Higgs mechanism and a composite Higgs boson, *Phys. Rev.*, vol. D91, p. 095 012, 2015. arXiv: 1501.07890 [hep-ph] (cit. on p. 118).
- [226] R. Barbieri, D. Greco, R. Rattazzi and A. Wulzer, The Composite Twin Higgs scenario, *JHEP*, vol. 08, p. 161, 2015. arXiv: 1501.07803 [hep-ph] (cit. on p. 118).
- [227] H.-C. Cheng, B. A. Dobrescu and J. Gu, Higgs Mass from Compositeness at a Multi-TeV Scale, *JHEP*, vol. 08, p. 095, 2014. arXiv: 1311.5928 [hep-ph] (cit. on p. 118).
- [228] J. Barnard, T. Gherghetta, T. S. Ray and A. Spray, The Unnatural Composite Higgs, *JHEP*, vol. 01, p. 067, 2015. arXiv: 1409.7391 [hep-ph] (cit. on p. 118).
- [229] H.-C. Cheng and J. Gu, Top seesaw with a custodial symmetry, and the 126 GeV Higgs, *JHEP*, vol. 10, p. 002, 2014. arXiv: 1406.6689 [hep-ph] (cit. on p. 118).
- [230] G. Ferretti, UV Completions of Partial Compositeness: The Case for a SU(4) Gauge Group, *JHEP*, vol. 06, p. 142, 2014. arXiv: 1404.7137 [hep-ph] (cit. on p. 118).
- [231] S. De Curtis, M. Redi and E. Vigiani, Non Minimal Terms in Composite Higgs Models and in QCD, *JHEP*, vol. 06, p. 071, 2014. arXiv: 1403.3116 [hep-ph] (cit. on p. 118).
- [232] A. Carmona and M. Chala, Composite Dark Sectors, *JHEP*, vol. 06, p. 105, 2015. arXiv: 1504.00332 [hep-ph] (cit. on p. 118).
- [233] V. Khachatryan *et al.*, Search for vector-like charge $2/3$ T quarks in proton-proton collisions at $\sqrt{s} = 8$ TeV, *Phys. Rev.*, vol. D93, no. 1, p. 012 003, 2016. arXiv: 1509.04177 [hep-ex] (cit. on p. 118).
- [234] G. Aad *et al.*, Search for production of vector-like quark pairs and of four top quarks in the lepton-plus-jets final state in pp collisions at $\sqrt{s} = 8$ TeV with the ATLAS detector, *JHEP*, vol. 08, p. 105, 2015. arXiv: 1505.04306 [hep-ex] (cit. on p. 118).
- [235] M. Backovic, T. Flacke, J. H. Kim and S. J. Lee, Search Strategies for TeV Scale Fermionic Top Partners with Charge $2/3$, *JHEP*, vol. 04, p. 014, 2016. arXiv: 1507.06568 [hep-ph] (cit. on p. 118).
- [236] A. Buckley, C. Englert, J. Ferrando, D. J. Miller, L. Moore, M. Russell and C. D. White, Global fit of top quark effective theory to data, *Phys. Rev.*, vol. D92, no. 9, p. 091 501, 2015. arXiv: 1506.08845 [hep-ph] (cit. on p. 118).

- [237] J. Serra, Beyond the Minimal Top Partner Decay, *JHEP*, vol. 09, p. 176, 2015. arXiv: 1506.05110 [hep-ph] (cit. on p. 118).
- [238] S. Dawson and E. Furlan, Yukawa Corrections to Higgs Production in Top Partner Models, *Phys. Rev.*, vol. D89, no. 1, p. 015 012, 2014. arXiv: 1310.7593 [hep-ph] (cit. on p. 118).
- [239] C. Grojean, O. Matsedonskyi and G. Panico, Light top partners and precision physics, *JHEP*, vol. 10, p. 160, 2013. arXiv: 1306.4655 [hep-ph] (cit. on p. 118).
- [240] M. Backović, T. Flacke, J. H. Kim and S. J. Lee, Boosted Event Topologies from TeV Scale Light Quark Composite Partners, *JHEP*, vol. 04, p. 082, 2015. arXiv: 1410.8131 [hep-ph] (cit. on p. 118).
- [241] E. Drueke, J. Nutter, R. Schwienhorst, N. Vignaroli, D. G. E. Walker and J.-H. Yu, Single Top Production as a Probe of Heavy Resonances, *Phys. Rev.*, vol. D91, no. 5, p. 054 020, 2015. arXiv: 1409.7607 [hep-ph] (cit. on p. 118).
- [242] J. Reuter and M. Tonini, Top Partner Discovery in the $T \rightarrow tZ$ channel at the LHC, *JHEP*, vol. 01, p. 088, 2015. arXiv: 1409.6962 [hep-ph] (cit. on p. 118).
- [243] O. Matsedonskyi, G. Panico and A. Wulzer, On the Interpretation of Top Partners Searches, *JHEP*, vol. 12, p. 097, 2014. arXiv: 1409.0100 [hep-ph] (cit. on p. 118).
- [244] B. Gripaios, T. Müller, M. A. Parker and D. Sutherland, Search Strategies for Top Partners in Composite Higgs models, *JHEP*, vol. 08, p. 171, 2014. arXiv: 1406.5957 [hep-ph] (cit. on p. 118).
- [245] C.-Y. Chen, S. Dawson and I. M. Lewis, Top Partners and Higgs Boson Production, *Phys. Rev.*, vol. D90, no. 3, p. 035 016, 2014. arXiv: 1406.3349 [hep-ph] (cit. on p. 118).
- [246] A. Banfi, A. Martin and V. Sanz, Probing top-partners in Higgs+jets, *JHEP*, vol. 08, p. 053, 2014. arXiv: 1308.4771 [hep-ph] (cit. on pp. 118, 135).
- [247] M. Carena, L. Da Rold and E. Pontón, Minimal Composite Higgs Models at the LHC, *JHEP*, vol. 06, p. 159, 2014. arXiv: 1402.2987 [hep-ph] (cit. on pp. 118, 127).
- [248] C. Niehoff, P. Stangl and D. M. Straub, Direct and indirect signals of natural composite Higgs models, *JHEP*, vol. 01, p. 119, 2016. arXiv: 1508.00569 [hep-ph] (cit. on p. 118).
- [249] J. Barnard and M. White, Collider constraints on tuning in composite Higgs models, *JHEP*, vol. 10, p. 072, 2015. arXiv: 1507.02332 [hep-ph] (cit. on p. 118).
- [250] G. Cacciapaglia, H. Cai, A. Deandrea, T. Flacke, S. J. Lee and A. Parolini, Composite scalars at the LHC: the Higgs, the Sextet and the Octet, *JHEP*, vol. 11, p. 201, 2015. arXiv: 1507.02283 [hep-ph] (cit. on p. 118).

- [251] A. Thamm, R. Torre and A. Wulzer, Future tests of Higgs compositeness: direct vs indirect, *JHEP*, vol. 07, p. 100, 2015. arXiv: 1502.01701 [hep-ph] (cit. on p. 118).
- [252] S. Kanemura, K. Kaneta, N. Machida and T. Shindou, New resonance scale and fingerprint identification in minimal composite Higgs models, *Phys. Rev.*, vol. D91, p. 115 016, 2015. arXiv: 1410.8413 [hep-ph] (cit. on p. 118).
- [253] N. Vignaroli, New W' signals at the LHC, *Phys. Rev.*, vol. D89, no. 9, p. 095 027, 2014. arXiv: 1404.5558 [hep-ph] (cit. on p. 118).
- [254] M. Redi, V. Sanz, M. de Vries and A. Weiler, Strong Signatures of Right-Handed Compositeness, *JHEP*, vol. 08, p. 008, 2013. arXiv: 1305.3818 (cit. on p. 118).
- [255] K. Agashe, A. Azatov, T. Han, Y. Li, Z.-G. Si and L. Zhu, LHC Signals for Coset Electroweak Gauge Bosons in Warped/Composite PGB Higgs Models, *Phys. Rev.*, vol. D81, p. 096 002, 2010. arXiv: 0911.0059 [hep-ph] (cit. on p. 118).
- [256] A. Carmona, M. Chala and J. Santiago, New Higgs Production Mechanism in Composite Higgs Models, *JHEP*, vol. 07, p. 049, 2012. arXiv: 1205.2378 [hep-ph] (cit. on p. 118).
- [257] R. Contino, D. Marzocca, D. Pappadopulo and R. Rattazzi, On the effect of resonances in composite Higgs phenomenology, *JHEP*, vol. 10, p. 081, 2011. arXiv: 1109.1570 [hep-ph] (cit. on p. 118).
- [258] D. Pappadopulo, A. Thamm and R. Torre, A minimally tuned composite Higgs model from an extra dimension, *JHEP*, vol. 07, p. 058, 2013. arXiv: 1303.3062 [hep-ph] (cit. on p. 118).
- [259] V. Sanz and J. Setford, Composite Higgses with seesaw EWSB, *JHEP*, vol. 12, p. 154, 2015. arXiv: 1508.06133 [hep-ph] (cit. on p. 118).
- [260] G. Panico, M. Redi, A. Tesi and A. Wulzer, On the Tuning and the Mass of the Composite Higgs, *JHEP*, vol. 03, p. 051, 2013. arXiv: 1210.7114 [hep-ph] (cit. on pp. 118, 128, 133).
- [261] M. Bauer, S. Casagrande, L. Grunder, U. Haisch and M. Neubert, Little Randall-Sundrum models: epsilon(K) strikes again, *Phys. Rev.*, vol. D79, p. 076 001, 2009. arXiv: 0811.3678 [hep-ph] (cit. on p. 119).
- [262] H. Davoudiasl, G. Perez and A. Soni, The Little Randall-Sundrum Model at the Large Hadron Collider, *Phys. Lett.*, vol. B665, pp. 67–71, 2008. arXiv: 0802.0203 [hep-ph] (cit. on pp. 119, 128).

- [263] T. A. collaboration, Search for resonances decaying to photon pairs in 3.2 fb^{-1} of pp collisions at $\sqrt{s} = 13 \text{ TeV}$ with the ATLAS detector, 2015 (cit. on p. 119).
- [264] C. Collaboration, Search for new physics in high mass diphoton events in proton-proton collisions at 13TeV , 2015 (cit. on p. 119).
- [265] H. Davoudiasl and C. Zhang, 750 GeV messenger of dark conformal symmetry breaking, *Phys. Rev.*, vol. D93, no. 5, p. 055 006, 2016. arXiv: 1512 . 07672 [hep-ph] (cit. on p. 119).
- [266] B. M. Dillon and V. Sanz, A Little KK Graviton at 750 GeV, 2016. arXiv: 1603 . 09550 [hep-ph] (cit. on p. 119).
- [267] A. Falkowski and J. F. Kamenik, Diphoton portal to warped gravity, *Phys. Rev.*, vol. D94, no. 1, p. 015 008, 2016. arXiv: 1603 . 06980 [hep-ph] (cit. on p. 119).
- [268] B. M. Dillon, D. P. George and K. L. McDonald, Regarding the Radion in Randall-Sundrum Models with Brane Curvature, *Phys. Rev.*, vol. D94, no. 6, p. 064 045, 2016. arXiv: 1605 . 03087 [hep-ph] (cit. on p. 119).
- [269] J. Hirn and V. Sanz, (Not) Summing over Kaluza-Kleins, *Phys. Rev.*, vol. D76, p. 044 022, 2007. arXiv: hep-ph/0702005 [HEP-PH] (cit. on p. 123).
- [270] L. Randall, V. Sanz and M. D. Schwartz, Entropy area relations in field theory, *JHEP*, vol. 06, p. 008, 2002. arXiv: hep-th/0204038 [hep-th] (cit. on p. 123).
- [271] G. Aad *et al.*, Measurements of the Higgs boson production and decay rates and coupling strengths using pp collision data at $\sqrt{s} = 7$ and 8 TeV in the ATLAS experiment, *Eur. Phys. J.*, vol. C76, no. 1, p. 6, 2016. arXiv: 1507 . 04548 [hep-ex] (cit. on p. 127).
- [272] G. Aad *et al.*, Constraints on new phenomena via Higgs boson couplings and invisible decays with the ATLAS detector, *JHEP*, vol. 11, p. 206, 2015. arXiv: 1509 . 00672 [hep-ex] (cit. on p. 135).
- [273] A. Azatov and A. Paul, Probing Higgs couplings with high p_T Higgs production, *JHEP*, vol. 01, p. 014, 2014. arXiv: 1309 . 5273 [hep-ph] (cit. on p. 135).
- [274] C. Grojean, E. Salvioni, M. Schlaffer and A. Weiler, Very boosted Higgs in gluon fusion, *JHEP*, vol. 05, p. 022, 2014. arXiv: 1312 . 3317 [hep-ph] (cit. on p. 135).
- [275] A. Banfi, B. M. Dillon and V. Sanz, In preparation, eprint: 2016 (cit. on p. 136).
- [276] C. T. Byrnes, M. Cort  s and A. R. Liddle, Curvaton scenarios with inflaton decays into curvatons, *Phys. Rev.*, vol. D94, no. 6, p. 063 525, 2016. arXiv: 1608 . 02162 [astro-ph.CO] (cit. on p. 140).

- [277] J. F. Dufaux, G. N. Felder, L. Kofman, M. Peloso and D. Podolsky, Preheating with tri-linear interactions: Tachyonic resonance, *JCAP*, vol. 0607, p. 006, 2006. arXiv: hep-ph/0602144 [hep-ph] (cit. on p. 141).
- [278] K. Enqvist, M. Karciauskas, O. Lebedev, S. Rusak and M. Zatta, Postinflationary vacuum instability and Higgs-inflaton couplings, *JCAP*, vol. 1611, p. 025, 2016. arXiv: 1608.08848 [hep-ph] (cit. on p. 141).
- [279] J. M. Cline, Is electroweak baryogenesis dead?, in *52nd Rencontres de Moriond on EW Interactions and Unified Theories (Moriond EW 2017) La Thuile, Italy, March 18-25, 2017*, 2017. arXiv: 1704.08911 [hep-ph]. [Online]. Available: <https://inspirehep.net/record/1597324/files/arXiv:1704.08911.pdf> (cit. on p. 141).